Quantifying Cognitive Workload and Mental Capacity from EEG Signals under Complex Cognitive Activities

Mengting Zhao

A Thesis

in

The Department

of

Concordia Institute for Information Systems Engineering (CIISE)

Presented in Partial Fulfillment of the Requirements

for the Degree of

Doctor of Philosophy (Information and Systems Engineering) at

Concordia University

Montréal, Québec, Canada

December 2022

CONCORDIA UNIVERSITY

School of Graduate Studies

This is to certify that the thesis prepared

By: **Ms. Mengting Zhao**

Entitled: **Quantifying Cognitive Workload and Mental Capacity from EEG Signals under Complex Cognitive Activities**

and submitted in partial fulfillment of the requirements for the degree of

Doctor of Philosophy (Information and Systems Engineering)

complies with the regulations of this University and meets the accepted standards with respect to originality and quality. Signed by the Final Examining Committee:

_____ Chair
Dr. Rajamohan Ganesan

_____ External Examiner
Dr. Chris W. Zhang

_____ External to Program
Dr. Chunyan Wang

_____ Examiner
Dr. Ben Hamza

_____ Examiner
Dr. Jun Yan

_____ Supervisor
Dr. Yong Zeng

_____ Co-supervisor
Dr. Dongyu Qiu

Approved by _____
Dr. Zachary Patterson, Graduate Program Director

_____ 2022 _____
Dr. Mourad Debbabi, Dean of Gina Cody School of Engineering and Computer Science

Abstract

Quantifying Cognitive Workload and Mental Capacity from EEG Signals under Complex Cognitive Activities

Mengting Zhao, Ph.D.

Concordia University, 2023

The objective of the present research is to quantify the changes in cognitive workload and mental capacity from EEG signals when people are conducting complex cognitive activities. Design activities are good examples of complex cognitive activities that require simultaneous involvements of multiple cognitive functions including problem understanding, analyzing, evaluating, and creating. As one of the fundamental human activities, design activities are where a designer's mental effort is applied to create product descriptions (design solutions) from an initial design problem, which involves looping and jumping among design problems, design knowledge, and design solutions. Using design activities as a starting point, the present study conducted a series of theoretical analyses and literature reviews to identify the opportunities and challenges for applying EEG to quantify designers' cognitive changes, including cognitive workload and mental capacity. The research objectives were formulated based on my pilot studies in applying and extending the stress model, leading to the methodology of the present research. A new framework (tEEG framework) has been proposed to address the identified challenges as a result of our past research attempts and theoretical analyses, which also serves as the foundation for the present research. Afterward, the proposed tEEG framework was applied for quantitatively monitoring changes in people's cognitive workload and mental capacity within and beyond the context of design, where mental capacity was considered as the umbrella of numerous cognitive factors including cognitive control. Finally, my future research goal is to apply the quantification results on cognitive workload and mental capacity to improving human mental effort under complex cognitive activities, which corresponds to the second research objective of the present research. Along this direction, the present research proposes

a quantitative approach to elaborate the impact of cognitive workload and mental capacity on mental effort that has been verified by simulation results. My future research will continue to test the approach in cognitive experiments including the ongoing N-back study, aiming to bridge the gap between most existing cognitive studies and their applications in real life.

Acknowledgments

My Ph.D. study at Concordia University has been such a long journey that so much changes have happened to me, my family, and the world during those years. The coronavirus pandemic has changed the whole world and people's lives, and a baby girl came to the world at St. Mary's hospital in Montreal on the day when the first positive case was identified in Montreal. As the mother of this baby girl, the experience of dealing with those challenges while pursuing my research goal makes me a totally different person while approaching the end of my Ph.D. journey. The person standing here to present her doctoral dissertation to the committee, is not afraid of any changes or problems in the future as she knows how to analyze the confronted problem step by step and where to put her effort for finding a solution for it.

In the first place, I would like to express my sincere gratitude to my supervisor, Prof. Yong Zeng, for his continuous supports throughout my study at Concordia. I appreciate his help in letting me participate in the NSERC CRD project led by him where I could not only test our proposed framework on a pilot training process beyond the context of design, but also get the chance to collaborate with the talents from the industry and other research institutions. I still remember the young lady full of confidence and motivations to achieve her research dream when I came to the university in 2017 right after my graduation from Paris-Saclay University. However, I didn't realize that I merely had any experience in conducting research as all of my past study programs were course-based. Changing my thinking style from a solution-driven engineer to a problem-driven researcher is not easy for me, which could also be challenging for my supervisor who has put so much confidence in me all the time. There were some tough moments when I thought about giving up my research, but thankfully Prof. Yong Zeng has always been here to encourage me and help me

getting through such moments. Even though I am not sure whether he is satisfied with my current research achievement, I really hope that he won't regret his time and effort in teaching and helping me with my research.

My gratitude also goes to my co-supervisor, Dr. Dongyu Qiu, for his continuous help with my research. Upon the reception of my submitted materials he would always get back to me as soon as possible with a list of detailed feedback, even though sometimes he needed to sacrifice his weekend for it. I am also grateful to Graduate Program Coordinator, CIISE staff, Research Grants Office staff, and other Concordia University staff who have helped me with my parental leave application, graduation application, and other requests. My special thanks go to Silvie Pasquarelli, who has provided continuous help in handling and double-checking my application materials.

I thank my colleagues from Design Lab for helping me with my research and the nice words that cheered me up. I learned a lot in collaborating and communicating with my colleagues despite our differences in educational background, cultural diversity, and personality. My special thanks go to Thanh An Nguyen, Suo Tan, and Philon Nguyen for explaining to me how to do use the research tools and giving me the chance to collaborate with them in the first year of my Ph.D. study. I also appreciate the support from Xiaoying Wang, Hongyi Cao, Cheligeer, Wenjun Jia, Jie Pan, Chang Su, Başak Tozlu, and Liang Fu, who have already become my lifelong friends.

I would like to express my appreciation and the deepest love to my family, I would never have been able to achieve such a goal without their support. My parents have always been there to comfort me when I am upset and to support me without any preconditions when I feel ready to restart. Although they kept sharing the good news with but hiding some bad news from me those years, I always know that they have carried much more burden than I could ever imagine from my faraway hometown. I also want to thank my husband, Daocheng Yang, who is also my best friend, for his understanding, support, and love. His accompany means a lot to me and I appreciate him for being the person holding my hands through all the happy and tough moments in the past ten years. My thanks also go to my beloved daughter Chloe Yang for her smile that has been my magic energy boost and her effort in keeping herself quiet at the age of two when mommy needs to work.

Contribution of Authors

This section presents a statement of the contributions of authors for the six co-authored research works that are included in the present thesis. These studies are discussed in chronological order as they appear in the thesis.

The study presented in Section 3.2.1 is a book chapter published in 2018 (Zhao, Yang, Liu, & Zeng, 2018), which is included in the sixth volume of the *Emotional Engineering* book series. This work is co-authored by Mengting Zhao, Daocheng Yang, Dr. Siyun Liu, and Dr. Yong Zeng. As the first author of this work, the candidate conducted the literature review, performed the theoretical analysis, and wrote the article. Daocheng Yang contributed to the literature review; Dr. Siyun Liu wrote the article; and Dr. Yong Zeng supervised the entire process and wrote the article.

The study discussed in Section 3.2.2 is a conference paper presented at *International Conference on Engineering Design* in 2019 (Zhao & Zeng, 2019). This work is co-authored by Mengting Zhao and Dr. Yong Zeng. As the first author of this work, the candidate analyzed the data and wrote the paper. Dr. Yong Zeng designed the experiment, supervised the data analysis, and wrote the paper.

The tEEG framework presented in Section 4.1 is proposed in the journal article published on *Design Science* in 2020 (Zhao et al., 2020). This article is co-authored by Mengting Zhao, Wenjun Jia, Daocheng Yang, Dr. Philon Nguyen, Dr. Thanh An Nguyen, and Dr. Yong Zeng. As the first author of this work, the candidate conducted the theoretical analysis, developed the framework, and wrote the article. Wenjun Jia contributed to the literature review on EEG related studies and wrote the article; Daocheng Yang contributed to the literature review on affective studies and reviewed the article; Dr. Philon Nguyen contributed to the development of framework and reviewed the article; Dr. Thanh An Nguyen contributed to the development of framework; Dr. Yong Zeng developed the

framework, supervised the analysis, and wrote the article.

The within design application of tEEG framework discussed in Section 5.1 is included in a journal article published on *Scientific Reports* in 2021 (Jia, von Wegner, Zhao, & Zeng, 2021). This research work is co-authored by Wenjun Jia, Dr. Frederic von Wegner, Mengting Zhao, and Dr. Yong Zeng. EEG-based analysis (including TRP and microstate analysis) has been conducted to investigate temporal dynamics of brain activity in response to distinct design activities during the conceptual design process under a loosely controlled setting. As the third author of this work, the candidate contributed to the EEG microstate analysis, conducted the statistical analysis, and wrote the article. Wenjun Jia pre-processed the data, conducted the TRP analysis and EEG microstate analysis, and wrote the article; Dr. Frederic von Wegner contributed to the EEG microstate analysis and wrote the article; Dr. Yong Zeng supervised the entire project, designed the experiment, and wrote the article. As a result, this thesis only covers the part of the EEG microstate analysis that is related to the candidate's contributions.

The beyond design application of tEEG framework discussed in Section 5.2 is included in a manuscript scheduled for submission to the journal *Nature Human Behaviour* upon agreement among all co-authors (Zhao, Jia, et al., 2022). This research work is co-authored by Mengting Zhao, Dr. Wenjun Jia, Sion Jennings, Andrew Law, Alain Bourgon, Hugh Grenier, Marie-Hélène Larose, Chang Su, David Bowness, and Dr. Yong Zeng. As the first author of this work, the candidate collected the data, pre-processed the data, analyzed the data, and wrote the article. Wenjun Jia contributed to the data analysis and wrote the article; Sion Jennings designed the experiment, collected the data, and wrote the article; Andrew Law designed the experiment and wrote the article; Alain Bourgon designed the experiment and wrote the article; Hugh Grenier designed the experiment and reviewed the article; Marie-Hélène Larose collected the data and reviewed the article; Chang Su collected the data and reviewed the article; David Bowness supervised the entire project and reviewed the article; Dr. Yong Zeng supervised the entire project and data analysis process, and wrote the article.

Section 5.3 presents the analysis and results included in a manuscript scheduled for submission to the journal *PloS One* (Zhao, Qiu, & Zeng, 2022). This work is co-authored by Mengting Zhao, Dr. Dongyu Qiu, and Dr. Yong Zeng, where the concept of human capacity zone locating between

the two workload equilibria is proposed to ensure the expected accomplishment of a collaborative task under a predefined deadline in a quantitative manner. As the first author of this work, the candidate conducted the analysis, performed the simulations, and wrote the article. Dr. Dongyu Qiu supervised the simulations and wrote the article; and Dr. Yong Zeng supervised the entire project, analyzed the results, and wrote the article.

List of Acronyms

AAHC	Atomize and Agglomerate Hierarchical Clustering
ANOVA	Analysis of Variance
CAD	Computer-Aided Design
DFA	Detrended Fluctuation Analysis
EBD	Environment-Based Design
ECG	Electrocardiogam
EEG	Electroencephalogram
EI	Engagement Index
ERD	Event Related Desynchronization
ERP	Event Related Potential
ERS	Event Related Synchronization
fNIRS	functional Near Infra-Red Spectroscopy
GFP	Global Field Power
GLR	Generalized Likelihood Ratio
GSR	Galvanic Skin Response
HRV	Heart Rate Variability

IE	Idea Evaluation
IG	Idea Generation
IPM	Integrated Physiological Monitoring
K-NN	K-Nearest Neighbours algorithm
LDA	Linear Discriminant Analysis
MARA	Multiple Artifact Rejection Algorithm
NASA-TLX	NASA Task Load Index
NEO	Nonlinear Energy Operator
PFD	Primary Flight Display
PSD	Power Spectral Density
PU	Problem Understanding
RIE	Rating Idea Evaluation
RIG	Rating Idea Generation
STFT	Short-term fast Fourier Transform
SVI	Sympathovagal Balance Index
SVM	Support Vector Machine
TLI	Task Load Index
TRP	Task Related Power
WM	Working Memory
WMC	Working Memory Capacity
WT	Wavelet Transform

Contents

List of Acronyms x

List of Figures xvii

List of Tables xxviii

1 Introduction 1

1.1 Research questions 3

1.2 Research objectives and contributions 5

1.3 Organization 7

2 Literature Review 8

2.1 Design as a complex cognitive activity 8

2.2 Cognitive workload under complex cognitive activities . . . 11

2.3 Mental capacity under complex cognitive activities 13

2.4 Failure to meet the deadline as a consequence of the mismatch between cognitive workload and mental capacity . . . 15

2.5 Applying EEG techniques to complex cognitive activities . . 18

3 Pilot Study: Formulation of Research Objectives **26**

3.1 The stress-effort model for design creativity 26

3.2 Applying stress-effort model for phenomena interpretation . 28

3.2.1 Role of emotion in engineering 28

3.2.2 Influence of information collection strategies on stress 31

3.3 Formulated research objectives 36

4 Research Methodology: A tEEG Framework for Conducting Loosely Controlled EEG Experimental Studies **39**

4.1 Proposing a new research framework for EEG-based cognitive design studies: The tEEG framework 40

4.1.1 Challenges with EEG-based cognitive design studies 40

4.1.2 The proposed tEEG framework 44

4.2 Applying tEEG framework within and beyond design for quantifying cognitive factors 47

4.2.1 A step-by-step guide for tEEG framework applications 48

4.2.2 Evaluation under different contexts 49

4.3 From stress model to a quantitative representation of human workload-effort relationship 50

4.3.1 The stress-effort model 51

4.3.2 From stress-effort model to a quantitative representation of human workload-effort relationship 53

5 Quantification of Phenomena under Complex Cognitive Activities: Results and Discussions **57**

5.1 An application of tEEG framework within design: A loosely controlled design experiment 57

5.1.1 Participants 58

5.1.2 Results on EEG microstate analysis 59

5.1.3 Quantification of cognitive control under different design activities 64

5.1.4 Quantification of cognitive workload under different design activities 66

5.1.5 Conclusion 66

5.2 An application of tEEG framework beyond design: A pilot training experiment 67

5.2.1 Experiment and participants 68

5.2.2 Pre-processing for data collected from loosely controlled experiment 71

5.2.3 Clustering-based segmentation: EEG microstate analysis 72

5.2.4 Segment-wise analysis 73

5.2.5 Results on performance evaluation, EEG spectral analysis, and EEG microstate analysis 74

5.2.6 Quantified cognitive control during a skill acquisition process 85
5.2.7 Quantified cognitive workload during a skill acquisition process 93
5.2.8 Quantitative changes in cognitive workload and cognitive control under varied task demands 96
5.2.9 Conclusion 98
5.3 Capacity zone: A quantitative approach for ensuring high efficiency by manipulating workload 99
5.3.1 Comparison between human workload-efficiency relationship and the ideal modeling 99
5.3.2 Results 102
5.3.3 Discussion 107
5.4 Ongoing exploration on the quantification and impact of mental capacity: An N-back working memory experiment . . 120
5.4.1 Experiment and participants 121
5.4.2 Data pre-processing 122
5.4.3 Feature extraction and analysis 123
5.4.4 Preliminary results 125
5.4.5 Discussions on the preliminary results 134

6 Conclusion and Future Work **140**

6.1 Conclusion 140
6.2 Future work 144

Bibliography **146**

List of Figures

Figure 2.1 Design evolution process 9

Figure 3.1 Depth-first and breadth-first information collection strategies 33

Figure 4.1 ERP waveform generated from averaging across events 41

Figure 4.2 Design process representation 43

Figure 4.3 The proposed tEEG framework 45

Figure 4.4 Human workload-effort relationship 55

Figure 5.1 Microstate coverage during rest (REST), problem understanding (PU), idea generation (IG), rating idea generation (IE), idea evaluation (IE), and rating idea evaluation (RIE). P-values between rest and other conditions are annotated by black dots ($p > 0.050$), blue dots ($p \leq 0.050$), yellow dots ($p \leq 0.010$), and red dots ($p \leq 0.005$). P-values between conditions are annotated by $^{*}(p \leq 0.050)$, $^{**}(p \leq 0.010)$, $^{***}(p \leq 0.005)$. 59

Figure 5.2 Microstate duration during rest (REST), problem understanding (PU), idea generation (IG), rating idea generation (IE), idea evaluation (IE), and rating idea evaluation (RIE). P-values between rest and other conditions are annotated by black dots ($p > 0.050$), blue dots ($p \leq 0.050$), yellow dots ($p \leq 0.010$), and red dots ($p \leq 0.005$). P-values between conditions are annotated by $^{*}(p \leq 0.050)$, $^{**}(p \leq 0.010)$, $^{***}(p \leq 0.005)$. 60

Figure 5.3 Microstate occurrence during rest (REST), problem understanding (PU), idea generation (IG), rating idea generation (IE), idea evaluation (IE), and rating idea evaluation (RIE). P-values between rest and other conditions are annotated by black dots ($p > 0.050$), blue dots ($p \leq 0.050$), yellow dots ($p \leq 0.010$), and red dots ($p \leq 0.005$). P-values between conditions are annotated by $^{*}(p \leq 0.050)$, $^{**}(p \leq 0.010)$, $^{***}(p \leq 0.005)$. 61

Figure 5.4 Entropy rate of microstate sequences during rest (REST), problem understanding (PU), idea generation (IG), rating idea generation (IE), idea evaluation (IE), and rating idea evaluation (RIE). P-values between rest and other conditions are annotated by black dots ($p > 0.050$), blue dots ($p \leq 0.050$), yellow dots ($p \leq 0.010$), and red dots ($p \leq 0.005$). P-values between conditions are annotated by $^{*}(p \leq 0.050)$, $^{**}(p \leq 0.010)$, $^{***}(p \leq 0.005)$. 62

Figure 5.5 Hurst exponent of microstate sequences averaged from 35 partitions during rest (REST), problem understanding (PU), idea generation (IG), rating idea generation (IE), idea evaluation (IE), and rating idea evaluation (RIE). P-values between rest and other conditions are annotated by black dots ($p > 0.050$), blue dots ($p \leq 0.050$), yellow dots ($p \leq 0.010$), and red dots ($p \leq 0.005$). P-values between conditions are annotated by $^{*}(p \leq 0.050)$, $^{**}(p \leq 0.010)$, $^{***}(p \leq 0.005)$. 63

Figure 5.6 Entropy rate of microstate sequences during each run for each tested condition (rest (REST), problem understanding (PU), idea generation (IG), rating idea generation (IE), idea evaluation (IE), and rating idea evaluation (RIE)). P-values between rest and other conditions are annotated by black dots ($p > 0.050$), blue dots ($p \leq 0.050$), yellow dots ($p \leq 0.010$), and red dots ($p \leq 0.005$). P-values between conditions are annotated by $^{*}(p \leq 0.050)$, $^{**}(p \leq 0.010)$, $^{***}(p \leq 0.005)$. 64

Figure 5.7 Hurst exponent of microstate sequences during each run for each tested condition (rest (REST), problem understanding (PU), idea generation (IG), rating idea generation (IE), idea evaluation (IE), and rating idea evaluation (RIE)). P-values between rest and other conditions are annotated by black dots ($p > 0.050$), blue dots ($p \leq 0.050$), yellow dots ($p \leq 0.010$), and red dots ($p \leq 0.005$). P-values between conditions are annotated by $^{*}(p \leq 0.050)$, $^{**}(p \leq 0.010)$, $^{***}(p \leq 0.005)$. 65

Figure 5.8 Flight instrument example 70

Figure 5.9 Quantitative assessment on each dimension with P-values for TASK and STAGE comparisons annotated by $^{*}(p \leq 0.050)$, $^{**}(p \leq 0.010)$, $^{***}(p \leq 0.005)$ 76

Figure 5.10 NASA-TLX subjective rating results for STAGE comparison (Training, PracticeA, and PracticeB). P-values for STAGE comparisons are annotated by $^{*}(p \leq 0.050)$, $^{**}(p \leq 0.010)$, $^{***}(p \leq 0.005)$ 78

Figure 5.11 EEG theta band power for Baseline tasks and Trial tasks during Training, PracticeA, and PracticeB. P-values for TASK and STAGE comparisons are annotated by $^{*}(p \leq 0.050)$, $^{**}(p \leq 0.010)$, $^{***}(p \leq 0.005)$. 80

Figure 5.12 EEG alpha band power for Baseline tasks and Trial tasks during Training, PracticeA, and PracticeB. P-values for TASK and STAGE comparisons are annotated by $^{*}(p \leq 0.050)$, $^{**}(p \leq 0.010)$, $^{***}(p \leq 0.005)$ 81

Figure 5.13 The spatial configuration of the seven microstate classes (A, B, C, D, E, F, and G) for across TASK and STAGE (global) and for each task type (Baseline and Trial) during different stages (Training, PracticeA, and PracticeB) 82

Figure 5.14 EEG microstate coverage for Baseline tasks and Trial tasks during Training, PracticeA, and PracticeB stages. P-values for TASK and STAGE comparisons are annotated by $^{*}(p \leq 0.050)$, $^{**}(p \leq 0.010)$, $^{***}(p \leq 0.005)$. 83

Figure 5.15 EEG microstate occurrence for Baseline tasks and Trial tasks during Training, PracticeA, and PracticeB stages. P-values for TASK and STAGE comparisons are annotated by $^{*}(p \leq 0.050)$, $^{**}(p \leq 0.010)$, $^{***}(p \leq 0.005)$. 85

Figure 5.16 EEG microstate duration for Baseline tasks and Trial tasks during Training, PracticeA, and PracticeB stages. P-values for TASK and STAGE comparisons are annotated by $^{*}(p \leq 0.050)$, $^{**}(p \leq 0.010)$, $^{***}(p \leq 0.005)$. 87

Figure 5.17 Entropy rate of microstate sequences for Baseline and Trial tasks during Training, PracticeA, and PracticeB stages. P-values for TASK and STAGE comparisons are annotated by $^{*}(p \leq 0.050)$, $^{**}(p \leq 0.010)$, $^{***}(p \leq 0.005)$. . 89

Figure 5.18 Hurst exponent of microstate sequences averaged across 35 partitions for Baseline and Trial tasks during Training, PracticeA, and PracticeB stages. P-values for TASK and STAGE comparisons are annotated by $^{*}(p \leq 0.050)$, $^{**}(p \leq 0.010)$, $^{***}(p \leq 0.005)$. 91

Figure 5.19 Modeling human beings' and the ideal workload-efficiency relationships at mental capacity $\beta = 1.0$ 101

Figure 5.20 Work efficiency and mental stress curves under varied mental capacity β when $W_T = W_{max} = 15000$. Task completion status is indicated by color: red for successful completion and black for failure. 104
Figure 5.21 Work efficiency and mental stress curves under varied mental capacity β when $W_T = W_{max} = 12500$. Task completion status is indicated by color: red for successful completion and black for failure. 105
Figure 5.22 Work efficiency and mental stress curves under varied mental capacity β when $W_T = W_{max} = 10000$. Task completion status is indicated by color: red for successful completion and black for failure. 105
Figure 5.23 Work efficiency and mental stress curves under varied mental capacity β when $W_T = W_{max} = 7500$. Task completion status is indicated by color: red for successful completion and black for failure. 105
Figure 5.24 Work efficiency and mental stress curves under varied mental capacity β when $W_T = W_{max} = 5000$. Task completion status is indicated by color: red for successful completion and black for failure. 106

Figure 5.25 Work efficiency and mental stress curves under varied mental capacity β when $W_T = W_{max} = 2500$. Task completion status is indicated by color: red for successful completion and black for failure. 106

Figure 5.26 Comparison between human beings' and the ideal workload-efficiency relationships for varying mental capacity at $\beta = 0.7, 1.0, 1.3$ 108

Figure 5.27 Comparison of human beings' and the ideal workload-efficiency relationships under maximum efficiency $\epsilon_{max} = 130$ and $\epsilon_{max} = 70$ 112

Figure 5.28 Human beings' **Capacity zone** and the state changing trends in different zones represented in workload-efficiency relationship at $\beta = 0.7$ 117

Figure 5.29 EEG theta band power for Spatial and Verbal N-back tasks with N equals to 1, 2, and 3. P-values for VERSION and DIFFICULTY comparisons are annotated by $^{*}(p \leq 0.050)$, $^{**}(p \leq 0.010)$, $^{***}(p \leq 0.005)$. 126

Figure 5.30 EEG alpha band power for Spatial and Verbal N-back tasks with N equals to 1, 2, and 3. P-values for VERSION and DIFFICULTY comparisons are annotated by $^{*}(p \leq 0.050)$, $^{**}(p \leq 0.010)$, $^{***}(p \leq 0.005)$. 127

Figure 5.31 EEG low Beta band power for Spatial and Verbal N-back tasks with N equals to 1, 2, and 3. P-values for VERSION and DIFFICULTY comparisons are annotated by $^{*}(p \leq 0.050)$, $^{**}(p \leq 0.010)$, $^{***}(p \leq 0.005)$. 128

Figure 5.32 EEG high Beta band power for Spatial and Verbal N-back tasks with N equals to 1, 2, and 3. P-values for VERSION and DIFFICULTY comparisons are annotated by $^{*}(p \leq 0.050)$, $^{**}(p \leq 0.010)$, $^{***}(p \leq 0.005)$. 129

Figure 5.33 EEG Gamma band power for Spatial and Verbal N-back tasks with N equals to 1, 2, and 3. P-values for VERSION and DIFFICULTY comparisons are annotated by $^{*}(p \leq 0.050)$, $^{**}(p \leq 0.010)$, $^{***}(p \leq 0.005)$. 130

Figure 5.34 Engagement index (EI) for Spatial and Verbal N-back tasks with N equals to 1, 2, and 3. P-values for VERSION and DIFFICULTY comparisons are annotated by $^{*}(p \leq 0.050)$, $^{**}(p \leq 0.010)$, $^{***}(p \leq 0.005)$. 131

Figure 5.35 Sample entropy for Spatial and Verbal N-back tasks with N equals to 1, 2, and 3. P-values for VERSION and DIFFICULTY comparisons are annotated by $^{*}(p \leq 0.050)$, $^{**}(p \leq 0.010)$, $^{***}(p \leq 0.005)$. 132

Figure 5.36 Permutation entropy for Spatial and Verbal N-back tasks with N equals to 1, 2, and 3. P-values for VERSION and DIFFICULTY comparisons are annotated by $^{*}(p \leq 0.050)$, $^{**}(p \leq 0.010)$, $^{***}(p \leq 0.005)$. 133

Figure 5.37 EEG microstate coverage for Spatial and Verbal N-back tasks with N equals to 1, 2, and 3. P-values for VERSION and DIFFICULTY comparisons are annotated by $^{*}(p \leq 0.050)$, $^{**}(p \leq 0.010)$, $^{***}(p \leq 0.005)$. 134

Figure 5.38 EEG microstate occurrence for Spatial and Verbal N-back tasks with N equals to 1, 2, and 3. P-values for VERSION and DIFFICULTY comparisons are annotated by $^{*}(p \leq 0.050)$, $^{**}(p \leq 0.010)$, $^{***}(p \leq 0.005)$. 135

Figure 5.39 EEG microstate duration for Spatial and Verbal N-back tasks with N equals to 1, 2, and 3. P-values for VERSION and DIFFICULTY comparisons are annotated by $^{*}(p \leq 0.050)$, $^{**}(p \leq 0.010)$, $^{***}(p \leq 0.005)$. 136

Figure 5.40 Entropy rate of microstate sequences for Spatial and Verbal N-back tasks with N equals to 1, 2, and 3. P-values for VERSION and DIFFICULTY comparisons are annotated by $^{*}(p \leq 0.050)$, $^{**}(p \leq 0.010)$, $^{***}(p \leq 0.005)$. 137

Figure 5.41 Hurst exponent of microstate sequences averaged across 35 partitions for Spatial and Verbal N-back tasks with N equals to 1, 2, and 3. P-values for VERSION and DIFFICULTY comparisons are annotated by $^{*}(p \leq 0.050)$, $^{**}(p \leq 0.010)$, $^{***}(p \leq 0.005)$. 138

List of Tables

Table 2.1 Mapping between EEG features and cognitive findings 24
Table 2.2 Classification methods in recognizing cognitive and affective states from EEG 25
Table 3.1 Dominant information collection strategy identification and segments 35
Table 4.1 Mapping between EEG features and affective findings 56
Table 5.1 Averaged results for each performance evaluation dimension under Baseline and Trial tasks. 75
Table 5.2 P-values for paired TASK and STAGE comparisons on each performance evaluation dimension. 77
Table 5.3 P-values for paired TASK and STAGE comparisons in theta band power. 79
Table 5.4 P-values for paired TASK and STAGE comparisons in alpha band power. 79
Table 5.5 P-values of paired TASK and STAGE comparisons on EEG microstate coverage. 84

Table 5.6 P-values of paired TASK and STAGE comparisons on EEG microstate occurrence. 86
Table 5.7 P-values of paired TASK and STAGE comparisons on EEG microstate duration. 88
Table 5.8 P-values for paired TASK and STAGE comparisons in entropy rate. 90
Table 5.9 P-values for paired TASK and STAGE comparisons in Hurst exponent. 90

Chapter 1

Introduction

Agreements have been achieved upon the importance of recognizing and understanding the changes in human factors such as emotion, fatigue, stress, and mental workload to achieve a good system productivity, system safety, and team performance as far as there is human involvement (Borghini, Astolfi, Vecchiato, Mattia, & Babiloni, 2014; Jaimes & Sebe, 2007; Love, Edwards, & Irani, 2010; Reddy, Thota, & Dharun, 2018; Reeves & Nass, 1996). Changes in any human factor will lead to variations in human beings' performance, which may result in unexpected decreases in the quality and quantity of the whole system if appropriate adaptation is not made. As a result, considerable efforts have been made to quantify human participants' cognitive factors, and to equip computers and machines with the ability to recognize and respond properly to human beings' time-varying cognitive states. Such computers and machines are described as intelligent, smart, adaptive, human-like, or emotional in emerging research areas like adaptive HCI (Bissoli, Lavino-Junior, Sime, Encarnação, & Bastos-Filho, 2019; Spezialetti, Placidi, & Rossi, 2020) and intelligent vehicle control (Horng, Chen, Chang, & Fan, 2004; Kar, Bhagat, & Routray, 2010; Zhang & Zhang, 2006).

What makes the quantification of certain cognitive factors even more difficult when human participants are conducting complex cognitive activities? Complex cognitive activities describe the activities that require multiple cognitive functions, especially high-level cognitive functions like reasoning and creating, to be involved simultaneously. That is, several cognitive functions can be

simultaneously involved in one complex cognitive activity, and one cognitive function may contribute to different complex cognitive activities. Basic cognitive functions never appear in isolation and interact heavily with each other. Design activities, as a typical example of complex cognitive activities, are used here to illustrate the difficulties in investigating the changes and complex relationships between different cognitive functions. Considering the co-evolutionary and recursive nature of a design process (Zeng, 2002, 2004), any changes in the environment will bring changes to the design behaviors, design solutions, as well as the environment as the design process evolves. Consequently, the causal relationships between stimuli and cognitive responses are extremely complex under such circumstances which could also explain the limited findings on the uncontrollable design activities (Abraham, 2013; Dietrich & Kanso, 2010; T. A. Nguyen & Zeng, 2014; Rieuf, Bouchard, Meyrueis, & Omhover, 2017).

Therefore, the investigations presented in this thesis cover theoretical analysis, framework development, experiment design, experimental data analysis to address the challenges in quantifying cognitive factors under complex cognitive activities. EEG-based analysis is applied in this paper as EEG signals are naturally less vulnerable to subjective factors and have less dependency on knowledge and experience compared to protocol analysis which has been widely applied in studying design phenomena. Meanwhile, the differences and difficulties of applying EEG to complex cognitive activities in comparison to most existing EEG studies should be well considered and addressed before conducting further investigations. Despite this, there is limited information in the literature along this line, and no appropriate protocol exists for quantifying cognitive factors from EEG signals under complex cognitive situations. Among the numerous cognitive factors, the present research further narrows the research focus on the quantification of cognitive workload and mental capacity. Mental capacity is considered as the umbrella of multiple cognitive factors as indicated in the stress-effort model (T. A. Nguyen & Zeng, 2012, 2017), where the influencing impact of cognitive workload on mental stress is also identified.

1.1 Research questions

Aiming to apply EEG techniques for the quantification of cognitive workload and mental capacity under complex cognitive activities, four research questions have been synthesized through reviewing the literature.

(1) **What are the complex cognitive activities under discussion and what are their characteristics?**

In this research, we adopted Bloom's taxonomy (L. W. Anderson & Krathwohl, 2001; Bloom, Engelhart, Furst, Hill, & Krathwohl, 1956) that recognized analysing and creating as the highest level of human cognitive states in describing complex cognitive activities. Cognitive activities that are considered complex require the simultaneous use of many cognitive functions, including the aforementioned high-level cognitive functions as well as lower-level cognitive functions according to Bloom's taxonomy, such as remembering, understanding, applying, and analyzing. Design activities are considered as representative examples of complex cognitive activities in this research as design activities require designers to understand the task and then to retrieve, search and digest the relevant and right knowledge for accomplishing the task by using the identified knowledge. Furthermore, learning processes and problem-solving under complex conditions are also examples of complex cognitive processes.

(2) **What makes EEG a suitable tool for monitoring cognitive changes under design and other complex cognitive activities?**

From the literature, EEG appears to be a suitable tool for investigating the temporal changes in human brains without adding unnecessary workload or interference when compared to self-reported measures and most event-related measures. A sound understanding of the complex stimulus-response relationships under complex cognitive activities is crucial to the reliability and quality of cognitive studies. In the context of design, EEG signals are naturally less vulnerable to subjective factors and have less dependency on knowledge and experience than protocol analysis that has been successfully applied in existing design studies.

(3) **Why is the research focus narrowed to cognitive workload and mental capacity instead**

of other cognitive factors?

There are two reasons for focusing the research on cognitive workload and mental capacity. The first reason lies in the importance of those two factors, whereas the other reason is their close relationship with mental effort according to the stress-effort model (T. A. Nguyen & Zeng, 2012). First, cognitive workload has been considered an important part of human mental states that needs to be closely monitored due to its close relationship with performance and other cognitive factors, while mental capacity describes one's overall mental readiness in dealing with the confronted task which could be seen as the umbrella of numerous cognitive factors. Second, the stress-effort model (T. A. Nguyen & Zeng, 2012) proposed by Nguyen and Zeng serves as the foundation of the present research, where cognitive workload and mental capacity are the two key influencing factors of mental stress. A better understanding of how those two factors vary under complex cognitive activities could contribute to further improvements in the overall efficiency of human-human or human-robot systems.

(4) **What are the challenges of conducting EEG-based cognitive studies under complex cognitive activities and how to address them?**

The critical challenge lies in how to find the hidden and complex stimulus-response relationships during complex cognitive activities, which calls for a new experimental paradigm for EEG-based cognitive studies. Taking design as the starting point, the challenges in conducting EEG-based cognitive design studies lie in: 1) design is a complex activity that consists of numerous basic cognitive activities; 2) complex relationships between designer, product, and environment add to the difficulty in experiment design and control; and 3) design process is continuous and unrepeatable.

A task-related EEG framework (tEEG framework) has been proposed to address the challenges, which can be applied to any complex cognitive task, though it was originally proposed for studying design phenomena. The framework focuses on investigating a complex design process by performing task-level analysis of different subtasks or subprocesses, which is enabled by loosely controlled experiments and a series of decompositions. Loosely controlled experiments are proposed to target the uncontrollable part of design activities whereas

additional processing/analysis is requisite to alleviate the dangers of informal "reverse inference" (Poldrack, 2006, 2011). As a result, clustering-based segmentation is proposed as a bridge from loosely controlled experiments to task-level analysis. The task-related framework consists of three main parts: data collection from loosely controlled experiments, clustering-based segmentation of unstructured design protocol, and EEG-based segment analysis.

1.2 Research objectives and contributions

The present research has two objectives for conducting EEG-based analysis to monitor the changes in cognitive workload and mental capacity under complex cognitive activities.

(1) **To quantify cognitive workload and mental capacity from EEG signals when human participants are conducting complex cognitive activities.**

(2) **To apply the quantification results on cognitive workload and mental capacity to improve human participants' mental effort during complex cognitive activities.**

In order to achieve the first objective, it is crucial to have a thorough understanding of the challenges that need to be addressed in EEG-based cognitive studies under complex cognitive activities. A new research framework is needed for applying EEG to investigate complex cognitive activities based on our literature review and a series of analyses on design and EEG techniques. And quantification results regarding cognitive workload and mental capacity in applying our proposed framework to design activities and learning activities are presented in Chapter 5. The second objective focuses on how to improve human participants' mental effort under complex cognitive activities with the quantitative feedback on cognitive workload and mental capacity obtained from EEG-based analysis. Our efforts in achieving the second objective would contribute to filling the gap between most existing EEG-based quantitative studies and their applications in interpreting real-life phenomena.

The first objective is a necessary prerequisite to the second objective, which has been achieved in the present research with a proposed research framework and two experimental applications. On the contrary, the second objective is more a direction of my future research and the current research

only covers the theoretical model and model verification based on simulation results. Further investigations along this direction will continue to test the quantitative model with experimental evidence, which would also add to the meaningfulness of the deliverable from the first objective and inspire applications of the proposed tEEG framework under different domains.

The contributions of the present research lie in the following aspects:

- **A new research framework conducting EEG-based cognitive studies in the context of design as well as other complex cognitive activities**

  We proposed a theoretical framework derived from our past research attempts and a series of theoretical analyses to guide scholars in determining how to use EEG to quantify designers' cognitive and affective states. With the research challenges well addressed, the tEEG framework takes better advantage of the emerging EEG techniques and facilitates further investigation into the uncontrollable parts of design activities. Moreover, it is possible to apply the tEEG framework to other complex cognitive activities, which has already been applied to a skill acquisition process 5.2. In the present research, the proposed tEEG framework has been successfully applied for quantifying trainees' cognitive workload and cognitive control while they learn and practice flight maneuvers, which may also shed light on future applications in different engineering and industrial areas.

- **Applications of the tEEG framework under or beyond the context of design in monitoring human participants' cognitive workload and mental capacity.**

  In the context of design, the tEEG framework has been applied to monitor designers' cognitive workload and cognitive control in a loosely controlled design experiment. We also believe that online application of the proposed tEEG framework could contribute to an adaptive computer aided design (CAD) system where designers can respond adaptively to their cognitive and affective states during a conceptual design process. In addition, the application discussed in 5.1 was the pioneering work in applying EEG microstate analysis to design activities, which noted that loosely controlled experiments proposed in the tEEG framework may be well supported by EEG microstate analysis, which appears to be an effective approach to facilitating ecologically valid neurocognitive studies.

Moreover, the framework can also be applied to a variety of complex cognitive activities other than design, such as monitoring trainees' cognitive workload and mental capacity during a training process (Section 5.2). The quantification results from this beyond design application will contribute to improving the precision and reliability of objective assessment of human participants' cognitive states toward the confronted task. Consequently, the effectiveness and efficiency of the training process could be enhanced by the availability of neurophysiological feedback and reliable objective assessments for skilled performance.

- **The capacity zone is proposed as a quantitative approach to allocate a "good" workload to human participants so that they can meet the deadline with a successful completion of the assigned task.**

  Built upon the stress model (T. A. Nguyen & Zeng, 2012), the proposed capacity zone provides a quantitative representation of the relationship between cognitive workload and mental effort that could be easily adapted for real-life practices. The applications of the proposed approach could improve the overall working efficiency through customizing the workload allocation strategies according to different individuals' capacity zones and providing timely interventions when they are found working beyond their capacity zone. Furthermore, the ongoing exploration on an N-back dataset aims to quantify different individuals' mental capacity and to detect when it reaches its limit, which could complement the theoretical approach with experimental evidence and also contribute to the determination of capacity zone.

1.3 Organization

The remainder of this thesis is organized as follows. Chapter 2 presents a literature review on the key concepts and the state of the art of related methods and techniques. Chapter 3 presents the research objectives that have been formulated based on the pilot studies in extending and applying the stress model. Chapter 4 introduces the research methodology along with a new research framework (tEEG framework). Chapter 5 covers the research findings obtained from a series of theoretical analyses, simulation results, and experimental evidence. Chapter 6 concludes this thesis and discusses my future research directions.

Chapter 2

Literature Review

2.1 Design as a complex cognitive activity

Design, as a basic human activity, is to create a new product to its environment. From this perspective, design activities are a set of interactions among and between designer (D), product (S) and environment (E) (Zeng, 2004). The environment represents all of the objects in this world other than the product itself. A product comes from the environment, serves the environment and changes the environment (Zeng, 2015). From the original design problem, a designer generates tentative solutions; the tentative solutions will not only improve designer's understanding but also help reformulate the design problem; with the new understanding, the designer adjusts the solutions to fit the newly redefined problem; the adjustment, in turn, triggers new problems. The idea of the evolving environment is also reflected in situatedness, "which emphasizes that the agent's view of a world changes depending on what the agent does" (Gero & Kannengiesser, 2004). Such a recursive process continues until the designer decides that a solution is satisfactory. The process described above implies the nature of design thinking, which is co-evolutionary and follows the recursive logic of design (Dong, 2005; Dorst & Cross, 2001; Gero & Kannengiesser, 2004; Hatchuel & Weil, 2009; Maher & Tang, 2003; T. A. Nguyen & Zeng, 2012; Roozenburg, 1993; Zeng & Gu, 1999). Design, which can be seen as a designer's mental effort to create product descriptions (design solution) from an initial design problem, involves looping and jumping among design problem, design knowledge, and design solutions. During such a recursive design process, the environment evolves (Zeng, 2002,

2004; Zeng & Gu, 1999) as illustrated in Figure 2.1. Each state of the evolution is a result of a primary design process cycle including defining problem, searching for knowledge, finding possible solutions, evaluating the solutions, and making decisions (Eekels, 2001; Gero, 1990; T. A. Nguyen & Zeng, 2012). A product will become a part of the environment (E) once it is taken as a design solution.

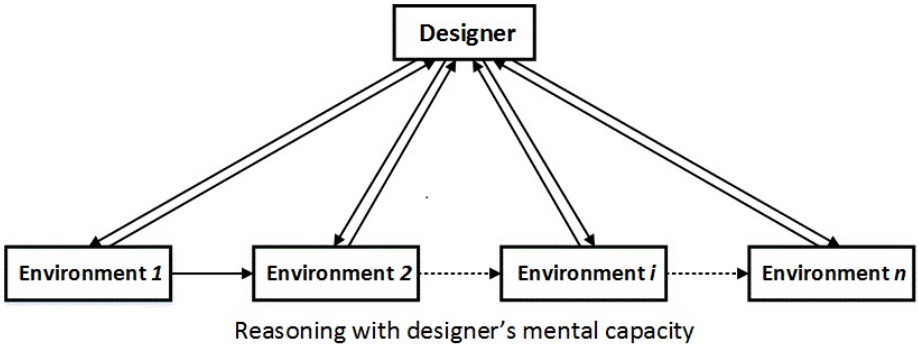

Figure 2.1: Design evolution process

Design activities could be considered as complex cognitive activities given the involvement of multiple complex cognitive functions. A lot of research has been endeavoring to model design as a rational problem-solving process (Simon, 1969), a "reflective conversation with the situation" (Schön, 2017), or a process involving both cognitive and affective components (T. A. Nguyen & Zeng, 2012). Despite the different interpretation and emphasis of each model, agreement has been achieved on the fact that design activities are supported by several cognitive functions such as reasoning and creating. According to Bloom's taxonomy (L. W. Anderson & Krathwohl, 2001), analysing and creating that have been recognized as the highest level of human cognitive states. Along this direction, design activities are good examples of complex cognitive activities that require designers to understand the task and then to retrieve, search and digest the relevant and right knowledge for accomplishing the task by using the identified knowledge (Zhao et al., 2020). In addition, both of the two identified influencing factors of mental stress (T. A. Nguyen & Zeng, 2012), namely knowledge and skills, are closely related to cognitive states like reasoning, memory, synthesis and so forth (Brun, Le Masson, & Weil, 2016; Fagin, Halpern, Moses, & Vardi, 2004; Gick & Holyoak, 1983; Thorndyke, 1977). Further design studies indicated that individual's knowledge could help in the solution generation, whereas the utilization of inappropriate knowledge may cause

design fixations (Crilly, 2015; Jansson & Smith, 1991; Viswanathan, Atilola, Esposito, & Linsey, 2014), which is somehow considered as a disadvantage of cognitive control in (Chrysikou, 2018; Chrysikou & Weisberg, 2005; Thompson-Schill, Ramscar, & Chrysikou, 2009). Existing research studies have reported considerable findings on designer's attention, memory, knowledge, reasoning, and problem solving (Balters & Steinert, 2017; Poldrack, 2011; Sylcott, Cagan, & Tabibnia, 2011), which could contribute to further investigation into the nature and mechanism of the design process. This effort generally falls into the realms of psychology and design. According to Bloom's taxonomy (Bloom et al., 1956), different cognitive aspects involved in a learning process include remembering, understanding, applying, analyzing, evaluating, and creating (Conklin, 2005; Krathwohl, 2002).

Protocol analysis has been widely applied to investigate designers' cognitive changes, which can be understood as a series of means to extract "reliable information about what people are thinking while they work on a task" (J. Austin & Delaney, 1998). Protocol analysis has been widely used by scholars to segment a complex design process into simpler processes (Dorst & Dijkhuis, 1995; Gero & Tang, 2001; Neill, Gero, & Warren, 1998). Verbal protocol analysis has been used as a tool for different objectives. In design domain, it has been used to study the designer's perception. Verbal protocol analysis has been used to compare the architects' perception and students' perception based on their own freehand sketches (Suwa & Tversky, 1997). The authors found that the architects think more deeply than students about the topic. Meanwhile, Suwa et al. used design protocol to code designer's cognitive actions in order to learn human design process (Suwa, Purcell, & Gero, 1998). In educational domain, researchers have used verbal protocol analysis to study human writing and reading process (Afflerbach & Johnston, 1984). However, scholars have challenged the effectiveness of verbal protocol analysis (Russo, Johnson, & Stephens, 1989; Smagorinsky, 1989). One frequently asked question is "do subjects really have the ability to describe the processes they perform?" (Ericsson & Simon, 1980). Concerns have been raised in terms of two different ways of collecting verbal protocol, namely concurrent verbal protocol and retrospective protocol. Chiu and Shu pointed out the limitation of verbal protocols with design experiments in which they mainly concerned about the data validity from several aspects (Chiu & Shu, 2010). For example, the application of concurrent verbal protocol may alter the design process because of changes in design

environment and emergent subtasks. Meanwhile, Gero and Tang compared the concurrent verbal protocol and retrospective verbal protocol in (Gero & Tang, 2001). Moreover, protocol segmentation and coding are usually done manually by domain experts and the results can be influenced by the experts' subjective opinions. The results of protocol analysis can be wrong as "even experts may make errors or are unable to correctly recall all of their behaviors and reasoning steps" (Pfeifer, Rothenfluh, Stolze, & Steiner, 1992). Hence, concerns about verbal protocol analysis can be summarized as follows: 1) it is sensitive to subjective factors; 2) there is no common standard to follow; and 3) such knowledge-based analysis is incomplete in most cases due to the limited knowledge of human beings.

2.2 Cognitive workload under complex cognitive activities

As one of the most discussed human factors, cognitive workload has attracted considerable research attention (Young, Brookhuis, Wickens, & Hancock, 2015), whereas there is no agreed definition of cognitive workload. Instead, researchers have been using different terms like cognitive workload, mental workload, perceived workload, operator workload, or as simple as workload to interchangeably describe the similar concept. Cognitive workload and mental workload emphasize the utilization of brain resources required by the task, which has been widely used in fields like neurocognition (Ghani, Signal, Niazi, & Taylor, 2020; T. A. Nguyen & Zeng, 2012, 2017) and human behavior studies (Wästlund, Norlander, & Archer, 2008; Wiebe, Roberts, & Behrend, 2010). Perceived workload, on the contrary, emphasizes the subjective perception of the task demands (Gabriel, Ramallo, & Cervantes, 2016) and is one of the influencing factors of a stress model (T. A. Nguyen & Zeng, 2012). In addition, HCI researchers use operator workload to describe human operator's workload to distinguish it from the computer related features (Borghetti, Giametta, & Rusnock, 2017; Liu & Nam, 2018; Prewett, Johnson, Saboe, Elliott, & Coovert, 2010). However, operator workload can be the human operator's cognitive workload, mental workload, or perceived workload as all of them represent human beings' workload. In this paper, cognitive workload is used to describe the utilization of brain resources under varied demands based on the confronted task (Baldwin, 2012; Ghani et al., 2020) without distinguishing it from mental workload.

Cognitive workload has been considered as an important part of human mental states that needs to be closely monitored due to its close relationship with performances and other cognitive factors (Dehais et al., 2019; Prewett et al., 2010; Sweller, 2010). High cognitive workload has been reported to be associated with increased human errors(Brown, 2016; Niederée, Jipp, Teegen, & Vollrath, 2012), vigilance decrement(Al-Shargie et al., 2019; Kamzanova, Kustubayeva, & Matthews, 2014), and bad performance(Wickens, 2002; Zahabi et al., 2021). Moreover, despite the positive relationship between increased task demands and cognitive workload, research findings also indicated decreasing cognitive workload under repetitive vigilance tasks (Grier et al., 2003; Helton et al., 2005; Manly, Robertson, Galloway, & Hawkins, 1999; Robertson, Manly, Andrade, Baddeley, & Yiend, 1997) where participants may "withdraw attentional effort over time and approach their assignment in a thoughtless, routinized manner" (Warm, Parasuraman, & Matthews, 2008). Mario et al. found that human beings could better "understand and actively manage their behaviour during tasks" if provided with the feedback of their mental workload, extracted from functional Near Infra-Red Spectroscopy (fNIRS) data (Maior, Wilson, & Sharples, 2018). Moreover, an adaptive workload allocation framework was proposed in a recent research for multi-human multi-robot (MH-MR) systems based on robots' performance conditions and human beings' stress conditions (Mina, Kannan, Jo, & Min, 2020). The framework could reduce the workload for "robots with deteriorated human and/or robot condition" and to allocate the surplus workload to "robots with better human and/or robot condition" (Mina et al., 2020). Researchers have reported a positive correlation between cognitive workload and task demands (Jia & Zeng, 2021; Shaw et al., 2019; Wickens, 2008). Referring to the stress model (T. A. Nguyen & Zeng, 2012), increases in cognitive workload may lead to increased mental stress which could then be reflected in variations in performance and vice versa.

Cognitive workload could be measured through subjective methods or objective methods (Charles & Nixon, 2019; Heard, Harriott, & Adams, 2018). Subjective measurements use questionnaires (i.e. NASA Task Load Index (NASA-TLX) (Hart & Staveland, 1988)) to collect human participants' feelings and self-ratings on the given tasks. On the contrary, objective measurements use performance and physiological signals (see (Charles & Nixon, 2019) for a comprehensive review) such as Electroencephalogram (EEG) and Electrocardiogam (ECG). One of the most extensively applied

EEG indices for cognitive workload is alpha power (Fink, Grabner, Neuper, & Neubauer, 2005), which has been reported to decrease with increasing cognitive workload (Gevins & Smith, 2003; Kamzanova et al., 2014; Keil, Mussweiler, & Epstude, 2006; Stipacek, Grabner, Neuper, Fink, & Neubauer, 2003). Researchers have also identified the brain areas associated with significant alpha decreases include the fronto-central and parietal regions (Fairclough, Venables, & Tattersall, 2005; Slobounov, Fukada, Simon, Rearick, & Ray, 2000). Moreover, numerous EEG studies have observed increases in frontal midline theta power under increasing cognitive workload (Jensen & Tesche, 2002; Klimesch, 1999; Pavlov & Kotchoubey, 2017; Raghavachari et al., 2001). Moreover, there are a few EEG indicator derived from the spectral power that have been reported to be related to variations in cognitive workload, such as the ERS/ERD, task load index (TLI), and engagement index (EI). TLI is defined as the ratior between frontal midline theta and parietal alpha (Kamzanova et al., 2014), event related synchronization (ERS) represents the cortical activation (Pfurtscheller, 1992), whereas event related desynchronization (ERD) represents inhibitory activities (Pfurtscheller, 1977).

2.3 Mental capacity under complex cognitive activities

Mental capacity describes the general intelligence which was once described as a metaphorical form of common mental energy underlying all cognitive processes by Spearman (Spearman, 1961). Besides mental capacity, researchers have also used varied terms, such as cognitive ability, cognitive capability, and mental capability, to distinguish such general intelligence from any specific cognitive function. Along the same line, mental capacity could be considered as the highest order factor in cognitive ability hierarchy (Johnson, Bouchard Jr, Krueger, McGue, & Gottesman, 2004; Johnson, te Nijenhuis, & Bouchard Jr, 2008; Lubinski, 2004), which involves the ability to "reason, plan, solve problems, think abstractly, comprehend complex ideas, learn quickly and learn from experience" (Gottfredson, 1997). Moreover, mental capacity was described as one's overall mental readiness in dealing with the confronted task in the stress model (T. A. Nguyen & Zeng, 2012), involving knowledge, skills, and affect. Along this direction, the present paper considers mental capacity as the umbrella of numerous cognitive factors other than cognitive workload and

mental stress, which is negatively associated with mental stress as illustrated in the stress model (T. A. Nguyen & Zeng, 2012).

Mental capacity has been related to varied types of performance in the literature with evidences from different domains (Kulikowski, 2021). For example, employees' mental capacity was considered as a predictor of their job performance (Ree, Earles, & Teachout, 1994; Salgado et al., 2003; F. L. Schmidt & Hunter, 2004). In addition, researchers have also observed positive correlations between mental capacity and academic performance (Kuncel, Hezlett, & Ones, 2004), socioeconomic success (Strenze, 2007), leadership (Judge, Colbert, & Ilies, 2004), as well as success in military settings (Duckworth et al., 2019). However, there is only a limited number of research that directly focused on the limit of mental capacity where burnout was sometimes considered as the sign of excess mental capacity (Kulikowski, 2021). Instead, considerable research efforts have been made to investigate certain cognitive functions (Bonnefond & Jensen, 2015; Borghini et al., 2014; Donoso, Collins, & Koechlin, 2014; Hanslmayr et al., 2007), which could contribute to a better understanding of mental capacity according to the aforementioned definition of mental capacity and the stress model (T. A. Nguyen & Zeng, 2012).

Among the varied cognitive functions, working memory capacity have attracted most research attention. Working memory capacity (WMC) describes the limited capacity of a person's working memory, which could stay relatively stable across different cognitive activities but differs from one individual to another (Kane & Engle, 2003). High working memory capacity (WMC) has been related to better performance at processing task-relevant information while being less distracted by task-irrelevant information (Kane, Bleckley, Conway, & Engle, 2001; Kane & Engle, 2003). Furthermore, recent studies have related WMC to specific factors of executive control, including inhibition, shifting, and updating (Miyake et al., 2000). Empirical evidences indicated positive correlations between WMC and each of the two factors of of executive control, namely inhibition and shifting (Keye, Wilhelm, Oberauer, & Van Ravenzwaaij, 2009; Oberauer, Süß, Wilhelm, & Sander, 2007; Oberauer, Süß, Wilhelm, & Wittman, 2003; Unsworth, Brewer, & Spillers, 2009). However, the relationship between WMC and the updating factor seems to be more complex due the difficulty in isolating WMC and updating during working memory updating tasks (Miyake et al., 2000; Wilhelm, Hildebrandt, & Oberauer, 2013). The commonly applied working memory updating

tasks include the n-back tasks, the running-memory task, and the memory-updating task, which are considered as good measures of WMC that "involve rapid updating of temporary bindings" (Wilhelm et al., 2013).

In addition, cognitive control also belongs to one's mental capacity which plays an important role in supporting the high cognitive functions involved in complex cognitive activities. Cognitive control describes the ability to coordinate mental resources to goal-directed performance while suppressing goal-irrelevant distractions (Hasher, Zacks, & May, 1999; Koechlin, Ody, & Kouneiher, 2003). However, cognitive control has not been as well investigated as cognitive workload in the literature. The study of Roberts and colleagues (Roberts, Anderson, & Husain, 2010) reported the associated differences in frontal and parietal white matter under different cognitive control levels that were measured by two behavioral paradigms, namely Eriksen Flanker (Eriksen & Eriksen, 1974) and change of plan tasks (Nachev, Rees, Parton, Kennard, & Husain, 2005). In the study (Borghini et al., 2017) (Borghini et al., 2017), EEG spectral features were analyzed in responding to different cognitive control levels that were represented by the difficulty levels of three kinds of events, namely Skill, Rule, and Knowledge based the SRK model proposed by Rasmussen (Rasmussen, 1983). In general, those studies either used behavioral performance for cognitive control assessment (Lopez, Previc, Fischer, Heitz, & Engle, 2012; Roberts et al., 2010) or treated cognitive control as an independent variable (Borghini et al., 2017; Krall, Menzies, & Davies, 2016). However, the former measured cognitive control in an indirect way which could lead to a reduced reliability, while the latter may interfere with the original tasks with the inserted events.

2.4 Failure to meet the deadline as a consequence of the mismatch between cognitive workload and mental capacity

Failing to meet the deadline could lead to direct and indirect damages not only to the involved individuals themselves, but also to the entire project, team, or system (Chetto & Chetto, 1989; Richardson, Sieh, & Elkateeb, 2001). Examples of direct and immediate personal consequences of failing to meet the deadline include blame from the director, salary reduction, and loss of job. Austin described such concern as *concern for career* that the individuals may worry about giving a

bad impression in the eyes of directors confessing that "he is behind schedule and his fellow agent does not" in his agency model (R. D. Austin, 2001). In addition, failure in meeting the deadline could lead to more severe consequences like entire system failure, costly damage to the employing company, and even some catastrophic consequences (G. C. Buttazzo & Sensini, 1999; Richardson et al., 2001; Stavrinides & Karatza, 2018). The failure of completing a certain task within the time limit may result in damage to the equipment as well as danger to the health and life of human operators in many real-life systems (Chetto & Chetto, 1989). Consider the situation when the patient and the emergency physician are waiting for the results from lab tests, where any delay may lead to further damage to the patient's health and life. Stress-related failures could be considered as part of the consequences of missing the deadline, which are particularly emphasized under high-risk environments, of which a typical example is aviation where the stress-related failures of decision making attributed to nearly half of fatal aviation accidents (McClernon, McCauley, O'Connor, & Warm, 2011; Wiegmann & Shappell, 1997). Meanwhile, gender differences in coping with time pressure have been considered as one of the important factors (Gneezy, Niederle, & Rustichini, 2003; Niederle & Vesterlund, 2007; Shurchkov, 2012) that make "women, even if as educated as men, continue to be heavily under-represented in many professions involving risky and high-pressure activities" (De Paola & Gioia, 2016). For those reasons, talking about the experience of struggling to complete a given task before the deadline could be difficult for some people as it reminds them of some unpleasant memories.

The key cause for the failures in meeting the deadline lies in the mismatch between workload and the individual's mental capacity, where mental stress plays a crucial role. Researchers have related increased stress, sometimes denoted as time pressure, to the situations when the individuals realize that they cannot complete the tasks before the deadline (R. D. Austin, 2001; Margheim, Kelley, Pattison, et al., 2005; Miletić & van Maanen, 2019). When required to complete a lot of work within a short period of time, human participants may feel stressed out from the beginning and end up with a failure. Increased physiological stress, as the reason behind the changes in individual's behaviours toward the confronted task under time pressure, was shown in the literature to increase risk taking (Buckert, Schwieren, Kudielka, & Fiebach, 2014; Putman, Antypa, Crysovergi, & van der Does, 2010; Starcke, Wolf, Markowitsch, & Brand, 2008) and inhibits strategic thinking

(Leder, Häusser, & Mojzisch, 2013). Researchers have observed a reduced decision quality as a result of time constrain in a decision-making process (Ahituv, Igbaria, & Sella, 1998; Sutter, Kocher, & Strauß, 2003), which could result in bad performance, burnout, and even some mental health problems like procrastination and depression (Hinds, Roberts, & Jones, 2004; Malone, 2018; Vesin, Mangaroska, & Giannakos, 2018; Whittaker, 2005; Yuksel et al., 2016). For example, the results on an experimental beauty-contest game showed a decrease in the quality of decision-making was observed as a result of time constrain (Kocher & Sutter, 2006). However, it is not an expected situation for companies and employers when their employees were given a very long time to complete a small amount of workload, which would lead to damage to the overall productivity and profit no matter they succeed or not at their tasks. In addition, we have also observed the cases where human participants were given a very long time limit to complete a small amount of workload but they still fail to accomplish the task. Under such circumstances, they may feel bored, make mistakes (Ryu & Myung, 2005), and merely do anything for a long time as meeting the deadline seems too easy for them until the moment when they realize the deadline is just ahead but the work hasn't been completed. Such phenomenon could be explained from the motivation point of view that the employees or learners will tend to cope cognitively and allocate less effort when given too little workload because they may "feel that the situation is negative and stable" (LePine, LePine, & Jackson, 2004). Although the mismatch between cognitive workload and mental capacity may not always reflect a lack of personal capability, it should be avoided with any possible effort.

Existing approaches to address the mismatch between cognitive workload and mental capacity can be categorized into the following directions, namely developing optimal workload allocation (Chen, Sekiyama, Cannella, & Fukuda, 2013; Parasuraman, Barnes, Cosenzo, & Mulgund, 2007), developing adaptive scheduling strategies (G. Buttazzo & Abeni, 2002; G. C. Buttazzo & Sensini, 1999; Vanheusden, Van Gils, Caris, Ramaekers, & Braekers, 2020), cognitive skills training (Anton, Bean, Hammonds, & Stefanidis, 2017; Radüntz, 2020), and optimizing stress management strategies (McClernon et al., 2011; Meichenbaum, 1985). The aforementioned approaches either aimed to adjust cognitive workload through optimal workload allocation and adaptive scheduling strategies, or to improve mental capacity through cognitive skill straining and stress management improvement. Considering the complexity in quantifying mental capacity, adjusting the workload

allocation based on each individual's mental capacity seems to be a promising and more direct way to help people in meeting a predefined deadline. Different from the existing research on workload allocation among several machines or computers (G. Buttazzo & Abeni, 2002; Verma, Cherkasova, Kumar, & Campbell, 2012; Y. Wang, Wu, Yuan, Liu, & Li, 2019), this research focuses on assigning varied amount of workload among different human participants. An optimal workload allocation was proposed for a multi-human multi-robot system (Malvankar-Mehta & Mehta, 2015), where human participants' performance and current cognitive workload were considered for workload allocation but individual difference in workload thresholds was not included. Similarly, a workplace design and task allocation system was presented in (Tsarouchi et al., 2017) based on multiple criteria defined upon user's requirements where both human and robot resources were modelled in a unified approach. Moreover, an adaptive workload allocation framework was proposed in a recent research for multi-human multi-robot (MH-MR) systems based on robots' performance conditions and human beings' stress conditions (Mina et al., 2020). The framework could reduce the workload for "robots with deteriorated human and/or robot condition" and to allocate the surplus workload to "robots with better human and/or robot condition" (Mina et al., 2020). However, there is limited information about what is or how to distinguish "good" workload from "bad" workload that could serve as the criteria for adaptive workload allocation.

2.5 Applying EEG techniques to complex cognitive activities

EEG, abbreviation for electroencephalogram, is the record of the fluctuation of brain waves generated by the neurons circuit. EEG signals directly measure "the dynamic, synchronous polarization of spatially aligned neurons in extended gray matter networks, with postsynaptic excitatory or inhibitory potentials being the main sources of the signal" (Michel & Koenig, 2018). The signals measured in voltage can be seen as a result of "the process of current flow through the tissues between the electrical generator and the recording electrode, which is called volume conduction" (Olejniczak, 2006). The two most important effects of volume conduction imply that: 1) an electrode at a given scalp location detects neuronal activity in simultaneously activated areas that far or near the electrode; 2) a single source activity affects simultaneously all scalp electrodes leading to

high correlation among multichannel EEG signals. This implication gives rise to an inverse problem in the EEG source localization that localizes the electrical activity in the brain according to EEG topographies. The inverse problem is that an EEG topography can be explained by different distributions of neuronal generators. However, the differences in EEG topographies might result from different distributions of activated neuronal generators.

As for the collection of EEG signals, EEG data can be collected through electrodes distributed on the scalp and the scalp EEG is an important tool for clinical usage (Niedermeyer and Lopes da Silva, 2005). The human cerebral cortex, i.e. the outermost layer of the brain, is divided into four lobes: frontal lobe, temporal lobe, occipital lobe, and parietal lobe. Parietal lobe and frontal lobe are separated by the central sulcus. EEG signals are recorded by electrodes which are positioned at specific locations following international standards such as 10/20, 10/10 and 10/5 placement systems (Chatrian, Lettich, & Nelson, 1985; Jasper, 1958; Oostenveld & Praamstra, 2001). EEG is collected at sampling rate between 250 Hz and 500 Hz, even up to several kHz by the nowadays human EEG recording system (Weiergräber, Papazoglou, Broich, & Müller, 2016). Due to its high temporal resolution, time-based and frequency-based EEG features have been applied to detect mental and functional abnormalities, as well as cognitive and affective states under external or internal stimuli (Acharya, Sree, Swapna, Martis, & Suri, 2013; Pidgeon et al., 2016). The time-based EEG features reflect the scalp potential of neuronal generators at a given moment in time. This information provides a possibility to study the temporal dynamics of whole-brain neuronal networks. The frequency-based EEG features reflect the rhythmic oscillations of neuronal generators in specific frequency bands. This information offers a possibility to investigate the characteristics of brain waves.

The collected EEG data imply information of the participants' cognitive and affective states as EEG signals relate regional brain activities to different cognitive and affective states (Delplanque, Silvert, Hot, Rigoulot, & Sequeira, 2006). Some EEG research was conducted based on the assumption that the frontal area plays an important role in the reflection of the valence level (Harmon-Jones & Allen, 1998; L. A. Schmidt & Trainor, 2001). The human parietal lobe was believed to be closely related to human perception, decision making and speech comprehension (Bisley & Goldberg, 2010). The occipital lobe is known to process visual information, which is related to object

detection and recognition (Dijkerman & De Haan, 2007; Malach et al., 1995). Studies also indicated that the two hemispheres of a brain are specialized for different tasks (Rhodes, 1985; Sergent & Bindra, 1981). "The right hemisphere mediates tasks requiring global, holistic processing such as facial effect recognition" whereas the left hemisphere is specified for detailed analysis (Holt et al., 2006). Nie et al. concluded from their experimental analysis that the EEG features related to emotional states "are mainly on the right occipital lobe and parietal lobe in alpha band, central site in beta band, left frontal lobe and right temporal lobe in gamma band" (Nie, Wang, Shi, & Lu, 2011). As a result, there are researchers trying to look at what's happening inside designer's brain during the design process.

Different methods have been applied to segment EEG data in time, frequency and time-frequency domains. In time-frequency domain, non-stationary EEG signals are broken down into pseudo-stationary segments during which statistical properties do not vary with time. Firstly, EEG signals need to be transformed from the time domain to time-frequency domain. Short-term fast Fourier transform (STFT) and wavelet transform (WT) are widely used to transform signals from the time to time-frequency domain. Secondly, several EEG features can be extracted in frequency domain, such as power, nonlinear energy operator (NEO) (Agarwal & Gotman, 1999) and generalized likelihood ratio (GLR) (Appel & Brandt, 1983). Thirdly, segmentation boundaries can be detected by comparing differences in EEG features between reference and sliding test window. If the sliding test window passes over a segment boundary, the differences would increase significantly leading to greater than a predefined threshold. If the sliding test window passes within a segment boundary, the sliding test and reference window would continually move based on different strategies (Wong & Abdulla, 2006). Alternatively, segmentation boundaries can be detected by clustering EEG features in overlap reference windows (Barlow, Creutzfeldt, Michael, Houchin, & Epelbaum, 1981; P. Nguyen, Nguyen, & Zeng, 2019).

In time domain, microstate analysis is used to identify successive short time periods during which the distribution of the scalp potential filed remains semi-stable. The changes of distribution of the scalp potential filed imply different activation of global network activity in the brain. Pascual-Marqui and his colleagues proposed a clustering-based method to identify the most dominant spatial components in the EEG topography series (Pascual-Marqui, Michel, & Lehmann, 1995). This

method was based on the k-means approach that clusters the scalp potential filed topographies into representative cluster centroids in terms of spatial correlations. The optimal number of cluster centroids is determined by cross-validation criterion (CV), which optimally explains the variance in each cluster. Murray and colleagues proposed an Atomize and Agglomerate Hierarchical Clustering (AAHC) to identify representative cluster centroids in a bottom-up manner (Murray, Brunet, & Michel, 2008). In contrast with the k-means approach that its results vary across runs due to a random selection of data points as seed clusters, the AAHC is a deterministic approach that its results are independent with the repetition of runs. Alternatively, other methods in factor analysis were applied to determine representative cluster centroids, including principal component analysis (PCA) (Pourtois, Delplanque, Michel, & Vuilleumier, 2008) and independent component analysis (ICA) (Makeig, Debener, Onton, & Delorme, 2004).

Once the EEG data are segmented, different features could extracted for further analysis varying from time domain to (time-) frequency domain, from scalar to matrix (like microstate). Scholars usually extract one or several features in order to recognize certain cognitive states or to compare the performance of different features regarding a specific research problem. The commonly applied EEG features and their corresponding cognitive findings are listed in Table 2.1 according to my literature review. Based on the extracted features, classification and other analysis algorithms could be applied to recognize cognitive factors, such as Support Vector Machine (SVM), K-Nearest Neighbours algorithm (K-NN), Linear Discriminant Analysis (LDA), as well as their derived algorithms and other analysis algorithms (Altman, 1992; Cortes & Vapnik, 1995). Numerous analysis methods have been applied to recognize cognitive and affective states from features in time domain, frequency domain, and time-frequency domain as summarized in Table 2.2.

Furthermore, physiological measures (such as EEG, fNIRS, ECG) have been applied to study pilots' cognitive changes, among which EEG has attracted the most research interest (Borghini et al., 2017; Causse, Chua, & Rémy, 2019; Jaquess et al., 2018). EEG is a suitable tool for investigating the temporal changes in trainees' brains without affecting the original process with additional workload or interference, leading to considerable research efforts along this direction. For example, research findings related alpha desynchronization to the demands on attentional resources (Başar, Başar-Eroglu, Karakaş, & Schürmann, 2001; Klimesch, 1999). Researchers observed the

decreases in alpha power with increasing cognitive workload (Gevins & Smith, 2003; Kamzanova et al., 2014; Stipacek et al., 2003) and identified the brain areas with significant alpha decreases such as such as the fronto-central and the parietal regions (Fairclough et al., 2005; Slobounov et al., 2000). Meanwhile, theta oscillations may support working memory (Jensen & Lisman, 1998; Raghavachari et al., 2001; Roux & Uhlhaas, 2014; Tesche & Karhu, 2000), cognitive control (Cavanagh & Frank, 2014), and rhythmic shifts of spatial attention (Fiebelkorn & Kastner, 2019) as reviewed by (Herweg, Solomon, & Kahana, 2020). Increases in EEG theta power were reported to be positively related to successful information encoding and memory retrieval during memory tasks (Addante, Watrous, Yonelinas, Ekstrom, & Ranganath, 2011; Guderian & Düzel, 2005; Staudigl & Hanslmayr, 2013). Research findings also related increases in theta activity to increased top-down control for attention allocation and information processing (Bosseler et al., 2013; Nyhus & Curran, 2010), but also identified the activation of certain brain areas that were involved during tasks requiring cognitive control, among which the active involvement of medial prefrontal cortex (mPFC) was highlighted (Veen & Carter, 2006). In particular, increases in the frontal midline theta was observed under under tasks with higher demands on cognitive control (Cavanagh, Cohen, & Allen, 2009; M. X. Cohen, Ridderinkhof, Haupt, Elger, & Fell, 2008; Eisma, Rawls, Long, Mach, & Lamm, 2021).

EEG-based analysis is therefore introduced to design studies EEG signals are naturally less vulnerable to subjective factors and have less dependency on knowledge and experience compared to protocol analysis. Research efforts have been made to investigate designers' cognitive changes using EEG techniques two decades (Göker, 1997; W.-L. Hu, Booth, & Reid, 2015; Liu & Nam, 2018; T. A. Nguyen & Zeng, 2010, 2014; Vieira et al., 2019). The results presented in (Göker, 1997) indicate that the activated brain areas are different for novices and experts during design problem solving. A preliminary study was conducted by (T. A. Nguyen & Zeng, 2010) which uses EEG to identify the regularities underlying a design process. The EEG results in (Hinterberger, Zlabinger, & Blaser, 2014) show the neurophysiological discriminability of three mental locations (intrapersonal, extrapersonal, perspective taking) and two attentional foci (self, object). A physiological study (T. A. Nguyen & Zeng, 2014) is conducted to investigate the relationship between designer's mental effort (cognitive aspect) and mental stress. Hu et al. provided psychophysiological evidence

for the role of warm-ups activities reducing inhibition during concept generation based on their analysis of EEG and galvanic skin response (GSR) (W.-L. Hu et al., 2015). In (Liang et al., 2017), EEG signals were analyzed to investigate the difference between expert designers' visual attention and association processes. By comparing the time-related neural responses, the EEG results show differences of the mechanical engineers' neurocognition in designing and problem-solving (Vieira et al., 2019). The use of EEG and other biometric measures in experimental design research were reviewed and discussed in (Borgianni & Maccioni, 2020).

Table 2.1: Mapping between EEG features and cognitive findings

EEG features		Cognitive findings	Research and authors
Frequency domain	Power spectral density (PSD)	Attention	(Almahasneh *et al.*, 2014)
		Cognitive workload	(Wang *et al.*, 2016), (Wang & Sourina, 2013)
		Reasoning and problem solving	(Amin *et al.*, 2014)
		Semantic memory recall	(Hanouneh *et al.*, 2016)
		Vigilance	(Shi *et al.*, 2013)
		Perception	(Kroupi *et al.*, 2014)
	Higher order crossings (HOC)	Cognitive load	(Jadhav *et al.*, 2016)
	Band power (theta, alpha, etc.)	Cognitive workload	(Wang & Sourina, 2013), (Wang *et al.*, 2016), (Blanco *et al.*, 2017)
		Creative thinking	(Fink *et al.*, 2009)
		Intelligence	(Jaarsveld *et al.*, 2015)
Time domain	ERP waveform (N2, P300, P3b, etc.)	Perception delay	(Chakraborty *et al.*, 2013)
		Sustained attention	(Gu *et al.*, 2016)
		Deductive reasoning	(Bonnefond *et al.*, 2014)
	Microstate	Transcendental meditation	(Faber *et al.*, 2017)
		Perceived task difficulty	(Nguyen *et al.*, 2015)
	Fractal distance (FD)	Cognitive workload	(Sharma & Gomes, 2015), (Wang & Sourina, 2013)
		Concentration	(Wang *et al.*, 2011)
		Meditation	(Harne, 2014)
		Vigilance	(Shi *et al.*, 2013)
	Entropy	Vigilance	(Shi *et al.*, 2013)
		Attention	(Thomas & Vinod, 2016)
	Amplitude based statistical features	Cognitive workload	(Wang *et al.*, 2016)
Time-frequency domain	Wavelet entropy	Cognitive workload	(Wang *et al.*, 2016), (Wang & Sourina, 2013)

Table 2.2: Classification methods in recognizing cognitive and affective states from EEG

Methods	Features	Affective work	Cognitive work
Support Vector Machine (SVM)	Time domain, frequency domain, time-frequency domain	(Blanco *et al.*, 2017), (Bono *et al.*, 2016), (Brown, Grundlehner, & Penders, 2011), (Duan, Zhu, & Lu, 2013), (Frantzidis *et al.*, 2010), (Liu, Sourina, & Nguyen, 2010), (Petrantonakis & Hadjileontiadis, 2010), (Yohanes *et al.*, 2012), (Singh, Singh, & Sandel, 2014), (Wang, Nie, & Lu, 2014), (Rozgić, Vitaladevuni, & Prasad, 2013), (Al-shargie *et al.*, 2016)	(Sharma & Gomes, 2015), (Shi, Jiao, & Lu, 2013), (Wang & Sourina, 2013), (Wang, Gwizdka, & Chaovalitwongse, 2016)
K Nearest Neighbors (KNN)	Frequency domain, time-frequency domain	(Blanco *et al.*, 2017), (Brown *et al.*, 2011), (Duan *et al.*, 2013), (Hadjidimitriou, Charisis, & Hadjileontiadis, 2015), (Khosrowabadi *et al.*, 2010), (Murugappan *et al.*, 2010), (Petrantonakis & Hadjileontiadis, 2010)	(Jadhav, Manthalkar, & Joshi, 2016), (Sharma & Gomes, 2015)
Linear discriminant analysis (LDA)	Time domain, time-frequency domain	(Blanco *et al.*, 2017), (Bono *et al.*, 2016), (Faber *et al.*, 2017), (Murugappan *et al.*, 2010)	
Multilayer perceptron (MLP)	Frequency domain, time-frequency domain	(Liu *et al.*, 2010)	
Naive Bayes nearest neighbour	Frequency domain	(Blanco *et al.*, 2017), (Rozgić *et al.*, 2013)	
Fuzzy c-Means, Fuzzy k-Means	Time domain, time-frequency domain	(Murugappan *et al.*, 2007)	(Chakraborty *et al.*, 2013), (Sharma & Gomes, 2015)
Correlation analysis	Time domain, frequency domain	(Kroupi, Yazdani, & Ebrahimi, 2011), (Nielsen & Chénier, 1999), (Reuderink, Mühl, & Poel, 2013)	(Hanouneh *et al.*, 2016)
Microstate analysis	Time domain		(Nguyen, Nguyen, & Zeng, 2015), (Faber *et al.*, 2017), (Nguyen, Nguyen, & Zeng, 2019)
Quadratic discriminant analysis (QDA)	Frequency domain,	(Brown *et al.*, 2011), (Petrantonakis & Hadjileontiadis, 2010)	

Chapter 3

Pilot Study: Formulation of Research Objectives

Starting from the stress-effort model (T. A. Nguyen & Zeng, 2012), the influencing effect of cognitive workload and mental capacity on mental effort has been identified and presented quantitatively based on a series of theoretical analyses in this research. Borrowed the concept of stress from the strength of materials, Nguyen and Zeng proposed a stress-effort model for the investigation on how creativity occurs in design phenomena (T. A. Nguyen & Zeng, 2012). This model took the axiomatic theory of design modeling (ATDM) (Zeng, 2002) as its formal tool and two postulates as its first principles. This model has already been applied to conduct in-depth investigations into a few typical phenomena within and beyond the context of design, such as sketching (T. A. Nguyen & Zeng, 2012), impact of human emotions in engineering (Zhao et al., 2018), and information collection in design (Zhao & Zeng, 2019).

3.1 The stress-effort model for design creativity

The stress-effort model was developed to address the research question how creativity occurs in design phenomena (T. A. Nguyen & Zeng, 2012). In this model, four factors were identified affecting designers' mental effort and the occurrence of creativity during the design process, namely perceived workload, knowledge, skills, and affect. The authors first analyzed designers' activities

and their characteristics within a design process, where the recursive nature of design process was highlighted. A design problem could be seen as an initial design state. The goal of solving such a problem was to achieve a new design state by applying appropriate design solutions which were generated from demanded design knowledge to this specific design problem. Once a new design state was defined, a new set of design knowledge would be determined considering its dependence on the design problem. Afterward, the relations between different design states were discussed where the design process was believed to have underlying nonlinear dynamics and possible to have chaotic motions. This led to the first postulate, denoted as the postulate of nonlinear design dynamics. This postulate indicated that the design process could be solved by environment-based design (EBD) (Zeng, 2004). It was also mentioned in this postulate that design reasoning was sensitive to initial conditions, based on which three routes leading to design creativity were then derived. Those three routes could be briefly described as formulating design problem differently, extending design knowledge, and changing the environment decomposition.

Starting from those identified three routes, the descriptive design model EBD was once again applied to find the factors that might cause initial conditions to change. The authors found that it was through mental capacity that the designers contributed to the changes in initial conditions. According to their analysis, there was great degree of uncertainty and unpredictability in the design evolution process. Such uncertainty and unpredictability will trigger mental stresses. This led to the postulate of the stress-creativity relation which indicated that designers' creativity was related with their mental stress following an inverted U shaped curve, by adapting findings from psychology (Yerkes & Dodson, 1908).

Finally, four major affecting factors were identified including the workload and the three factors affecting mental capacity as illustrated in Eq.(3). Among the four factors influencing mental stress, knowledge *K(t)*, skills *S(t)*, and affect *A(t)* constitute a person's mental capacity, the level of which reflects how well the person is at the current work. As mentioned in (T. A. Nguyen & Zeng, 2012), knowledge *K(t)* is influenced by knowledge and experience related to the given workload. Skills *S(t)* refer to a person's thinking styles, thinking strategies or reasoning ability. The level of affect *A(t)* could determine how much of the person's knowledge and skills can be effectively used in accomplishing the workload.

$$\sigma(t) = \frac{W(t)}{(K(t) + S(t))A(t)}, \quad \text{A(t)} \in (0, 1) \tag{1}$$

where $\sigma(t)$ denotes a person's stress at time *t*, which is determined by four influencing factors including workload *W(t)*, knowledge *K(t)*, skills *S(t)*, and affect *A(t)*. Please note that Eq. (3) represents a qualitative relation.

3.2 Applying stress-effort model for phenomena interpretation

Though firstly proposed for studying design phenomena, the stress model can be applied to any task as long as there is human participation (Yang, Yang, Quan, & Zeng, 2021). This section covers two studies that applied and extended the stress-effort model to interpret the typical phenomena including the influence of human emotions in engineering (Zhao et al., 2018) and the effect of information collection strategies on stress (Zhao & Zeng, 2019).

3.2.1 Role of emotion in engineering

This section aims to apply the mental stress to explaining how emotion affects performance in the existing literature on engineering (T. A. Nguyen & Zeng, 2012). A wide variety of research topics on emotional engineering has demonstrated that emotional engineering has attracted a lot of attention recently, and more researchers have realized the importance of emotion in engineering. Some of the efforts are focused on the application of emotion to different phases within a product lifecycle, namely conceive stage, design stage, realize stage, and service stage; other efforts are directed at proposing emotion-based approaches like Kano model (Sauerwein, Bailom, Matzler, & Hinterhuber, 1996) and Kansei engineering (Nagamachi, 1995), where related psychological mechanisms (e.g., the expectation effect theory, categorization of emotion in psychology) are explained. All of the above-mentioned research considered emotion as an imperative element in the process of product design that aims to help customers to achieve better performance in product use. Still, there is a need to build up a strong causal connection between emotion and engineering.

First, the influence of emotion on engineering was discussed based on a brief literature review of emotional engineering (Zhao et al., 2018). Different stages within the entire product lifecycle

are discussed separately hoping to acquire a good understanding of how emotion participates in engineering. Given that a product lifecycle can be divided into four major phases including conceive, design, realize, and service, a literature review of emotional engineering is developed in the order chronologically corresponding to lifecycle phases. In addition, a lack of theoretical support for emotion-performance relation in existing research works on emotional engineering is identified through our review. Further efforts are required to address this theoretical deficiency so that the influence of emotion to engineering can be better understood. Therefore, two application examples in emotional engineering are presented below to illustrate how the stress model (T. A. Nguyen & Zeng, 2012) could be applied for phenomena interpretation for filling the gap between emotion and performance in engineering.

- **Example 1: applying stress model to a TV rating system**

  The BROAFERENCE rating system (Aoki & Kowalik, 2011) was considered as an example, where emotional parameters were extracted by utilizing FACS for facial expressions observed by cameras. The FACS system defined forty-six atomic action units, whereas the current proposed rating system considered only a restricted number of action units which indicated happiness and surprise.

  In order to apply the stress model to it, the studied performance of users here is their willingness to watch a TV program. The required knowledge is little under such circumstance, and identified skills are changing channels, volume adjustment, and other possible TV operations in which every individual seems quite skilled. Then we can start by quantifying the workload as the duration of the program. With those mentioned variables controlled, a relative clear emotion-performance relation is established. For the quantification of emotion, we can distribute different weights to different action units within FACS, and among them AU2 and AU12 get the highest scores. Any possible facial expression could be described by a combination of some of those units. As Nguyen and Zeng once explained the influence of emotion as "affect will determine how much one's knowledge and skills can be effectively used," larger numbers represent better exertion of knowledge and skills resulting in less stress. In addition, TV programs are never too short so that the common goal is to make the stressful audience

less stressful. In other words, we can assume that we are working on the right side of the inverse U shaped relation between stress and performance where less stress indicates better performance.

The improvements are obvious after applying the stress model. The former results of BROAFERENCE are capable to tell good quality from bad quality of TV programs. However, their results are too vague and the reason was not explained for why AU2 and AU12 represent good quality. Combined with the model, the rating results now can be used to rank different TV programs. This means more information could be figured out such as how every TV program is selling and if it is well made in audience's opinion. Theoretical support is also given to correlate their calculated emotional parameters to audience performance, i.e., their willingness to continue watching a TV program.

- **Example 2: applying stress model to PET bottle design**

  Another example is the PET bottle design (Widiyati & Aoyama, 2013), where the expected performance is that customers purchase such PET bottle and perhaps recommend it to others afterward. In addition, customer's knowledge and skills related to the usage of the PET bottle are easy to control mainly for two reasons. Firstly, the requirements for knowledge and skills in this case are so little that we can assume customers' knowledge and skill levels as constant. Secondly, the changing part is restricted to the shape of the bottle resulting in relative stable product functionality. Moreover, the second reason can also be used in explaining why workload is treated unvaried given that changes in product functionality will increase or decrease the required skills and the workload as well. So we can easily keep those three variables within the stress model stable and leave emotion the only varying factor. Now we should concentrate on the quantification of customers' emotion. This time we should take the whole inverse U shaped curve into consideration which is different from that in the example of TV rating system. That is to say, finding the optimal stress level becomes more complicated than dealing with the relation following a monotonic function. In the authors' original work, weight adjustment of each criterion was performed by multiplying the adjustment coefficient with each Kano category where Kano model was integrated. With the purpose of introducing

the stress model, we could make use of the criteria obtained from Kansei words analysis. Extreme scores are distributed to each pair of Kansei words under the assumption that the optimum appears as a compromise. For instance, we can fix Masculine at 1 and Feminine at 5 for the Masculine–Feminine pair, and among the numerous methods of finding the optimal value we start by finding the median value for simplicity. Those calculated optimal values will replace the original Kansei points and participate in later steps.

The surprising result is that we find a way to integrate the stress model together with Kano model in the PET bottle design. According to our discussion in (Zhao et al., 2018), those two models emphasize on different aspects: Kano model focuses on relating emotional factors to different characteristics and elements of a product; stress model, on the other side, establishes the relation between human emotion and his own performance which helps in explaining why certain emotions should be considered regarding a target performance. In the meanwhile, the design workload is not much elevated because what we utilize for emotion quantification has existed already. Therefore, with all those efforts we aim to provide an improved methodology with the complete relation considered which occurs during product-user communication.

To sum up, the presented examples of using stress-effort model to interpret the effect of emotion in engineering applications not only supported the model's expanded applicability beyond the context of design but also could inspire future potential applications in different fields. In order to realize and facilitate future applications of the stress-effort model in engineering and other fields, the need for a quantitative representation of the stress model as well as the quantification of the related factors was also pointed out in this study.

3.2.2 Influence of information collection strategies on stress

The studied phenomenon, information collection, is an essential part within a decision making process, which is not limited to a design process. This research tested it with a design experiment, aiming to investigate how designers' mental stress would vary when different information collection strategy is applied. As a continuous analysis of (X. Wang, Nguyen, Zeng, et al., 2015), we assumed that designers would naturally apply depth-first strategy or breadth-first strategy during

information search. Designers' stress was then quantified from HRV data and was compared under two strategies to see if "designer's mental stress in breadth-first dominant process is higher than that in depth-first dominant process".

Information collection strategies are believed to be related to the quality of decisions as one's choice of searching strategies differed from time to time during the entire decision-making process (Cook, 1993). Similar studies have supported this claim by analysing the influence of information collection strategies on consumer's shopping choices, student's performance in school, as well as human performance in other cases (Eysenbach & Köhler, 2002; Scott & O'Sullivan, 2005; Wilczynski & Haynes, 2004). When it comes to design activities, information collection may also affect the design quality and designer's performance through changing the structure of information and the way how information is searched and organized (Bardwell, 1991; X. Wang et al., 2015). The information identified will subsequently reformulate the design problem. According to the Environment-Based Design (EBD) (Zeng, 2004), searching for information during a design process is to search for environment components and their relationships, where the environment includes existing knowledge about customers, technologies, and other relevant product related components. From this point of view, the application of different information collection strategies corresponds to the order in which different objects are studied.

As a continued work from the analysis presented in (X. Wang et al., 2015), the present research started with a comparison between the three information collection strategies, namely depth-first, breadth-first and hybrid. Information is collected from the top layer to the end along each branch before moving to another branch under depth-first strategy as illustrated in Figure 3.1. However, the information at the same level within different branches will be collected before moving to a deeper level when breadth-first strategy is applied. Then the hybrid strategy can be seen as a compromise of both depth-first and breadth-first strategies. It can be seen from Figure 3.1 that several possible states or factors are explored regarding the current object when breadth-first strategy is applied whereas only the current object is studied with depth-first strategy. Reif argues that depth-first strategy is inherently sequential which means that the nodes from other branches are temporarily "forgotten" in (Reif, 1985). More branches of information can lead to more workload due to the different natures of the branches. From this point of view, designers seem to have less workload under depth-first

process than breadth-first process by ”forgetting” about other branches. However, as designers go deeper with a certain branch under depth-first strategy the target information becomes more and more specific which is difficult both to find and to understand. An increase in workload may be expected as designers continue with depth-first strategy.

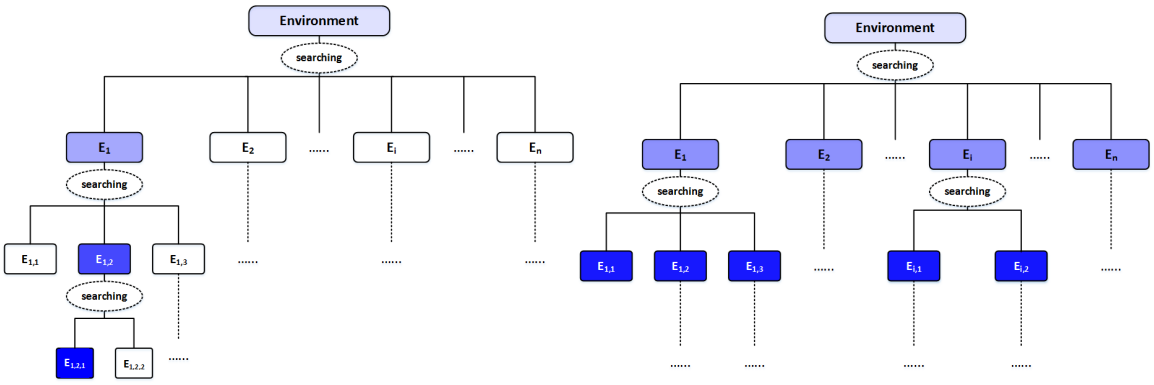

(a) Depth-first strategy (b) Breadth-first strategy

Figure 3.1: Depth-first and breadth-first information collection strategies

In the meantime, within a depth-first process detailed information about the studied object will be collected which belongs to a certain domain. Depth-first process is more domain-specific than breadth-first process and designer’s domain knowledge is more likely to be activated during such a process. On the contrary, within a breadth-first process the successively studied objects are usually from the same level which tend to be less related to each other as with depth-first process. As those objects may belong to different fields and a wide range of knowledge is needed, designers are more likely to feel the shortage of knowledge with breadth-first process. It seems that more domain dependent knowledge will be activated with depth-first process than that with breadth-first process. We may infer how designer’s mental stress changes under breadth-first process and under depth-first process by integrating the aforementioned analysis into Eq. (1). With reduced workload and more activated domain knowledge, designer’s mental stress may be lower when depth-first instead of breadth-first strategy is applied. This seems in accord with our sentiment that the depth-first approach can enhance the designer’s mastering of the global picture of the design and thus reduce the feeling of uncertainty, which is closely related to stress. Furthermore, as participants were not given any instructions about information collection strategy we assume that designers would

naturally adopt hybrid strategy. Design is a recursive process (T. A. Nguyen & Zeng, 2012; Zeng & Cheng, 1991) where solutions to a sub-design problem may depend on those for another sub-problem. Any new pieces of design information (either of design problem, design solutions, and design knowledge) would reframe the problem, which could generate a new tree for search. As a result, though some designers may prefer either depth-first or breadth-first strategy, they would have to turn to the other strategy either because the current design needs information from another sub-design problem or because they cannot move deeper or wider with the available information. From this point of view, any application examples can be relatively seen as hybrid processes if the boundaries are defined as far as possible from the studied node. However, such hybrid processes may still have a dominant strategy, depth-first or breadth-first, as people may have a preference on one of them. And our previous analysis on these two information collection strategies may also apply for hybrid cases dominated by those two strategies. Therefore, the research hypothesis is formulated as follows:

- **Designer's mental stress in breadth-first dominant process is higher than that in depth-first dominant process.**

Based on the aforementioned research hypothesis, a dataset that was collected from a design experiment conducted at Concordia University was considered here to test the hypothesis (T. A. Nguyen, Xu, Zeng, et al., 2013). This pilot study was conducted based on the data collected from six subjects with engineering background aged from 25 to 35. The participants' design behaviours were recorded by a tablet screen recorder and four cameras whereas their HRV data were recorded by an HRV monitor-Polar RS800G3. The experiment protocol was approved by Human Research Ethics and Compliance, Concordia University. During the experiment, each participant was assigned the same design task so that the workload was the same for all participants in the beginning of the design. Besides, participants were given unlimited time to develop their design solutions and they were clearly told that their solutions would not be marked. The objective is to reduce the possibility that participants experience extreme emotions (affect) during the entire process. Participants were using their comfortable approaches during the experiment as we did not specify the strategy, who appeared to be in a relative calm state during the experiment based on

their facial expressions in the recorded videos. In addition, we assume that all participants have the design skills needed in the case, and that skills and emotions are not going to experience noticeable changes during a short period of time as skills gaining usually requires a relative long training process. Therefore, skills are treated as a stable parameter in our analysis. To sum up, participants have the same initial workload and their skills stay stable during the experiment.

The collected data were firstly segmented based on the results of protocol analysis on the recorded design behaviours. Besides observable actions shown in the screen recording video, participants' answers during the interview stage were also used to calibrate the segmentation result. Afterward, several criteria were developed for recognizing the applied dominant strategy based on our analysis mentioned above and the analysis of the three different information collection strategies. When breadth-first dominant strategy is applied, objects at the same level, which may belong to different branches, are studied. In the meantime, some closely related information may be collected repetitively while subjects investigate objects from the same branch at different stages of their design process. However, in a depth-first dominant process subjects may include more details in their solutions, which is enabled by the increase of certain domain knowledge. From another perspective, more efforts and time are required from the subjects whose solutions include more details than those with less detailed solutions. According to our discussions about relative hybrid process, we may use efforts and time as an indicator of one's preference to depth-first strategy. Therefore, the criteria used in our analysis to recognize the applied information collection strategy are as following: A sample is identified as a depth-first dominant process if it satisfies the following two conditions simultaneously: 1) there is little jumping between different branches; and 2) details are added for certain items. Otherwise, the sample is recognized as a breadth-first dominant process. Therefore, the information strategy identification results are listed with the number of segments for each participant in Table 3.1.

Table 3.1: Dominant information collection strategy identification and segments

Participants	1	2	3	4	5	6
Dominant strategy	DF	DF	BF	DF	BF	BF
Number of segments	142	54	211	139	235	216

In the meanwhile, the collected HRV data were computed and clustered for the quantification

of subject's mental stress during design processes. The collected HRV data were analyzed by the HRVAS software (Ramshur, 2010) and the LF/HF ratio was calculated from the computed the Discrete Wavelet Transform (DWT) coefficients. According to the literature, a group of features extracted from the collected Heart Rate Variability (HRV) have been considered as useful indicators, such as the mean of RR intervals (mRR), and power spectra in very low (VLF), low (LF), and high (HF) frequency ranges, are believed to be affected by mental stress (Hjortskov et al., 2004; Kumar, Weippert, Vilbrandt, Kreuzfeld, & Stoll, 2007; Salahuddin, Cho, Jeong, & Kim, 2007). The LF/HF ratio derived from the mentioned features, which is sometimes noted as Sympathovagal Balance index (SVI), was applied to indicate the participants' mental stress level by scholars (Boonnithi & Phongsuphap, 2011; Healey & Picard, 2005; Karthikeyan, Murugappan, & Yaacob, 2011). The LF/HF ratio for a given segment was computed by dividing the accumulated results by the time length of the segment. Afterward, K-means was applied to the normalized LF/HF ratios to cluster the segment LF/HF ratios across subjects with K varing from 2 to 12. Finally, a weighted average stress value was computed for each participant based on the obtained stress distribution.

In conclusion, as a continuous work of the analysis in (X. Wang et al., 2015), the hypothesis was derived by descriptively analyzing how the related factors would change under different information collection strategies using the stress model. The results obtained from the pilot analysis on HRV data indicate that higher mental stress is more likely to happen to designers under a breadth-first dominant process than a depth-first dominant one. Further studies are needed to provide more evidence for the tested research hypothesis with a larger sample size as the current analysis only covered the data collected from six participants. Meanwhile, the protocol analysis applied during the segmentation step relies heavily on subjective factors such as expert knowledge and emotions, and is also time-consuming, which would be a promising direction for my future research. Along this direction, integrating EEG-based analysis into our analysis appears to be a promising candidate.

3.3 Formulated research objectives

The necessity for a quantitative representation of the stress model as well as the quantification of the involved cognitive factors like cognitive workload and mental capacity can be identified in the

aforementioned application examples of the stress model. In general, those pilot studies in applying stress-effort model for phenomenon interpretation are somehow limited to a descriptive level. Although the pilot study on the effect of information collection strategies quantitatively analyzed the HRV data to test the hypothesis, the stress-effort model was also applied in a descriptive manner for the hypothesis development by analyzing the possible variations of different factors. As a result, the aforementioned applications on phenomena interpretation revealed the need for a quantitative representation of the stress model.

As we seek to establish a general quantitative system that will simplify the applications of the stress model in quantitative cognitive studies, we should first consider the quantification of the influencing factors of mental stress, namely cognitive workload and mental capacity. Moreover, a quantitative representation of the stress model may serve as a bridge between the quantification of certain cognitive factors and mental effort, which could enrich most existing and future cognitive studies. Once both of the two cognitive factors are quantified with a few features extracted from the collected EEG data, further investigations could be conducted to investigate the relationships between those cognitive factors as well as their effect on stress as well as mental effort. As a result, my future research will focus on the effect of the quantified cognitive workload and mental capacity on mental effort under complex cognitive activities. The research findings would enable real-life applications that are adaptive to individual differences and time-varying cognitive states in order to achieve high efficiency.

In summary, two research questions arise from the aforementioned efforts in applying and extending the stress model for phenomena interpretation:

(1) **How to quantify cognitive workload and mental capacity that have been identified in the stress model?**

(2) **How to quantitatively describe the effect of variations in those cognitive factors on one's mental effort?**

The above-mentioned questions correspond to the two objectives of this research as mentioned in Chapter 1 under Section 1.2. Meanwhile, a research methodology has been developed to address

these questions, on the basis of which the present study is structured. The two research objectives are:

(1) **To quantify cognitive workload and mental capacity from EEG signals when human participants are conducting complex cognitive activities.**

(2) **To apply the quantification results on cognitive workload and mental capacity to improve human participants' mental effort during complex cognitive activities.**

Chapter 4

Research Methodology: A tEEG Framework for Conducting Loosely Controlled EEG Experimental Studies

The research methodology is developed based on the two research objectives identified in Chapter 3. As a result, the research methodology consists of three main stages, among which the necessity for the first stage comes from the lack of investigations into the uncontrolled part of complex cognitive activities and the challenges and opportunities in integrating EEG techniques such research. In particular, the first stage is to develop a new research framework to address the challenges identified by synthesizing the knowledge on design and EEG techniques through literature review, conducting theoretical analysis, and combining preliminary results. Upon the proposition of the framework, the second stage is to apply the framework, denoted as tEEG framework, to investigate some typical cognitive phenomena. We followed the tEEG framework when designing experiments and analyzing data for the target research question. Not only would the obtained results provide evidence of performance improvements with quantified cognitive workload and mental capacity, but they would also serve as examples of how to apply the tEEG framework outside of the context of design. Afterward, the third stage proposes and tests a quantitative approach for ensuring high mental effort with the quantitative feedback on participants' cognitive workload and mental capacity. Starting from

the stress model (T. A. Nguyen & Zeng, 2012), a quantitative representation of the workload-effort relationship was developed and was then tested with simulation results. Furthermore, an ongoing study aims to test the proposed quantitative approach with experimental evidence where we designed a cognitive experiment based on the N-back WM paradigm. In summary, the first two stages have been completed, which aim at the first objective by quantifying changes of cognitive workload and mental capacity from EEG data under complex cognitive activities, whereas the third stage is a continuous work of my current research that targets at the second objective.

4.1 Proposing a new research framework for EEG-based cognitive design studies: The tEEG framework

A task-related research framework, tEEG framework, is proposed aiming to guide scholars' research on EEG-based cognitive and affective studies in the context of design. A theoretical analysis of the design process is conducted in the first place to show that it is necessary and promising to look into designers' cognitive and affective states for further investigation of the design process. Afterward, several difficulties with EEG-based design studies are summarized by reviewing and analysing current EEG applications in design research. Therefore, the tEEG framework is presented to address these difficulties.

4.1.1 Challenges with EEG-based cognitive design studies

In order to take full advantage of EEG techniques, an overall understanding of the existing EEG studies is not only important but also necessary for any other analysis. Most of the existing EEG-based neuro-cognitive research relies strongly on event-related techniques (Friedman & Johnson Jr, 2000; Kutas & Federmeier, 2011). In particular, event-related potential (ERP) method has been widely applied in investigations of simple cognitive activities through well-controlled experiments. Event-related potential (ERP) is the brain's potential generated in response to an event or a stimulus. The ERP waveform, as shown in Figure 4.1, is computed by averaging EEG signals time-locked to an event across multiple trials. The underlying assumption is that the fundamental cognitive response to an event is invariant. Therefore, by averaging EEG signals across multiple trials, the

noises and artifacts in the signals could be canceled. An ERP waveform consists of negative (labeled as N) and positive (labeled as P) amplitudes. These are ERP components and are denoted by the direction of the polarity (either P or N) followed by the latency of the occurrence or the position of the component. For instance, P300 is a positive component occurring at 300 milliseconds, and N1 is the first negative component in the ERP. ERP components characterize the brain's potential in reaction to the event. ERP method can be used to investigate the invariant nature of cognitive response but may not applicable to most real-life applications where complex cognitive activities are involved.

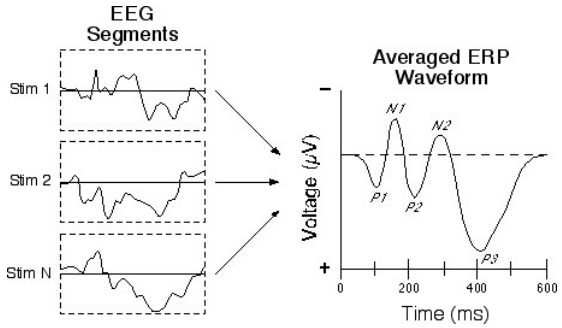

Figure 4.1: ERP waveform generated from averaging across events

In addition, the characteristics of design activities need to be carefully considered when conducting EEG-based design studies. Design research differs from current EEG studies in that 1) design is a complex activity that consists of numerous basic cognitive activities; 2) complex relationships between designer, product and environment contribute to the increase of difficulty in experiment design and control; and 3) design process is continuous and unrepeatable. As a result, EEG-based design research is embedded with difficulties summarized in the following:

- **Task driven and delayed responses:** The initial design task will drive the reformulation of the design problem, which is the stimulus for a design, throughout the entire design process; thus, the stimuli for design activities keep changing and are not always observable. Behavioral responses to a stimulus may be delayed in that a designer may not show what comes into his/her mind right away. For example, a solution that a designer brought forth at certain moment may have been generated any time before that moment. Therefore, finding a causal stimulus-response relationship under such circumstances is not a straightforward effort.

- **Complex relationships:** Design activities are so complicated that there may not be a direct causal relationship between a stimulus and its response, especially if one intends to examine primitive cognitive activities. When investigating the effect of knowledge on design performance, it is expected that the designer's perception of workload, skills, and affect would remain stable, based on the stress model. As discussed above, this ideal condition is unrealistic since artificial controls will change the outcome of a real design even if the control were practicable.

- **Continuousness and nonrepetitiveness of design activity:** According to the previous discussion in the paper about the evolution of the design process, design activities cannot be repeated because of their inherent recursive logic. The impossibility of repetition makes event-related potential (ERP) analysis unsuitable for full-scale design studies. Design activities, in whole and in part, are not time-locked and thus cannot be reduced to ERP analysis.

The difficulties identified above also lead to the key challenge of conducting EEG-based cognitive design studies, that is to find the hidden stimulus-response relationships during the design process. If we describe the design process as the entire process from a design problem to the generation of a final design solution, it inputs the initial design problem and outputs the design solution. Such a process consists of a series of sub-processes resulting from the dynamic evolving characteristic of design process (Zeng & Gu, 1999) as illustrated in Figure 4.2. Each synthesis process describes the process in which a designer tries to conceive a solution to the current design problem. Once a design solution is produced, the designer is able to redefine the design problem and to retrieve the related design evaluation knowledge. This process is denoted as evaluation (Figure 4.2) and the new design problem becomes the input for another synthesis process with more detailed product descriptions (solution) and designer's updated design knowledge. Therefore, a design process is constantly fed with evolving input, which is a design problem formulation, resulting in evolving design solutions as the output (Figure 4.2). The input and output variables of a design process belong respectively to sets "X" and "Y" where each x_i represents a certain design problem whose corresponding design solution (selected from multiple candidates) is denoted as y_i. Additionally, control variables belong to the set "C" while designer's behavior and biometrics belong to the set "Z"

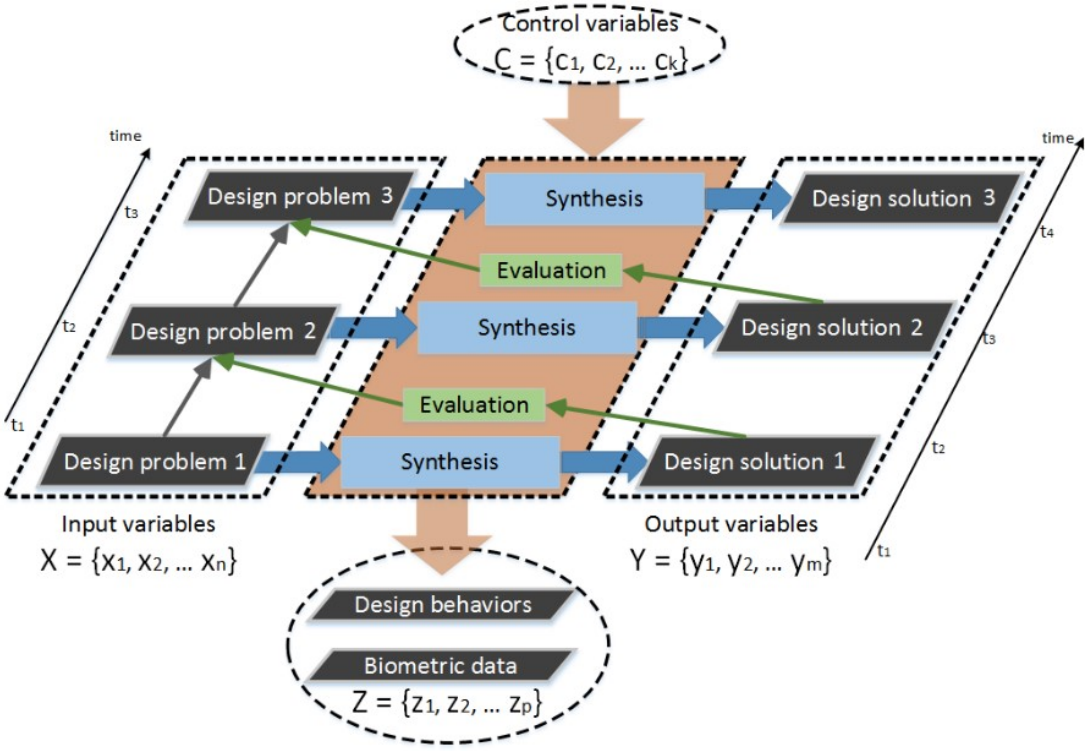

Figure 4.2: Design process representation

The equations below show how such a complex process is mathematically formulated:

$$\begin{aligned} &\overrightarrow{y} = f_1(\overrightarrow{x}), \overrightarrow{z} = f_2(f_1, \overrightarrow{c}), \\ &y_j = g_1(y_q), \text{ where } j \neq q, 1 \leq j \leq m, 1 \leq q \leq m \end{aligned} \tag{2}$$

where $\overrightarrow{x} = \{x_1, x_2, ..., x_n\}$ represents input variables, $\overrightarrow{y} = \{y_1, y_2, ..., y_m\}$ represents output variables, $\overrightarrow{c} = \{c_1, c_2, ..., c_k\}$ represents control variables, $\overrightarrow{z} = \{z_1, z_2, ..., z_p\}$ represents behavioral and biometric data, f_1 describes the mapping from input ($\overrightarrow{x}$) to output variables ($\overrightarrow{y}$), which is a design process. Meanwhile, the design process f_1 together with other factors ($\overrightarrow{c}$) may cause changes in designer's behaviors and biometric data ($\overrightarrow{z}$), which is represented by f_2. Certain relationships between different output variables may be related to each other by relations represented by g_1. The numbers of variables of input, output, control variables and other changes are denoted as n, m, p, and k respectively, which are independent from each other.

Eq. (2) presents a general experimental design research framework that structures unstructured data from design activities, which aims to identify the hidden stimulus-response relationships. This

calls for a new experimental paradigm for EEG studies of design cognition.

4.1.2 The proposed tEEG framework

A task-related framework is proposed for investigating the cognitive and affective activities during design processes with the mentioned challenges addressed. As depicted in Figure 4.3, the overall design process inputs the initial design problem and outputs the final design solutions if viewed from a high level perspective. The data collected during loosely controlled experiments include designer's behaviors, biometric data and design solutions based on the target design problem. Loosely controlled experiments are designed and conducted regarding the studied research topic where participants' design activities could happen. Secondly, clustering-based segmentation can be used to identify the hidden structured stimulus-response data pairs from the unstructured data. Several subprocesses can be extracted from a complex design after this step. Last but not least, each individual segment can be analyzed using the traditional hypothesis test method. It is during this step that some of the existing results and techniques on EEG-based cognitive and affective states may be adopted and integrated.

Loosely controlled experiments are proposed for design studies which should be less controlled compared to traditional ERP experiments based on our previous discussions of design process. The surrounding environment of a product consists of everything other than the product itself and the designer. Additional controls will bring changes to the environment resulting in different design solutions as those controls change the environment in which the product is to be designed (Dong, 2005; Dorst & Cross, 2001; Maher & Tang, 2003; T. A. Nguyen & Zeng, 2012). This means that loosely controlled experiments will be conducted without control of certain extraneous variables. Typical of such experiments is that they can last much longer than traditional ERP experiments, during which various cognitive activities may take place. Meanwhile, loosely controlled experiments are proposed to target the uncontrollable part of design activities while current EEG-based design studies mainly investigate basic and clear stimulus-response relationships under experiments with better controls. The consistency of the nature of loosely controlled experiments and that of complex design scenarios indicates more possibilities and new directions for design studies. Finally, different loosely controlled experiments can be designed depending on the complexity of the

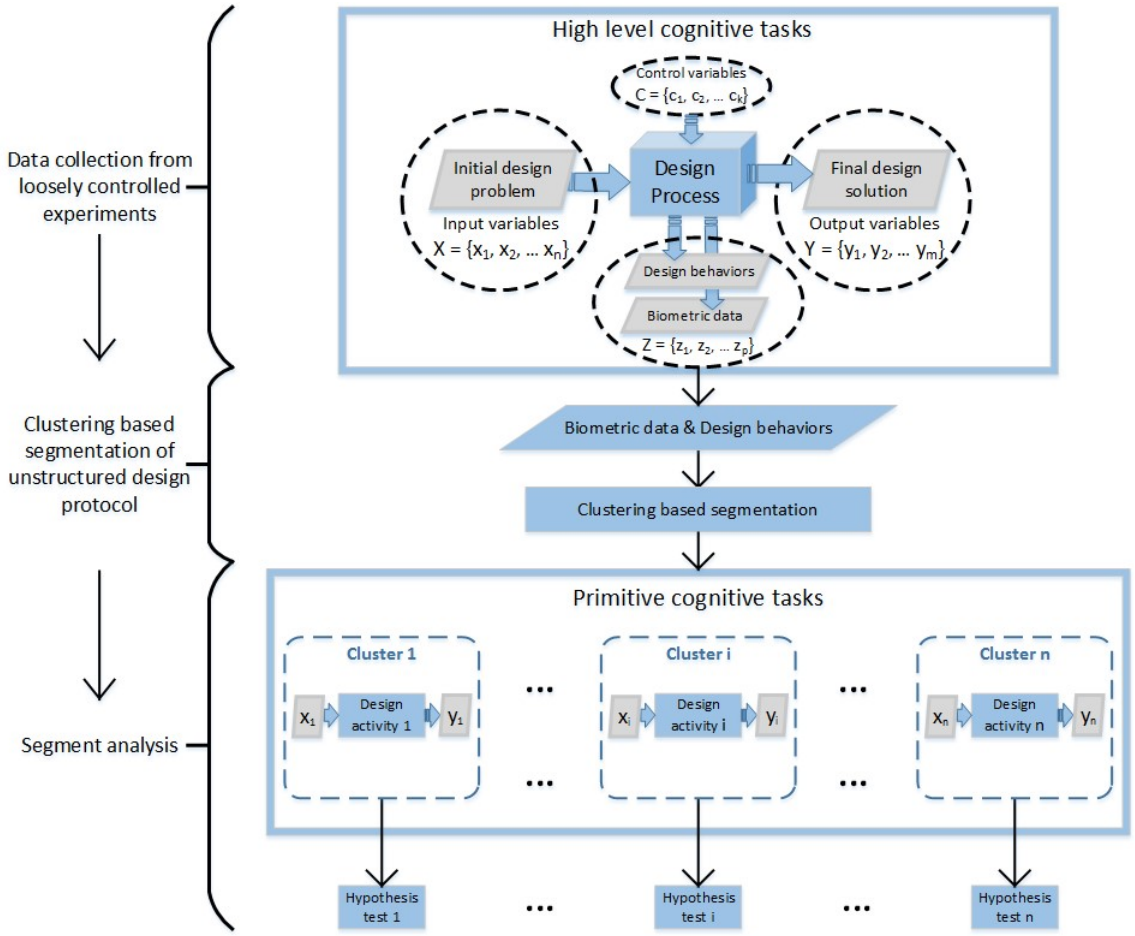

Figure 4.3: The proposed tEEG framework

studied scenario and the cognitive/affective aspect of interest. That is to say, designers need to have an overall understanding of the research topic and be aware of the characteristics of this kind of experiment when designing a loosely controlled experiment. A basic principle of experiment design for studying design activities is to ensure the emergence of regularities related to the phenomena under observation while applying minimum controls.

Since a design experiment consists of numerous stages and processes of solving different subtasks and evolves over time, designer's cognitive and affective states should also vary from time to time. Different cognitive, affective, and behavioral states may be dominant at different stages so that the recognition results should reflect the designer's cognitive and affective states in a basic design activity. Consequently, cognitive and affective states can be identified for each individual sub-process instead of the entire process, either by segmenting the object of study into primitive

ones or by segmenting the duration into shorter ones or by both. Each segment will have a clear stimulus-response relationship that can be effectively tested by using existing hypothesis test methods. Afterwards, appropriate analysis methods should be applied to different sub-tasks and/or at a shorter duration for their corresponding hypothesis tests. Clustering algorithms could be integrated to find the relative "structured" groups from the unstructured data. Clustering aims to separate an unlabeled data set into several clusters by capturing the hidden similarity and dissimilarity within the data (Jain, 2010; Jain, Murty, & Flynn, 1999; R. Xu & Wunsch, 2005). In terms of the aforementioned concerns, the influence of subjective factors can be attenuated by taking into consideration the data-driven analysis results that are obtained by applying clustering algorithms to the collected data. Besides, a common standard could be developed to apply clustering algorithms for segmenting unstructured data. Clustering, as an unsupervised classification method, has less dependency on knowledge and experience compared to protocol analysis as it deals with unlabeled data. Within the proposed tEEG framework, EEG data are the main source of the unstructured data on which clustering algorithms are performed. Thus, clustering-based segmentation is proposed to process unstructured data collected during loosely controlled experiments. Additionally to the advantages of clustering-based segmentation regarding the three concerns of traditional protocol analysis, the incorporation of EEG data during data segmentation may improve the accuracy of (protocol analysis based) segmentation results.

As illustrated in Figure 4.3, the last step is conducting segment analysis where the extracted primitive tasks will thereafter be tested by a series of corresponding hypotheses. Each individually extracted segment is analyzed following the traditional hypothesis test method considering that each segmented sub-process may be dominated by a stimulus-response relationship. The purpose of EEG-based segment analysis is to identify causal relations in the segmented design process. The captured causal relations can be used to infer cognitive and affective states that have been widely tested in the field of cognition and psychology during the design process. It is during this step that some of the existing results and techniques on EEG-based cognitive and affective states may be adopted and integrated.

4.2 Applying tEEG framework within and beyond design for quantifying cognitive factors

Experimental applications have been conducted to quantify different cognitive factors not only under design activities, but also for other complex cognitive activities beyond the context of design. Within the context of design, there are four experimental applications that apply the tEEG framework to investigate designers' cognitive factors and their relationships. Among those four design applications, three of them have already been completed before the proposition of tEEG framework (Zhao et al., 2020), which will be discussed in the paper. The other design application (Jia & Zeng, 2021) investigates designers' cognitive workload and cognitive control during different design activities when they work on six different design problems, which will be carefully discussed in this paper under Section 5. As for the beyond design application, the tEEG framework has been applied to a flight simulator-based training experiment designed to simulate different flight scenarios while pilot trainees (participants) were asked to perform basic elements of lateral and vertical navigation.

For example, the study (T. A. Nguyen & Zeng, 2014) published on Computer-Aided Design was discussed in (Zhao et al., 2020) as the first example of tEEG framework application. This study aims to investigate the relationship between designer's mental effort (mental capacity aspect) and mental stress. One potential contribution of this study is for the development of the next generation of computer-aided design (CAD) systems where the interactions between designers and design tools should be well considered. The results show that designers' mental effort reduces at high levels of stress (among the studied three stress levels), indicating that workflow and interfaces of computer aided conceptual design tools should be designed so as not to add unnecessary mental stress. Another application example is the study that used EEG signals to test different hypotheses on the cognitive and quantitative aspects of design process (P. Nguyen, Nguyen, & Zeng, 2018). The quantified cognitive factors include mental stress, fatigue which is closely related to one's mental capacity, and creativity which could be seen as part of one's performance. There is a loose connection between cognitive states and the design process as undertaken by a subject that can be interpreted from a physiological perspective using for example EEG signals. EEG signals can measure cognitive states although these cognitive states labelled as fatigue, mental stress or creativity

may no longer retain the same semiological content as their natural language counterparts and take a more operational and experimental meaning.

4.2.1 A step-by-step guide for tEEG framework applications

In general, the proposed tEEG framework consists of three parts including data collection from loosely controlled experiments, clustering-based segmentation, and EEG-based segment analysis. For each of these three parts, related algorithms and techniques are summarized from existing literature covering a broad spectrum of fields and resources. We propose loosely controlled experiments to investigate uncontrollable parts and complex relationships within design processes. Afterwards, clustering-based segmentation is proposed to find structured sub-datasets from the unstructured dataset collected during loosely controlled experiments. As a result, a complex design process is segmented into different primitive activities that can be studied using traditional hypothesis tests. Lastly, during the segment analysis step the extracted segments are examined one by one, which can be viewed as several hypothesis tests. In the meantime, tEEG framework makes existing EEG techniques and analysis methods applicable for EEG-based design studies.

Collecting data during loosely controlled experiment

Despite the difference in experiment design, EEG data collection under loosely controlled design experiments will be similar to that under current EEG studies. EEG data will be collected throughout the experiment while subjects are asked to solve a design problem. Moreover, behavioral data will also be collected which will be used in clustering-based segmentation as illustrated in Figure 4.3. In the meantime, only ambient noises will be filtered from EEG data and artifacts are kept for further analysis, which is different from the data filtering step in current EEG studies. Those artifacts can be used for clustering-based segmentation given that the so-called artifacts may be an indirect reflection of participants' cognitive/affective activities.

Conducting clustering-based segmentation

Combining the theoretical analysis and our previous attempts, the procedure of the proposed clustering-based segmentation can be explained as follows:

(1) Conduct protocol analysis and apply clustering algorithms on EEG data simultaneously;

(2) Use the part with high confidence from the protocol analysis results as the criteria to assess the reliability of the applied clustering algorithm. If the reliability is not satisfying, a different clustering algorithm can be applied until the clustering analysis results can be accepted; and

(3) The segments obtained based on clustering analysis are labelled by the protocol analysis results.

Performing segment analysis

It is during this step that feature extraction, feature selection, classification and statistical analysis will be performed as has been done in most existing EEG studies. Every extracted feature has its specific aspect of information for which some information will be lost. For example, frequency domain features can hardly describe temporal (time) information. Furthermore, information is organized in different ways and representation forms differ from one feature to another. As a result, a comprehensive understanding of various features is essential as each feature represents a different way of information selection and organization. Table 4.1 and Table 2.1 list the applied EEG features and their corresponding affective and cognitive findings reviewed in the development of tEEG framework, hoping to assist scholars in choosing appropriate EEG features in their tEEG framework applications.

4.2.2 Evaluation under different contexts

In the context of design and other complex cognitive activities, the crucial challenge for evaluating the indices of cognitive factors extracted from physiological data lies in the lack of ground truth, which could be related to the complex relationships involved in complex cognitive activities as well as our limited knowledge of the functions of human brain. Taking design as an example, the recursive and complex process makes it merely possible for researchers to concentrate on a specific stimulus-response relationship with other potential influencing factors well controlled. Several cognitive functions can be simultaneously involved in one complex cognitive activity, whereas one cognitive function may contribute to multiple complex activities in different ways. Existing research

findings cannot provide sufficient evidence about how one cognitive function supports a specific complex task and how it interacts with other cognitive functions. As a result, the evaluation of a certain method or feature in quantifying one specific cognitive factor could be challenging and may combine different evaluation methods, which is exactly what has been done in the present research.

In order to evaluate the effectiveness and reliability of a loosely controlled experiment, classical features like spectral power were applied for comparisons with the validated findings available in the literature. Before applying any advanced features or applying a relative popular feature to a new phenomenon, aligning our findings with other validated evidence was considered as the first step in evaluating the performance and quality of our analysis. In the meantime, a consistent conclusion obtained through multiple features that have been proved to be related to the same cognitive function could add to the reliability of our analysis, which serves as another evaluation step. Moreover, the results extracted from EEG-based analysis could further be evaluated through comparisons with subjective ratings and performance evaluations depending on the availability under varied circumstances. However, subjective ratings are not necessarily the ground truth, as they may be inaccurate in reflecting the real changes in cognition (T. A. Nguyen & Zeng, 2017), which is just one metric considered in the analysis. Performance evaluations could be a more reliable measure in comparison to subjective ratings, even though the evaluation conclusion obtained from correlation analysis is built upon one or a series of well accepted assumptions between cognitive functions and performance when the research question is more about cognitive functions instead of performance dimensions. Therefore, the present research combined the aforementioned evaluation methods to achieve a convergent conclusion.

4.3 From stress model to a quantitative representation of human workload-effort relationship

A quantitative representation is developed based on the original stress model (T. A. Nguyen & Zeng, 2012) for describing the impact of stress and cognitive factors like workload and mental capacity on mental effort. As the third stage within the research methodology, this section presents a quantitative representation of human workload-effort relationship, which could be further tested

with simulations and experiments. The simulation results lead to a quantitative approach for ensuring high work efficiency and successfully meeting the deadline, denoted as the capacity zone model. Moreover, a cognitive experiment was designed using an N-back WM paradigm to provide experimental evidence to the proposed capacity zone. The simulation results and the preliminary results obtained on the N-back dataset are discussed in Chapter 5 under Section 5.3 and Section 5.4 respectively.

Aiming to develop a quantitative description of the relationship between cognitive factors and mental effort, the important role of mental stress in mediating the influence of cognitive workload and other cognitive factors on mental effort should be well considered in the first place. Therefore, the stress-effort model (T. A. Nguyen & Zeng, 2012, 2017) was introduced into our analysis. The stress-effort model not only described an inverted U shaped relationship between designer's mental stress and mental effort but also identified a group of cognitive factors that could positively or negatively influence one's mental stress. Starting from the stress-effort model, we quantitatively represented the relationship between cognitive workload and mental effort, which then directly led to the human workload-efficiency relationship based on a series of simplifications. Afterward, we modeled the ideal workload-efficiency relationship corresponding to the case when the influence from human beings' limited capacity and other human factors could be ignored. By adding the ideal modeling line to the original human workload-efficiency curve, two intersections were generated which result in three different zones identified on the workload-efficiency curve. Thereafter, time-course simulations were conducted to capture the changes in human work efficiency under different zones considering possible variations in workload assignment and the factors, which will be discussed in the Results section. Note that we distinguish the cognitive workload that is perceived by the human participants from the actual amount of workload assigned to them. It is the former that affects a person's mental stress and is closely related to other human factors (Young et al., 2015), whereas manipulating the latter could affect the initial value of the former.

4.3.1 The stress-effort model

The stress-effort model concentrated on the relationship between mental stress and mental effort as well as the influencing factors on mental stress (T. A. Nguyen & Zeng, 2012). Inspired by the

Yerkes-Dodson Law from psychology (Yerkes & Dodson, 1908), the stress-effort model described an inverted U shaped relationship between mental stress and mental effort. Moreover, four factors have been identified as influencing factors of designers' mental stress which could thus affect the occurrence of creativity during the design process. The authors first analyzed designers' activities and their characteristics within a design process, where the recursive nature of design process was highlighted. A design problem could be seen as an initial design state. The goal of solving such a problem was to achieve a new design state by applying appropriate design solutions which were generated from demanded design knowledge to this specific design problem. Once a new design state was defined, a new set of design knowledge would be determined considering its dependence on the design problem. Afterward, the relations between different design states were discussed where the design process was believed to have underlying nonlinear dynamics and possible to have chaotic motions. This led to the first postulate, denoted as the postulate of nonlinear design dynamics. This postulate indicated that the design process could be solved by environment-based design (EBD) (Zeng, 2004). It was also mentioned in this postulate that design reasoning was sensitive to initial conditions, based on which three routes leading to design creativity were then derived. Those three routes could be briefly described as formulating design problem differently, extending design knowledge, and changing the environment decomposition.

Starting from those identified three routes, the descriptive design model EBD was once again applied to find the factors that might cause initial conditions to change. The authors found that it was through mental capacity that the designers contributed to the changes in initial conditions. According to their analysis, there was great degree of uncertainty and unpredictability in the design evolution process. Such uncertainty and unpredictability will trigger mental stresses. This led to the postulate on the relationship between mental stress and mental effort which indicated that designers' mental effort was related to their mental stress following an inverted U shaped curve and also identified the four influencing factors of mental stress as described in Eq. (3) (T. A. Nguyen & Zeng, 2012, 2017).

$$\sigma(t) = \frac{W(t)}{(K(t) + S(t))A(t)}, \quad \text{A(t)} \in (0, 1)\ , \tag{3}$$

where $\sigma(t)$ denotes a person's stress at time *t*, which is determined by four influencing factors including workload *W(t)*, knowledge *K(t)*, skills *S(t)*, and affect *A(t)*. Please note that Eq. (3) represents a qualitative relation.

The aforementioned influencing factors of mental stress include perceived workload *W(t)*, knowledge *K(t)*, skills *S(t)*, and affect *A(t)*, among which knowledge *K(t)*, skills *S(t)*, and affect *A(t)* constitute a person's mental capacity. The level of mental capacity reflects how well the person is at the current work. As described in the stress-effort model (T. A. Nguyen & Zeng, 2012), knowledge *K(t)* is influenced by knowledge and experience related to the given workload. Skills *S(t)* refer to a person's thinking styles, thinking strategies or reasoning ability. The level of affect *A(t)* could determine how much of the person's knowledge and skills can be effectively used in accomplishing the workload. Continuous efforts have been made to investigate the relationships between mental stress and the potential factors (Jia & Zeng, 2021; P. Nguyen et al., 2018; T. A. Nguyen & Zeng, 2014, 2017; Petkar, Dande, Yadav, Zeng, & Nguyen, 2009; Tang, Zeng, et al., 2009; Zhu, Yao, & Zeng, 2007), which lay a solid foundation for the present research. The stress-effort model, though firstly proposed for studying design phenomena, can be applied to any task that is involved with human participation (Yang et al., 2021).

4.3.2 From stress-effort model to a quantitative representation of human workload-effort relationship

With the mathematical representation of stress-effort model described in Eq. (3), it is assumed in the current study that a person's knowledge *K(t)*, skills *S(t)*, and affect *A(t)* will stay stable throughout a short-term task completion process, which could thus be considered as constants. Under such simplification, Eq.(3) can be written as:

$$\sigma(t) = \frac{W(t)}{(K+S)A} = \frac{W(t)}{\beta}, \tag{4}$$

where β is defined as a person's mental capacity for a given task, which is determined by the person's knowledge K, skills S, and affect A. A larger value of β represents a better mental status regarding the given workload, and vice versa. As we can see from Eq. (4), the smaller β becomes,

the more sensitive the person's stress to workload becomes.

The raised-cosine function, one of the bell-shaped functions, was then applied to model the inverted U-shaped relationship between mental stress and mental effort in this study as illustrated in Eq. (5). The application of raised-cosine function does not indicate any unsuitability of other bell-shaped functions for modeling the stress-effort relationship. Instead, it is possible to try alternative functions for the stress-effort modeling as no additional requirements are needed to limit the application of other bell-shaped functions.

$$E(t) = f(\sigma(t)) = \begin{cases} \frac{1}{2}[1 + \cos(\frac{\sigma(t) - \frac{1}{2}\sigma_{max}}{\frac{1}{2}\sigma_{max}}\pi)], & \text{if } 0 \leq \sigma(t) \leq \sigma_{max}\ , \\ 0, & \text{otherwise}\ , \end{cases} \tag{5}$$

where $E(t)$ denotes a person's mental effort at time t and σ_{max} represents the maximum stress the person can tolerate. We assume that the optimal stress level for human beings to achieve their maximum efficiency is half of the stress limit σ_{max} that they can tolerate. The present function is symmetric around $\frac{1}{2}\sigma_{max}$ as $f(\sigma(t) + \frac{1}{2}\sigma_{max}) = f(-\sigma(t) + \frac{1}{2}\sigma_{max})$ and a person's mental effort achieves its maximum at $\frac{1}{2}\sigma_{max}$. Starting from this maximum effort level, the mental effort will gradually decrease to zero when the stress increases to σ_{max} or decreases to 0. Note that although we assume a symmetric function for simplicity, the analysis and simulation results still hold even if the function is not symmetric.

By integrating the aforementioned Eq. (4) into the stress-effort relationship, Eq. (5) can be written as below:

$$E(t) = \begin{cases} \frac{1}{2}[1 + \cos(\frac{W(t) - \frac{1}{2}\beta\sigma_{max}}{\frac{1}{2}\beta\sigma_{max}}\pi)], & \text{if } 0 \leq W(t) \leq \beta\sigma_{max}\ , \\ 0, & \text{otherwise.} \end{cases} \tag{6}$$

A visualization of the modeling result is presented in Figure 4.4, where the cognitive workload

changes from 0 to 200 with $\epsilon_{max} = 100$, $\sigma_{max} = 200$, and $\beta = 1.0$.

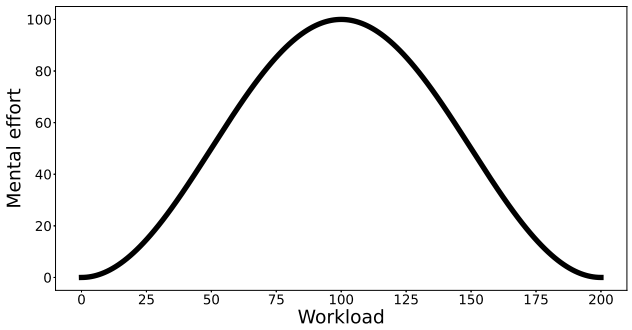

Figure 4.4: Human workload-effort relationship

Table 4.1: Mapping between EEG features and affective findings

EEG features		Affective findings	Research and authors
Frequency domain	Power spectral density (PSD)	Discrete emotional states like happy, sad, fear and relax.	(Yohanes *et al.*, 2012), (Sourina, Kulish, & Sourin, 2009), (Liu *et al.*, 2010)
		Emotions under the 2D valence-arousal model.	(Kroupi *et al.*, 2011), (Reuderink *et al.*, 2013)
		Positive, negative (and neutral) states.	(Brown *et al.*, 2011), (Duan *et al.*, 2013), (Wang *et al.*, 2014)
		Mental stress.	(Al-shargie *et al.*, 2016)
	Higher order crossings (HOC)	Discrete emotional states like happy, sad, fear and angry.	(Petrantonakis & Hadjileontiadis, 2010)
		Emotions under the 2D valence-arousal model.	(Frantzidis *et al.*, 2010), (Hadjidimitriou *et al.*, 2015)
	Coherence	Discrete emotional states like happy, sad, fear and calm.	(Khosrowabadi *et al.*, 2010)
		Negative emotion during dreaming.	(Nielsen & Chénier, 1999)
	Rational asymmetry (RASM12) and differential asymmery (DASM12)	Discrete emotional states like pleasant, sad, angry and joyful.	(Liu *et al.*, 2010)
		Positive and negative states.	(Duan *et al.*, 2013)
	Other techniques: synchronization likelihood, NN voting histogram, Dirichlet distribution parameters, etc.	Emotions under the 2D valence-arousal model.	(Rozgić *et al.*, 2013)
		Positive, negative and neutral states.	(Faber *et al.*, 2017)
Time domain	ERP waveform (P100, N100, P200, N200, etc.)	Discrete emotional states like happy, sad, fear, satisfied and frustrated.	(Bar-Haim *et al.*, 2005)
		Emotions under the 2D valence-arousal model.	(Frantzidis *et al.*, 2010), (Hadjidimitriou *et al.*, 2015), (Singh *et al.*, 2014)
		Positive, negative (and neutral) states.	(Bono *et al.*, 2016)
	Fractal distance (FD)	Discrete emotional states like happy, sad, fear, satisfied and frustrated.	(Liu *et al.*, 2011), (Yohanes *et al.*, 2012), (Sourina *et al.*, 2009)
		Emotions under the 2D valence-arousal model.	(Kroupi *et al.*, 2011), (Frantzidis *et al.*, 2010), (Hadjidimitriou *et al.*, 2015)
		Positive, negative (and neutral) states.	(Faber *et al.*, 2017)
	Entropy	Positive, negative (and neutral) states.	(Duan *et al.*, 2013), (Wang *et al.*, 2014)
	Functional connectivity	Positive, negative and neutral states.	(Bono *et al.*, 2016)
Time-frequency domain	Wavelet coefficient energy	Discrete emotional states like happy, sad, fear and disgust.	(Murugappan *et al.*, 2007), (Murugappan *et al.*, 2010), (Sourina *et al.*, 2009), (Yohanes *et al.*, 2012)
		Positive, negative (and neutral) states.	(Wang *et al.*, 2014)
		Mental stress.	(Al-shargie *et al.*, 2016)

Chapter 5

Quantification of Phenomena under Complex Cognitive Activities: Results and Discussions

5.1 An application of tEEG framework within design: A loosely controlled design experiment

This study aims to quantify designers' cognitive workload and mental capacity when they are conducting design activities. As an application of the tEEG framework, it involves a loosely controlled design experiment consisting of six runs corresponding to six different design problems: design a birthday cake, design a recycle bin, design a toothbrush, design a wheelchair, design a workspace, and design a drinking fountain. Each run consists of five successive design activities: problem understanding, idea generation, rating idea generation, idea evaluation, and rating idea evaluation. By dividing a design process into the five design activities mentioned above, we aimed to reduce the difficulty in investigating such a complex design process and adding certain 'structure' to the unstructured data. Such segmentation is the main control applied in the experiment, meaning that despite the task description showing on the screen from the beginning of each design activity, any additional control including time limit, oral instructions, or 'think-aloud' related control, was avoided

during the experiment. In the meantime, the presented experiment is loosely controlled in that participants were provided with unlimited response times during each design activity and were given sufficient freedom to complete the given task as they chose without interruption or interference. In this manner, the characteristics of the design process can be better modeled, as sufficient time and freedom are essential to allow participants to explore possible solutions naturally and recursively complete the given task. The two rests are placed at the beginning and end of this experiment. As this section will mainly cover the parts related to EEG microstate analysis, more information could be found in (Jia et al., 2021).

First, we simulated design creation using loosely controlled settings in a series of open-ended creation tasks, such as understanding problems, generating ideas, evaluating ideas, and self-rating them. In a loosely controlled setting, considerable freedom is provided regarding response time (self-paced) and response action (integrating the thinking and drawing phases) while maintaining certain levels of control. The effectiveness of loosely controlled settings was also demonstrated in a recent creativity study (Jia & Zeng, 2021). To align our findings with other validated evidence, we investigated the regional contribution of brain oscillations in the classical frequency bands (delta, theta, alpha, and beta) to the different open-ended creation tasks through TRP analysis. In terms of data analysis, however, loosely controlled settings add new challenges. Several cognitive functions can be simultaneously involved in one open-ended creation task, and one cognitive function may contribute to different open-ended creation tasks. Basic cognitive functions never appear in isolation and interact heavily with each other. Consequently, causal relationships between stimuli and responses are extremely complex under loosely controlled settings. To facilitate the loosely controlled experimental setting, we used EEG microstate analysis to segment the unstructured EEG signals into a set of microstates. Each microstate reflects activity in large-scale brain networks whose induced scalp potential fields remain quasi-stable during successive short time periods.

5.1.1 Participants

A total of 42 participants took part in this experiment, who were graduate students in the Gina Cody School of Engineering and Computer Science, Concordia University. A gift card of CAD100 was given as compensation to the best design. Three participants were excluded from data analysis since

they have not completed all the experiments. Eleven participants were excluded from data analysis due to technical errors such as missing markers. One participant was excluded from data analysis due to large electrode impedances and poor data quality. The final samples included 27 participants (8 women, 19 men) aged from 24 to 39. All participants had normal or corrected-to-normal vision. The experimenters helped subjects wear the HRV chest strap, GSR finger strap, respiration rate belt and EEG cap. The experimenters briefed each participant the experimental tasks; impedance of all the EEG electrodes was below 10 kΩ; participants completed the experiment by following the experimental procedures specified in the experimental design. EEG signals were recorded by a 64 channel BrainVision actiCHamp at 500 Hz during the experiment. The EEG was referenced to Cz and the electrode placement was based on the international 10-10 system. The experimental protocol was approved by Human Research Ethics Committee (HREC) of Concordia University. All sections of the experiment were performed in accordance with relevant guidelines and regulations. All subjects signed the informed consent form before taking the experiment.

5.1.2 Results on EEG microstate analysis

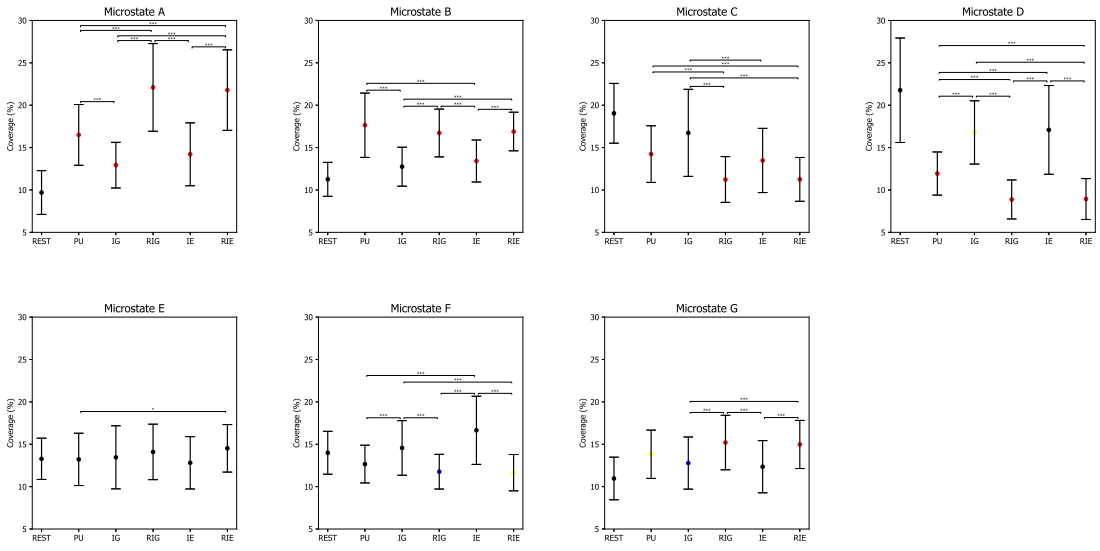

Figure 5.1: Microstate coverage during rest (REST), problem understanding (PU), idea generation (IG), rating idea generation (IE), idea evaluation (IE), and rating idea evaluation (RIE). P-values between rest and other conditions are annotated by black dots ($p > 0.050$), blue dots ($p \leq 0.050$), yellow dots ($p \leq 0.010$), and red dots ($p \leq 0.005$). P-values between conditions are annotated by $^{*}(p \leq 0.050)$, $^{**}(p \leq 0.010)$, $^{***}(p \leq 0.005)$.

Figure 5.1 shows the error bars of microstate coverage in each tested condition. In particular, the coverage of microstate class A was the lowest during REST compared to during PU, IG, RIG, IE, and RIE ($p = 0.000$), while the coverage of microstate class B was the lowest during REST compared to PU, RIG, IE, and RIE ($p < 0.005$). Similarly, the coverage of microstate class G was the lowest during REST compared to during PU, IG, RIG, and RIE ($p < 0.040$). On the contrary, the coverage of microstate class C was the highest during REST compared to during PU, RIG, IE, and RIE ($p < 0.001$), while the coverage of microstate class D was the highest during REST compared to PU, IG, RIG, and RIE ($p < 0.009$). The coverage of microstate class F was higher during REST compared to during RIG and RIE ($p < 0.021$). In addition, the coverage of microstate class A decreased significantly from RIG and RIE to PU, IG, and IE ($p < 0.001$), as well as from PU to IG ($p = 0.001$). The coverage of microstate class B increased significantly from IG and IE to PU, RIG, and RIE ($p < 0.001$). The coverage of microstate class C decreased significantly from IG

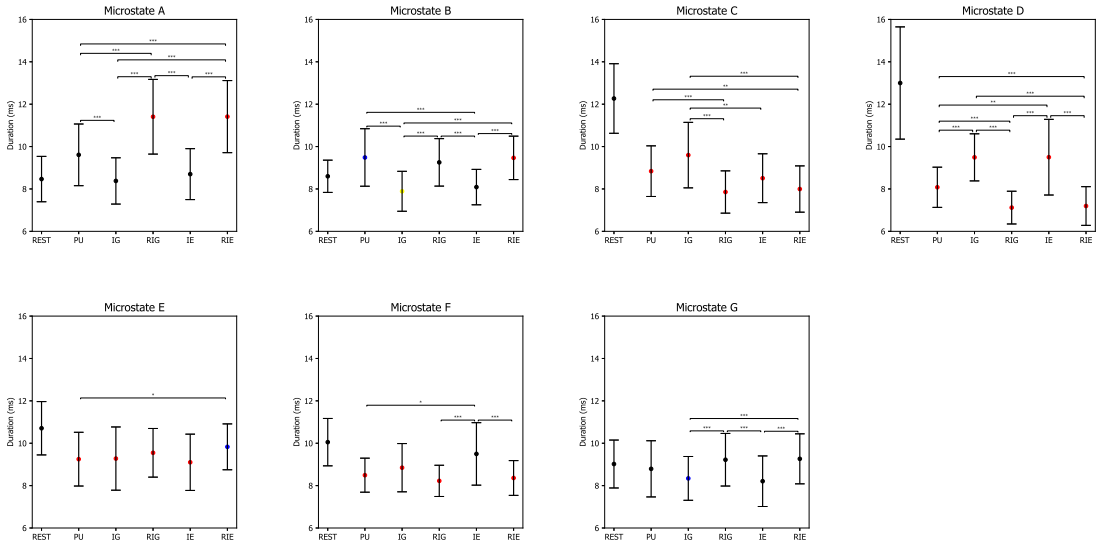

Figure 5.2: Microstate duration during rest (REST), problem understanding (PU), idea generation (IG), rating idea generation (IE), idea evaluation (IE), and rating idea evaluation (RIE). P-values between rest and other conditions are annotated by black dots ($p > 0.050$), blue dots ($p \leq 0.050$), yellow dots ($p \leq 0.010$), and red dots ($p \leq 0.005$). P-values between conditions are annotated by $^{*}(p \leq 0.050)$, $^{**}(p \leq 0.010)$, $^{***}(p \leq 0.005)$.

Figure 5.2 shows the error bars of microstate duration under each condition. In particular, the duration of microstate class A was lower during REST compared to during RIG and RIE ($p = 0.000$). The duration of microstate class B was lower during REST compared to during PU ($p =$

0.044), whereas it was higher during REST compared to during IG ($p = 0.007$). The duration of microstate classes C, D and E was the lowest during REST compared to PU, IG, RIG, IE, and RIE ($p < 0.002$). The duration of microstate class F was higher during REST compared to during PU, IG, RIG, and RIE ($p < 0.004$). The duration of microstate class G was higher during REST compared to that during IG ($p = 0.027$). Besides, the duration of microstate class A decreased significantly from RIG and RIE to PU, IG, and IE ($p < 0.001$), as well as from PU to IG ($p = 0.001$). The duration of microstate class B increased significantly from IG and IE to PU, RIG, and RIE ($p < 0.001$). The duration of microstate class C decreased significantly from PU to RIG and RIE ($p < 0.007$), as well as from IG to RIG, IE, and RIE ($p < 0.006$). The duration of microstate class D decreased from PU to RIG and RIE ($p < 0.002$), as well as from IG and IE to PU, RIG, and RIE ($p < 0.001$). The duration of microstate class E decreased significantly from RIE to PU ($p = 0.018$). The duration of microstate class F decreased significantly from IE to PU, RIG, and RIE ($p < 0.034$). The duration of microstate class G decreased significantly from RIG and RIE to IG and IE ($p < 0.001$).

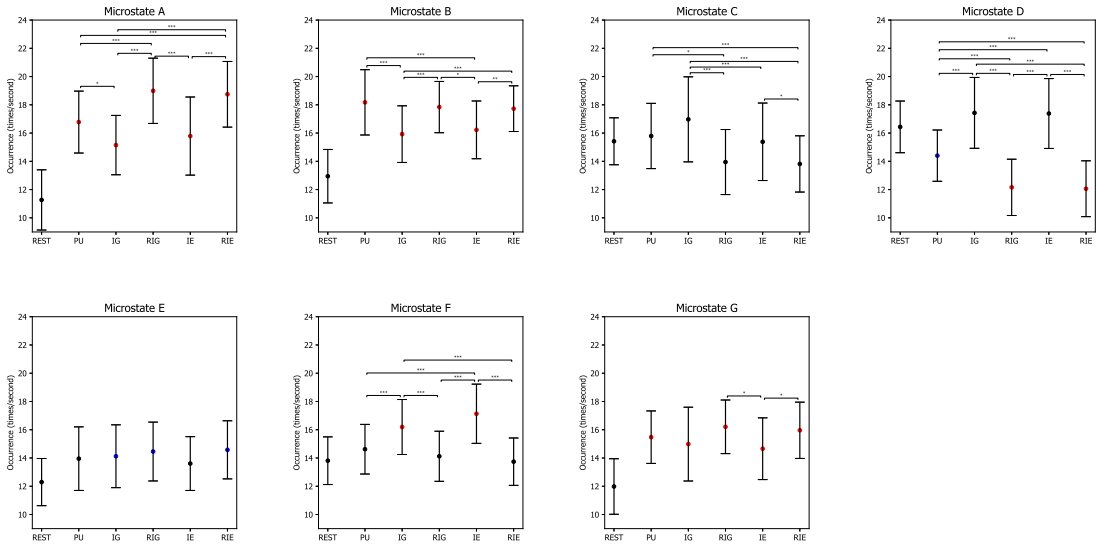

Figure 5.3: Microstate occurrence during rest (REST), problem understanding (PU), idea generation (IG), rating idea generation (IE), idea evaluation (IE), and rating idea evaluation (RIE). P-values between rest and other conditions are annotated by black dots ($p > 0.050$), blue dots ($p \leq 0.050$), yellow dots ($p \leq 0.010$), and red dots ($p \leq 0.005$). P-values between conditions are annotated by $^{*}(p \leq 0.050)$, $^{**}(p \leq 0.010)$, $^{***}(p \leq 0.005)$.

Figure 5.3 shows the error bars of microstate occurrence under each tested condition. In particular, the occurrence of microstate classes A, B, and G increased significantly from REST to PU, IG, RIG, IE, and RIE ($p = 0.000$). Similarly, the occurrence of microstate class E increased significantly from REST to IG, RIG, and RIE ($p < 0.043$), while the occurrence of microstate class F increased significantly from REST to IG and IE ($p = 0.000$). On the contrary, the occurrence of microstate class D decreased significantly from REST to PU, RIG, and RIE ($p < 0.011$). In addition, the occurrence of microstate class A decreased significantly from RIG and RIE to PU, IG, and IE ($p < 0.003$), as well as from PU to IG ($p = 0.014$). The occurrence of microstate class B increased significantly from IG and IE to PU, RIG, and RIE ($p < 0.011$). The occurrence of microstate class C decreased significantly from PU to RIG and RIE ($p < 0.014$), from IG to RIG, IE, and RIE($p < 0.002$), as well as from IE to RIE ($p = 0.016$). The occurrence of microstate class D decreased significantly from PU to RIG and RIE ($p < 0.001$), as well as from IG and IE to PU, RIG, and RIE ($p < 0.001$). The occurrence of microstate class F decreased significantly from IG and IE to PU, RIG, and RIE ($p < 0.001$). The occurrence of microstate class G increased significantly from IE to RIG and RIE ($p < 0.047$).

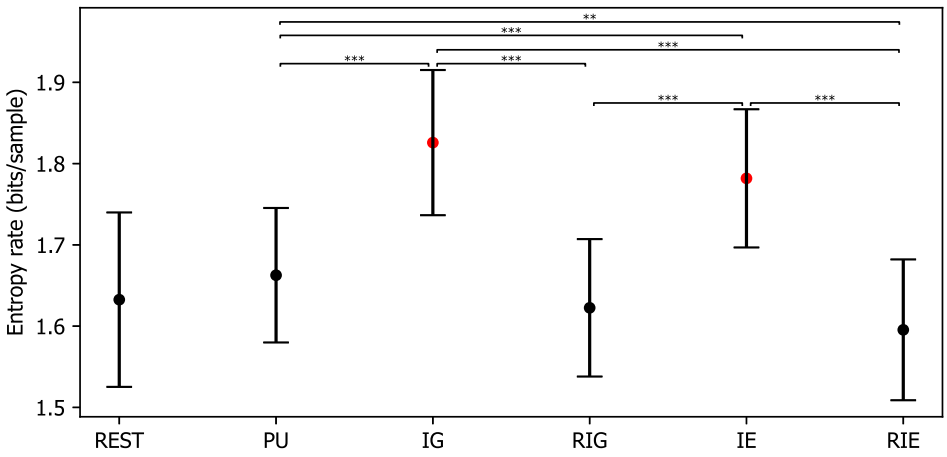

Figure 5.4: Entropy rate of microstate sequences during rest (REST), problem understanding (PU), idea generation (IG), rating idea generation (IE), idea evaluation (IE), and rating idea evaluation (RIE). P-values between rest and other conditions are annotated by black dots ($p > 0.050$), blue dots ($p \leq 0.050$), yellow dots ($p \leq 0.010$), and red dots ($p \leq 0.005$). P-values between conditions are annotated by $^{*}(p \leq 0.050)$, $^{**}(p \leq 0.010)$, $^{***}(p \leq 0.005)$.

In addition, the finite entropy rate was computed as one of the temporal dependency features of

the generated microstate sequences in this study. The computed entropy rate was 1.633 bits/sample (SE = 0.021) for REST, 1.663 bits/ sample (SE = 0.016) for PU, 1.826 bits/sample (SE = 0.018) for IG, 1.623 bits/sample (SE = 0.017) for RIG, 1.782 bits/sample (SE = 0.017) for IE, and 1.595 bits/sample (SE = 0.017) for RIE, when considering the previous 6 microstate labels. The repeated measures ANOVA revealed a significant effect CONDITION ($F(3.237, 84.153) = 40.629$, $p = 0.000$, $\eta^2 = 0.610$). Post hoc paired t tests with Bonferroni correction as shown in Figure 5.4 indicated that the entropy rate was higher during IG and IE compared to during REST, PU, RIG, and RIE ($p < 0.001$), while the entropy rate was higher during PU compared to during RIE ($p = 0.006$).

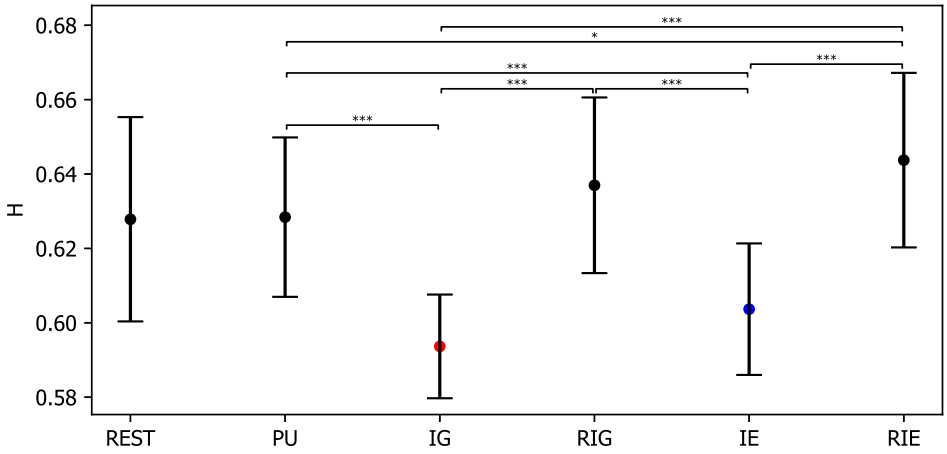

Figure 5.5: Hurst exponent of microstate sequences averaged from 35 partitions during rest (REST), problem understanding (PU), idea generation (IG), rating idea generation (IE), idea evaluation (IE), and rating idea evaluation (RIE). P-values between rest and other conditions are annotated by black dots ($p > 0.050$), blue dots ($p \leq 0.050$), yellow dots ($p \leq 0.010$), and red dots ($p \leq 0.005$). P-values between conditions are annotated by $^{*}(p \leq 0.050)$, $^{**}(p \leq 0.010)$, $^{***}(p \leq 0.005)$.

the Hurst exponent averaged from 35 partitions was 0.628 (SE = 0.005) for REST, 0.628 (SE = 0.004) for PU, 0.594 (SE = 0.003) for IG, 0.637 (SE = 0.005) for RIG, 0.604 (SE = 0.003) for IE, and 0.644 (SE = 0.005) for RIE. The repeated measures ANOVA revealed a significant effect CONDITION ($F(3.276, 85.182) = 24.696$, $p = 0.000$, $\eta^2 = 0.487$). Post hoc paired t tests with Bonferroni correction as shown in Figure 5.5 revealed that the Hurst exponent was significantly lower during IG and IE compared to during REST, PU, RIG, and RIE ($p < 0.041$), while the Hurst exponent was significantly lower during PU compared to during RIE ($p = 0.025$).

In the meantime, the entropy rate and Hurst exponent were computed for comparing between

each of the six runs under each tested condition as shown in Figure 5.6 and Figure 5.7 respectively. Even through this task-wise comparison was not covered in the published paper (Jia et al., 2021), the results could shed light on how designers' mind changes as the design process continues. Further research is needed to continue with this direction.

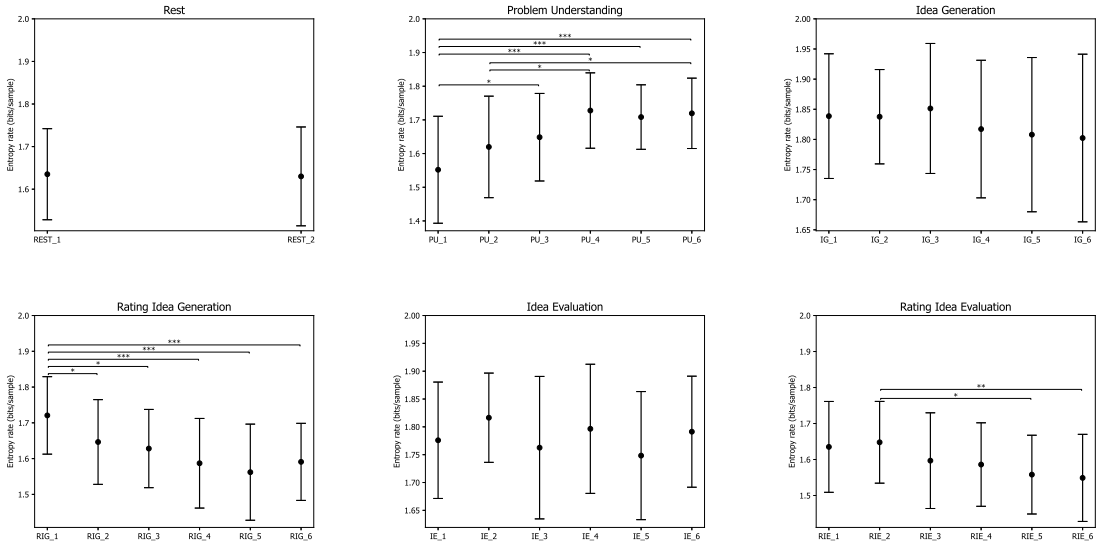

Figure 5.6: Entropy rate of microstate sequences during each run for each tested condition (rest (REST), problem understanding (PU), idea generation (IG), rating idea generation (IE), idea evaluation (IE), and rating idea evaluation (RIE)). P-values between rest and other conditions are annotated by black dots ($p > 0.050$), blue dots ($p \leq 0.050$), yellow dots ($p \leq 0.010$), and red dots ($p \leq 0.005$). P-values between conditions are annotated by $^{*}(p \leq 0.050)$, $^{**}(p \leq 0.010)$, $^{***}(p \leq 0.005)$.

5.1.3 Quantification of cognitive control under different design activities

The quantification of cognitive control was quantified combining the results obtained from EEG microstate analysis and task-related power (TRP) analysis. The EEG microstate parameters indicated that IG was associated with the most microstate C than other design activities, supported by the coverage, duration, and occurrence of microstate C. Moreover, the temporal dependencies on the microstate sequences showed the maximum entropy rate and the lowest Hurst exponent during IG in comparison with other design activities. In our framework, the increasing entropy rate and the decreasing Hurst exponent is mediated by a relaxation of cognitive control mechanisms.

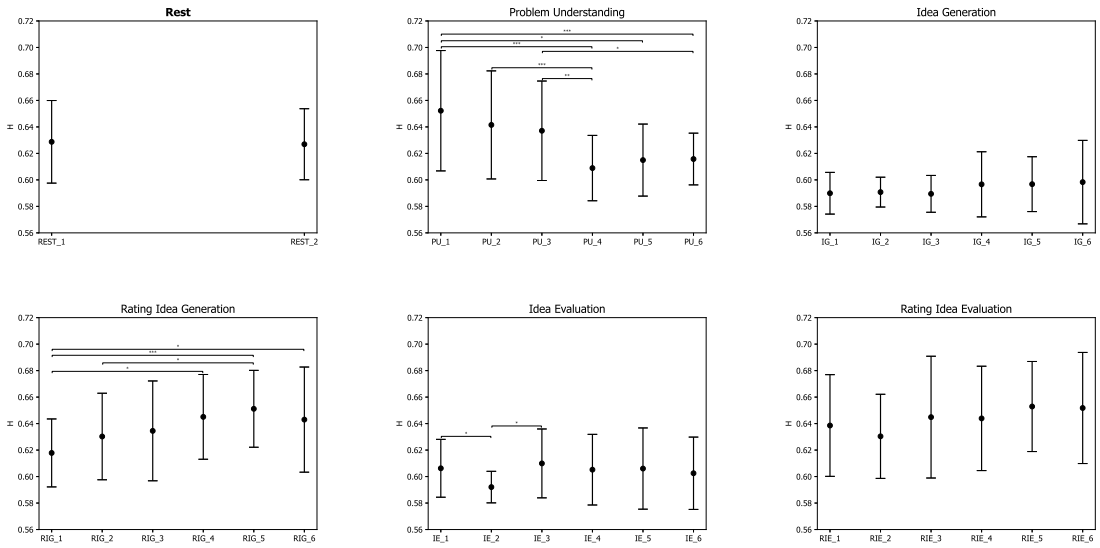

Figure 5.7: Hurst exponent of microstate sequences during each run for each tested condition (rest (REST), problem understanding (PU), idea generation (IG), rating idea generation (IE), idea evaluation (IE), and rating idea evaluation (RIE)). P-values between rest and other conditions are annotated by black dots ($p > 0.050$), blue dots ($p \leq 0.050$), yellow dots ($p \leq 0.010$), and red dots ($p \leq 0.005$). P-values between conditions are annotated by $^{*}(p \leq 0.050)$, $^{**}(p \leq 0.010)$, $^{***}(p \leq 0.005)$.

The TRP analysis in delta, theta, and beta bands suggests differences among three groups of experimental conditions, which are IG, IE, and PU/RIG/RIE. It was found that delta, theta, and beta power increased over frontal sites from REST to PU/RIG/RIE and IE, whereas they decreased over all sites from REST to IG. A comparison within design activities indicated that delta, theta, and beta power increased significantly over almost all sites from IG to IE, and PU/RIG/RIE, as well as from IE to PU/RIG/RIE, while delta, theta, and beta power did not show significant differences over almost all sites in PU/RIG/RIE. Increased theta power over the frontal sites has been viewed as a function of working memory and cognitive control. Generally, increased frontal theta activity has been interpreted as a need for increased cognitive control in response to conflict (Cavanagh & Frank, 2014; Cavanagh, Zambrano-Vazquez, & Allen, 2012), encoding and retrieval of information from working memory (Karakaş, 2020; Sauseng, Griesmayr, Freunberger, & Klimesch, 2010), while increased beta activity is associated with the maintenance of intended status quo (Engel & Fries, 2010). Besides, increases in delta power have been associated with heightened attention during mental tasks. In summary, EEG microstate analysis and TRP analysis revealed that IG triggered the least cognitive control among the tested five design activities.

5.1.4 Quantification of cognitive workload under different design activities

Cognitive workload was quantified by the task-related power (TRP) results on alpha band, which is then compared to the subjective rating results obtained from NASA-TLX. The TRP analysis results on alpha band suggests differences among three groups of experimental conditions, which are IG, IE, and PU/RIG/RIE. It was found that IG, IE, and PU/RIG/RIE were associated with decreases in alpha power while the degree of decreases in alpha power was the largest over almost all sites during IG, followed by during IE and PU/RIG/RIE. Alpha power has been considered as a reliable indicator of cognitive workload (Fink et al., 2005) where the extent of decreases in alpha power is associated with increases in cognitive workload (Keil et al., 2006). The TRP results on alpha band indicated that the IG task triggered the highest cognitive workload, followed by IE and PU/RIG/RIE. In the meantime, the obtained NASA-TLX results indicated that mental demand, time demand, effort, and stress decreased significantly from IG to IE, supporting the hypothesis that IG would trigger the highest cognitive workload.

5.1.5 Conclusion

Our research findings can be summarized as below. The results on EEG microstate parameters indicated that microstate C, being negatively associated with the cognitive control network, was more prevalent in idea generation. Furthermore, the EEG microstate sequence analysis indicated that idea generation was consistently associated with the shortest temporal correlation times concerning finite entropy rate, autoinformation function, and Hurst exponent. This finding suggests that the interplay of functional networks appears less restricted while the brain has more degrees of freedom in choosing the next network configuration. In the meantime, the task-related power (TRP) analysis also revealed that idea generation in comparison with other design activities including problem understanding, idea generation, idea evaluation, and self-rating, was associated with the highest cognitive workload and lowest cognitive control due to the most significant decreases in theta, alpha, and beta power (Jia et al., 2021). Taken together, the TRP and EEG microstate results support that idea generation would be associated with the highest cognitive workload and lowest cognitive control during a design process.

5.2 An application of tEEG framework beyond design: A pilot training experiment

This study applied the proposed tEEG framework to training process, where trainees' cognitive control and cognitive workload were quantitatively monitor as the skill acquisition process continued (Zhao, Jia, et al., 2022). This study could also serve as a good application example of the proposed tEEG framework beyond the context of design. As mentioned in Chapter 4, when the performance evaluation is not available the evaluation focuses on whether our results are aligned with the literature and if the applied features could lead to a convergent conclusion. A pilot training process is designed to equip students with the knowledge, judgement, and skills required for maintaining aircraft control and responding to critical flight situations. The present research aims to investigate the changes in trainees' cognitive control and cognitive workload along a skill acquisition process while they underwent training on basic flight maneuvers. EEG microstate analysis and spectral power features were applied to assess the variations in trainees' cognitive workload and cognitive control during different stages within a pilot training process. The experimental results indicated that trainees' cognitive workload decreased during the skill acquisition process, whereas their cognitive control improved toward the end of the process. As the study demonstrated, even under varied task demands, EEG microstate features were able to capture improvements in cognitive control throughout the skill acquisition process.

We hypothesized that trainees' cognitive workload would decrease whereas their cognitive control would improve under the same task demands through a skill acquisition process. Aiming to test our hypothesis under a skill acquisition process, a pilot training experiment was designed with a series of preparation steps and a familiarization session before the commencement of EEG data collection. According to the skill acquisition theory (J. R. Anderson, 1982, 1987), trainees could be considered as possessing the declarative knowledge for the upcoming flight tasks throughout the recorded training process under the current experimental settings. In this way, the physiological measures may capture trainees' cognitive changes that could happen during a skill acquisition process as the twenty-two sessions under study corresponded to the proceduralization and automatization of knowledge within a skill acquisition process, where trainees applied the declarative

knowledge in the execution of the target maneuvers through practicing (DeKeyser, 2020). Moreover, the first part of the hypothesis is the decrease in cognitive workload during a skill acquisition process. Given that cognitive workload describes the balance between the task demands and the available resources to the confronted task (Welford, 1978; Young et al., 2015), skill acquisition adds to the available resources leading to a decreased cognitive workload with unvaried task demands. The other part of the hypothesis is that cognitive control may improve along a skill acquisition process. Enhanced cognitive control has been associated with improvements in information processing, reasoning, planning, and decision-making (J. D. Cohen, 2017; Musslick & Cohen, 2021), all of which could happen as the skill acquisition process continues. In the context of pilot training, the aforementioned cognitive changes are well aligned with the expected changes in trainees after a training process. Therefore, we tested the hypothesis by assessing and comparing trainees' cognitive workload and cognitive control when they were performing the same Baseline tasks along the tested pilot training process. To be more precise, STAGE comparisons were conducted by dividing the twenty-two Baseline tasks within the pilot training process into three stages: Training stage, PracticeA stage, and PracticeB stage. In the meantime, paired comparisons were conducted between Baseline tasks and Trial tasks within the same stage to align our results with the effect of varied task demands on cognitive workload and cognitive control reported in the literature. And the effect of skill acquisition through our pilot training process was tested based on the quantitative assessment results. Furthermore, STAGE comparisons were also conducted on the twenty-two Trial tasks to see whether we will still be able to observe the same effect of skill acquisition on trainees' cognitive workload and cognitive control under varied task demands.

5.2.1 Experiment and participants

The experiment was conducted on a custom aircraft flight simulator built by Marinvent Corporation. Aircraft dynamics reflected a Boeing 737 and were modelled using XPlane 11 from Laminar Research on a computer running the Windows operating system. The simulator controls included a yoke, pedals, rudder and throttle quadrant. During this experiment, participants did not have an out-the-window view. Instead they referred to only a primary flight display (PFD) shown Figure 5.8 for

knowledge of the aircraft attitude, altitude, heading, climb rate and speed. Participants used the aircraft yoke to control aircraft pitch and roll. An autopilot controlled throttles (for speed maintenance) and pedals (for turn coordination). As a result, participants operated only the yoke.

To equip the participants with a basic understanding of the flight instruments and flight maneuvers, a few preparation steps were added before the commencement of the pilot training process in this experiment. Participants were asked to read a flight briefing presentation, watch four training videos, and take a familiarization session accompanied by the test director in the selected simulator to practice the basic maneuvers presented in the videos. They outline the Yoke as a flight control and its effects on pitch and roll to control the desired parameters. How to interpret control and performance indications on the PFD as well as some basic strategies were also covered.

Once the pilot training process started, participants' physiological data and learning behaviours were recorded till the end of the experiment by the National Research Council's Integrated Physiological Monitoring (IPM) (Law A & S., 2017) and synchronised with the aircraft simulator using a network time protocol server. An iPad located to the left of the participant presented task instructions and collected NASA-TLX ratings and other questionnaire data (e.g. fatigue ratings). Instructions were presented and data were collected using Qualtrics software. The recorded physiological data includes: Electroencephalogram (EEG), Electrocardiogram (ECG), Galvanic Skin Response (GSR), and Eye tracking, while participants' learning behaviors were recorded in the training devices together with three cameras placed at the top, front and side of the participants. EEG data was collected using a 64-channel BioSemi ActiveTwo system placed according to the international 10–20 system at a sampling rate of 2048 Hz. The results from other recorded physiological data were not included in this research. For comparative analysis, subjective real-time evaluation by an instructor was not possible due to COVID-19 health restrictions but was conducted post-experiment by a review of parametric data and video of the sessions.

Twenty-four participants aged between 21-41 (11 males, 13 females) were recruited to conduct the experiments. All participants reported to be in general good health without any neurological or psychiatric disorder. In addition, all participants had normal vision or could achieve normal vision with contact lenses, as glasses were not accepted for this experiment. Each participant received $100 CAD compensation together with $80 CAD as trip compensation after completing the experiments.

Figure 5.8: Flight instrument example

All participants signed the informed consent forms before taking the experiment and filled out a questionnaire related to the training tasks, based on which the experimenters may interview the participants for more information. Participants were asked to rest for two minutes with their eyes open and closed right before the training process. The pilot training process consists of twenty-two sessions and the instructions for the required maneuvers were displayed on an iPad placed in front of the participants under the supervision of the Test Director. The experimental protocol was approved by the Concordia Human Research Ethics Committee as well as the research ethics board of the National Research Council Canada.

During each session, the participants were instructed to complete a Baseline task during 30 seconds, a Trial task during 90 seconds, and a NASA-TLX questionnaire on the iPad to rate their perceived workload before moving on to the next session. All maneuvers requested in Baseline tasks were the same and the participant maintained straight and level flight at a constant heading and altitude. Following the baseline, the simulator was paused and the participant read the twizzle instructions and moved to the Trial stage. The maneuvers requested in Trial tasks varied in difficulty on three levels:

- Level 1: a climb, descent, or turn in one direction.
- Level 2: a climb, descent, or turn with reversal.
- Level 3: a climb or descent with reversal combined with a turn in one direction; or a turn with reversal combined with a climb or descent.

Those twenty-two sessions were divided into three stages to better monitor different stages during a training process, which are denoted as Training (7 Baseline and 7 Trial tasks), PracticeA (8 Baseline and 8 Trial tasks), and PracticeB (7 Baseline and 7 Trial tasks) in chronological order. During the Training stage, the test director provided the participant with feedback on their performance and all participants were given the same sequence of maneuvers. By comparison, in the Practice A and Practice B stages, no test instructor feedback was provided and the sequence of maneuvers was pseudo-randomized across participants. Specifically, maneuvers were presented in blocks of three that contained one twizzle from each of Level 1, Level 2 and Level 3 difficulties. Moreover, the first Trial task in a new block could not be the same level as the last Trial task of the previous block.

5.2.2 Pre-processing for data collected from loosely controlled experiment

The EEGLAB toolbox was applied during pre-processing for removing noises and artifacts from the EEG data (Delorme & Makeig, 2004). The collected EEG data were referenced to mastoids and then filtered between 1 and 40Hz using a zero-phase Hamming windowed-sinc FIR filter. Afterward, the channels that satisfied one or more criteria below were isolated as bad channels. The applied criteria for bad channel detection include: 1) the channel kept flat for more than 5 seconds; 2) the correlation between the channel and its nearby channels is smaller than 0.8; and 3) the amplitude of the channel was greater than 3 standard deviation from the mean. For artifact removal, the multiple artifact rejection algorithm (MARA) was applied where the IC components having more than 40% chance to be labelled as artifacts (eye-blink, eye-movement, muscle-generated, and other artifacts) were removed. Moreover, the signals were segmented in 2-second epochs for detecting bad segments and bad local channels within each segment (Gabard-Durnam, Mendez Leal, Wilkinson, & Levin, 2018). The detected bad segments were rejected and the bad local channels detected by applying FASTER

(Nolan, Whelan, & Reilly, 2010) criteria were interpolated using spherical splines. Finally, the obtained clean signals were re-referenced to average reference and downsampled to 250Hz.

5.2.3 Clustering-based segmentation: EEG microstate analysis

The seven microstate classes (A, B, C, D, E, F, G) were computed following the approach proposed in (Pascual-Marqui et al., 1995). The Global Field Power (GFP) of the pre-processed EEG data was computed for each task at each stage and only the EEG data at the computed GFP peaks were sent to the modified k-means algorithm with the cost function defined in Eq. (7). We applied 100 repetitions to select the optimal microstate classes based on the cross-validation defined in Eq. (8) from the microstate classes computed from each repetition.

$$F = \frac{1}{N_T(N_S-1)} \sum_{t=1}^{N_T} ||V_t - \sum_{k=1}^{N_K} a_{kt}\Gamma_k||^2, \tag{7}$$

$$CV = \frac{\sum_{t=1}^{N_T}(V_t' \cdot V_t - (V_t' \cdot \Gamma_k)^2)}{N_T(N_S-1)} \cdot (\frac{N_S-1}{N_S-1-N_K})^2, \tag{8}$$

where N_T is the sample length, V_t is a $N_S \times 1$ vector consisting of the electric potential at time point t, N_K is the number of microstate classes, Γ_k is a normalized $N_S \times 1$ vector representing the k-th microstate class, a_{kt} is the intensity of the k-th microstate class at the time point t.

Afterward, a full permutation procedure was applied to compute the group-wise microstate classes from the microstate classes obtained in each participtant's single task, which were denoted as the global microstate classes. The global microstate classes were then used to represent the pre-processed EEG data in the time domain by assigning one of the global microstate classes to each time point. During this fitting back process, the highest spatical correlation was used as the criterion for mocrostate class assignment and the polarity of the microstate classes was ignored. Furthermore, no smoothing parameters were applied in our analysis to avoid any modification to the temporal dynamics of the generated microstate sequences.

5.2.4 Segment-wise analysis

- **EEG microstate features**

  Three microstate parameters were computed for the 44 microstate sequences generated for each participant's different tasks during varied stages. The three parameters were duration, occurrence, and coverage, which were used to describe at an average level how long a microstate could remain stable, how many times a microstate appeared per second, and the fraction of the total analysis time covered by a microstate, perspectively.

  Moreover, a finite estimate of the entropy rate (Von Wegner, 2018) and Hurst exponent estimated by detrended fluctuation analysis (DFA) (Peng, Havlin, Stanley, & Goldberger, 1995) were applied to measure the temporal dependencies of different microstates in this research. In particular, the entropy rate was computed to measure the short-range temporal dependencies, whereas the computed Hurst exponent aimed to measure the long-range temporal dependencies (Jia & Zeng, 2021). Moreover, the generated microstate sequences needed to be mapped intro the metric space $S_0 = \{-1, +1\}$ before applying DFA for Hurst exponent computation. A total of 35 partitions were obtained for the seven microstate classes, and the Hurst exponent was computed for the mapped sequences generated under each partition. Therefore, the arithmetic average of the Hurst exponents computed from 35 partitions was used in this research to describe the long-range temporal dependencies.

- **Spectral analysis**

  The power spectral density (PSD) was estimated by applying the Welch periodogram method with 50% overlapping Hamming windows of a length of 2 seconds to the pre-processed EEG data. Afterward, the theta band (4-7.5 Hz) power and alpha band (8-12.5 Hz) power (García-Martínez, Martinez-Rodrigo, Alcaraz, & Fernández-Caballero, 2019) were computed from the PSD for each Trial task and Baseline task within the tested training process (22 Trial tasks, and 22 Baseline tasks). Under each task, the band powers at 64 EEG channels were then grouped into five cortical areas (frontal, central, temporal, parietal, and occipital) (Agnoli, Zanon, Mastria, Avenanti, & Corazza, 2020; Jia & Zeng, 2021) for including AREA comparisons in repeated measures ANOVA.

- **Statistical anlaysis**

  The EEG spectral power changes in theta and alpha bands were analyzed separately by a 2 (TASK) $\times 3$ (STAGE)$\times 5$ (AREA) repeated measures ANOVA. The three within subject factors were TASK (Baseline and Trial), STAGE (Training, PracticeA, and PracticeB), and AREA (Frontal, Central, Temporal, Parietal, and Occipital). Greenhouse-Geisser correction was applied in the case of sphericity violations. Post hoc paired t-test was conducted at each tested AREA between TASK and between STAGE and Bonferroni correction was applied for multiple comparisons.

  For each of the computed EEG microstate parameters (coverage, occurrence, and duration), a 2 (TASK) $\times 3$ (STAGE)$\times 7$ (CLASS) repeated measures ANOVA was applied to analyze the effects of different factors. The three within subject factors were TASK (Baseline and Trial), STAGE (Training, PracticeA, and PracticeB), and CLASS (A, B, C, D, E, F, and G). Greenhouse-Geisser correction was applied in the case of sphericity violations. Post hoc paired t-test was conducted at each microstate CLASS between TASK and between STAGE and Bonferroni correction was applied for multiple comparisons.

  The temporal dependencies measured by entropy rate and Hurst exponent were analyzed separately by a 2 (TASK) $\times 3$ (STAGE) repeated measures ANOVA. The two within subject factors were TASK (Baseline and Trial) and STAGE (Training, PracticeA, and PracticeB). Greenhouse-Geisser correction was applied in the case of sphericity violations. Post hoc paired t-test was conducted between TASK and between STAGE and Bonferroni correction was applied for multiple comparisons.

5.2.5 Results on performance evaluation, EEG spectral analysis, and EEG microstate analysis

Performance evaluation results

The performance evaluation of each trial and baseline used a combination of qualitative and quantitative assessment. The evaluator looked at each trial and baseline and measured them along three dimensions; the quality of the dataset, a quantitative assessment of performance in accomplishing

the task, and a descriptive analysis of the trainee's actions during the trial. The scale of the grading level was selected by a panel of two instructors and tailored to the expected level of performance of ab-initio trainees for each parameter. A single qualified instructor was used to evaluate trainee's performance attempt to minimize variations in assessments.

Among the three evaluated dimensions, the quality of the dataset can be reflected in the results on quantitative assessment of the trainees' performance, whereas the descriptive analysis provides additional information that may explain for the trainee's good or bad performance. Therefore, this research only focused on the quantitative assessment dimension to reflect trainees' performance evaluation results throughout the training process. The quantitative assessment was composed of five dimensions in total including three types of performance (heading, altitude, and rate climb/descent) and three types of control management evaluations (roll and pitch), which were denoted as P-H, P-A, P-R, C-R, and C-P in Table 5.1 and 5.2.

Table 5.1: Averaged results for each performance evaluation dimension under Baseline and Trial tasks.

Mean (SE)	Training		PracticeA		PracticeB	
	Baseline	Trial	Baseline	Trial	Baseline	Trial
P-H	3.88 (0.042)	3.68 (0.066)	3.98 (0.012)	3.72 (0.000)	4.00 (0.000)	3.77 (0.065)
P-A	3.73 (0.067)	3.13 (0.124)	3.92 (0.034)	3.34 (0.098)	3.89 (0.036)	3.50 (0.091)
P-R	2.92 (0.140)	2.36 (0.107)	3.21 (0.118)	2.38 (0.121)	3.27 (0.121)	2.49 (0.121)
C-R	3.83 (0.047)	3.38 (0.082)	3.93 (0.030)	3.27 (0.087)	3.99 (0.008)	3.46 (0.066)
C-P	2.83 (0.158)	2.21 (0.110)	3.16 (0.132)	2.27 (0.095)	3.23 (0.119)	2.27 (0.124)

The quantitative assessment decreased significantly from Baseline tasks to Trial tasks for all the five evaluated dimensions throughout the training process (including Training, PracticeA, and PracticeB stages) as shown in Figure 5.9a-5.9e. The averaged evaluation results are listed in Table 5.1 and the related p-values for paired TASK comparisons can be found in Table 5.2. As for STAGE comparisons on Baseline tasks, significant increases from Training to PracticeA stage were observed under three evaluated dimensions, namely performance (altitude) (Figure 5.9b), performance (rate climb/descent) (Figure 5.9c), and control management (pitch) (Figure 5.9e). In the meantime, such significant increases were also observed from Training to PracticeB stages for all the five evaluated dimensions (Figure 5.9a-5.9e) when trainees were conducting Baseline tasks. As for STAGE comparisons on Trial tasks, performance (altitude) was the only dimension that showed

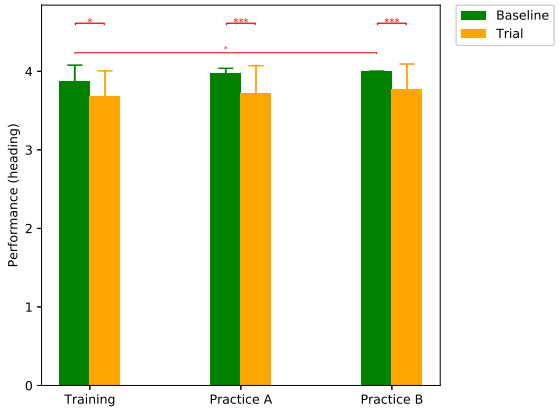

(a) Performance (heading)

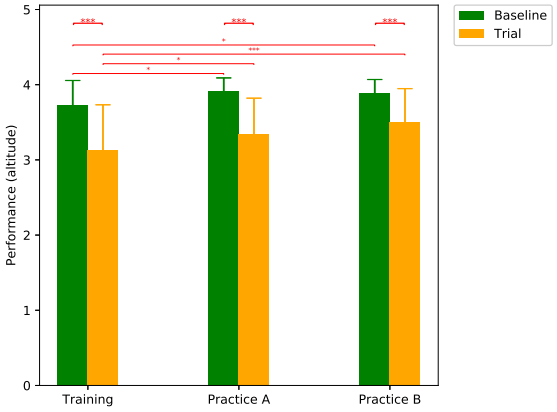

(b) Performance (altitude)

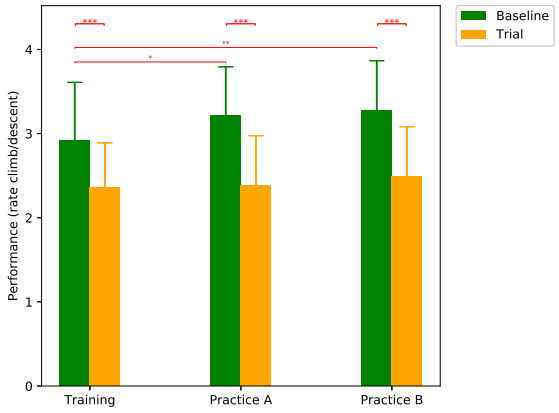

(c) Performance (rate climb/descent)

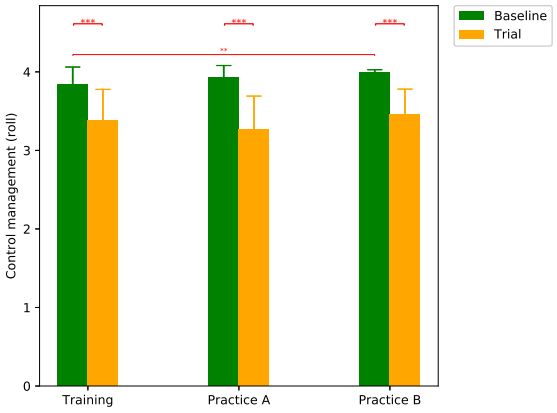

(d) Control management (roll)

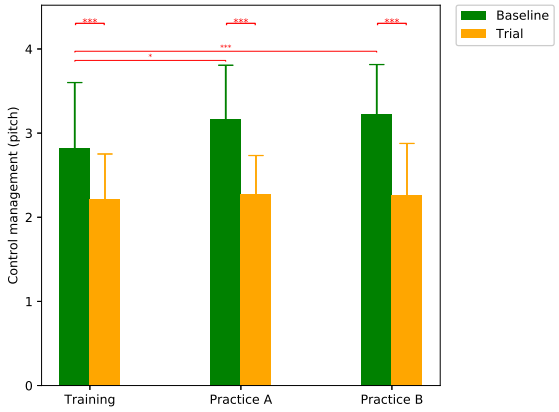

(e) Control management (pitch)

Figure 5.9: Quantitative assessment on each dimension with P-values for TASK and STAGE comparisons annotated by $^{*}(p \leq 0.050)$, $^{**}(p \leq 0.010)$, $^{***}(p \leq 0.005)$

Table 5.2: P-values for paired TASK and STAGE comparisons on each performance evaluation dimension.

Comparison	Dimension				
	P-H	P-A	P-R	C-R	C-P
S1:B-T	0.021^{*} ↘	0.0^{***} ↘	0.0^{***} ↘	0.0^{***} ↘	0.0^{***} ↘
S2:B-T	0.001^{***} ↘	0.0^{***} ↘	0.0^{***} ↘	0.0^{***} ↘	0.0^{***} ↘
S3:B-T	0.002^{***} ↘	0.0^{***} ↘	0.0^{***} ↘	0.0^{***} ↘	0.0^{***} ↘
B:S1-S2	0.072	0.017^{*} ↗	0.039^{*} ↗	0.148	0.016^{*} ↗
B:S1-S3	0.022^{*} ↗	0.021^{*} ↗	0.006^{**} ↗	0.009^{**} ↗	0.002^{***} ↗
B:S2-S3	0.311	1.0	1.0	0.23	1.0
T:S1-S2	1.0	0.046^{*} ↗	1.0	0.463	1.0
T:S1-S3	0.567	0.001^{***} ↗	0.942	1.0	1.0
T:S2-S3	1.0	0.066	0.949	0.13	1.0

* $\rho \leq 0.050$, ** $\rho \leq 0.010$, *** $\rho \leq 0.005$
↗ Quantitative assessment increases
↘ Quantitative assessment decreases

significant increases from Training to PracticeA as well as from Training to PracticeB stage (Figure 5.9b). The related p-values for STAGE comparisons with Bonferroni correction are listed in Table 5.2.

Subjective ratings

By averaging the six dimensions, the global score of NASA-TLX for training was 5.85 (SD=0.97), for practiceA was 5.52(SD=0.98), and for practiceB was 5.31(SD=1.03). As shown in Figure 5.10, the results of NASA-TLX revealed that trainees' cognitive workload decreases during the tested pilot training process. In particular, significant decreases were observed from Training to PracticeA (p=0.038), and from Training to PracticeB (p=0.024) according the post hoc analysis.

EEG spectral power results

In the theta band, the $2 \times 3 \times 5$ repeated measures ANOVA revealed two significant main effects of TASK ($F(1, 23) = 13.110$, $p = 0.001$, $\eta^2 = 0.368$) and AREA ($F(4, 92) = 34.337$, $p = 0.000$, $\eta^2 = 0.600$), as well as one significant interaction effect of TASK $\times$ AREA ($F(4, 92) = 15.604$, $p = 0.000$, $\eta^2 = 0.420$). Figure 5.11 presents the comparison results on TASK and STAGE on each brain area. And the p-values for pairwise comparisons of theta spectral power with Bonferroni correction on each area are listed in Table 5.3, where $B-$ and $T-$ represent the two TASK types,

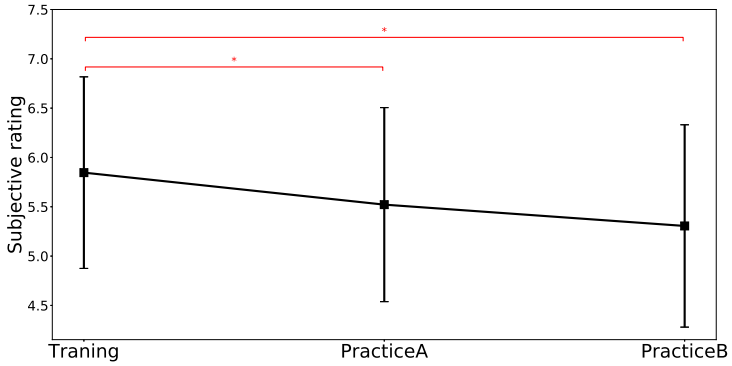

Figure 5.10: NASA-TLX subjective rating results for STAGE comparison (Training, PracticeA, and PracticeB). P-values for STAGE comparisons are annotated by $^{*}(p \leq 0.050)$, $^{**}(p \leq 0.010)$, $^{***}(p \leq 0.005)$

namely Baseline tasks and Trial tasks respectively), whereas $S1$, $S2$, and $S3$ correspond to Training, PracticeA, and PracticeB stages respectively. As shown in Figure 5.11, trainees' theta spectral power decreased significantly from Baseline tasks to Trial tasks over frontal sites under PracticeA stage and PracticeB stage, over central sites for all three stages (Training, PracticeA, and PracticeB), and over temporal sites under PracticeA stage and PracticeB stage. In the meantime, significant increases of theta band powers were observed from Baseline tasks to Trial tasks over parietal and occipital sites under Training stage, PracticeA stage, and PracticeB stage. As for STAGE comparison on Baseline tasks, the spectral power results in theta band showed significant increases from Training stage to PracticeA stage over central, temporal, parietal, and occipital sites, as well as from Training stage to PracticeB stage over frontal, central, and temporal sites. However, no significant changes were observed between different stages while the trainees were conducting Trial tasks over the five brain areas.

In the alpha band, the $2\times3\times5$ repeated measures ANOVA revealed three significant main effects of TASK ($F(1,23) = 45.253$, $p = 0.000$, $\eta^2 = 0.663$), STAGE ($F(2,46) = 4.004$, $p = 0.048$, $\eta^2 = 0.148$), and AREA ($F(4,92) = 35.845$, $p = 0.000$, $\eta^2 = 0.609$), as well as one significant interaction effect of TASK $\times$ AREA ($F(4,92) = 21.992$, $p = 0.000$, $\eta^2 = 0.495$). Figure 5.12 presents the results on TASK comparisons and STAGE comparisons in each brain area, and the p-values for pairwise comparisons of alpha spectral power with Bonferroni correction on each area are listed in Table 5.4. For the TASK comparisons, trainees' alpha band power significantly decreased

Table 5.3: P-values for paired TASK and STAGE comparisons in theta band power.

Comparison	Area									
	Frontal		Central		Temporal		Parietal		Occipital	
S1:B-T	0.094		0.007^{**}	↘	0.086		0.0^{***}	↗	0.0^{***}	↗
S2:B-T	0.0^{***}	↘	0.0^{***}	↘	0.0^{***}	↘	0.0^{***}	↗	0.0^{***}	↗
S3:B-T	0.0^{***}	↘	0.0^{***}	↘	0.003^{***}	↘	0.001^{***}	↗	0.0^{***}	↗
B:S1-S2	0.314		0.019^{*}	↗	0.008^{**}	↗	0.034^{*}	↗	0.02^{*}	↗
B:S1-S3	0.049^{*}	↗	0.048^{*}	↗	0.046^{*}	↗	0.173		1.0	
B:S2-S3	0.317		1.0		1.0		1.0		0.097	
T:S1-S2	0.124		0.3		1.0		1.0		1.0	
T:S1-S3	0.906		1.0		1.0		0.094		1.0	
T:S2-S3	0.828		0.848		1.0		0.174		1.0	

* $\rho \leq 0.050$, ** $\rho \leq 0.010$, *** $\rho \leq 0.005$
↗ Theta band power increases
↘ Theta band power decreases

from Baseline tasks to Trial tasks over frontal and central sites for all the three stages (Training, PracticeA, and PracticeB), whereas significant increases were also observed over parietal sites during Training and PracticeA stages as well as over occipital sites for all the three stages (Training, PracticeA, and PracticeB). As for the STAGE comparisons on Baseline tasks, significant increases in alpha band power were observed from Training stage to PracticeA stage over central sites, as well as from Training stage to PracticeB stage over central and parietal sites. However, no significant changes in alpha band power were observed the STAGE comparisons on Trial tasks.

Table 5.4: P-values for paired TASK and STAGE comparisons in alpha band power.

Comparison	Area									
	Frontal		Central		Temporal		Parietal		Occipital	
S1:B-T	0.029^{*}	↘	0.008^{**}	↘	0.161		0.0^{***}	↗	0.0^{***}	↗
S2:B-T	0.0^{***}	↘	0.0^{***}	↘	0.106		0.0^{***}	↗	0.0^{***}	↗
S3:B-T	0.0^{***}	↘	0.0^{***}	↘	0.09		0.404		0.0^{***}	↗
B:S1-S2	1.0		0.021^{*}	↗	0.108		0.15		0.053	
B:S1-S3	1.0		0.024^{*}	↗	0.067		0.014^{*}	↗	0.612	
B:S2-S3	0.813		1.0		1.0		0.841		1.0	
T:S1-S2	0.255		1.0		0.792		1.0		1.0	
T:S1-S3	0.43		1.0		0.364		0.165		1.0	
T:S2-S3	1.0		1.0		1.0		0.391		1.0	

* $\rho \leq 0.050$, ** $\rho \leq 0.010$, *** $\rho \leq 0.005$
↗ Alpha band power increases
↘ Alpha band power decreases

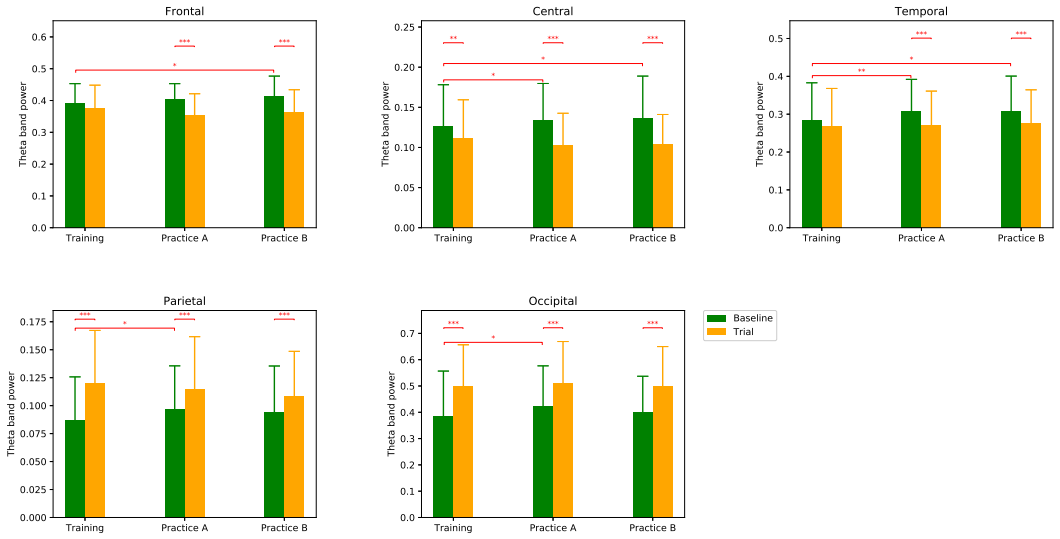

Figure 5.11: EEG theta band power for Baseline tasks and Trial tasks during Training, PracticeA, and PracticeB. P-values for TASK and STAGE comparisons are annotated by $^{*}(p \leq 0.050)$, $^{**}(p \leq 0.010)$, $^{***}(p \leq 0.005)$.

EEG microstate results

Figure 5.13 shows the topographic maps of seven global microstate classes across TASK and across STAGE, as well as for each task type (Baseline or Trial) during different stages, namely Training, PracticeA, and PracticeB. The seven microstate classes were labelled as A, B, C, D, E, F, and G (Custo et al., 2017; Jia & Zeng, 2021; Michel & Koenig, 2018). For Baseline tasks, the seven microstate classes explained 66.685% $(SE = 0.347)$ of the global variance of the original EEG topographies corresponding to peaks of GPF for Training stage, 67.628% $(SE = 0.294)$ for PracticeA stage, 68.749% $(SE = 0.312)$ for PracticeB stage. As for Trial tasks, the seven microstate classes explained 67.127% $(SE = 0.348)$ of the global variance of the original EEG topographies corresponding to peaks of GPF for Training stage, 67.894% $(SE = 0.264)$ for PracticeA stage, 68.342% $(SE = 0.301)$ for PracticeB stage.

The computed EEG microstate parameters include coverage, occurrence, and duration. For microstate coverage analysis, the $2 \times 3 \times 7$ repeated measures ANOVA revealed one significant main

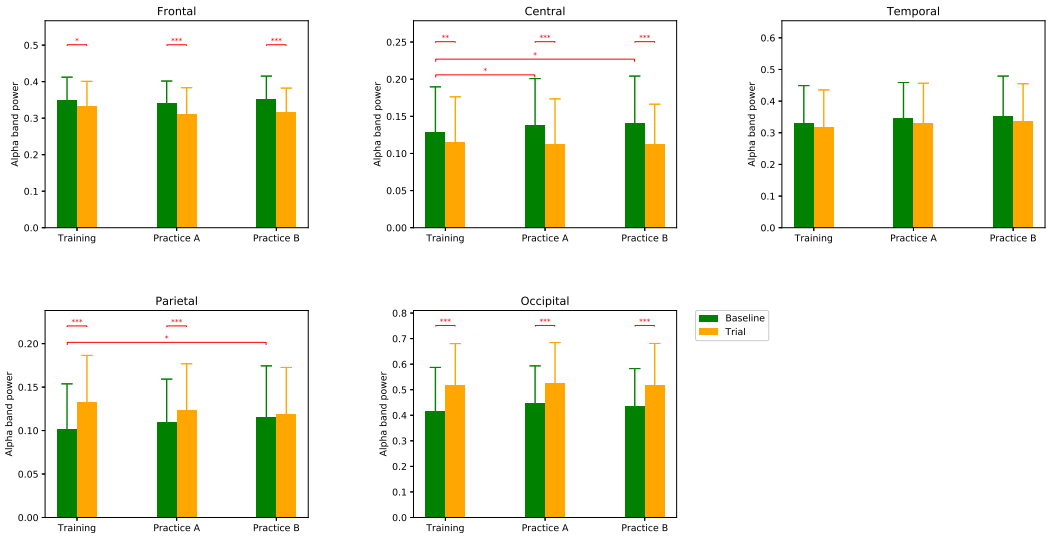

Figure 5.12: EEG alpha band power for Baseline tasks and Trial tasks during Training, PracticeA, and PracticeB. P-values for TASK and STAGE comparisons are annotated by $^{*}(p \leq 0.050)$, $^{**}(p \leq 0.010)$, $^{***}(p \leq 0.005)$

effect of CLASS ($F(6, 138) = 52.261$, $p = 0.000$, $\eta^2 = 0.694$), as well as one significant interaction effect of TASK $\times$ CLASS ($F(6, 138) = 37.493$, $p = 0.000$, $\eta^2 = 0.620$). Figure 5.14 presents the coverage comparison results on TASK and STAGE for each of the seven EEG microstate classes, while the p-values for pairwise comparisons with Bonferroni correction on each microstate class are listed in Table 5.5. For TASK comparison, significant increases in the coverage of microstate B from Baseline tasks to Trial tasks were observed for Training and PracticeA stages; the significant changes from Baseline to Trial tasks were also observed for the coverage of microstate C for PracticeA (increasing); the coverage of microstate D for Training (increasing), PracticeA (increasing), and PracticeB (increasing); the coverage of microstate E for Training (decreasing), PracticeA (decreasing), and PracticeB (decreasing); the coverage of microstate F for PracticeA (increasing) and PracticeB (increasing); the coverage of microstate G for Training (decreasing), PracticeA (decreasing), and PracticeB (decreasing). The results on EEG microstate coverage showed no significant difference in STAGE comparisons in all of the seven microstate classes.

In addition, the $2 \times 3 \times 7$ repeated measures ANOVA on EEG microstate occurrence revealed

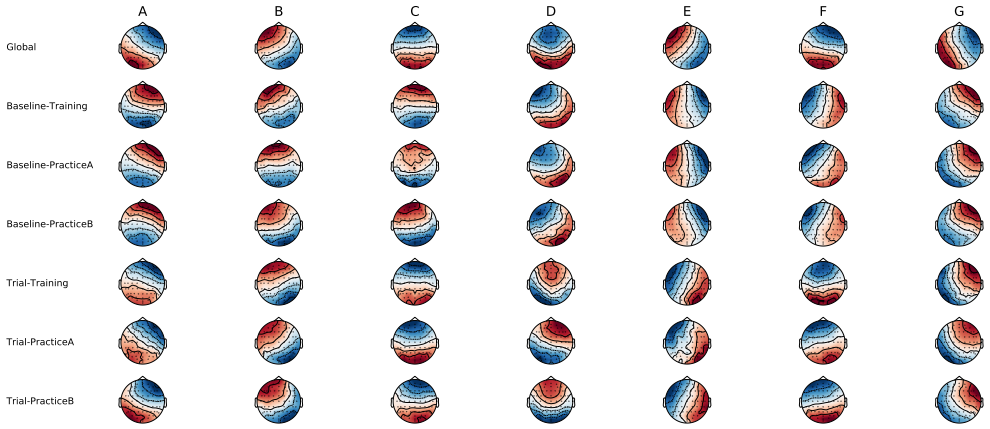

Figure 5.13: The spatial configuration of the seven microstate classes (A, B, C, D, E, F, and G) for across TASK and STAGE (global) and for each task type (Baseline and Trial) during different stages (Training, PracticeA, and PracticeB)

two significant main effects of TASK ($F(1, 23) = 17.349$, $p = 0.000$, $\eta^2 = 0.430$) and CLASS ($F(6, 138) = 91.163$, $p = 0.000$, $\eta^2 = 0.799$), as well as one significant interaction effect of TASK $\times$ CLASS ($F(6, 138) = 32.424$, $p = 0.000$, $\eta^2 = 0.585$). Figure 5.15 presents the occurrence comparison results on TASK and STAGE for each of the seven EEG microstate classes, while the p-values for pairwise comparisons with Bonferroni correction on each microstate class are listed in Table 5.6. For TASK comparison, significant differences between Baseline tasks and Trial tasks were observed for all of the three stages (Training, PracticeA, and PracticeB) in the occurrence of microstate B, C, D, E, F, and G despite the polarity of the changes. To be more precise, significant increases were observed in the occurrence of microstate B, C, D, and F during Training, PracticeA, and PracticeB, whereas significant decrease were observed in the occurrence of microstate E and G during Training, PracticeA, and PracticeB. No significant difference was observed in the occurrence of microstate A under TASK comparisons. As for STAGE comparison, the occurrence of microstate D decreased significantly from PracticeA stage to PracticeB stage for Baseline tasks, whereas non of the seven microstate classes showed any significant occurrence difference in STAGE comparisons for Trial tasks.

Moreover, the $2 \times 3 \times 7$ repeated measures ANOVA on EEG microstate duration revealed two significant main effect of TASK ($F(1, 23) = 12.140$, $p = 0.002$, $\eta^2 = 0.345$) and CLASS

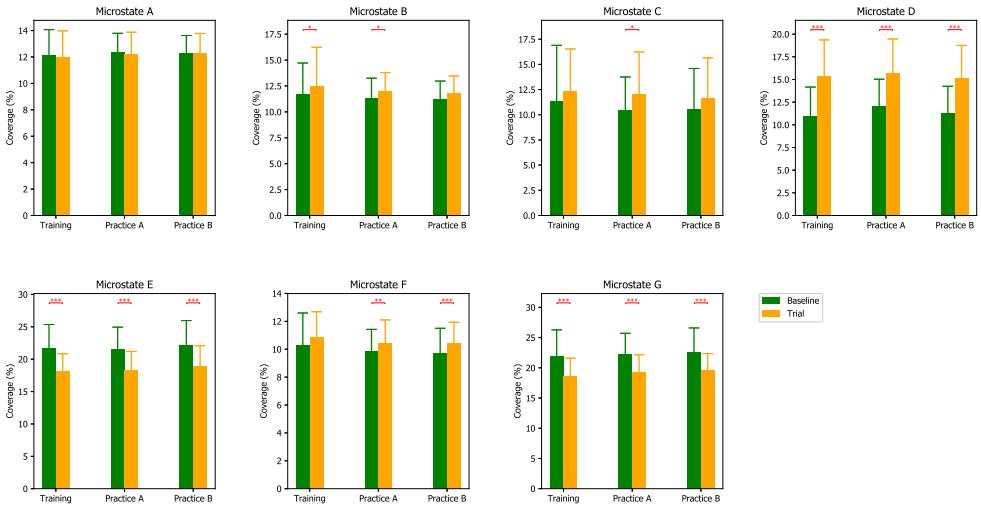

Figure 5.14: EEG microstate coverage for Baseline tasks and Trial tasks during Training, PracticeA, and PracticeB stages. P-values for TASK and STAGE comparisons are annotated by $^{*}(p \leq 0.050)$, $^{**}(p \leq 0.010)$, $^{***}(p \leq 0.005)$.

($F(6, 138) = 35.832$, $p = 0.000$, $\eta^2 = 0.609$), as well as one significant interaction effect of TASK $\times$ CLASS ($F(6, 138) = 31.065$, $p = 0.000$, $\eta^2 = 0.575$). Figure 5.16 presents the duration comparison results on TASK and STAGE for each of the seven EEG microstate classes, while the p-values for pairwise comparisons with Bonferroni correction on each microstate class are listed in Table 5.7. For TASK comparison, significant increases in the duration of microstate D from Baseline tasks to Trial tasks were observed for Training, PracticeA, and PracticeB stages, whereas the duration of microstate A, E, and G decreased significantly from Baseline to Trial tasks for Training, PracticeA, and PracticeB stages. No significant differences between Baseline tasks and Trial tasks were observed in the duration of microstate B, C, and F across different stages. In the meantime, the results on EEG microstate duration showed no significant difference in STAGE comparisons for all of the seven microstate classes for both task types (Baseline and Trial).

Table 5.5: P-values of paired TASK and STAGE comparisons on EEG microstate coverage.

Comparison	Microstate classes						
	Class A	Class B	Class C	Class D	Class E	Class F	Class G
S1:B-T	0.606	0.018^{*} ↗	0.269	0.0^{***} ↗	0.0^{***} ↘	0.084	0.0^{***} ↘
S2:B-T	0.218	0.03^{*} ↗	0.014^{*} ↗	0.0^{***} ↗	0.0^{***} ↘	0.007^{**} ↗	0.0^{***} ↘
S3:B-T	0.924	0.091	0.1	0.0^{***} ↗	0.0^{***} ↘	0.002^{***} ↗	0.0^{***} ↘
B:S1-S2	0.92	0.987	0.377	0.15	1.0	0.337	1.0
B:S1-S3	1.0	0.806	0.721	1.0	1.0	0.228	0.451
B:S2-S3	1.0	1.0	1.0	0.097	0.475	1.0	0.521
T:S1-S2	1.0	0.944	1.0	1.0	1.0	0.165	0.672
T:S1-S3	0.585	0.723	0.71	1.0	0.606	0.315	0.086
T:S2-S3	1.0	1.0	1.0	0.634	0.507	1.0	1.0

* $\rho \leq 0.050$, ** $\rho \leq 0.010$, *** $\rho \leq 0.005$
↗ Microstate coverage increases
↘ Microstate coverage decreases

Temporal dependency results on EEG microstates

For Baseline tasks, the finite entropy rate was 1.607 $bits/sample$ ($SE = 0.020$) during Training, 1.623 $bits/sample$ ($SE = 0.019$) during PracticeA, and 1.604 $bits/sample$ ($SE = 0.018$) during PracticeB. As for Trial tasks, the finite entropy rate was 1.771 $bits/sample$ ($SE = 0.015$) during Training, 1.776 $bits/sample$ ($SE = 0.015$) during PracticeA, and 1.766 $bits/sample$ ($SE = 0.017$) during PracticeB. The 2×3 repeated measures ANOVA revealed one significant main effect of TASK ($F(1, 23) = 291.901$, $p = 0.000$, $\eta^2 = 0.927$). Figure 5.17 presents the entropy rate results for TASK and STAGE comparisons, whereas the p-values for pairwise comparisons with Bonferroni correction are listed in Table 5.8. For TASK comparison, the averaged entropy rate of microstate sequences increased significantly from Baseline tasks to Trial tasks for all of the three tested stages including Training, PracticeA, and PracticeB. As for STAGE comparisons, the entropy results showed significant decreases from PracticeA to PractiveB stage, whereas no significant difference in STAGE comparisons were observed for Trial tasks.

Moreover, the Hurst exponent averaged across 35 partitions was 0.649 ($SE = 0.005$) for Training, 0.642 ($SE = 0.004$) for PracticeA, and 0.647 ($SE = 0.004$) for PracticeB. As for Trial tasks, the finite entropy rate was 0.608 ($SE = 0.003$) for Training, 0.607 ($SE = 0.00.$) for PracticeA,

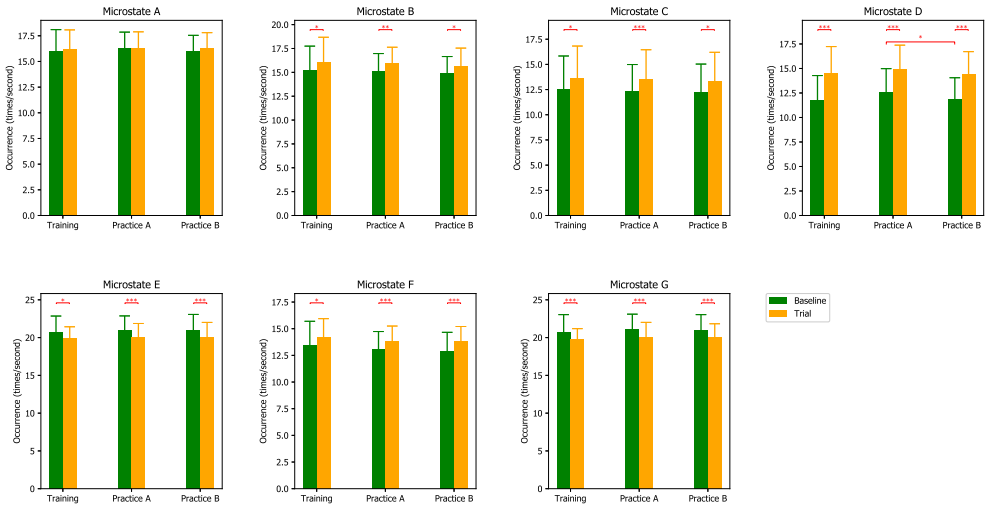

Figure 5.15: EEG microstate occurrence for Baseline tasks and Trial tasks during Training, PracticeA, and PracticeB stages. P-values for TASK and STAGE comparisons are annotated by $^{*}(p \leq 0.050)$, $^{**}(p \leq 0.010)$, $^{***}(p \leq 0.005)$.

and 0.611 $(SE = 0.003)$ for PracticeB. The 2×3 repeated measures ANOVA revealed one significant main effect of TASK ($F(1, 23) = 221.604$, $p = 0.000$, $\eta^2 = 0.906$). Figure 5.18 presents the averaged Hurst exponent for TASK and STAGE comparisons, whereas the p-values for pairwise comparisons with Bonferroni correction are listed in Table 5.9. For TASK comparison, significant decreases were observed in the averaged Hurst exponent of microstate sequences from Baseline tasks to Trial tasks for all of the three tested stages including Training, PracticeA, and PracticeB. However, no significant difference was observed in the Hurst exponent results on STAGE comparisons for both Baseline and Trial tasks.

5.2.6 Quantified cognitive control during a skill acquisition process

Trial tasks were associated with decreased cognitive control than Baseline tasks

The TASK comparisons indicated decreases in trainees' cognitive control when they were confronted with larger task demands under Trial tasks in comparison to Baseline tasks, which was supported by decreased theta spectral power, increases in the parameters of microstate C, increased entropy rate, and decreased Hurst exponent under Trial tasks. For EEG spectral powers in theta

Table 5.6: P-values of paired TASK and STAGE comparisons on EEG microstate occurrence.

Comparison	Microstate classes						
	Class A	Class B	Class C	Class D	Class E	Class F	Class G
S1:B-T	0.435	$0.011^{*}\nearrow$	$0.012^{*}\nearrow$	$0.0^{***}\nearrow$	$0.024^{*}\searrow$	$0.011^{*}\nearrow$	$0.004^{***}\searrow$
S2:B-T	0.726	$0.006^{**}\nearrow$	$0.005^{***}\nearrow$	$0.0^{***}\nearrow$	$0.002^{***}\searrow$	$0.002^{***}\nearrow$	$0.0^{***}\searrow$
S3:B-T	0.085	$0.013^{*}\nearrow$	$0.018^{*}\nearrow$	$0.0^{***}\nearrow$	$0.005^{***}\searrow$	$0.0^{***}\nearrow$	$0.003^{***}\searrow$
B:S1-S2	1.0	1.0	1.0	0.157	1.0	0.69	0.377
B:S1-S3	1.0	0.627	0.724	1.0	1.0	0.225	0.748
B:S2-S3	0.377	0.53	1.0	$0.023^{*}\searrow$	1.0	0.79	1.0
T:S1-S2	1.0	1.0	1.0	1.0	1.0	0.298	0.521
T:S1-S3	1.0	0.806	1.0	1.0	1.0	0.551	0.4
T:S2-S3	1.0	0.636	1.0	0.287	1.0	1.0	1.0

* $\rho \leq 0.050$, ** $\rho \leq 0.010$, *** $\rho \leq 0.005$
$\nearrow$ Microstate occurrence increases
$\searrow$ Microstate occurrence decreases

band, significant decreases from Baseline tasks to Trial tasks were observed for Training stage over central sites, and for both PracticeA and PracticeB stages over frontal, central, and temporal sites. In the literature, increased theta power over the frontal sites has been viewed as a reliable index of working memory and cognitive control (Cavanagh et al., 2009; Cooper et al., 2019), which could be related to increased cognitive control in encoding and retrieval of information from working memory (Karakaş, 2020; Sauseng et al., 2010). In general, our analysis results on theta spectral powers indicated decreases in trainees' cognitive control under increased task demands and increased uncertainty under Trial tasks, whereas the significant theta increases over parietal and occipital sites could be related to increased visual loads.

Among the seven computed EEG microstate states, microstate C was discussed here due to its close relationship with cognitive control. Researchers have reported both positive and negative correlations of microstate class C with cognitive control mechanisms as reviewed in (Michel & Koenig, 2018). As a result, TASK comparisons were conducted on the three parametes of microstate C, namely coverage, occurrence, and duration, and the results indicated increased microstate C under Trial tasks. To be more precise, the coverage of microstate C increased from Baseline tasks to Trial tasks during Training stage (non-significant), PracticeA stage (significant), and PracticeB stage (non-significant) as shown in Figure 5.14. The occurrence of microstate C significantly increased from Baseline tasks to Trial tasks throughout the pilot training process (Training, PracticeA,

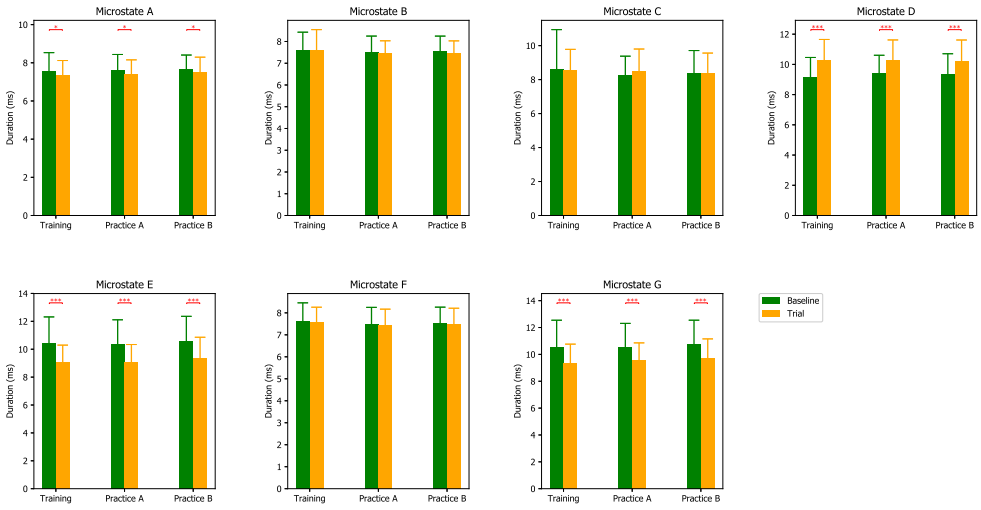

Figure 5.16: EEG microstate duration for Baseline tasks and Trial tasks during Training, PracticeA, and PracticeB stages. P-values for TASK and STAGE comparisons are annotated by $^{*}(p \leq 0.050)$, $^{**}(p \leq 0.010)$, $^{***}(p \leq 0.005)$.

and PracticeB) (Figure 5.15), whereas the duration of microstate showed non-significant decreases under Training stage and non-significant increases under PracticeA and PracticeB stages (Figure 5.16). Combining the observations on microstate C and those indicated by other EEG quantities, the increased microstate C under Trial tasks indicated that trainees' cognitive control decreased under larger task demands with increased uncertainty. Therefore, our results supported the notion that microstate class C is negatively correlated to task demands, which was consistent with the the studies suggesting microstate C's role in reflecting activities in the default mode network (DMN) (Bréchet et al., 2019; Seitzman et al., 2017; X. Xu, Yuan, & Lei, 2016).

The entropy rate computed from EEG microstate sequences described how random the sequences were, as it described how random or free the brain was in choosing the next network configuration (Jia & Zeng, 2021). The more random a microstate sequence was, the larger the computed entropy rate became. On the contrary. the more organized a sequence was, the smaller the entropy rate could be. In other words, decreased entropy rate would be associated with a higher cognitive control as both of them indicated a more organized microstate sequence in our analysis. Our paired TASK comparisons showed that entropy rate significantly increased from Baseline tasks to Trial

Table 5.7: P-values of paired TASK and STAGE comparisons on EEG microstate duration.

Comparison	Microstate classes						
	Class A	Class B	Class C	Class D	Class E	Class F	Class G
S1:B-T	$0.041^{*}\searrow$	0.693	0.904	$0.0^{***}\nearrow$	$0.0^{***}\searrow$	0.583	$0.0^{***}\searrow$
S2:B-T	$0.03^{*}\searrow$	0.38	0.263	$0.0^{***}\nearrow$	$0.0^{***}\searrow$	0.611	$0.0^{***}\searrow$
S3:B-T	$0.041^{*}\searrow$	0.532	0.913	$0.0^{***}\nearrow$	$0.0^{***}\searrow$	0.516	$0.0^{***}\searrow$
B:S1-S2	1.0	1.0	0.728	0.222	1.0	0.556	1.0
B:S1-S3	0.717	1.0	1.0	0.563	1.0	0.83	0.628
B:S2-S3	1.0	1.0	1.0	1.0	0.598	1.0	0.292
T:S1-S2	0.96	0.393	1.0	1.0	1.0	0.415	0.911
T:S1-S3	0.339	0.984	0.861	1.0	0.485	0.898	0.221
T:S2-S3	0.543	1.0	1.0	1.0	0.213	1.0	0.962

* $\rho \leq 0.050$, ** $\rho \leq 0.010$, *** $\rho \leq 0.005$
$\nearrow$ Microstate duration increases
$\searrow$ Microstate duration decreases

tasks across the three stages (Training, PracticeA, and PracticeB) within a pilot training process as shown in Figure 5.17. Given the negative correlation between entropy rate and cognitive control, our analysis on the entropy rate of microstate sequences revealed that trainees' cognitive control was lower when they were confronted with increased task demands and increased uncertainty under Trial tasks, which was consistent with the changing trend indicated by theta band power and the parameters of microstate C.

Hurst exponent, as an indicator of long-range dependency, reflected the long-range correlation in the EEG microstate sequences. The larger the Hurst exponent was, the more temporally correlated the microstates were, whereas Hurst exponent at 0.5 represented a completely uncorrelated microstate sequence. From this standpoint, increases in Hurst exponent may indicate a higher cognitive control, both of which are associated with a more predictable microstate sequence. According to our paired TASK comparison results, significant decreases in the computed average Hurst exponent were observed from Baseline to Trial tasks throughout the pilot training process (Traing, PracticeA, and PracticeB) as shown in Figure 5.18. Considering the aforementioned positive correlation between Hurst exponent and cognitive control, our results indicated a lower cognitive control when trainees were confronted with increased task demands and increased uncertainty under Trial tasks. Such observations were also consistent with those indicated by theta spectral power, the parameters of microstate C, as well as entropy rate.

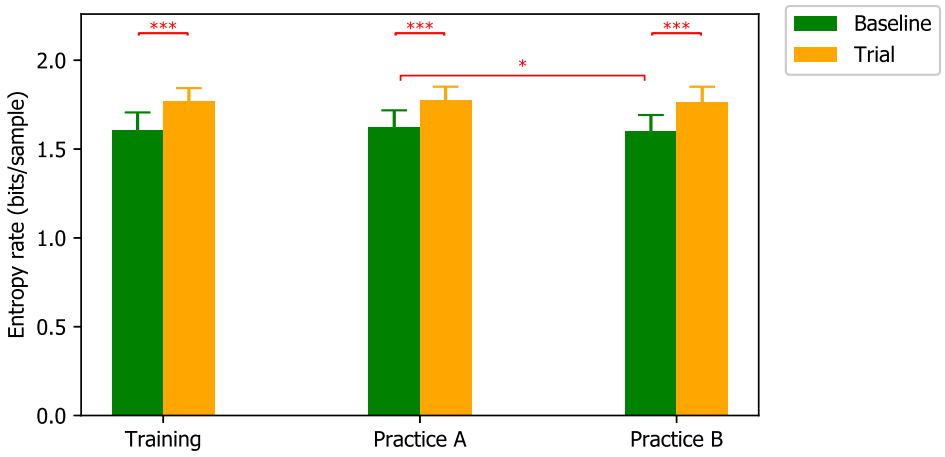

Figure 5.17: Entropy rate of microstate sequences for Baseline and Trial tasks during Training, PracticeA, and PracticeB stages. P-values for TASK and STAGE comparisons are annotated by $^{*}(p \leq 0.050)$, $^{**}(p \leq 0.010)$, $^{***}(p \leq 0.005)$.

To sum up, our results on TASK comparisons indicated reduced cognitive control when trainees were confronted with larger task demands and increased uncertainty under Trial tasks. The quantitative performance evaluation results also indicated that trainees were less skilled and were having more difficulty in completing the Trial tasks than Baseline tasks, which was reflected in the significant decreases in each evaluated dimension across the training process (Training, PracticeA, PracticeB). In addition, our analysis on cognitive control was consistent with the negative correlation between cognitive control and uncertainty reported in the existing studies. Such consistency across the applied EEG quantities and with the literature confirmed the reliability of our analysis regarding cognitive control.

Trainees' cognitive control improved after a skill acquisition process under unvaried task demands

The STAGE comparisons on Baseline tasks showed significant or non-significant increases in theta band power from Training stage to PracticeA stage, as well as from Training stage to PracticeB stage. In particular, significant increases in theta band power from Training stage to PracticeA stage over central, temporal, parietal, and occipital sites, as well as non-significant increases over frontal sites. Similarly, significant theta increases were observed from Training stage to PracticeB stage

Table 5.8: P-values for paired TASK and STAGE comparisons in entropy rate.

Comparison	Entropy rate	
B-S1 Vs. T-S1	0.0^{***}	↘
B-S2 Vs. T-S2	0.0^{***}	↘
B-S3 Vs. T-S3	0.0^{***}	↘
B-S1 Vs. B-S2	0.426	
B-S1 Vs. B-S3	1.0	
B-S2 Vs. B-S3	0.039^{*}	↘
T-S1 Vs. T-S2	1.0	
T-S1 Vs. T-S3	1.0	
T-S2 Vs. T-S3	0.492	

* $\rho \leq 0.050$, ** $\rho \leq 0.010$, *** $\rho \leq 0.005$
↗ Entropy rate increases
↘ Entropy rate decreases

Table 5.9: P-values for paired TASK and STAGE comparisons in Hurst exponent.

Comparison	Hurst exponent	
B-S1 Vs. T-S1	0.0^{***}	↘
B-S2 Vs. T-S2	0.0^{***}	↘
B-S3 Vs. T-S3	0.0^{***}	↘
B-S1 Vs. B-S2	0.192	
B-S1 Vs. B-S3	1.0	
B-S2 Vs. B-S3	0.27	
T-S1 Vs. T-S2	1.0	
T-S1 Vs. T-S3	1.0	
T-S2 Vs. T-S3	0.346	

* $\rho \leq 0.050$, ** $\rho \leq 0.010$, *** $\rho \leq 0.005$
↗ Hurst exponent increases
↘ Hurst exponent decreases

over frontal, central, and temporal sites, as well as non-significant theta increases over parietal and occipital sites. In addition, no significant changes in theta spectral powers were observed from PracticeA stage to PracticeB stage. According to the literature, increased theta power over the frontal sites has been viewed as a reliable index of working memory and cognitive control (Cavanagh et al., 2009; Cooper et al., 2019), which could be related to a higher cognitive control in encoding and retrieval of information from working memory (Karakaş, 2020; Sauseng et al., 2010). Along the same direction, our EEG spectral analysis in theta band indicated that Training stage was associated with the lowest cognitive control in comparison with the other two stages (PracticeA and PracticeB)

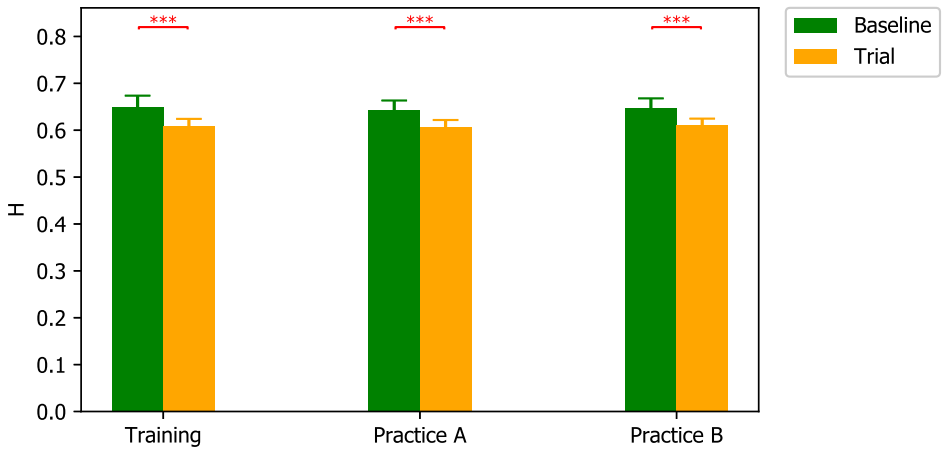

Figure 5.18: Hurst exponent of microstate sequences averaged across 35 partitions for Baseline and Trial tasks during Training, PracticeA, and PracticeB stages. P-values for TASK and STAGE comparisons are annotated by $^{*}(p \leq 0.050)$, $^{**}(p \leq 0.010)$, $^{***}(p \leq 0.005)$.

and that trainees' cognitive control improved within a skill acquisition process.

In terms of the STAGE comparisons on microstate C, no significant changes were observed throughout the pilot training process (Training, PracticeA, and PracticeB) for all the three microstate parameters, namely coverage, occurrence, and duration. The mean coverage of microstate C decreased non-significantly from 11.403 (Trainging) to 10.480 (PracticeA), and then increased non-significantly to 10.582 (PracticeB). The mean occurrence of microstate C decreased non-significantly from 12.600 (Training) to 12.366 (PracticeA), and then decreased non-significantly to 12.212 (PracticeB). The mean duration of microstate C also decreased non-significantly from 8.635 (Trainging) to 8.258 (PracticeA), and then increased non-significantly to 8.376 (PracticeB). To sum up, our results showed that Training stage could be associated with the most microstate C and that microstate C decreased after repeated practices. By referring to the negative relationship between microstate C and cognitive control, our STAGE comparisons on Baseline tasks indicated that trainees' cognitive control improved after a skill acquisition process, which was the lowest during Training stage in comparison with the other two stages (PracticeA and PracticeB).

The STAGE comparisons on entropy rate increased non-significantly from Training stage to PracticeA stage, then decreased non-significantly from PracticeA to PracticeB stage, as well as decreased non-significantly from Training stage to PracticeB stage under Baseline tasks (Figure 5.17).

In particular, the entropy rate increased from 1.607 in Training to 1.623 in PracticeA, and then decreased significantly from 1.623 (PracticeA) to 1.604 (PracticeB) under Baseline tasks. Considering the negative relationship between entropy rate and cognitive control, our STAGE comparison results indicated that PracticeB stage was associated with the highest cognitive control and that trainees' cognitive control improved significantly from PracticeA stage to PracticeB stage.

In addition, the STAGE comparisons on Hurst exponent showed non-significant decreases from Training stage to PracticeA stage and non-significant increases from PracticeA stage to PracticeB stage under unvaried task demands (Figure 5.18). That is, the STAGE comparisons on the twenty-two Baseline tasks indicated that the averaged Hurst exponent experienced U-shaped changes by decreasing from 0.649 (Training) to 0.642 (PracticeA) and increasing from 0.642 (PracticeA) to 0.647 (PracticeB) afterward. Therefore, the results on Hurst exponent indicated that trainees' cognitive control experienced a U-shaped changing trend, which was the highest during Training stage and improved from PracticeA stage to PracticeB stage. As discussed in TASK comparisons, the high cognitive control observed during Training stage could be related to the reduced uncertainty with the help from the instructor.

The aforementioned results on unvaried task demands (Baseline tasks) indicated that trainees' cognitive control improved along the skill acquisition process, even though such improvements were observed at different moments as indicated by different features. In general, the theta band power and microstate parameters indicated that trainees' cognitive control was the lowest during Training stage and their cognitive control improved after a skill acquisition process. Such improvement in trainees' cognitive control was reflected in the comparisons between PraciceA stage and Training stage, as well as PracticeB stage and Training stage as indicated by theta band power and microstate parameters. We also observed non-significant decreases in trainees' cognitive control from PracticeA stage to PracticeB stage as indicated by the coverage and duration of microstate C, as well as the theta band power over temporal, parietal, and occipital sites. We may infer from those observations that trainees' cognitive control improved along the skill acquisition process, which may happen at the end of the skill acquisition process or even earlier. Meanwhile, the slight decreases in cognitive control observed toward the end of the skill acquisition process may be related to improved neural efficiency once the trainees became better trained and skilled (Gobel, Parrish,

& Reber, 2011; Hatfield, Haufler, Hung, & Spalding, 2004; Kerick, Douglass, & Hatfield, 2004). The other two features (entropy rate and Hurst exponent) indicated a U-shaped changing trend in trainees' cognitive control, which differed from our original hypothesis on an increasing cognitive control along the skill acquisition. The discrepancy lies in the cognitive control decreases observed from Training stage to PracticeA stage, which could be interpreted from the negative correlation between uncertainty and cognitive control. PracticeA stage could be associated with increased uncertainty as the absence of instructor's help may be the reason for the increased uncertainty when trainees moved from Training stage to PracticeA stage. From this standpoint, PracticeA stage corresponds to the low cognitive control situation where trainees did not know when or where to control or intervene for achieving a good performance (Botvinick, Braver, Barch, Carter, & Cohen, 2001; Verguts & Notebaert, 2009). Despite the aforementioned discrepancy, the observed increases in cognitive control from PracticeA stage to PracticeB stage were somehow consistent with our original hypothesis. Improvements in cognitive control could be explained from the skill acquisition point of view as tested by the pilot training process, which could contribute to a broad set of cognitive functions that were improved after repeated practices (Amer, Campbell, & Hasher, 2016; Unsworth, Fukuda, Awh, & Vogel, 2015). Overall, our STAGE comparisons on Baseline tasks indicated that trainees' cognitive control improved along the skill acquisition which may be observed toward the end of the process (from Training to PracticeB, or from PracticeA to PracticeB) or even earlier (from Training to PracticeA). Meanwhile, the quantitative assessment results indicated improved performance (heading, altitude, and rate climb/decent) (Figure 5.9a-5.9c) and control management (roll and pitch) (Figure 5.9d and 5.9e) from Training to PracticeA and from Training to PracticeB in conducting the same tasks during a skill acquisition process.

5.2.7 Quantified cognitive workload during a skill acquisition process

Trial tasks were associated with increased cognitive workload than Baseline tasks

According to our experiment procedure, trainees were confronted with larger task demands, increased task difficulty, and increased uncertainty under Trial tasks in comparison to Baseline tasks.

Despite the different time length for each Baseline (30 seconds) and Trial task (90 seconds), Baseline tasks differed from Trial tasks in that trainees were required to complete the same maneuvers across the twenty-two Baseline tasks. On the contrary, the instructions of the twenty-two Trial tasks varied from one to another and the required maneuvers under Trial tasks were more difficult than those under Baseline tasks in general. Therefore, paired comparisons were conducted between the two types of tasks, namely Baseline tasks and Trial tasks, to align our research with the reported effect of task demands and uncertainty on cognitive workload in the literature.

The paired comparisons on alpha spectral powers indicated that trainees' cognitive workload was higher while they were conducting Trial tasks in comparison to Baseline tasks. In particular, the TASK comparisons on alpha spectral powers showed significant decreases from Baseline tasks to Trial tasks throughout the pilot training process (Training, PracticeA, and PracticeB) over frontal and central sites, while non-significant decreases from Baseline tasks to Trial tasks were observed over temporal sites for all the three stages. Meanwhile, significant increases in alpha band power from Baseline to Trial tasks were observed over parietal sites for Training and PracticeA stages, as well as over occipital sites for all the three stages, and such alpha increases may indicate increased visual attention when trainees were confronted with increases task loads under Trial tasks (Fu et al., 2001; Hohaia, Saurels, Johnston, Yarrow, & Arnold, 2022; Yamagishi et al., 2003). Considering the differences between the two types of tasks, the alpha decreases from Baseline to Trial tasks (over frontal, central, and temporal sites) may indicate an increased cognitive workload in responding to larger task demands with increased task difficulty. This observation was aligned with the positive correlation between cognitive workload and task demands in the literature (Jia & Zeng, 2021; Shaw et al., 2019; Wickens, 2008), which also confirmed the reliability of our analysis on cognitive workload assessment.

To sum up, our results on TASK comparisons indicated increased cognitive workload when trainees were confronted with larger task demands and increased uncertainty under Trial tasks. The quantitative performance evaluation results also indicated that trainees were less skilled and were having more difficulty in completing the Trial tasks than Baseline tasks. In particular, the significant decreases in each evaluated dimension across the training process (Training, PracticeA, PracticeB)

could complement the EEG features in indicating that people may experience more cognitive workload at the tasks that seem to be difficult and challenging for them. By referring to the literature, our analysis on cognitive workload added evidences to the positive correlation between cognitive workload and task demands. As a result, such consistency across the applied EEG quantities and with the literature confirmed the reliability of our analysis regarding cognitive workload, which laid the foundation for our further investigations.

Trainees' cognitive workload decreased under unvaried task demands during a pilot training process

The time-course changes of cognitive workload along the training process were reflected in the STAGE comparisons on the EEG alpha band power and NASA-TLX subjective ratings. The STAGE comparisons on Baseline tasks showed significant increases in trainees' alpha band power from Training stage to PracticeA stage over central sites, as well as from Training stage to PracticeB stage over central and parietal sites. In addition, non-significant increases in alpha band power were observed from Training stage to PracticeA stage over temporal, parietal, and occipital sites, and from Training stage to PracticeB stage over frontal, temporal and occipital sites, as well as from PracticeA stage to PracticeB stage over frontal, central, temporal, and parietal sites. Alpha power has been considered as a reliable indicator of cognitive workload (Fink et al., 2005) where the extent of decreases in alpha power is associated with increases in cognitive workload (Keil et al., 2006). Alpha power has also been associated with task difficulty (Brouwer, Hogervorst, Holewijn, & van Erp, 2014; Jaquess et al., 2018; Jaušovec & Jaušovec, 2000), semantic memory process (Doppelmayr, Klimesch, Hödlmoser, Sauseng, & Gruber, 2005; Klimesch, 1999), and attention (Klimesch, 2012). Therefore, the STAGE comparisons of alpha spectral power under unvaried task demands (Baseline tasks) indicated a decreasing trend in trainees' cognitive workload within the pilot training process.

Furthermore, such decreasing trend in trainees' cognitive workload was confirmed in the subjective rating results as shown in Figure 5.10. In particular, trainees' cognitive workload decreased significantly from Training stage to PracticeA stage, as well as from Training stage to PracticeB stage. In addition, non-significant decreases were observed from PracticeA stage to PracticeB stage

(Figure 5.10). Considering the chronological order of those stages within the tested pilot training process, the subjective rating results indicated a decreasing cognitive workload along a pilot training process where trainees' subjective perception of the workload was captured at each stage without distinguishing the TASK types.

Taken together, the EEG spectral power results in alpha band and the subjective rating results both indicated that trainees' cognitive workload decreased along the tested pilot training process (from Training, to PracticeA, and then to PracticeB). This was consistent with our hypothesis on the decreasing cognitive workload within a skill acquisition process when compared to the performance evaluation results. The significant increases in the assessment of all of the five evaluated dimensions under Baseline tasks from Training to PracticeB and the significant/non-significant increases from Training to PracticeA showed the effectiveness of the tested skill acquisition process where trainees improved their skills and achieved better performance through the pilot training process.

5.2.8 Quantitative changes in cognitive workload and cognitive control under varied task demands

Apart from the aforementioned analysis on Baseline tasks (unvaried task demands), the present research also investigated the changes in trainees' cognitive workload and cognitive control under varied task demands. The research question is whether we would be able to observe the same changes as indicated by the analysis on Baseline tasks if the same analysis was applied on Trial tasks with varied task demands. First of all, no significant changes were captured by any of the tested features in the STAGE comparisons on Trial tasks. Among the non-significant changes, the parameters of microstate C indicated that trainees' cognitive control improved along the skill acquisition process. In particular, the mean coverage decreased from Training stage to PracticeA stage and then decreased to PracticeB stage, such decreasing trend was also observed in the mean occurrence and duration of microstate C. In the meantime, the temporal dependency features, both entropy rate and Hurst exponent, indicated that PracticeB stage was associated with the highest cognitive control in comparison with Training and PracticeA stages. To be more precise, entropy rate showed an inverted U-shaped changing trend whereas Hurst exponent indicated a U-shaped changing trend. However, the changes in alpha band power showed more variations across the five

brain areas, and such varied changing trend was also observed in theta band power. And both alpha and theta band power shared a high similarity between the observed changing patterns under Trial tasks. In particular, both features showed a U-shaped changing trend over frontal and central sites, an increasing trend over temporal sites, a decreasing trend over parietal sites, and an inverted U-shaped trend over occipital sites. Based on those observations, the spectral changes in theta band and alpha band may reflect the varied neural activation over different brain areas in responding to the varied flight tasks, instead of being interpreted from cognitive control or workload point of view.

What can be learned from the similarity and discrepancy between the results obtained on Trial tasks and the aforementioned results obtained on Baseline tasks? EEG microstate features seemed to be more robust in reflecting trainees' cognitive changes under varied tasks than spectral features, whereas the spectral features could be more sensitive to changes in task demands and difficulty levels. Trainees were instructed to conduct the same maneuvers across the twenty-two Baseline tasks along the pilot training process, whereas the maneuvers in the twenty-two Trial tasks varied from one to another with a varied difficulty level presented in a pseudo-randomized order. From this standpoint, the cognitive changes captured by certain features under Trial tasks could be triggered by the variations of task demands, whereas under Baseline tasks the effect of task demands could be avoided. The observed changes on Baseline tasks may reflect the actual changes in trainees' cognitive workload and cognitive control along the pilot training process. In the meantime, the quantitative assessment results seem to complement the EEG microstate features in indicating trainees' changes through the skill acquisition process. Among the five evaluated assessment dimensions, the three performance dimensions (heading, altitude, and rate climb/descent) showed an increasing trend from Training to PracticeA and then to PracticeB (Figure 5.9a-5.9c). This could reflect trainees' improvement as the skill acquisition process continues, despite of the fact that performance (altitude) was the only dimension that showed significant increases from Training to PracticeA and also from Training to PracticeB under Trial tasks (Figure 5.9b). Moreover, the control management (roll) dimension indicated a U-shaped changing trend without any significant changes (Figure 5.9d), which seemed to be consistent with the U-shaped changing cognitive control indicated by the two temporal dependency features on microstate sequences (entropy rate and Hurst exponent). To sum up, we may conclude that trainees' cognitive workload decreased whereas their cognitive control

improved along the skill acquisition process as indicated by the results on Baseline tasks (unvaried task demands). And the effect of skill acquisition on trainees' cognitive control improvement could be captured by microstate features, including microstate parameters and the temporal dependency quantities like entropy rate and Hurst exponent, even under varied tasks.

5.2.9 Conclusion

The present study aimed to capture the changes in trainees' cognitive workload and cognitive control within a skill acquisition process. Trainees' cognitive control was quantified using EEG microstate analysis and spectral features, while the quantification of cognitive workload was based on spectral analysis and subjective ratings. A series of STAGE comparisons and TASK comparisons were conducted to investigate the time-course changes and to align our analysis with other findings reported in the literature respectively. In particular, our results on TASK comparisons indicated that Trial tasks were associated with higher cognitive workload but lower cognitive control than Baseline tasks, which were also reflected in the decreased performance under Trial tasks as indicated by the quantitative evaluation results. The EEG-indicated changes in trainees' cognitive workload were aligned with the research findings on increased cognitive workload triggered by larger task demands (Gevins & Smith, 2003; Shaw et al., 2019; Wickens, 2008). In comparison to Baseline tasks, our results showed decreased cognitive control under Trial tasks which may be related to increased uncertainty (Jia & Zeng, 2021). Afterward, the same EEG quantities were applied in STAGE comparisons to test our hypothesis. We would expect decreases in trainees' cognitive workload and increases in their cognitive control from the experimental results during a skill acquisition process. The STAGE comparisons on Baseline tasks indicated that trainees' cognitive workload decreased whereas their cognitive control improved along the tested pilot training process, where pilot trainees' skilled performance improved as indicated by the quantitative performance evaluation results. Moreover, the cognitive control changes within a skill acquisition process could be captured by EEG microstate features even under varied task demands (Trial tasks), which was also aligned with the performance evaluation results. Overall, the results presented in this research indicated that trainees' cognitive control improved whereas their cognitive workload decreased during a skill acquisition process.

5.3 Capacity zone: A quantitative approach for ensuring high efficiency by manipulating workload

This research investigates how much workload is a "good" workload for human beings to achieve a satisfactory level of mental effort. This study belongs to the third stage within the research methodology, where simulations were conducted to model human participants' time-varying work efficiency and mental stress under a problem-solving process within limited time. Besides testing the quantitative workload-efficiency representation with simulations in this application, the findings obtained from them could contribute to a general problem-solving process. Moreover, it will shed light on the quantification of other related cognitive factors and how they influence performance in our future research.

When given a "good" workload, human beings can efficiently accomplish the assigned task within the time limit, whereas they could fail to complete it due to low efficiency when given a "bad" workload. The objective of the present research is thus to investigate how much workload is a "good" workload for a human being to meet the deadline with a successful completion of the assigned task. A high work efficiency can be achieved through manipulating the workload assignment and assigning to different human beings at the right moment. It should be noted that multitasking and open-ended tasks are not covered in the present research as we keep our focus on the scenarios where human beings are requested to complete a given task within a predefined deadline. The scenarios under discussion can be widely observed in many fields including industry, education, and medicine (Hinds et al., 2004; Malone, 2018; Vesin et al., 2018; Whittaker, 2005; Yuksel et al., 2016), which could lead to various consequences due to the mismatch between the workload and the limited time resource.

5.3.1 Comparison between human workload-efficiency relationship and the ideal modeling

Taking the definition of mental effort as the amount of mental energy devoted to the confronted task, the amount of workload the person can complete with one unit of mental energy per time unit could be considered as positively proportional to the capacity level. That is to say, human beings'

work efficiency accumulates the amount of workload completed by each mental effort unit within a time unit, which is also influenced by their mental capacity level. As a result, a quantitative representation of the relationship between mental stress and work efficiency based on the raised-cosine representation (Eq. (6)) could be written as shown in Eq. (9):

$$\epsilon(t) = \beta * \epsilon_{max} * E(t)$$
$$\begin{cases} \beta * \frac{1}{2}\epsilon_{max}[1 + \cos(\frac{W(t) - \frac{1}{2}\beta\sigma_{max}}{\frac{1}{2}\beta\sigma_{max}}\pi)], & \text{if } 0 \leq W(t) \leq \beta\sigma_{max}\ , \\ 0, & \text{otherwise.} \end{cases} \tag{9}$$

where ϵ_{max} denotes the maximum work efficiency the person could achieve per unit of mental effort.

As shown in Eq. (9), a person's work efficiency depends on the current workload $W(t)$, maximum efficiency ϵ_{max}, stress limit σ_{max}, and mental capacity β. Among those influencing factors, we assume that the maximum efficiency ϵ_{max} and stress limit σ_{max} can be obtained from a person's previous performance and behavioral data. According to Eq.(4), β, considered as a constant variable, describes the extent to which a person is good at the current workload. Thereafter, we are able to plot human beings' work efficiency as a function of their workload.

As for the ideal modeling, the general idea of modeling the workload-efficiency relationship is to see how work efficiency responds to varied workload assignment without the influence of human factors or limits. However, in the real case the work efficiency will be as much as the expected amount of workload required to be completed within a time unit, where the the person's limited capacity and the influence of other human factors are not considered. Such ideal case could help explaining why human beings are sometimes assigned with too much workload in real-life practices. However, human beings' responses to varied workload are so different from the ideal case that their efficiency is affected by their stress and other human factors. Therefore, ignoring the influence of human factors could result in fatigue, stress, or some severe mental health problems in human beings after long-term exposure to high workload. Mathematically, the ideal workload-efficiency relationship can be described as:

$$\epsilon(t) = W(t)\,, \tag{10}$$

where $W(t)$ represents a person's workload to be completed at time t and $\epsilon(t)$ represents the person's ideal work efficiency at time t.

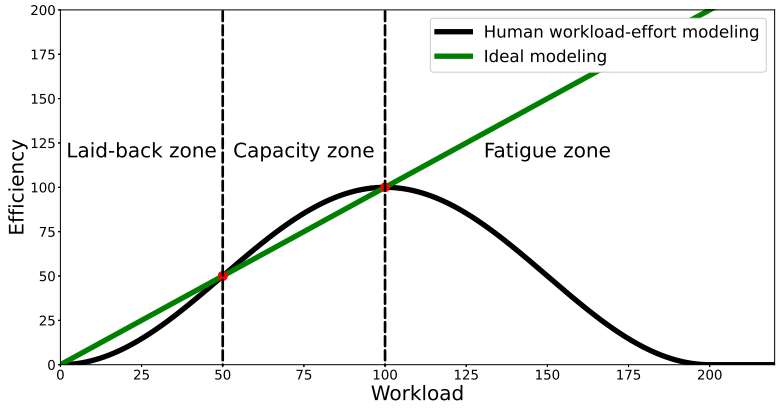

Figure 5.19: Modeling human beings' and the ideal workload-efficiency relationships at mental capacity $\beta = 1.0$

An ideal workload-efficiency relationship line was then added to the original modeling of human beings' workload-efficiency relationship as shown in Figure 5.19, with $\epsilon_{max} = 100$, $\sigma_{max} = 200$, and $\beta = 1.0$. As shown in Figure 5.19, two intersections have been generated between human beings' workload-efficiency curve and the ideal workload-efficiency line. For simplicity, we name the intersection corresponding to a smaller workload as the first intersection and the one with larger workload as the second intersection. As a result, the human workload-efficiency curve is divided into three parts by the two interactions, one zone locating on the left side of the first intersection, another zone locating between the two intersections, and the other zone locating on the right side of the second intersection as shown in Figure 5.19. Intuitively, we named those three zones as **Laid-back zone**, **Capacity zone**, and **Fatigue zone** based on the corresponding workload range. In particular, **Laid-back zone** corresponds to the situation where human beings are assigned with too little workload so that they may behave lazily, **Capacity zone** describes the situation where human beings are given a moderate amount of workload assignment that is somehow compatible to the person's mental capacity, **Fatigue zone** could describe the overwhelmed situation where human beings

are given too much workload. Apart from the aforementioned differences, the aforementioned three zones seem to be related to different cases where people are assigned with varied amount of workload. Therefore, simulations were performed to monitor changes in human beings' work efficiency and mental stress under different zones.

5.3.2 Results

Time-course simulations were conducted to capture the changes in human work efficiency and mental stress when given a fixed amount of workload assignment under varied mental capacity. The initial point may fall in different zones as indicated in Figure 5.19) due to the variations in mental capacity even though the given workload assignment is the same. As a consequence, different working patterns have been recognized based on our observations on the simulation results, which are closely related to the the aforementioned zones.

To avoid any confusion on distinguishing a person's cognitive workload and the total assigned workload given by the computer, we named the latter as the workload assignment W_T. Within our analysis, we used workload to describe human beings' subjective conception of the given task, whereas the workload assignment was used to represent the objective workload demands. We assume a very basic strategy here that human beings' workload is determined by balancing the remaining workload (in total) and the remaining time resource. More precisely speaking, the considered workload determination strategy is to compute human beings' workload by dividing the remaining total workload with the remaining time. From a different point of view, this strategy is consistent with our current simplification in which human beings' time resources are constantly changing whereas other resources are either treated as constants or neglected. Mathematically, the applied workload determination strategy can be described as:

$$W(t) = \frac{W_T - \sum_0^t \epsilon(\tau)\Delta\tau}{T - t}\,, \tag{11}$$

where $W(t)$ denotes a person's cognitive workload at time t, W_T denotes the workload assignment, T represents the time length within which the person is asked to finish the assigned workload,

$\sum_0^t \epsilon(\tau)\Delta\tau$ represents the completed workload which sums the person's efficiency from the beginning to the time point t, $T - t$ denotes the remaining time.

Simulation results on time-varying work efficiency and mental stress

The tested workload assignments are set as 15000, 12500, 10000, 7500, 5000, and 2500, whereas the other parameters are fixed as time limit T at 100, stress limit σ_{max} at 200, and maximum efficiency ϵ_{max} at 100. Besides, we compared three different mental capacity levels under each simulated case. The tested mental capacity levels include the mental capacity $\beta = 1.0$ as indicated in Figure 5.19, one smaller capacity $\beta = 0.7$, as well as one larger capacity $\beta = 1.3$. In addition, the task completion status is also indicated in Figure 5.20-5.25 by color: red for successful completion and black for failure.

The simulation results indicate that when given a large amount of workload assignment such as $W_T = 15000$, human beings' work efficiency decreases to zero whereas their mental stress increases to the maximum along the process under under $\beta = 1.0$ and $\beta = 1.3$ (Figure 5.20). Moreover, human beings' work efficiency stays at zero and their mental stress stays at the maximum level when the mental capacity decreases to $\beta = 0.7$, which could be seen as the extreme case of the aforementioned trends observed under $\beta = 1.0$ and $\beta = 1.3$. According to the initial settings, the mental stress of the human beings with a mental capacity at $\beta = 0.7$ would achieve the maximum limit from the beginning till the end leading to a minimum level of work efficiency throughout the process. In addition, the simulation results indicated that human beings fail to complete the given workload assignment $W_T = 15000$ for all the three tested mental capacity levels $\beta = 0.7$, $\beta = 1.0$, and $\beta = 1.3$.

As shown in Figure 5.21, when the workload assignment is $W_T = 12500$ the human beings with a mental capacity at $\beta = 1.3$ succeed in completing the given workload assignment with both of their work efficiency and mental stress keep decreasing throughout the process. Whereas for the other two tested cases with a smaller mental capacity at $\beta = 1.0$ and $\beta = 0.7$, human beings' work efficiency decreases to zero while their mental stress increases to the maximum. In addition, the simulation results also indicate that human beings with a mental capacity at $\beta = 1.0$ and $\beta = 0.7$ fail to complete the given workload assignment (Figure 5.21).

As shown in Figure 5.22, when given a workload assignment at $W_T = 10000$ human beings seem to achieve a stable state where both of their work efficiency and mental stress stay stable throughout the process under $\beta = 1.0$. For the case with a larger mental capacity at $\beta = 1.3$, human beings' efficiency and mental stress both keep decreasing along the process. However, human beings' efficiency decreases to zero whereas their mental stress increases to the maximum under a smaller mental capacity value $\beta = 0.7$. Among the three tested mental capacity levels, human beings with a mental capacity at $\beta = 1.0$ and $\beta = 1.3$ succeed in completing the workload assignment within the time limit, whereas those with a mental capacity at $\beta = 0.7$ fail to complete the given workload assignment as shown in Figure 5.22.

When assigned with a workload assignment at $W_T = 7500$ (Figure 5.23), the simulated curves for work efficiency and mental stress resemble those observed under $W_T = 10000$ (Figure 5.22). However, the stable state observed under $W_T = 10000$ with $\beta = 1.0$ disappears under $W_T = 7500$. In particular, both work efficiency and mental stress keep decreasing throughout the process with $\beta = 1.0$ and $\beta = 1.3$, whereas work efficiency decreases to zero but mental stress increases to the maximum with $\beta = 0.7$. In the meanwhile, human beings can successfully accomplish the workload assignment at the tested two mental capacity values $\beta = 1.0$ and $\beta = 1.3$ but fail in completing the task for $\beta = 0.7$.

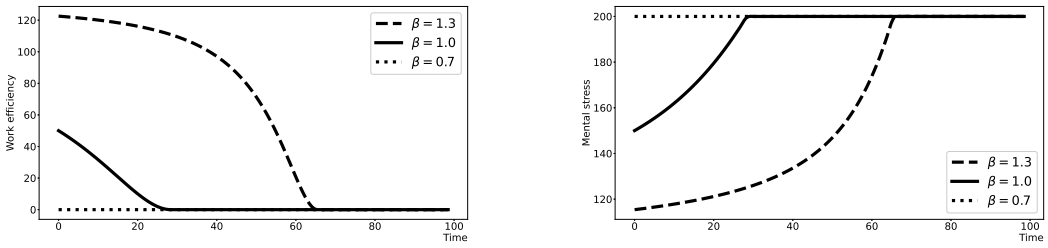

(a) Work efficiency curves

(b) Mental stress curves

Figure 5.20: Work efficiency and mental stress curves under varied mental capacity β when $W_T = W_{max} = 15000$. Task completion status is indicated by color: red for successful completion and black for failure.

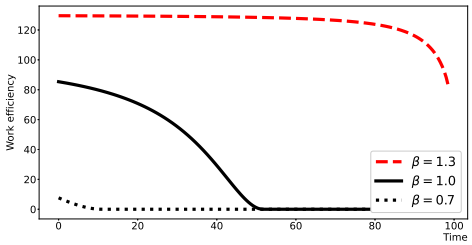

(a) Work efficiency curves

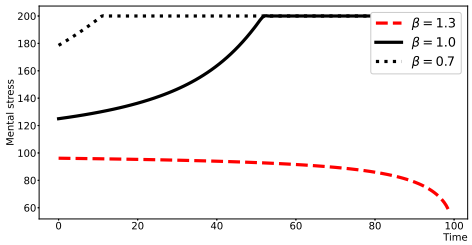

(b) Mental stress curves

Figure 5.21: Work efficiency and mental stress curves under varied mental capacity β when $W_T = W_{max} = 12500$. Task completion status is indicated by color: red for successful completion and black for failure.

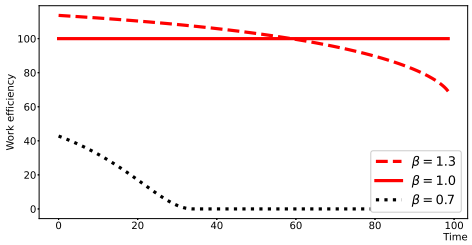

(a) Work efficiency curves

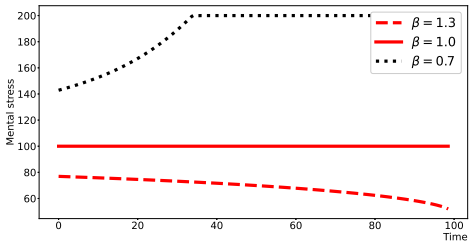

(b) Mental stress curves

Figure 5.22: Work efficiency and mental stress curves under varied mental capacity β when $W_T = W_{max} = 10000$. Task completion status is indicated by color: red for successful completion and black for failure.

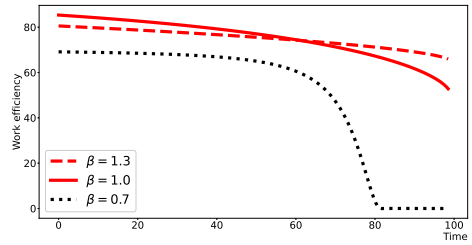

(a) Work efficiency curves

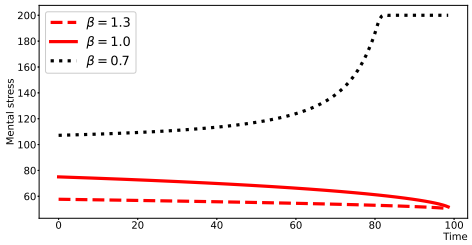

(b) Mental stress curves

Figure 5.23: Work efficiency and mental stress curves under varied mental capacity β when $W_T = W_{max} = 7500$. Task completion status is indicated by color: red for successful completion and black for failure.

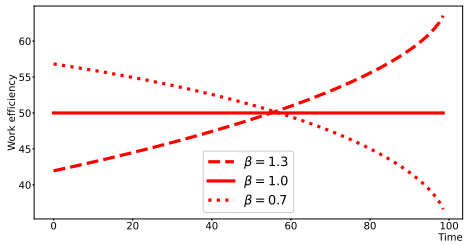

(a) Work efficiency curves

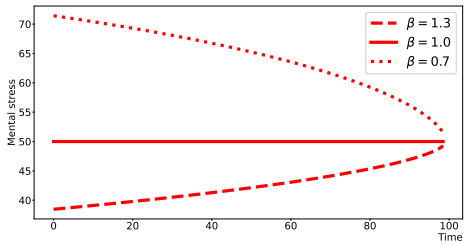

(b) Mental stress curves

Figure 5.24: Work efficiency and mental stress curves under varied mental capacity β when $W_T = W_{max} = 5000$. Task completion status is indicated by color: red for successful completion and black for failure.

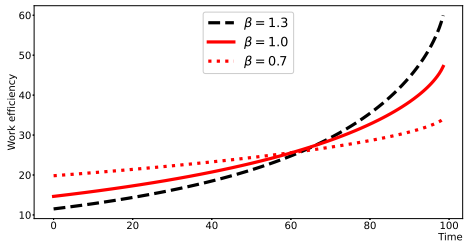

(a) Work efficiency curves

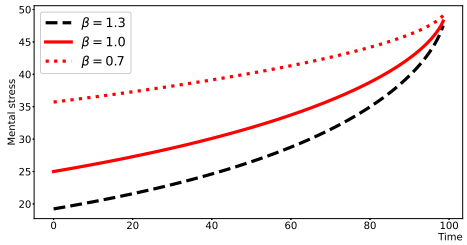

(b) Mental stress curves

Figure 5.25: Work efficiency and mental stress curves under varied mental capacity β when $W_T = W_{max} = 2500$. Task completion status is indicated by color: red for successful completion and black for failure.

When the workload assignment is reduced to $W_T = 5000$ (Figure 5.24), the stable state observed at mental capacity $\beta = 1.0$ under $W_T = 10000$ (Figure 5.22) appears again. As shown in Figure 5.24, with a mental capacity at $\beta = 1.0$ human beings' work efficiency keeps stable almost throughout the process at a value which is only half of that observed under $W_T = 10000$. The simulation results indicate that for the human beings with a mental capacity at $\beta = 1.3$ both of their work efficiency and mental stress keep increasing along the process, whereas for those with a mental capacity at $\beta = 0.7$ both of their work efficiency and mental stress keep decreasing. Despite the aforementioned different trends in work efficiency and mental stress, the simulation results indicate that human beings succeed in completing the given workload assignment under all of the three tested mental capacity levels ($\beta = 0.7$, $\beta = 1.0$, and $\beta = 1.3$).

When the workload assignment decreases to $W_T = 2500$ (Figure 5.25), the stable states observed at mental capacity $\beta = 1.0$ under the workload assignment $W_T = 10000$ (Figure 5.22) and $W_T = 5000$ (Figure 5.24) disappears again. Instead, human beings' work efficiency and mental stress both keep increasing throughout the process with a mental capacity at $\beta = 1.0$. Moreover, the same increasing trends in work efficiency and mental stress are also observed for the other two tested mental capacity levels, namely $\beta = 0.7$ and $\beta = 1.3$. In the meantime, according to the simulation results human beings with a mental capacity at $\beta = 0.7$ and $\beta = 1.0$ succeed in completing the given workload assignment, whereas those with a mental capacity at $\beta = 1.3$ end up with a failure.

To sum up, the aforementioned observations seem to indicate that human beings' work efficiency and mental stress may follow a specific pattern or trend when the initial point falls in different zones according to the given workload assignment W_T and a predefined mental capacity β. Therefore, the following section aims to identify the possible patterns under different settings and to investigate how can the identified patterns be mapped to the three zones identified in Figure 5.19.

5.3.3 Discussion

Three working zones corresponding to three working patterns

The ideal case modeling line is added to the corresponding human beings' workload-efficiency curves under the tested three mental capacity levels, namely $\beta = 0.7$, $\beta = 1.0$, $\beta = 1.3$. As shown in Figure 5.26, two intersections are generated under each tested mental capacity between the ideal modeling and the human workload-efficiency curves. In particular, the two intersections under $\beta = 0.7$ locate at $W(t) = 35$ and $W(t) = 70$, the intersections under $\beta = 1.0$ locate at $W(t) = 50$ and $W(t) = 100$, and the intersections under $\beta = 1.3$ locate at $W(t) = 65$ and $W(t) = 130$.

Let's recall the time-varying word efficiency and mental stress curves observed in Figure 5.20 under the workload assignment at $W_T = 15000$. The corresponding initial workload equals to 150, which is larger than all the intersections generated between human beings and the ideal workload-efficiency curves under the three mental capacity levels. That is to say, the initial point falls in **Fatigue zone** under all the three tested mental capacity levels as shown in Figure 5.26. As shown

in Figure 5.20, human beings fail to complete the given workload assignment across the tested mental capacity levels ($\beta = 0.7, 1.0, 1.3$), while their work efficiency decreases to zero and their mental stress increases to the maximum limit. The work efficiency and mental stress curves observed under $\beta = 0.7$ are the extreme cases of the aforementioned pattern where work efficiency decreases directly to zero and mental stress increases directly to the maximum at the beginning. The aforementioned changing trends in work efficiency and mental stress may indicate a specific pattern under **Fatigue zone**.

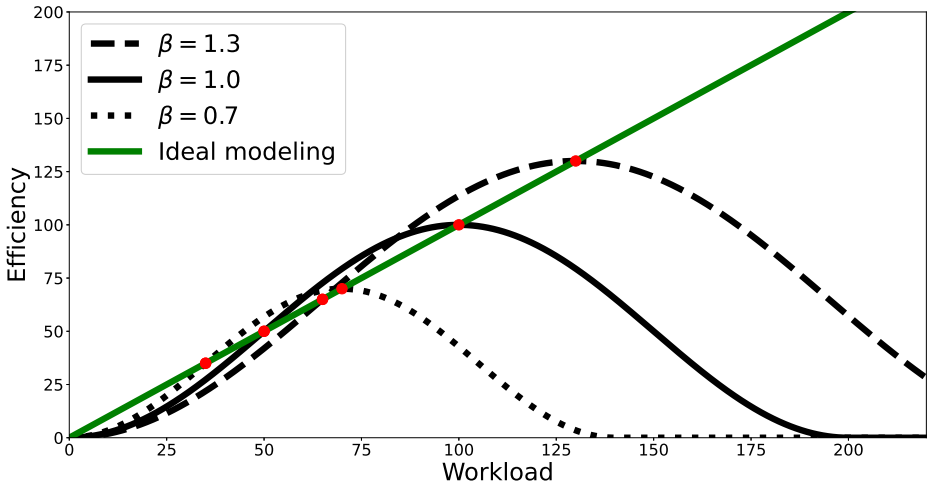

Figure 5.26: Comparison between human beings' and the ideal workload-efficiency relationships for varying mental capacity at $\beta = 0.7, 1.0, 1.3$

When the given workload assignment is set at $W_T = 12500$, the corresponding initial workload equals to 125. By referring to the modeling results shown in Figure 5.26, the initial point falls in **Capacity zone** ($65 < 125 < 130$) for the mental capacity at $\beta = 1.3$ whereas for the other two mental capacity levels at $\beta = 1.0$ and $\beta = 0.7$ the initial point falls in **Fatigue zone**. As indicated in Figure 5.21, both of work efficiency and mental stress keep decreasing throughout the process when the initial point falls in **Capacity zone** under $\beta = 1.3$, where the human beings succeed in completing the given workload assignment. However, the human beings with a mental capacity at $\beta = 0.7, 1.0$ fail to complete the workload assignment $W_T = 12500$ and the changing trends of the work efficiency and mental stress resemble what have been seen under $W_T = 15000$. This similarity might be explained by the location of the initial point that belong to **Fatigue zone** for a

mental capacity at $\beta = 0.7, 1.0$ under $W_T = 12500$ and for all the three mental capacity levels under $W_T = 15000$.

The original workload corresponding to the workload assignment at $W_T = 10000$ is $W(t = 0) = 100$, locating exactly at the one of the intersections under $\beta = 1.0$ (Figure 5.26). As for the other two tested mental capacity levels, the original point falls within **Capacity zone** for $\beta = 1.3$ and within **Fatigue zone** for $\beta = 0.7$. As shown in Figure 5.22, the work efficiency and mental stress stay at the initial level throughout the process when the original point locates at the intersection under $\beta = 1.0$. In the meantime, the trends of work efficiency and mental stress resemble what have been observed under $W_T = 12500$ when the initial point falls in **Capacity zone** and **Fatigue zone** for $\beta = 1.3$ and $\beta = 0.7$ respectively. The simulation results also indicate that human beings are able complete the given workload assignment when the initial point falls within **Capacity zone** including the intersection positions.

As the workload assignment reduced to $W_T = 7500$ as shown in Figure 5.23, the corresponding initial workload equals to 75, which locates within **Capacity zone** under $\beta = 1.0, 1.3$ and within **Fatigue zone** under $\beta = 0.7$ (Figure 5.26). Similar to the aforementioned observations, both of work efficiency and mental stress keep decreasing throughout the process when the initial point falls in **Capacity zone**, whereas human beings' work efficiency decreases to zero whereas their mental stress increases to the maximum when the initial point falls in **Fatigue zone**.

The original workload corresponding to the workload assignment at $W_T = 5000$ is $W(t = 0) = 50$, which once again locates exactly at the one of the intersections under $\beta = 1.0$ (Figure 5.26). Similar to the stable state observed under $W_T = 10000$, human beings' work efficiency and mental stress both stay stable throughout the process under $\beta = 1.0$ as shown in Figure 5.24. As for the other two tested mental capacity levels, the initial point falls in **Capacity zone** under $\beta = 0.7$ and in **Laid-back zone** under $\beta = 1.3$. This is the first time that the initial point falls in **Laid-back zone** based on our observations so far, human beings' work efficiency and mental stress both keep increasing throughout the process as indicated in Figure 5.24 for $\beta = 1.3$. The decreasing work efficiency and mental stress under $\beta = 0.7$ resembles what have been observed with the initial point within **Capacity zone**. Moreover, the simulation results indicated that human beings can succeed in completing the given workload assignment when working at **Capacity zone** as well as **Laid-back**

zone.

When the workload assignment reduced to $W_T = 2500$ as shown in Figure 5.25, the corresponding initial workload equals to 25 locating in **Laid-back zone** for all the three tested mental capacity levels. According to Figure 5.25, human beings' work efficiency and mental stress both keep increasing throughout the process when the initial point falls in **Laid-back zone**. In addition, the simulation results indicate that human beings may succeed or fail in completing the given workload assignment when working at **Laid-back zone**.

To sum up, based on our observations so far there seems to be a mapping between different changing patters reflecting human beings' work efficiency and mental stress and the three zones identified under the three tested mental capacity levels as shown in Figure 5.26. Therefore, three patterns have been identified as:

> **Pattern I**: observed within **Laid-back zone**, where both of work efficiency and mental stress keep increasing, human beings may succeed or fail in completing the workload assignment.
>
> **Pattern II**: observed within **Capacity zone**, where both of work efficiency and mental stress keep decreasing, human beings succeed in completing the workload assignment.
>
> **Pattern III**: observed within **Fatigue zone**, where work efficiency decreases to zero and mental stress increases to the maximum level, human beings fail to complete the given workload assignment.

Our simulation results show that under **Pattern I** human beings keep working at a very low efficiency even though the workload assignment can be successfully completed in some cases. This is not an expected situation as they are actually capable to complete much more workload assignment instead of just completing the given small amount of workload assignment. On the contrary, **Pattern III** seems to be accompanied with a high stress level but low efficiency when the human beings are confronted with a large amount of workload assignment. Such low efficiency may explain the human beings' failure under this working pattern. Besides, long-term exposure to such overwhelmed situation may lead to fatigue and other mental health problems. **Pattern II** describes the situation where human beings are not given too much or too little workload and can therefore

succeed in completing the workload assignment at a relative high efficiency. In spite of the decreasing trend observed in human beings' work efficiency, their work efficiency keeps at a relative high level throughout the process. In addition, by monitoring their cognitive workload under **Pattern II** we may infer that the workload is well managed under such working pattern due to the decreasing workload trend. Among the three patterns, **Pattern II** is the only working pattern under which a successful completion of the given workload assignment can be ensured. However, human beings always fail to complete the workload assignment within the time limit under **Pattern III** and they may fail or succeed in completing the workload assignment under **Pattern I**. In addition, more workload assignment can be completed under **Pattern II** when compared to the successful cases under **Pattern I**. Therefore, **Pattern II** appears to be the preferred working pattern for human beings.

The Capacity zone and workload equilibrium

According to our observations so far, human beings are actually able to complete more workload assignment when the initial workload falls in **Laid-back zone**, where their work efficiency and mental stress keep increasing as the process continues (**Pattern I**). When working at **Laid-back zone**, human beings tend to lay back considering that they do not feel any challenge or stress towards the assigned workload, which could also lead to a bad performance reflected in a low efficiency and sometimes a failure in completing the given task. When the initial workload locates in **Fatigue zone**, human beings' work efficiency decreases to zero whereas their mental stress increases to the maximum as described in **Pattern I**. In addition, the process always ends with a failure in completing the given task, the reason for which may be found in the name indicating that human beings would feel fatigue when given too much workload when working at **Fatigue zone**. This is unexpected in real-life practices in terms of efficiency and effectiveness as human being always fail to complete the workload assignment and may lead to potential mental health problems. As a result, **Fatigue zone** should firstly be avoided. Similarly, **Laid-back zone** is not an expected working zone either given that human beings are working at a very low efficiency and behaving lazily toward the assigned work, even though they may not always fail in completing the workload assignment. The most important characteristics shared by the two zones discussed above is that

human beings can only accomplish a relatively small amount of workload assignment regardless of the completion results. On the contrary, when working under **Capacity zone** located between the two intersections, human beings can keep working at a high efficiency throughout the process and succeed in completing the given workload assignment within the time limit. Thereafter, the concept of **Capacity zone** is proposed in this paper to ensure the successful completion and a high efficiency for the task handled by human beings.

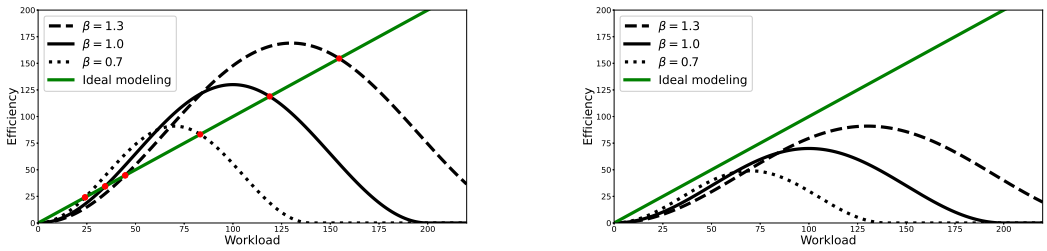

(a) Intersections under $\beta = 0.7, 1.0, and 1.3$ (b) Intersections under $\epsilon_{max} = 70, 100, and 130$

Figure 5.27: Comparison of human beings' and the ideal workload-efficiency relationships under maximum efficiency $\epsilon_{max} = 130$ and $\epsilon_{max} = 70$

The two intersections between human beings' and the ideal modeling seem to serve as the boundaries of human beings' **Capacity zone**, with the first intersection as the lower boundary and the second intersection as the upper boundary. Considering the working patterns identified under the three working zones during simulations, the stable states observed observed at $W_T = 5000$ and $W_T = 10000$ correspond to the two intersections generated under $\beta = 1.0$. Moreover, by including more workload assignment values into our simulations **Pattern II** was observed in all the tested cases when human beings' initial workload falls in **Capacity zone**. When the initial workload is smaller than 50, **Pattern I** was observed in all of the tested cases where human beings will be working at their **Laid-back zone** with increasing work efficiency and increasing mental stress. This may suggest that human beings' efficiency is very low when working under **Laid-back zone** and they gradually increase their efficiency in order to complete the assigned workload. However, when corresponding initial workload is larger than 100, **Pattern III** appeared where human beings can no longer complete the workload assignment working at their **Fatigue zone**. The decreasing efficiency and increasing mental stress under **Pattern III** indicate that human beings are having difficulty in handling the task and their working states are moving away from the second intersection while

working at their **Fatigue zone**. Moreover, the ideal case modeling line is added to the corresponding human beings' workload-efficiency curves under $\epsilon_{max} = 130$ and $\epsilon_{max} = 70$ (Figure 5.27b). Two intersections are generated between the ideal modeling and the human workload-efficiency curve under each of the three tested mental capacity levels under $\epsilon_{max} = 130$, whereas no interaction was generated under $\epsilon_{max} = 70$ across the tested mental capacity levels. From a practical viewpoint, $\epsilon_{max} \geq 100$ can be considered as one of the requirements in selecting the right human beings to complete the target task. That is, the human beings with a maximum efficiency $\epsilon_{max} \geq 100$ are considered unqualified for the confronted task under the current settings. When the maximum efficiency is set to 130, the generated intersections include two intersections located at $W(t) = 44.71$ and $W(t) = 154.55$ for $\beta = 1.3$, two intersections at $W(t) = 34.39$ and $W(t) = 118.89$ for $\beta = 1.0$, and two intersections at $W(t) = 24.08$ and $W(t) = 83.22$ for $\beta = 0.7$. The aforementioned boundary effect of the generated intersections has been confirmed across the three different mental capacity levels under $\epsilon_{max} = 130$. Thereafter, we name the two intersections as the workload equilibrium points considering their important role in defining human beings' **Capacity zone** and separating the corresponding working patterns. The definition of human beings' **Capacity zone** as well as the other two working zones could thus be summarized as follows.

> **Laid-back zone**: corresponds to the workload values smaller than the first workload equilibrium, where both of work efficiency and mental stress keep increasing and human beings may succeed or fail in completing the workload assignment.
>
> **Capacity zone**: corresponds to the workload values between the two workload equilibrium points, where both of work efficiency and mental stress keep decreasing and human beings always succeed in completing the workload assignment.
>
> **Fatigue zone**: corresponds to the workload values larger than the second workload equilibrium, where work efficiency decreases to zero and mental stress increases to the maximum level and human beings always fail to complete the given workload assignment.

Figure 5.28 presents a summary of human beings' workload equilibrium, **Capacity zone**, and the changing trends within different zones at a reduced mental capacity example for $\beta = 0.7$ (needs

to be updated with the new parameters). The proposed **Capacity zone** is highlighted with colored background in Figure 5.28, where the arrows indicate different changing trends and the workload equilibrium is marked by solid or hollow circle regarding its stability. Based on our observations, human beings are only able to complete the a large amount of workload assignment within the pre-defined time limit when working at the **Capacity zone**. When working outside of the **Capacity zone**, human beings can only handle a very limited amount of workload assignments, even though they do not always fail to complete the given assignment. The increasing work efficiency observed under **Laid-back zone** (corresponding to the right-oriented black arrow in Figure 5.28) does not mean a good performance, considering that human beings keep working at a relatively low efficiency level throughout the process and they keep approaching the first workload equilibrium. As for **Fatigue zone**, only a small portion of the task can be completed even though a larger amount of workload is assigned to the human beings than that for **Capacity zone**. Moreover, the increasing workload when working at the **Fatigue zone** (corresponding to the right-oriented black arrow in Figure 5.28) may lead to fatigue and stress related health problems if such condition continues for a long time, which should be avoided. However, human beings are able to work at a relatively high efficiency and can always succeed in completing the workload assignment when working at the **Capacity zone**. Despite the fact that human beings' efficiency keeps decreasing toward the first workload equilibrium (corresponding to the red arrows within in Figure 5.28), they are still working at a relatively high efficiency which contributes to the successful task completion. The word "capacity" is used to highlight the good matching between this working zone and human beings' current mental capacity β level, which is reflected in the successful completion of the task and a good performance (efficiency). In the meanwhile, this way of naming emphasizes the paired application and close relationship between human beings' **Capacity zone** and their mental capacity β. Human beings' mental capacity β reflects a general mental status regarding the given task considering their knowledge, skills, and affect. The determination of a **Capacity zone** could not be done without a fixed mental capacity β. This means that the application of **Capacity zone** should always be in pair with a known mental capacity β as any changes in the mental capacity will change the position and shape of the corresponding **Capacity zone**.

Furthermore, the proposed **Capacity zone** could provide theoretical interpretation to the deadline related as well as the mental capacity related phenomena reported in the literature (Chong, Van Eerde, Chai, & Rutte, 2010; Gonzalez-Mulé, Carter, & Mount, 2017; Kulikowski, 2021; Phillips, 2008; Schmitt, Ohly, & Kleespies, 2015). Meanwhile, the three identified working zones and their corresponding working patterns showed high consistency with the challenging and hindering effect of time pressure on performance (Baethge, Vahle-Hinz, Schulte-Braucks, & van Dick, 2018; Kunzelmann & Rigotti, 2021). The proposed **Capacity zone** located between the two workload equilibrium points under varied initial settings could help in theoretically explaining the dual effect of cognitive abilities on burnout proposed in a recent study (Kulikowski, 2021). That is, the **Proposition 1** in that paper saying that "cognitive ability indirectly decreases burnout via increasing job resources" , could be explained by the differences in individual's **Capacity zone** under varied mental capacity as illustrated in Figure 5.27a, and the **Proposition 2** may be explained with the cases presented in Figure 5.27b. Consider an individual with a mental capacity at 0.7 works at the **Fatigue zone** whereas another individual with a mental capacity at 1.0 works within the **Capacity zone** when both of them are required to work on an assigned task with a corresponding initial workload around 100 (Figure 5.27a). Under such circumstance, the latter is associated with a decrease on burnout in comparison with the former case considering that burnout is a typical consequence of continuously working at the **Fatigue zone**. In addition, the **Proposition 2** in the study (Kulikowski, 2021) mentioned that individuals with higher cognitive abilities may also receive more task demands and have higher performance pressure compared to the individuals with lower cognitive abilities, which could be explained with the cases shown in Figure 5.27b. Employers seem to have very high expectation in the employees with high cognitive abilities, which may be represented as the employer tend to overestimate those individuals' maximum efficiency whereas their actual efficiency limit may be much lower due to varied reasons. In this way, more tasks and workload assignments will be given to this employer which may result in long-term working at then **Fatigue zone** and increases in burnout.

Is there an optimal position within human beings' **Capacity zone** that should be suggested for real-life practice? Considering that the **Capacity zone** describes the area between the two workload equilibrium points, we may start with those two points located at the boundaries of the preferred

working zone. Should we recommend the workload equilibrium? The answer is no due to the following two reasons. First, the first workload equilibrium is the only stable equilibrium point because it could "attract" the state point back to it with any displacements (in the **Laid-back zone** or **Capacity zone**). However, human beings can only complete a relatively small amount of workload when working at or around this stable equilibrium compared to the rest area within **Capacity zone**. As the result, the first workload equilibrium should not be recommended. Second, the second workload equilibrium is an unstable equilibrium which should not be recommended either. In Figure 5.28, it is distinguished from the stable equilibrium by a hollow circle marker. Human beings complete the most amount of workload if working exactly at this point from the beginning, but at the risk that the state point will leave further and further with any slight displacement. What about the position corresponding to human beings' maximum efficiency ϵ_{max}? We should not recommend the maximum efficiency point either because human beings' efficiency will keep decreasing toward the first workload equilibrium instead of staying at the maximum value. That is to say, the maximum efficiency point in Figure 5.28 only means the starting point of human beings' time-course efficiency, but the completed workload amount is not very large compared to the amount of workload completed at the second workload equilibrium. Therefore, there is not a specific position that should be considered as the optimal position to be recommended. However, there is an area within the **Capacity zone** that could be suggested to computers as the preferred area.

Based on the aforementioned discussions, we would suggest to facilitate the positions within human beings' **Capacity zone** that locate near the second workload equilibrium when assigning workload to different individuals. At those positions, human beings could work at a high efficiency and end with a successful completion of the given task with a large amount of workload completed. Moreover, those positions may locate on the right side of the maximum efficiency point, meaning that human beings will work at a high efficiency for a period of time by approaching and then leaving from their maximum efficiency. Last but not least, keeping a certain distance from the second workload equilibrium can reduce the risk of exceeding the **Capacity zone**. As human beings' state point keeps moving toward the first workload equilibrium while working at their **Capacity zone**, it will never reach the second workload equilibrium not to mention exceeding the preferred working zone.

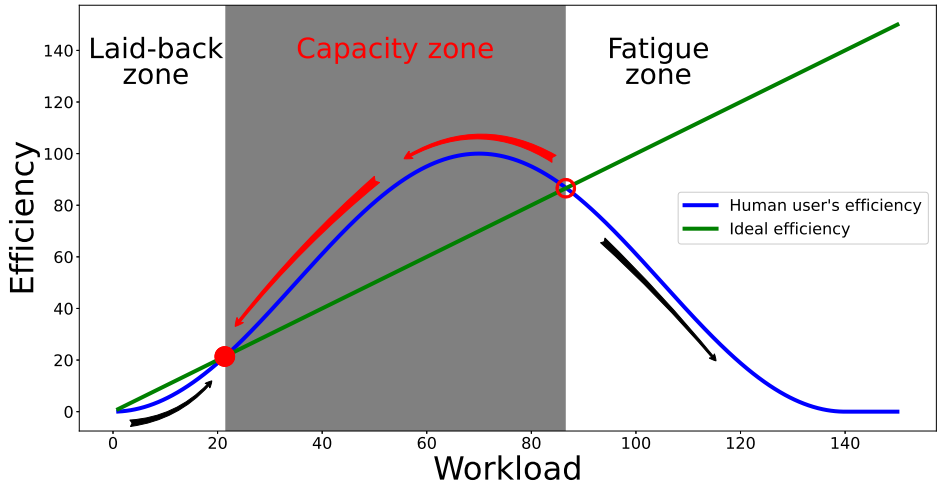

Figure 5.28: Human beings' **Capacity zone** and the state changing trends in different zones represented in workload-efficiency relationship at $\beta = 0.7$

Determining and applying human beings' Capacity zone

In terms of the determination of human beings' **Capacity zone**, it could be done by identifying the two workload equilibrium points on the workload-efficiency curve corresponding to the intersections generated between human beings' and the ideal modeling. Mathematically, this can be done by solving Eq. (9) and Eq. (11) under predefined β and ϵ_{max} values. The smaller one's mental capacity β is, the narrower the corresponding **Capacity zone** becomes while moving toward the left side. On the contrary, a larger mental capacity leads to a wider range for the corresponding **Capacity zone** locating more toward the right side on the workload-efficiency curves. Based on the current assumptions, the maximum efficiency also increases with a larger mental capacity level. With regard to variations in the maximum efficiency ϵ_{max}, a larger value corresponds to a broader and higher **Capacity zone**, and vice versa. Considering that the positions of the original workload-efficiency curves won't change under varied maximum efficiency, the changing trend of **Capacity zone** is not as obvious as that under varied mental capacity. Moreover, a large maximum efficiency ϵ_{max} may be able to compensate the deficiency of mental capacity β.

Furthermore, a four-step protocol is proposed below for applying and facilitating human participants' **Capacity zone** in real-life practices. First, the workload-efficiency modeling for the involved

human participants can be done based on their previous performance (to obtain his maximum efficiency ϵ_{max}) and other recordings (to obtain his mental capacity β). Second, an ideal workload-efficiency modeling line can be added to the original modeling in order determine the corresponding **Capacity zone** located between the workload equilibrium points. Third, a computer or human instructor should adjust the workload allocation strategy to assign a "good" workload amount to different human participants so that they can work at their **Capacity zone**. Fourth, the computer or human instructor should frequently update human participants' mental capacity β values used in the workload-efficiency modeling based on the timely feedback from them. The fourth step needs to be addressed in our future work as human participants' mental capacity is considered stable throughout the problem-solving process in the current research.

Limitations and future directions

This research has a few limitations which need to be addressed in our future work. First, the current research proposes human beings' **Capacity zone** that is determined on a predefined mental capacity and maximum efficiency. However, the current discussions do not cover how to extract the values of those two parameters from behavioural and physiological data. In our future work, further investigation will be conducted regarding what kinds of data should be used and how to obtain human beings' mental capacity and maximum efficiency from the data. Second, interventions from computers or human instructors are suggested to pull human participants back to their capacity zone when they are found working outside of it, whereas the details of how to inform computers of human participants' current working zone and the exact working position are not covered in the present research. As a result, our future work will address the questions including what quantification methods are suitable to extract human beings' cognitive workload and what else should be added if workload itself is not enough. Third, the current research does not consider the differences in workload determination strategies across individuals. For example, some people prefer to complete as much workload as they can in the early stage whereas some may prefer to leave most of the workload till the last few days or weeks before the deadline. Another example is that human beings may apply different problem-solving strategies like depth-first or breadth-first strategies, and varied strategies for workload/task decomposition. It is also possible that some human participants are able to get

back to their capacity zone by themselves thanks to their applied strategies in coping with "bad" workload or stress. Covering those differences in our future work will also add more dimensions to our analysis and make it more adaptive to different scenarios that may happen in real-life practices. Last but not the least, our current observations are based on the theoretical analysis and simulation results built upon the stress-effort model. Part of our future work is to identify human beings' capacity zone from their behavioural and physiological data recorded during experiments.

Conclusions

This paper proposes the concept of human beings' capacity zone located between the two workload equilibrium points to ensure a successful accomplishment of a collaborative task under a predefined deadline. Computers or human instructors are suggested to facilitate human beings' capacity zone and to intervene when they are working outside their capacity zone to ensure a high efficiency of the entire systems or teams. According to our discussions above, human beings could always succeed in accomplishing the given task with a large amount of workload completed in the end if they work within their capacity zone. This characteristic of capacity zone is highlighted under a collaborative project where the successful completion of the each human participant's task is crucial to the overall success. The proposed capacity zone should be used together with a mental capacity β value and a maximum efficiency ϵ_{max} level that could vary between different individuals. Those two parameters not only contribute to the initial determination of one's capacity zone but also keep reshaping it in responding to any variations in the parameters during the process.

We suggest that a computer or human instructor should intervene with human participants when they are working outside their capacity zone. The necessity of such intervention results from our observations that human beings are not able to come back to their capacity zone by themselves once working outside. However, only a limited amount or workload assignment can be done if they continue to work outside their capacity zone. Therefore, we suggest that interventions are required under those cases to pull them back to their capacity zone. In this way, a successful accomplishment of each human participant's task and a high overall efficiency can be ensured. Moreover, an area right before the second workload equilibrium is highlighted in order to achieve a even better performance with a larger amount of completed workload compared to the rest positions

within the capacity zone. In terms of possible intervention actions, a computer or human instructor could directly adjust the workload assignment amount for different human participants depending on their current mental capacity levels. For example, when a human participant is working at the laid-back zone, the computer or human instructor may intervene by adding more workload assignment or updating the deadline to an earlier time (smaller T) to pull the person back to the capacity zone. On the contrary, possible interventions for a human participant who is working at the fatigue zone include extending the time limit or taking out some workload assignment from the person.

5.4 Ongoing exploration on the quantification and impact of mental capacity: An N-back working memory experiment

This ongoing study aims to test the proposed quantitative approach with experimental evidence where we designed a cognitive experiment based on the N-back WM paradigm, which falls under the third stage of the research methodology toward the second research objective. One research goal of this study, a continuation of the one presented in Section 5.3, is to quantify different individuals' mental capacities as well as their limits that would contribute to the determination of capacity zones. Taking it as the ultimate goal of this study, the current preliminary analysis might contribute to the other two research questions listed below. From this perspective, the current analysis can be seen as the first step to measuring a person's capacity limit and detecting when it is reached. Overall, this study was designed to answer three questions, of which the third corresponds to the ultimate objective, which requires further discussion among the research team in order to summarize the existing findings and add additional analysis. Though the current analysis did not yield sufficient results to measure or detect one's capacity limit, I will continue to finalize the analysis and conduct further investigations along this direction in my future research.

(1) How would the tested features respond to different workload as N increases from 1 to 2 and then to 3 in an N-back WM paradigm?

(2) Do the EEG-based results differentiate between spatial and verbal information under an N-back WM paradigm?

(3) If some participants have already reached their capacity limit in an N-back WM paradigm with N up to 3, can we detect it from their network oscillations?

In the meantime, the experiment design was motivated by our discussions with a few experienced pilots and observations on a pilot training process within the study presented in Section 5.2. A number of well-established EEG features were tested under an N-back WM paradigm under varying conditions to see how they responded and how sensitive they were to a particular changing dimension. Participants in this study are sometimes called ”pilot trainees” since they have been hired for both this N-back experiment and the aforementioned pilot training experiment. In this vein, the research outcome from this ongoing study which might also provide useful information to the study (Zhao, Jia, et al., 2022) in improving the reliability and precision of the quantification of pilot trainees' cognitive changes within a skill acquisition process.

5.4.1 Experiment and participants

The N-back experiment in this study was adapted from the N-back protocol applied in (Nystrom et al., 2000), which contrasted WM processes with letters (verbal) versus spatial locations. Under an N-back WM paradigm, participants are presented with a sequence of visual stimuli and are asked to answer if the current item is the same as the one presented N items prior. Our N-back experiment consists of two versions, namely the verbal version and the spatial version. The stimuli used for both versions were the same group of letters showing at varying locations on the screen, which could ensure that participants receive identical visual stimuli to “eliminate a potential confound between WM and differential low-level visual experience” (Nystrom et al., 2000). The only difference between the two versions lied in the task instructions presented in the beginning of the block, indicating whether the letter (for verbal version) or the location (for spatial version) should be considered in making a judgement.

Three workload levels were tested during the experiment with N equals to 1, 2, and 3 for both verbal and spatial versions. General instructions were displayed to the participants at the beginning of the experiment, indicating how the experiment works and the tasks to be completed. The trials were grouped in blocks, there were instructions at the beginning of each block indicating the version

(spatial or verbal) and difficulty level (1-back, 2-back, or 3-back) of the current block. Participants were asked to complete 12 blocks in total and each block consisted of 50 sequential trials. Those 12 blocks were presented in a predefined order starting with 3 spatial blocks (1-back, 2-back, and 3-back), 3 verbal blocks (1-back, 2-back, and 3-back), followed by another 3 spatial blocks and 3 verbal blocks. At the beginning of each trial, a cross appeared at the center of the screen for 0.2 s. After 1.1 s following the offset of the cross, the stimulus (a random letter) appeared at a random location for 0.2 s. After the offset of the stimulus, participants were given 3.0 s to indicate their response. In our experiment, participant were allowed to change their responses and only the latest press before the time limit was considered as their final response. In addition, participants were instructed to practice the spatial and non-spatial version of the N-back task on all three difficulties (1-back, 2-back, 3-back) before starting the experiment.

Twenty-four participants aged between 21-41 (11 males, 13 females) were recruited to conduct the experiments. All participants reported to be in general good health without any neurological or psychiatric disorder.In addition, all participants had normal vision or could achieve normal vision with contact lenses, as glasses were not accepted for this experiment. Each participant received $\$50$ CAD compensation together with $\$80$ CAD as trip compensation after completing the experiments. Participants' physiological data and behavioural data were recorded throughout the experiment. The recorded physiological data includes: Electroencephalogram (EEG), Electrocardiogram (ECG), Galvanic Skin Response (GSR), and Eye tracking, while participants' behavioural data were recorded by the computer. EEG data was collected using a 64-channel BioSemi ActiveTwo system placed according to the international 10–20 system at a sampling rate of 2048 Hz. The results from other recorded physiological data were not included in this research. The data collected from three subjects have been removed for further analysis due to bad data quality or unexpected interruptions, resulting in a data sample consisted of 21 subjects for further analysis.

5.4.2 Data pre-processing

The EEGLAB toolbox was applied during pre-processing for removing noises and artifacts from the EEG data (Delorme & Makeig, 2004). The collected EEG data were referenced to mastoids and then filtered between 1 and 40Hz using a zero-phase Hamming windowed-sinc FIR filter. Afterward, the

channels that satisfied one or more criteria below were isolated as bad channels. The applied criteria for bad channel detection include: 1) the channel kept flat for more than 5 seconds; 2) the correlation between the channel and its nearby channels is smaller than 0.8; and 3) the amplitude of the channel was greater than 3 standard deviation from the mean. For artifact removal, the multiple artifact rejection algorithm (MARA) was applied where the IC components having more than 40% chance to be labelled as artifacts (eye-blink, eye-movement, muscle-generated, and other artifacts) were removed. According to the experiment protocol, the collected data were segmented into 4.5-second epochs, among which only those with correct answers were kept for further analysis. The kept 4.5-second epochs were then analyzed for detecting bad segments and bad local channels within each segment (Gabard-Durnam et al., 2018). The detected bad segments were rejected and the bad local channels detected by applying FASTER (Nolan et al., 2010) criteria were interpolated using spherical splines. Afterward, the obtained clean signals were re-referenced to average reference and downsampled to 250Hz. Finally, baseline correction was applied to the pre-processed epochs using the 1.3-second fixation period. As a result, the pre-processed epochs used for further analysis were 3.2-second epochs starting from the presence of the trigger letter.

5.4.3 Feature extraction and analysis

- **Spectral analysis:** The power spectral density (PSD) was estimated by applying the Welch periodogram method with 50% overlapping Hamming windows of a length of 2 seconds to the pre-processed EEG data. Afterward, the theta band (4-7.5 Hz) power, alpha band (8-12.5 Hz) power, low beta band (13-19.5 Hz) power, high beta band (20-30 Hz) power, and gamma band (30.5-40 Hz) power were computed from the PSD for each individual's trials with correct answers. In the meantime, we also computed a few features derived from the band power features that have been reported to be associated with engagement, mental effort, and fatigue in the literature (Fernandez Rojas et al., 2020; Freeman, Mikulka, Scerbo, & Scott, 2004; J. Hu & Min, 2018; Ismail & Karwowski, 2020; Khare & Bajaj, 2020). The engagement index (Freeman, Mikulka, Prinzel, & Scerbo, 1999; Pope, Bogart, & Bartolome, 1995) has been applied to describe how engaged the individual is at the confronted task, which represents the ratio between beta power and the sum of theta and alpha power associated

with certain EEG measurement channels. Two types of entropies were computed, namely sample entropy (Richman & Moorman, 2000) and permutation entropy (Bandt & Pompe, 2002) according to the reported applications on fatigue detection. Under each trial, the band powers and power derived features at 64 EEG channels were then grouped into five cortical areas (frontal, central, temporal, parietal, and occipital) (Agnoli et al., 2020; Jia & Zeng, 2021) for including AREA comparisons in repeated measures ANOVA.

- **EEG microstate features:** The seven microstate classes (A, B, C, D, E, F, G) were computed following the same approach as described in Section 5.2. The Global Field Power (GFP) was computed for each trial and only the EEG data at the computed GFP peaks were sent to the modified k-means algorithm with the cost function. We applied 100 repetitions to select the optimal microstate classes based on the cross-validation defined in Eq. (8) from the microstate classes computed from each repetition. Afterward, a full permutation procedure was applied to compute the group-wise microstate classes from the microstate classes obtained in each individual's single block, which were denoted as the global microstate classes. The global microstate classes were then used to represent the pre-processed EEG data in the time domain by assigning one of the global microstate classes to each time point. During this fitting back process, the highest spatical correlation was used as the criterion for mocrostate class assignment and the polarity of the microstate classes was ignored. Furthermore, no smoothing parameters were applied in our analysis to avoid any modification to the temporal dynamics of the generated microstate sequences.

  Three microstate parameters, namely duration, occurrence, and coverage, were computed for the microstate sequences generated for each individual's different trials. Moreover, a finite estimate of the entropy rate and Hurst exponent estimated by detrended fluctuation analysis (DFA) were applied to measure the temporal dependencies of different microstates in this research. More detailed information could be found in Section 5.2.

- **Statistical anlaysis:** The EEG spectral features were analyzed separately by a 2 (VERSION) $\times$3 (DIFFICULTY)$\times$5 (AREA) repeated measures ANOVA. The three within subject factors were VERSION (Spatial and Verbal), DIFFICULTY (1-back, 2-back, and 3-back), and AREA

(Frontal, Central, Temporal, Parietal, and Occipital). Greenhouse-Geisser correction was applied in the case of sphericity violations. Post hoc paired t-test was conducted at each tested AREA between VERSION and between DIFFICULTY and Bonferroni correction was applied for multiple comparisons.

For each of the computed EEG microstate parameters (coverage, occurrence, and duration), a 2 (VERSION) $\times$3 (DIFFICULTY)$\times$7 (CLASS) repeated measures ANOVA was applied to analyze the effects of different factors. The three within subject factors were VERSION (Spatial and Verbal), DIFFICULTY (1-back, 2-back, and 3-back), and CLASS (A, B, C, D, E, F, and G). Greenhouse-Geisser correction was applied in the case of sphericity violations. Post hoc paired t-test was conducted at each microstate CLASS between VERSION and between DIFFICULTY and Bonferroni correction was applied for multiple comparisons.

The temporal dependencies measured by entropy rate and Hurst exponent were analyzed separately by a 2 (VERSION) $\times$3 (DIFFICULTY) repeated measures ANOVA. The two within subject factors were VERSION (Spatial and Verbal), DIFFICULTY (1-back, 2-back, and 3-back). Greenhouse-Geisser correction was applied in the case of sphericity violations. Post hoc paired t-test was conducted between VERSION and between DIFFICULTY and Bonferroni correction was applied for multiple comparisons.

5.4.4 Preliminary results

In the theta band, the $2 \times 3 \times 5$ repeated measures ANOVA revealed one significant main effect of AREA ($F(4, 80) = 13.945, p = 0.000, \eta^2 = 0.411$). Figure 5.29 presents the comparison results on VERSION and DIFFICULTY on each brain area. As shown in Figure 5.29, trainees' theta spectral power increased significantly from Spatial 1-back to Verbal 1-back tasks over frontal sites, and from Spatial 3-back tasks to Verbal 3-back tasks over central and parietal sites. As for DIFFICULTY comparison, the theta band power results over frontal sites showed significant increases from Spatial 1-back to 2-back, as well as from 1-back to 3-back conditions. However, significant decreases in theta band power were observed from Spatial 1-back to 2-back over temporal site, from Spatial 1-back to 3-back over parietal and occipital sites, as well as from Verbal 1-back to 2-back and from

Verbal 1-back to 3-back over occipital sites.

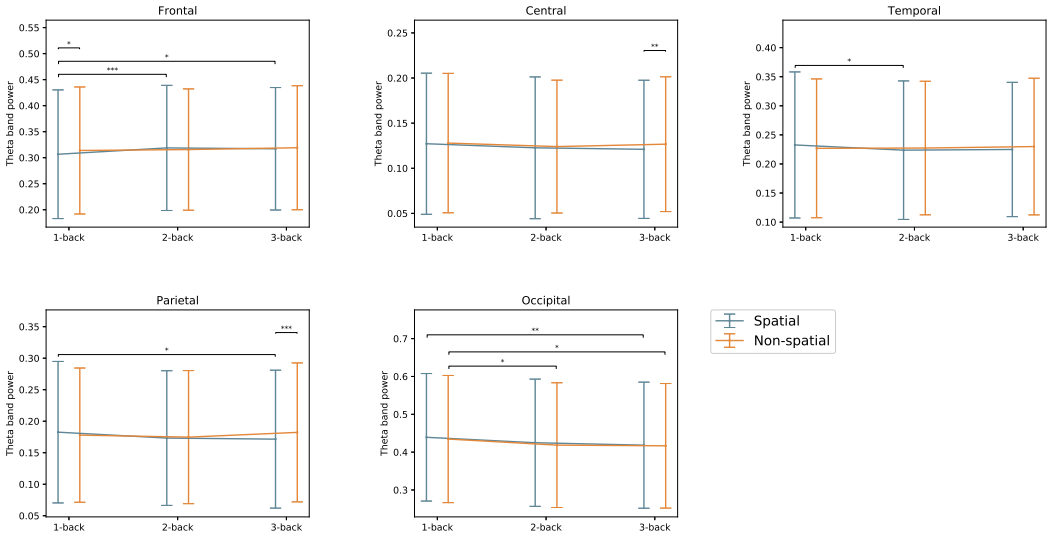

Figure 5.29: EEG theta band power for Spatial and Verbal N-back tasks with N equals to 1, 2, and 3. P-values for VERSION and DIFFICULTY comparisons are annotated by $^{*}(p \leq 0.050)$, $^{**}(p \leq 0.010)$, $^{***}(p \leq 0.005)$.

In the alpha band, the $2 \times 3 \times 5$ repeated measures ANOVA revealed one significant main effect of AREA ($F(4, 80) = 12.480$, $p = 0.000$, $\eta^2 = 0.384$). Figure 5.30 presents the comparison results on VERSION and DIFFICULTY on each brain area. As shown in Figure 5.30, trainees' alpha spectral power increased significantly from Spatial 1-back tasks to Verbal 1-back tasks over frontal and parietal sites, from Spatial 2-back to Verbal 2-back tasks over frontal sites, and from Spatial 3-back tasks to Verbal 3-back tasks over occipital sites. In the meantime, significant alpha decreases were observed from Spatial 3-back to Verbal 3-back tasks over central and temporal sites. As for DIFFICULTY comparison, the alpha band power increased significantly from Spatial 1-back to 3-back over central sites whereas significant decreases in alpha band power were observed from Spatial 1-back to 3-back over occipital sites. However, no significant decreases in alpha band power were observed in paired DIFFICULTY comparisons on Verbal N-back tasks across the tested brain areas.

In the low Beta band, the $2 \times 3 \times 5$ repeated measures ANOVA revealed two significant main

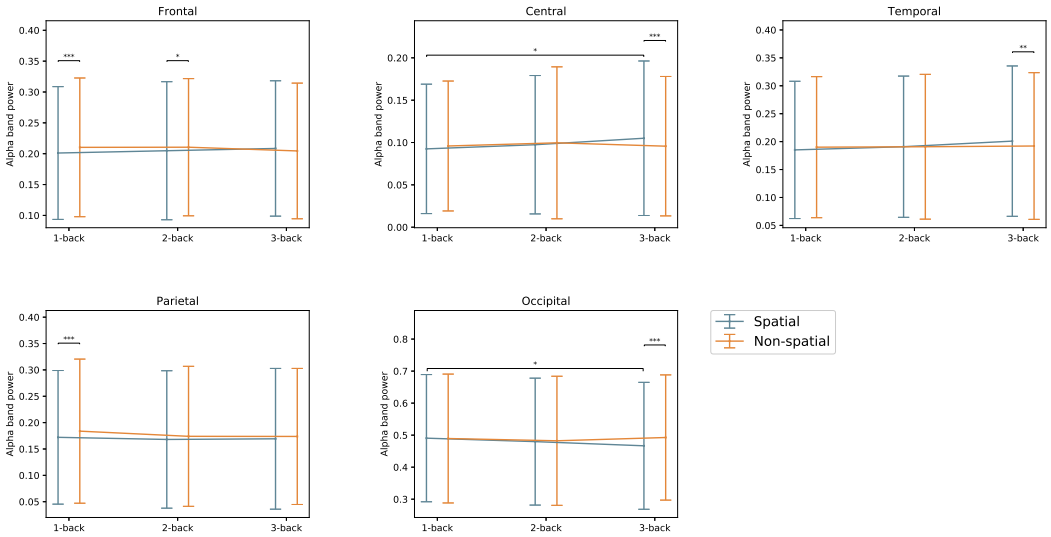

Figure 5.30: EEG alpha band power for Spatial and Verbal N-back tasks with N equals to 1, 2, and 3. P-values for VERSION and DIFFICULTY comparisons are annotated by $^{*}(p \leq 0.050)$, $^{**}(p \leq 0.010)$, $^{***}(p \leq 0.005)$.

effects of DIFFICULTY ($F(2, 40) = 17.850$, $p = 0.000$, $\eta^2 = 0.472$) and AREA ($F(4, 80) = 43.245$, $p = 0.000$, $\eta^2 = 0.684$), as well as one significant interaction effect of DIFFICULTY $\times$ AREA ($F(8, 160) = 6.947$, $p = 0.015$, $\eta^2 = 0.258$). Figure 5.31 presents the comparison results on VERSION and DIFFICULTY on each brain area. As shown in Figure 5.31, trainees' low Beta spectral power decreased significantly from Spatial 1-back to Verbal 1-back tasks over frontal sites, from Spatial 2-back to Verbal 2-back tasks over frontal sites. However, significant increases in low Beta band power were observed from Spatial 2-back to Verbal 2-back tasks over parietal and occipital sites, as well as from Spatial 3-back to Verbal 3-back tasks over occipital sites. As for DIFFICULTY comparison, the low Beta band power decreased significantly from Spatial 1-back to 2-back tasks over parietal and occipital sites, from Spatial 1-back to 3-back tasks over frontal and parietal sites, from Verbal 1-back to 2-back tasks over parietal sites, from Verbal 1-back to 3-back tasks over central and parietal sites, as well as from Verbal 2-back to 3-back tasks over frontal sites. However, no significant changes in low Beta band power were observed over temporal sites either for VERSION or DIFFICULTY paired comparisons.

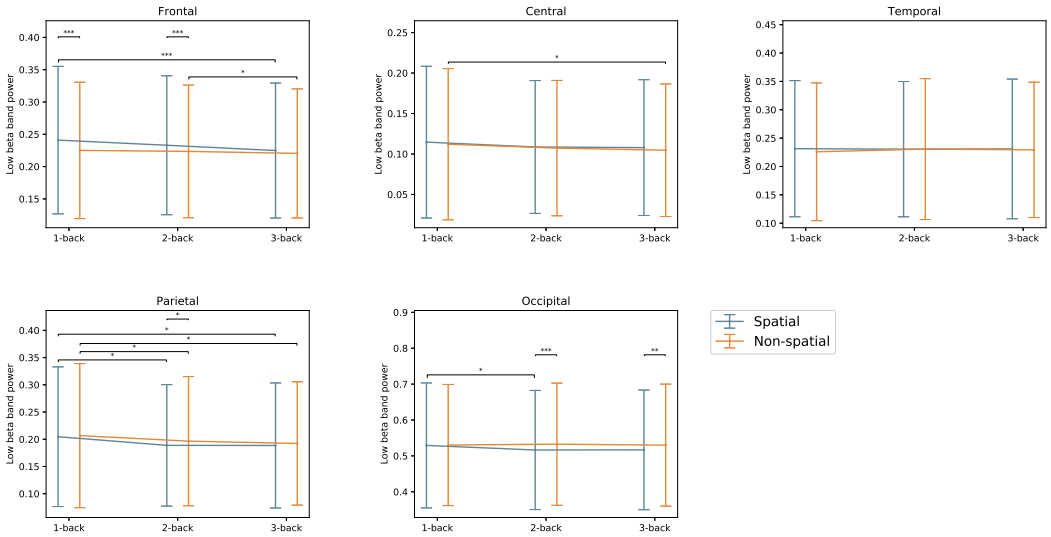

Figure 5.31: EEG low Beta band power for Spatial and Verbal N-back tasks with N equals to 1, 2, and 3. P-values for VERSION and DIFFICULTY comparisons are annotated by $^{*}(p \leq 0.050)$, $^{**}(p \leq 0.010)$, $^{***}(p \leq 0.005)$.

In the low Beta band, the $2 \times 3 \times 5$ repeated measures ANOVA revealed two significant main effects of DIFFICULTY ($F(2, 40) = 6.547$, $p = 0.010$, $\eta^2 = 0.247$) and AREA ($F(4, 80) = 36.033$, $p = 0.000$, $\eta^2 = 0.683$), as well as one significant interaction effect of VERSION $\times$ DIFFICULTY ($F(2, 40) = 4.005$, $p = 0.036$, $\eta^2 = 0.167$). Figure 5.32 presents the comparison results on VERSION and DIFFICULTY on each brain area. As shown in Figure 5.32, trainees' high Beta spectral power decreased significantly from Spatial 1-back to Verbal 1-back tasks over occipital sites, whereas significant increases in high Beta power were observed from Spatial 2-back to Verbal 2-back tasks over parietal sites. As for DIFFICULTY comparison, the significant decreases in high Beta band power were observed from Spatial 1-back to 3-back tasks over frontal, central, and parietal sites, as well as from Verbal 1-back to 3-back tasks over frontal and parietal sites. Meanwhile, no significant changes in high Beta band power were observed over temporal sites either for VERSION or DIFFICULTY paired comparisons.

In the Gamma band, the $2 \times 3 \times 5$ repeated measures ANOVA revealed two significant main effects of VERSION ($F(1, 20) = 4.447$, $p = 0.0478$, $\eta^2 = 0.182$) and AREA ($F(4, 80) = 26.316$,

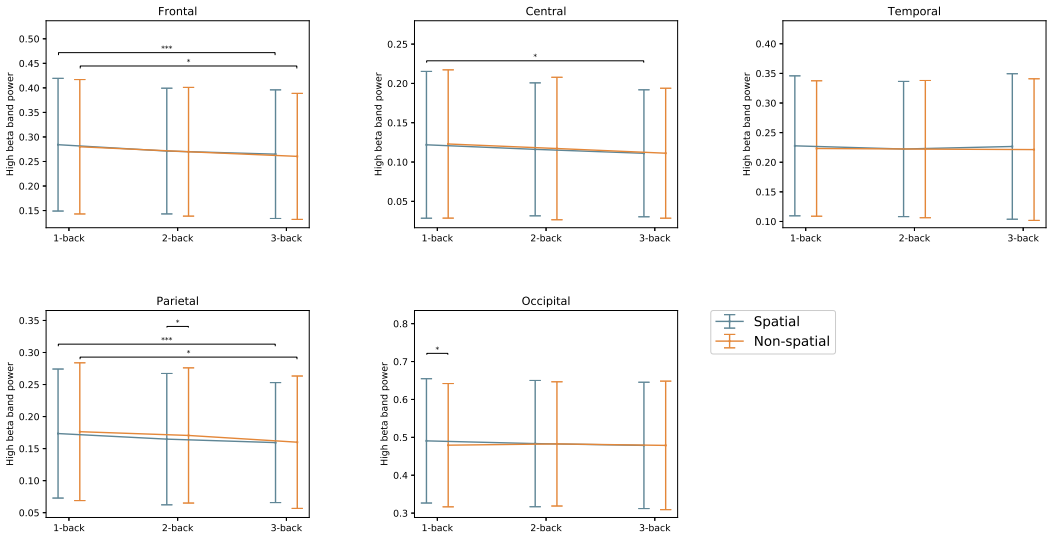

Figure 5.32: EEG high Beta band power for Spatial and Verbal N-back tasks with N equals to 1, 2, and 3. P-values for VERSION and DIFFICULTY comparisons are annotated by $^{*}(p \leq 0.050)$, $^{**}(p \leq 0.010)$, $^{***}(p \leq 0.005)$.

$p = 0.000$, $\eta^2 = 0.568$). Figure 5.33 presents the comparison results on VERSION and DIFFICULTY on each brain area. As shown in Figure 5.33, trainees' Gamma spectral power increased significantly from Spatial 1-back to Verbal 1-back tasks over central, temporal, and parietal sites. However, significant decreases in gamma band power were observed from Spatial 2-back to Verbal 2-back tasks over central and temporal sites, as well as from Spatial 3-back to Verbal 3-back tasks over frontal and occipital sites. Meanwhile, no significant changes were observed in the Gamma band power in any paired DIFFICULTY comparisons across the tested brain areas.

Besides the aforementioned band power features, the results on engagement index and two entropy features will be presented below. In the analysis on engagement index, the $2 \times 3 \times 5$ repeated measures ANOVA revealed one significant main effect of VERSION ($F(1, 20) = 4.911$, $p = 0.038$, $\eta^2 = 0.197$), as well as one significant interaction effect of DIFFICULTY $\times$ AREA ($F(8, 160) = 3.930$, $p = 0.032$, $\eta^2 = 0.164$). Figure 5.34 presents the comparison results on VERSION and DIFFICULTY on each brain area. As shown in Figure 5.34, trainees' engagement index decreased significantly from Spatial 1-back to Verbal 1-back tasks and from Spatial 2-back

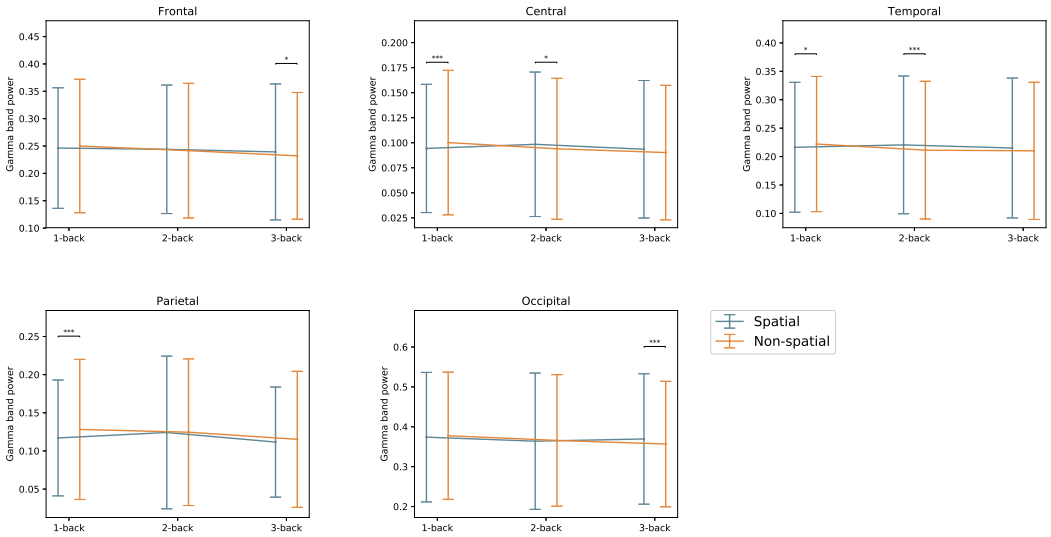

Figure 5.33: EEG Gamma band power for Spatial and Verbal N-back tasks with N equals to 1, 2, and 3. P-values for VERSION and DIFFICULTY comparisons are annotated by $^{*}(p \leq 0.050)$, $^{**}(p \leq 0.010)$, $^{***}(p \leq 0.005)$.

tasks to Verbal 2-back tasks over frontal sites. In the meantime, significant increases in engagement index were observed from Spatial 2-back to Verbal 2-back tasks over occipital sites, as well as from Spatial 3-back to Verbal 3-back tasks over central sites. As for DIFFICULTY comparison, trainees' engagement index decreased significantly from Spatial 1-back to 3-back tasks over frontal sites. However, their engagement index increased significantly from Spatial 1-back to 3-back, from Verbal 1-back to 2-back, and from Verbal 1-back to 3-back tasks over occipital sites. In addition, no significant changes in engagement index were observed over temporal and parietal sites either for VERSION or DIFFICULTY paired comparisons. Similarly, the results obtained on sample entropy and permutation are presented in Figure 5.35 and 5.36. The DIFFICULTY comparison results on sample entropy showed significant decreases from Spatial 1-back to 3-back tasks over the frontal sites as well as significant increases from Spatial 1-back to 2-back tasks over the Parietal sites. In the meantime, the DIFFICULTY comparison results on sample entropy showed significant increases from Spatial 1-back to 2-back tasks as well as from Verbal 1-back to 2-back tasks over the parietal sites. In terms of VERSION comparisons, permutation entropy seemed to be more sensitive to

the content or format of information as significant changes were observed between Spatial 2-back and Verbal 2-back tasks over frontal, temporal, and occipital sites, as well as from Spatial 3-back to Verbal 3-back tasks over frontal, central, temporal, and parietal sites. However, the VERSION comparisons on sample entropy did not show any significant changes across the five brain areas under discussion.

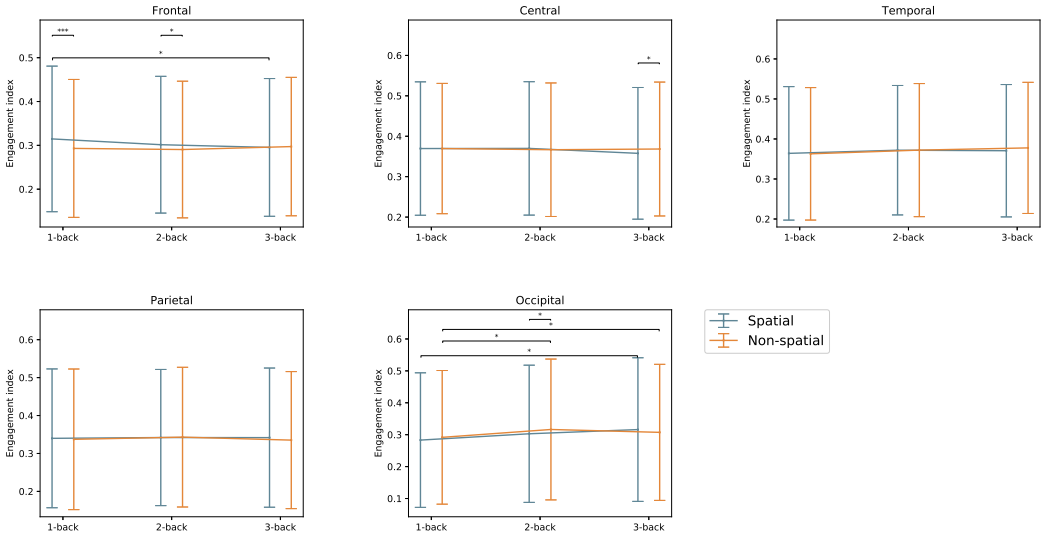

Figure 5.34: Engagement index (EI) for Spatial and Verbal N-back tasks with N equals to 1, 2, and 3. P-values for VERSION and DIFFICULTY comparisons are annotated by $^{*}(p \leq 0.050)$, $^{**}(p \leq 0.010)$, $^{***}(p \leq 0.005)$.

In the meantime, microstate parameters and the temporal dependency features on microstate sequences were computed under each of the tested condition followed by post hoc paired t tests with Bonferroni correction when needed. Figure 5.37 presents the microstate coverage comparison results on VERSION and DIFFICULTY for each of the seven EEG microstate classes plotted with annotations based on the p-values from pairwise comparisons. For VERSION comparison, significant decreases in the coverage of microstate G from Spatial 1-back to Verbal 1-back tasks, whereas the coverage of other microstates didn't show any significant changes between Spatial and Verbal tasks across the tested difficulty levels (1-back, 2-back, and 3-back). In the meantime, no significant differences were observed in DIFFICULTY comparisons for all of the seven microstate classes for

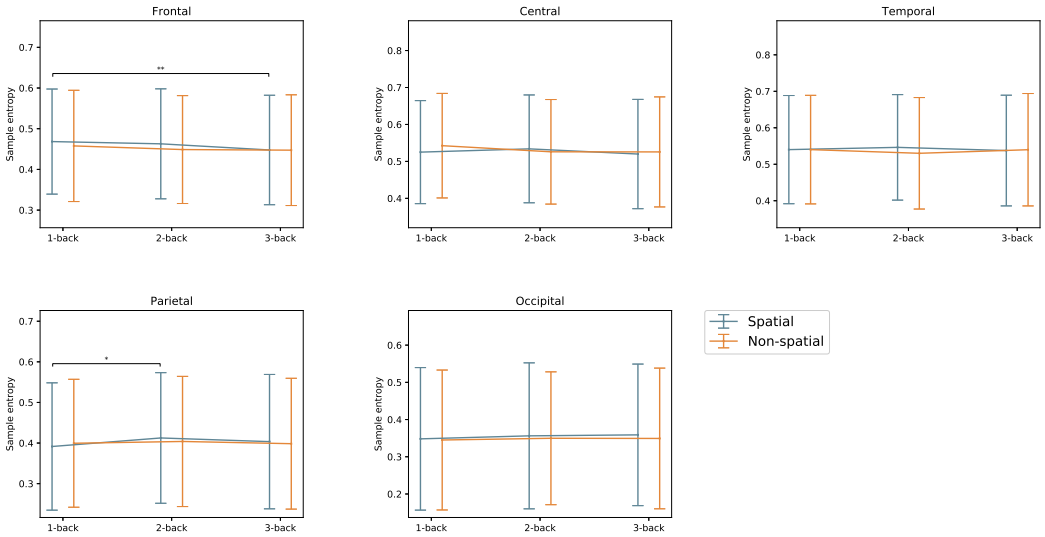

Figure 5.35: Sample entropy for Spatial and Verbal N-back tasks with N equals to 1, 2, and 3. P-values for VERSION and DIFFICULTY comparisons are annotated by $^{*}(p \leq 0.050)$, $^{**}(p \leq 0.010)$, $^{***}(p \leq 0.005)$.

both task types (Spatial and Verbal).

The occurrence comparison results on VERSION and DIFFICULTY for each of the seven EEG microstate classes plotted with annotations based on the p-values from pairwise comparisons as shown in Figure 5.38. For VERSION comparison, significant decreases in the occurrence parameter were observed from Spatial 1-back to Verbal 1-back tasks on microstate B, E, and G, and such significant occurrence decreases were also observed from Spatial 2-back to Verbal 2-back tasks on microstate B, C, E, and G. However, no significant changes were observed between Spatial 3-back and Verbal 3-back tasks across the seven microstate classes. In terms of DIFFICULTY comparison, the occurrence of microstate C and F significantly decreased from Verbal 1-back to 2-back tasks, the occurrence of microstate F significantly decreased from Spatial 1-back to 3-back tasks, whereas significant increases in the occurrence of microstate B, C, and E were observed from Verbal 2-back to 3-back tasks.

The duration comparison results on VERSION and DIFFICULTY for each of the seven EEG microstate classes plotted with annotations based on the p-values from pairwise comparisons as

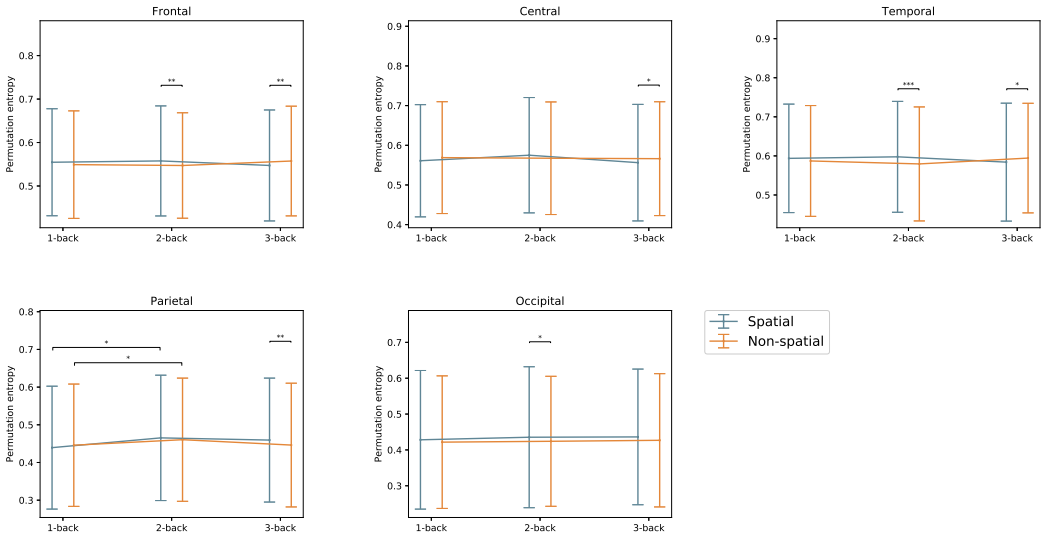

Figure 5.36: Permutation entropy for Spatial and Verbal N-back tasks with N equals to 1, 2, and 3. P-values for VERSION and DIFFICULTY comparisons are annotated by $^{*}(p \leq 0.050)$, $^{**}(p \leq 0.010)$, $^{***}(p \leq 0.005)$.

shown in Figure 5.39. For VERSION comparison, significant increases in the duration parameter were observed from Spatial 1-back to Verbal 1-back tasks on microstate A, B, C, D, and E, and such significant increases were also observed from Spatial 2-back to Verbal 2-back tasks on microstate A, B, C, and F. However, no significant duration changes were observed between Spatial 3-back and Verbal 3-back tasks across the seven microstate classes. In terms of DIFFICULTY comparison, the duration of microstate G significant increased from Spatial 1-back to 2-back as well as from Verbal 1-back to 2-back tasks. In addition, the duration of microstate B and F significantly decreased from Verbal 2-back to 3-back tasks.

Moreover, the VERSION and DIFFICULTY comparison results on entropy rate of the generated microstate sequences are plotted with annotations based on the p-values from pairwise comparisons as shown in Figure 5.40. For VERSION comparison, significant increases were observed from Spatial 1-back to Verbal 1-back tasks and also from Spatial 2-back to Verbal 2-back tasks, whereas non-significant decreases were observed from Spatial 3-back to Verbal 3-back tasks. In terms of DIFFICULTY comparison, the computed entropy rate significant decreased from Verbal 2-back to

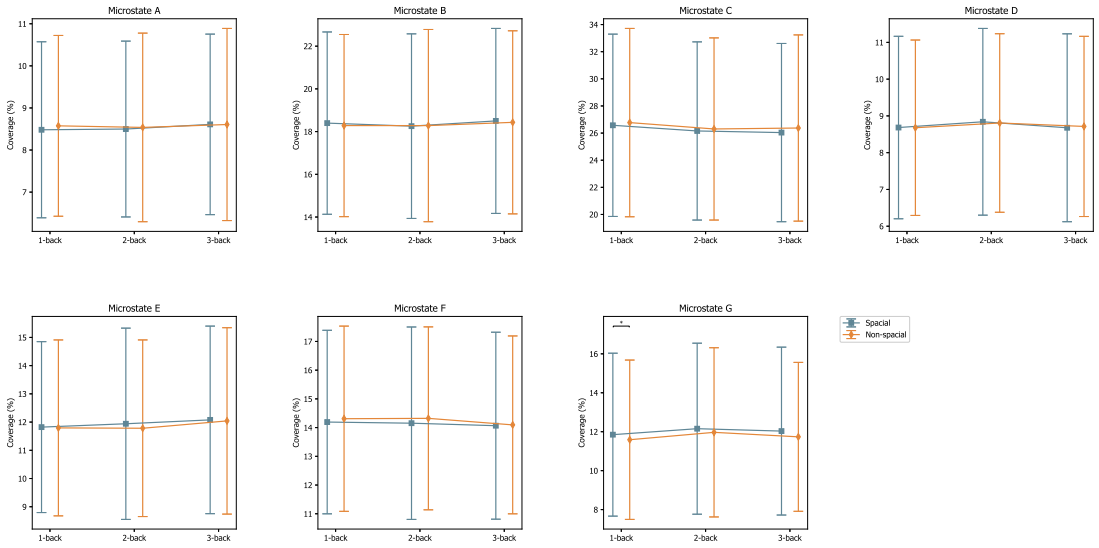

Figure 5.37: EEG microstate coverage for Spatial and Verbal N-back tasks with N equals to 1, 2, and 3. P-values for VERSION and DIFFICULTY comparisons are annotated by $^{*}(p \leq 0.050)$, $^{**}(p \leq 0.010)$, $^{***}(p \leq 0.005)$.

3-back tasks.

the Hurst exponent averaged across 35 partitions was computed and compared as another temporal dependency feature in this research. And the the pairwise comparison results on the computed Hurst exponent showed no significant changes either in VERSION comparisons or DIFFICULTY comparisons as shown in Figure 5.41. The comparison results are are plotted with annotations based on the p-values from pairwise comparisons followed by Bonferroni correction was for multiple comparisons when needed.

5.4.5 Discussions on the preliminary results

The results on theta band power showed significant increases from Spatial 1-back to 2-back as well as from Spatial 1-back to 3-back tasks over the frontal sites. In the meantime, the theta band power increased non-significantly from Verbal 1-back to 2-back and then to 3-back tasks. Considering the aforementioned association between increased frontal theta activity with increased cognitive control (Cavanagh & Frank, 2014; Karakaş, 2020; Sauseng et al., 2010), our results on theta band power indicated an increasing need of cognitive control, information retrieval, and conflict encoding as N increases from 1 to 3 under an N-back WM paradigm for both of the tested versions (Spatial and

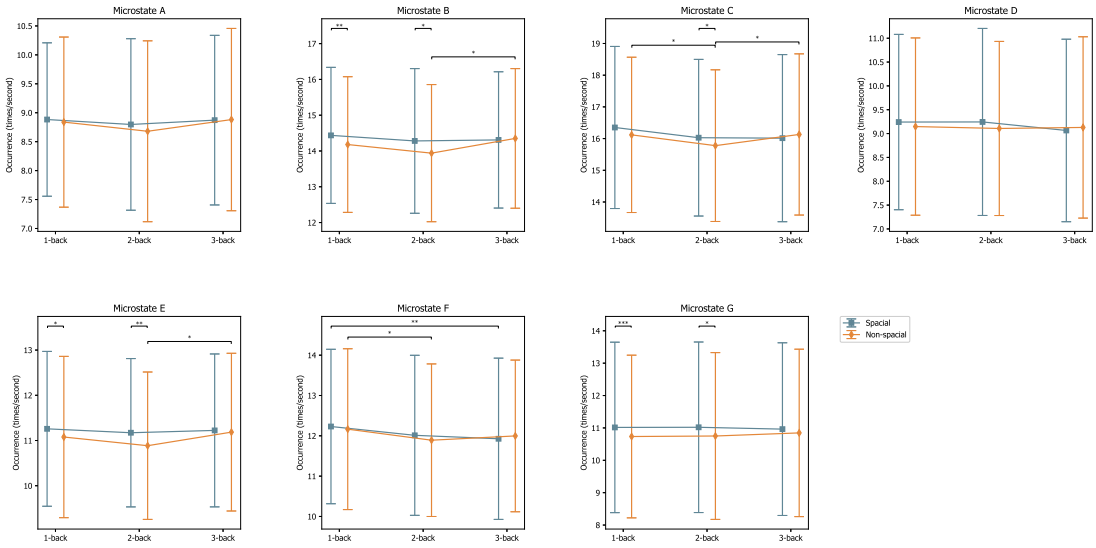

Figure 5.38: EEG microstate occurrence for Spatial and Verbal N-back tasks with N equals to 1, 2, and 3. P-values for VERSION and DIFFICULTY comparisons are annotated by $^{*}(p \leq 0.050)$, $^{**}(p \leq 0.010)$, $^{***}(p \leq 0.005)$.

Verbal). However, the effect of VERSION on theta band power is not significant and the DIFFICULTY comparison results on theta band showed a decreasing trend on the other four investigate brain areas either supported by significant or non-significant differences. Such decreasing trend and some of the non-significant changes in theta band power are worth studying for achieving a better understanding of the research topic, which will be covered in my future research.

The results on alpha band power showed significant increases from Spatial 1-back to 3-back over the central sites whereas significant decreases were observed from Spatial 1-back to 3-back over occipital sites. In the meantime, the alpha band power changes among the three Verbal tasks (1-back, 2-back, and 3-back) showed diverse changing trends despite the fact none of those changes was significant. In addition, the VERSION comparisons showed both significant increases and significant decreases from Spatial tasks to Verbal tasks over different brain areas as shown in Figure 5.30. Besides the aforementioned relationship between alpha activation and cognitive workload, alpha band oscillations have also been linked to top-down modulation of attention (Palva & Palva, 2007; Sauseng et al., 2005). And there are studies supporting that "alpha-band power follows the focus of spatial attention, by decreasing over task-relevant areas and increasing over brain regions that represent distracting information (Händel, Haarmeier, & Jensen, 2011; Klimesch, 2012; Payne,

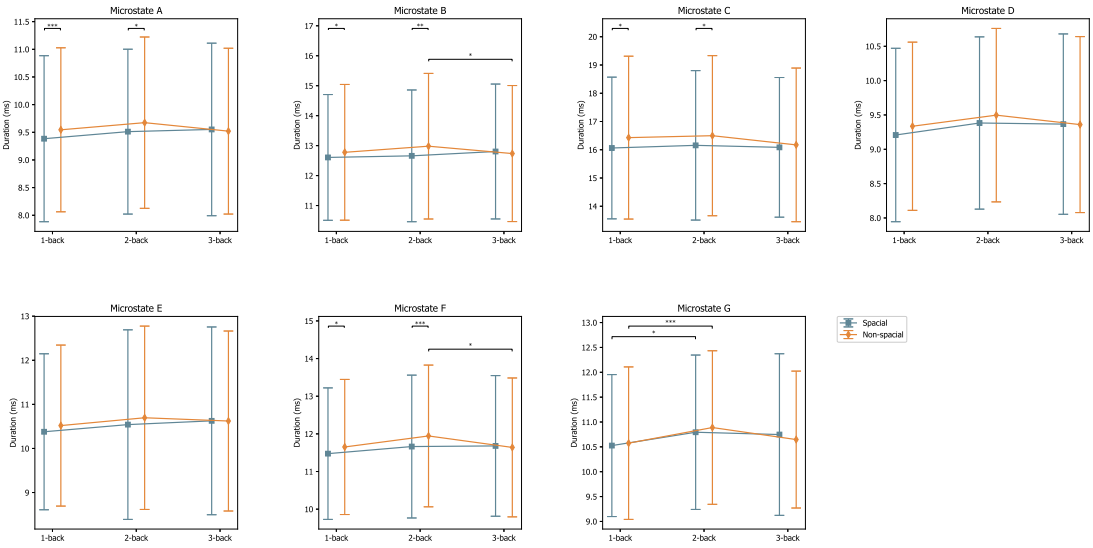

Figure 5.39: EEG microstate duration for Spatial and Verbal N-back tasks with N equals to 1, 2, and 3. P-values for VERSION and DIFFICULTY comparisons are annotated by $^{*}(p \leq 0.050)$, $^{**}(p \leq 0.010)$, $^{***}(p \leq 0.005)$.

Guillory, & Sekuler, 2013; Payne & Sekuler, 2014; Sauseng et al., 2009; Snyder & Foxe, 2010)" (Fodor, Marosi, Tombor, & Csukly, 2020). Therefore, continued analysis is needed to look into the reasons for the observed alpha increases and decreases reported in the literature as well as from our analysis.

Moreover, my future research will also include the results obtained on the other six computed spectral features including three band powers (low beta band, high beta band, and gamma band), engagement index, sample entropy, and permutation entropy, which have already showed some changing trends worth studying. For example, the DIFFICULTY comparisons on low beta band power showed a decreasing trend over frontal, central, and parietal sites for both Spatial and Verbal tasks supported by significant or non-significant changes (Figure 5.31). Similarly, such decreasing trend was also observed in high beta band power over the aforementioned three brain areas for both types of tasks when N varied from 1 to 3 (Figure 5.32). However, gamma band power seemed to be more sensitive to VERSION effect than DIFFICULTY effect as the DIFFICULTY comparisons on gamma band did not show any significant changes (Figure 5.33), which was also supported by the ANOVA results. The VERSION comparisons showed significant increases from Spatial 1-back to Verbal 1-back tasks over central, temporal, and parietal sites, whereas significant decreases were

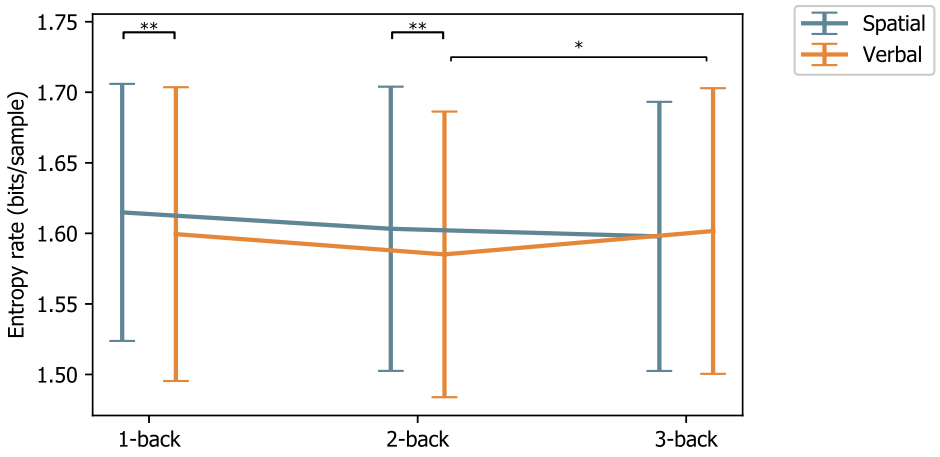

Figure 5.40: Entropy rate of microstate sequences for Spatial and Verbal N-back tasks with N equals to 1, 2, and 3. P-values for VERSION and DIFFICULTY comparisons are annotated by $^{*}(p \leq 0.050)$, $^{**}(p \leq 0.010)$, $^{***}(p \leq 0.005)$.

observed from Spatial 2-back to Verbal 2-back tasks over central and temporal sites, as well as from Spatial 3-back to Verbal 3-back tasks over frontal and occipital sites.

Among the seven computed EEG microstate states, our previous discussions in Section 5.1 and 5.2 highlighted microstate C due to its close relationship with cognitive control. Therefore, the three parametes of microstate C, namely coverage, occurrence, and duration, were discussed in the first place in the investigation of trainees' cognitive changes under N-back tasks. The coverage of microstate C showed a decreasing trend under Spatial N-back tasks when N changed from 1 to 3, whereas a U-shaped changing coverage was observed under Verbal tasks (Figure 5.37). Of note, the coverage of microstate C and the other six microstates (A, B, D, E, F, and G) did not show any significant changes in both DIFFICULTY and VERSION comparisons except for the only significant decrease from Spatial 1-back to Verbal 1-back in the coverage of microstate G.

The occurrence of microstate C also showed a decreasing trend under Spatial tasks as well as a U-shaped changing trend under Verbal tasks (Figure 5.38). The supporting evidences include significant decreases from Verbal 1-back to 2-back tasks, significant increases from Verbal 2-back to 3-back tasks, as well as non-significant changes in the paired DIFFICULTY comparisons under Spatial tasks. In the meantime, the occurrence of microstate F also indicated a decreasing trend under Spatial tasks and a U-shaped trend under Verbal tasks, supported by significant decreases

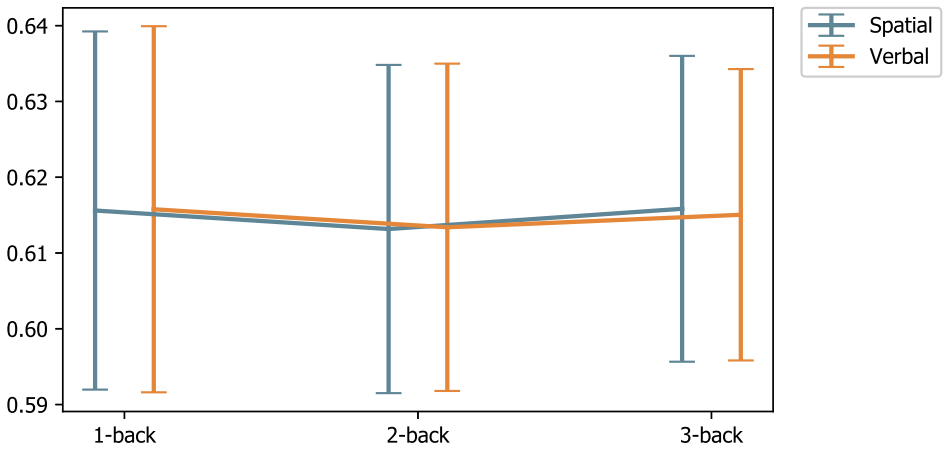

Figure 5.41: Hurst exponent of microstate sequences averaged across 35 partitions for Spatial and Verbal N-back tasks with N equals to 1, 2, and 3. P-values for VERSION and DIFFICULTY comparisons are annotated by $^{*}(p \leq 0.050)$, $^{**}(p \leq 0.010)$, $^{***}(p \leq 0.005)$.

from Spatial 1-back to 3-back tasks as well as from Verbal 1-back to 2-back. Also, the occurrence parameter seemed to be more sensitive to the content or format of information as the results on VERSION comparisons showed significant occurrence decreases from Spatial 1-back to Verbal 1-back tasks in microstate B, E, and G, as well as from Spatial 2-back to Verbal 2-back tasks in microstate B, C, E and G.

However, the duration of microstate C followed an inverted-U changing trend under both types of tasks (Spatial and Verbal) as shown in Figure 5.39. The comparison results of duration parameter under Verbal tasks seemed to follow an inverted-U shaped trend across the computed seven microstates. The supporting evidences include the significant duration increases from Verbal 1-back to 2-back tasks in microstate G, significant duration decreases from Verbal 2-back to 3-back tasks in microstate B and F, as well as the non-significant changes in the paired comparisons. And the VERSION comparisons on duration showed significant increases from Spatial 1-back to Verbal 1-back tasks as well as from Spatial 2-back to Verbal 2-back tasks in microstate A, B, C, and F. Although the aforementioned observations on the duration parameter were so different from what have been observed on the other two microstate parameters (coverage and occurrence), the results on duration seemed to achieve a certain consistency among the seven microstates. Continued analysis is needed to interpret such differences and consistency through combining theoretical support

and experimental evidences in my future research.

Moreover, entropy rate computed from the generate microstate sequences showed a decreasing trend under Spatial tasks and followed a U-shaped trend under Verbal tasks as shown in Figure 5.40. Entropy rate increased significantly from Verbal 2-back to 3-back tasks, whereas the other evidences are non-significant changes obtained in DIFFICULTY comparisons for the decreasing and U-shaped trends under Spatial and Verbal tasks respectively. Following our previous analysis on the negative correlation between entropy rate and cognitive control, our results indicated that participants' cognitive control increased under Spatial N-back tasks while N increased from 1 to 3, whereas their cognitive control increased from 1-back to 2-back then decreased from 2-back to 3-back when conducting Verbal N-back tasks. This is consistent with the cognitive control variations indicated by the coverage and occurrence of microstate C, considering its role in reflecting activities in the default mode network (Bréchet et al., 2019; Seitzman et al., 2017; X. Xu et al., 2016). Furthermore, the computed Hurst exponent, as the other temporal dependency feature on the microstate sequences, decreased from 1-back to 2-back tasks and then decreased from 2-back to 3-back tasks under both Spatial and Verbal N-back WM paradigms (Figure 5.41). Adopting the positive relationship between Hurst exponent and cognitive control from our precious analysis, the U-shaped changing trend in Hurst exponent indicated that participants' cognitive control decreased from 1-back to 2-back and then then increased from 2-back to 3-back under both of the two tested versions of N-back WM paradigm. That is, the observations from Hurst exponent results were so different from that obtained on entropy rate as well as the coverage and occurrence of microstate C that additional analysis is needed to interpret such phenomena.

Chapter 6

Conclusion and Future Work

6.1 Conclusion

This research aims to quantify cognitive workload and mental capacity while people perform complex cognitive activities from their EEG signals. Overall, the present research covers theoretical analysis, framework development, experiment design, and experimental data analysis to address the challenges in quantifying cognitive workload, mental capacity from EEG signals under complex cognitive activities. The tEEG framework was proposed in the first place to address the challenges in EEG-based cognitive design studies, which might fill the gap between the existing EEG studies and the cognitive studies under complex cognitive activities. The tEEG framework has then been applied for the quantification of cognitive workload and mental capacity from the EEG signals within and beyond the context of design. In particular, cognitive workload was quantified by combining the spectral analysis results on EEG data and confirmed with the results obtained from subjective ratings. The quantification of cognitive control, as part of mental capacity, was based on the EEG microstate features and spectral analysis, which has been confirmed with the subjective evaluation results from pilot instructors. In addition, these applications indicated that the loosely controlled experiments proposed in the tEEG framework could be well supported by EEG microstate analysis, which appears to offer an effective approach to investigating the cognitive changes under complex cognitive activities.

The present research was structured and developed following a three-stage research methodology. Two research objectives have been formulated in the first place based on the pilot studies (Zhao et al., 2018; Zhao & Zeng, 2019) in applying and extending the stress model, based on which a series of theoretical analyses and literature review were conducted leading to a three-stage methodology. According to the research methodology, a new research framework was proposed during the first stage for conducting EEG-based analysis to quantify designers' cognitive changes based on our past research efforts and a series of theoretical analyses (Zhao et al., 2020). Design activities are considered as representative examples of complex cognitive activities and EEG appears to be a promising tool for monitoring designers' cognitive changes within a design process as indicated in the literature. The proposed tEEG framework was then applied to quantitatively monitor changes in people's cognitive workload and mental capacity within and beyond the context of design, during the second stage in the research methodology. These applications not only illustrate how the tEEG framework can be used but also provide feedback for further developing the framework and contribute in various ways to specific fields, such as design and learning. Moreover, the third stage aims at establishing a quantitative representation of the stress model to relate the quantification results on the mentioned cognitive factors to human mental effort as well as the behavioral variations, which is more a future direction of my current research. Along this direction, investigations would be conducted into the impact of cognitive workload and mental capacity on mental effort, which would be one step further to apply my current research findings and most existing quantitative cognitive findings in real-life scenarios. Even though it is still at an early stage as explained in this research, my future research will continue to conduct further investigations toward the second research objective. Research outputs from every stage (mainly for the first two stages) of the methodology are summarised one by one in the following paragraphs, as well as their contributions to the studied phenomenon and corresponding field.

A task-related framework, denoted as tEEG framework, is proposed for conducting EEG-based analysis to investigate designers' cognitive changes under different design activities (Zhao et al., 2020). As one of the key outcomes of the present research, the proposed tEEG framework consists of three main parts, namely data collection from loosely controlled experiments, clustering-based segmentation of unstructured data, and EEG-based segment analysis. The overall design process

inputs the initial design problem and outputs the final design solutions if viewed from a high level perspective. The data collected during loosely controlled experiments include designer's behaviors, biometric data, and design solutions based on the target design problem. Loosely controlled experiments are designed and conducted regarding the studied research topic where participants' design activities happen. Secondly, clustering-based segmentation can be conducted to identify the hidden structured stimulus-response data pairs from the unstructured data. Several sub-processes can be extracted from a complex design after this step. Last but not least, each extracted segment can be analyzed using traditional hypothesis test method. It is during this step that some of the existing results and techniques on EEG-based cognitive and affective states may be adopted and integrated. Moreover, the results obtained in later applications indicated that loosely controlled experiments proposed in the tEEG framework can be well supported by EEG microstate analysis, which appears to offer an effective approach to facilitating an ecologically valid neurocognitive study.

Within the context of design, the first application simulated the design process in a loosely controlled setting, aiming to quantify the design-related workload and cognitive control and uncover their temporal dynamics (Jia et al., 2021). The TRP and EEG microstate results suggest that idea generation is associated with the highest cognitive workload and lowest cognitive control during open-ended creation tasks. In particular, the results indicated that idea generation and idea evolution were associated with decreases in alpha power, while the decreases were significantly larger during idea generation compared to idea evolution. In addition, problem understanding, rating idea generation, and rating idea evaluation were shown to be associated with increases in theta and beta power while the increases were largest during problem understanding, which are in line with those from visual creativity and higher-order cognition research based on ERD/ERS and TRP. The effectiveness of loosely controlled experiments proposed in our tEEG framework was successfully tested in this research by comparing the findings on the studied phenomena that have been effectively studied by validated experimental research.

Beyond the context of design, the second research strictly followed the steps within our tEEG framework to capture the changes in trainees' cognitive control and workload while they underwent training on basic flight maneuvers (Zhao, Jia, et al., 2022). This is also the first application that followed the framework from experiment design to each step of data analysis for testing the

hypothesis that trainees' cognitive workload would decrease whereas their cognitive control would improve under the same task demands through a skill acquisition process. EEG microstate analysis and spectral power features were applied in this research to assess trainees' cognitive workload and cognitive control variations during different stages within a pilot training process. Our results revealed that trainees' cognitive workload decreased along the pilot training process whereas their cognitive control improved toward the end of the process under unvaried task demands. Our investigations also indicated that even under varied task demands the effect of skill acquisition on cognitive control could be captured by EEG microstate features.

As for the third stage, a quantitative representation for describing the impact of cognitive workload and mental capacity on mental effort was established and modeled based on the stress-effort model. The model has been verified with simulations and applied for phenomena interpretations under the condition when a collaborative task needs to be completed within a limited period. The concept of capacity zone was proposed to ensure high efficiency that lies between the two workload equilibrium points (Zhao, Qiu, & Zeng, 2022). Human instructors or computers should facilitate human beings' capacity zones and intervene when they are found working outside the capacity zone. This characteristic is emphasized in collaborative projects, in which each individual's task is crucial to the overall success of the project. The proposed capacity zone should be used together with a mental capacity value and a maximum efficiency level of each human participant. These parameters not only contribute to the initiation of capacity zone, but also continuously reshape them as parameters change. Furthermore, the proposed quantitative approach would be tested with experimental evidence based on an N-back WM paradigm in the ongoing research presented in Section 5.4. Even though the current research only covers some preliminary results on the N-back dataset, my future with continue to finalize the current analysis and I believe that the deliverable from my research will pave the way to achieving the second research goal step by step.

6.2 Future work

Two future research directions have been identified based on the aforementioned research findings and the preliminary results obtained from the ongoing exploration. One future direction is to measure different individual's mental capacity from their physiological recordings by continuing with my current analysis on the dataset collected under an N-back WM paradigm, which corresponds to the third stage within my research methodology aiming at the second research objective. The research outcome could enable the application of the capacity zone model under varied real-life scenarios with customized workload allocation strategies and timely interventions. In this vein, the goal is to increase the overall efficiency of the project, team, or system by providing quantitative feedback on the mental capacity of each individual. The processes that rely heavily on subjective criteria like expert evaluations and judgments would benefit greatly from objective feedback on human participants' mental capacity. As an example of such a process, pilot training, in which the instructors can use such objective metrics to give a more precise assessment, adjust the training tasks, provide timely interventions, and supervise more trainees simultaneously, the efficiency of the training process can be improved.

The other future direction is to conduct further analysis to identify which parts of subjective evaluations can be replaced by physiological metrics and whether physiological metrics can supplement expert evaluations with additional information. This is motivated by the similarity and differences that have been observed between EEG quantities and quantitative assessment provided by the experts on the study of pilot training process (Zhao, Jia, et al., 2022). There are a few things that could be considered to continue in this direction: 1) may include more EEG features included into my analysis; 2) may incorporate other physiological measures into the current EEG-based analysis; and 3) may follow a recursive process to improve the precision and reliability. For example, we may ask the experts to calibrate the current subjective evaluations based on the physiological metrics and then come back to modify the metrics based on the updated expert evaluations. The process could be repeated a number of times until both physiological metrics and subjective evaluations are relatively stable. Research along this line would continue to improve the accuracy and reliability of objective assessments of human participants' performance, which may also shed light

on the studies of other cognitive functions.

References

Abraham, A. (2013). The promises and perils of the neuroscience of creativity. *Frontiers in Human Neuroscience*, *7*, 246.

Acharya, U. R., Sree, S. V., Swapna, G., Martis, R. J., & Suri, J. S. (2013). Automated EEG analysis of epilepsy: a review. *Knowledge-Based Systems*, *45*, 147–165.

Addante, R. J., Watrous, A. J., Yonelinas, A. P., Ekstrom, A. D., & Ranganath, C. (2011). Prestimulus theta activity predicts correct source memory retrieval. *Proceedings of the National Academy of Sciences*, *108*(26), 10702–10707.

Afflerbach, P., & Johnston, P. (1984). On the use of verbal reports in reading research. *Journal of Reading Behavior*, *16*(4), 307–322.

Agarwal, R., & Gotman, J. (1999). Adaptive segmentation of electroencephalographic data using a nonlinear energy operator. In *1999 IEEE International Symposium on Circuits and Systems (ISCAS)* (Vol. 4, pp. 199–202).

Agnoli, S., Zanon, M., Mastria, S., Avenanti, A., & Corazza, G. E. (2020). Predicting response originality through brain activity: An analysis of changes in EEG alpha power during the generation of alternative ideas. *NeuroImage*, *207*, 116385.

Ahituv, N., Igbaria, M., & Sella, A. V. (1998). The effects of time pressure and completeness of information on decision making. *Journal of Management Information Systems*, *15*(2), 153–172.

Al-Shargie, F., Tariq, U., Mir, H., Alawar, H., Babiloni, F., & Al-Nashash, H. (2019). Vigilance decrement and enhancement techniques: a review. *Brain Sciences*, *9*(8), 178.

Altman, N. S. (1992). An introduction to kernel and nearest-neighbor nonparametric regression.

The American Statistician, *46*(3), 175–185.

Amer, T., Campbell, K. L., & Hasher, L. (2016). Cognitive control as a double-edged sword. *Trends in Cognitive Sciences*, *20*(12), 905–915.

Anderson, J. R. (1982). Acquisition of cognitive skill. *Psychological Review*, *89*(4), 369.

Anderson, J. R. (1987). Skill acquisition: Compilation of weak-method problem situations. *Psychological Review*, *94*(2), 192.

Anderson, L. W., & Krathwohl, D. R. (2001). *A taxonomy for learning, teaching, and assessing: A revision of bloom's taxonomy of educational objectives*. Longman,.

Anton, N. E., Bean, E. A., Hammonds, S. C., & Stefanidis, D. (2017). Application of mental skills training in surgery: a review of its effectiveness and proposed next steps. *Journal of Laparoendoscopic & Advanced Surgical Techniques*, *27*(5), 459–469.

Aoki, T., & Kowalik, U. (2011). BROAFERENCE: A prototype of an emotion-based TV quality rating system. In *Emotional Engineering* (pp. 223–245). Springer.

Appel, U., & Brandt, A. V. (1983). Adaptive sequential segmentation of piecewise stationary time series. *Information Sciences*, *29*(1), 27–56.

Austin, J., & Delaney, P. F. (1998). Protocol analysis as a tool for behavior analysis. *The Analysis of Verbal Behavior*, *15*(1), 41–56.

Austin, R. D. (2001). The effects of time pressure on quality in software development: An agency model. *Information Systems Research*, *12*(2), 195–207.

Baethge, A., Vahle-Hinz, T., Schulte-Braucks, J., & van Dick, R. (2018). A matter of time? challenging and hindering effects of time pressure on work engagement. *Work & Stress*, *32*(3), 228–247.

Baldwin, C. L. (2012). *Auditory cognition and human performance: Research and applications*. CRC Press.

Balters, S., & Steinert, M. (2017). Capturing emotion reactivity through physiology measurement as a foundation for affective engineering in engineering design science and engineering practices. *Journal of Intelligent Manufacturing*, *28*(7), 1585–1607.

Bandt, C., & Pompe, B. (2002). Permutation entropy: a natural complexity measure for time series. *Physical Review Letters*, *88*(17), 174102.

Bardwell, L. V. (1991). Problem-framing: A perspective on environmental problem-solving. *Environmental Management*, *15*(5), 603–612.

Barlow, J., Creutzfeldt, O., Michael, D., Houchin, J., & Epelbaum, H. (1981). Automatic adaptive segmentation of clinical EEGs. *Electroencephalography and Clinical Neurophysiology*, *51*(5), 512–525.

Başar, E., Başar-Eroglu, C., Karakaş, S., & Schürmann, M. (2001). Gamma, alpha, delta, and theta oscillations govern cognitive processes. *International Journal of Psychophysiology*, *39*(2-3), 241–248.

Bisley, J. W., & Goldberg, M. E. (2010). Attention, intention, and priority in the parietal lobe. *Annual Review of Neuroscience*, *33*, 1.

Bissoli, A., Lavino-Junior, D., Sime, M., Encarnação, L., & Bastos-Filho, T. (2019). A human–machine interface based on eye tracking for controlling and monitoring a smart home using the internet of things. *Sensors*, *19*(4), 859.

Bloom, B. S., Engelhart, M. D., Furst, E., Hill, W. H., & Krathwohl, D. R. (1956). Handbook i: cognitive domain. *New York: David McKay*.

Bonnefond, M., & Jensen, O. (2015). Gamma activity coupled to alpha phase as a mechanism for top-down controlled gating. *PloS One*, *10*(6), e0128667.

Boonnithi, S., & Phongsuphap, S. (2011). Comparison of heart rate variability measures for mental stress detection. In *2011 Computing in Cardiology* (pp. 85–88).

Borghetti, B. J., Giametta, J. J., & Rusnock, C. F. (2017). Assessing continuous operator workload with a hybrid scaffolded neuroergonomic modeling approach. *Human Factors*, *59*(1), 134–146.

Borghini, G., Aricò, P., Di Flumeri, G., Cartocci, G., Colosimo, A., Bonelli, S., ... others (2017). EEG-based cognitive control behaviour assessment: An ecological study with professional air traffic controllers. *Scientific Reports*, *7*(1), 1–16.

Borghini, G., Astolfi, L., Vecchiato, G., Mattia, D., & Babiloni, F. (2014). Measuring neurophysiological signals in aircraft pilots and car drivers for the assessment of mental workload, fatigue and drowsiness. *Neuroscience & Biobehavioral Reviews*, *44*, 58–75.

Borgianni, Y., & Maccioni, L. (2020). Review of the use of neurophysiological and biometric

measures in experimental design research. *AI EDAM*, *34*(2), 248–285.

Bosseler, A., Taulu, S., Pihko, E., Mäkelä, J., Imada, T., Ahonen, A., & Kuhl, P. (2013). Theta brain rhythms index perceptual narrowing in infant speech perception. *Frontiers in Psychology*, *4*, 690.

Botvinick, M. M., Braver, T. S., Barch, D. M., Carter, C. S., & Cohen, J. D. (2001). Conflict monitoring and cognitive control. *Psychological Review*, *108*(3), 624.

Bréchet, L., Brunet, D., Birot, G., Gruetter, R., Michel, C. M., & Jorge, J. (2019). Capturing the spatiotemporal dynamics of self-generated, task-initiated thoughts with EEG and fMRI. *Neuroimage*, *194*, 82–92.

Brouwer, A.-M., Hogervorst, M. A., Holewijn, M., & van Erp, J. B. (2014). Evidence for effects of task difficulty but not learning on neurophysiological variables associated with effort. *International Journal of Psychophysiology*, *93*(2), 242–252.

Brown, J. P. (2016). The effect of automation on human factors in aviation. *The Journal of Instrumentation, Automation and Systems*, *3*(2), 31–46.

Brun, J., Le Masson, P., & Weil, B. (2016). Designing with sketches: The generative effects of knowledge preordering. *Design Science*, *2*.

Buckert, M., Schwieren, C., Kudielka, B. M., & Fiebach, C. J. (2014). Acute stress affects risk taking but not ambiguity aversion. *Frontiers in Neuroscience*, *8*, 82.

Buttazzo, G., & Abeni, L. (2002). Adaptive workload management through elastic scheduling. *Real-Time Systems*, *23*(1), 7–24.

Buttazzo, G. C., & Sensini, F. (1999). Optimal deadline assignment for scheduling soft aperiodic tasks in hard real-time environments. *IEEE Transactions on Computers*, *48*(10), 1035–1052.

Causse, M., Chua, Z. K., & Rémy, F. (2019). Influences of age, mental workload, and flight experience on cognitive performance and prefrontal activity in private pilots: A fNIRS study. *Scientific Reports*, *9*(1), 1–12.

Cavanagh, J. F., Cohen, M. X., & Allen, J. J. (2009). Prelude to and resolution of an error: EEG phase synchrony reveals cognitive control dynamics during action monitoring. *Journal of Neuroscience*, *29*(1), 98–105.

Cavanagh, J. F., & Frank, M. J. (2014). Frontal theta as a mechanism for cognitive control. *Trends*

in Cognitive Sciences, *18*(8), 414–421.

Cavanagh, J. F., Zambrano-Vazquez, L., & Allen, J. J. (2012). Theta lingua franca: A common mid-frontal substrate for action monitoring processes. *Psychophysiology*, *49*(2), 220–238.

Charles, R. L., & Nixon, J. (2019). Measuring mental workload using physiological measures: A systematic review. *Applied Ergonomics*, *74*, 221–232.

Chatrian, G. E., Lettich, E., & Nelson, P. L. (1985). Ten percent electrode system for topographic studies of spontaneous and evoked EEG activities. *American Journal of EEG Technology*, *25*(2), 83–92.

Chen, F., Sekiyama, K., Cannella, F., & Fukuda, T. (2013). Optimal subtask allocation for human and robot collaboration within hybrid assembly system. *IEEE Transactions on Automation Science and Engineering*, *11*(4), 1065–1075.

Chetto, H., & Chetto, M. (1989). Some results of the earliest deadline scheduling algorithm. *IEEE Transactions on Software Engineering*, *15*(10), 1261.

Chiu, I., & Shu, L. (2010). Potential limitations of verbal protocols in design experiments. In *International Design Engineering Technical Conferences and Computers and Information in Engineering Conference* (Vol. 44137, pp. 287–296).

Chong, D. S., Van Eerde, W., Chai, K. H., & Rutte, C. G. (2010). A double-edged sword: The effects of challenge and hindrance time pressure on new product development teams. *IEEE Transactions on Engineering Management*, *58*(1), 71–86.

Chrysikou, E. G. (2018). The costs and benefits of cognitive control for creativity.

Chrysikou, E. G., & Weisberg, R. W. (2005). Following the wrong footsteps: fixation effects of pictorial examples in a design problem-solving task. *Journal of Experimental Psychology: Learning, Memory, and Cognition*, *31*(5), 1134.

Cohen, J. D. (2017). Cognitive control: Core constructs and current considerations. *The Wiley Handbook of Cognitive Control*, 1–28.

Cohen, M. X., Ridderinkhof, K. R., Haupt, S., Elger, C. E., & Fell, J. (2008). Medial frontal cortex and response conflict: evidence from human intracranial EEG and medial frontal cortex lesion. *Brain Research*, *1238*, 127–142.

Conklin, J. (2005). *A taxonomy for learning, teaching, and assessing: A revision of bloom's*

taxonomy of educational objectives complete edition. JSTOR.

Cook, G. J. (1993). An empirical investigation of information search strategies with implications for decision support system design. *Decision Sciences*, *24*(3), 683–698.

Cooper, P. S., Karayanidis, F., McKewen, M., McLellan-Hall, S., Wong, A. S., Skippen, P., & Cavanagh, J. F. (2019). Frontal theta predicts specific cognitive control-induced behavioural changes beyond general reaction time slowing. *Neuroimage*, *189*, 130–140.

Cortes, C., & Vapnik, V. (1995). Support-vector networks. *Machine Learning*, *20*(3), 273–297.

Crilly, N. (2015). Fixation and creativity in concept development: The attitudes and practices of expert designers. *Design Studies*, *38*, 54–91.

Custo, A., Van De Ville, D., Wells, W. M., Tomescu, M. I., Brunet, D., & Michel, C. M. (2017). Electroencephalographic resting-state networks: source localization of microstates. *Brain Connectivity*, *7*(10), 671–682.

Dehais, F., Duprès, A., Blum, S., Drougard, N., Scannella, S., Roy, R. N., & Lotte, F. (2019). Monitoring pilot's mental workload using ERPs and spectral power with a six-dry-electrode EEG system in real flight conditions. *Sensors*, *19*(6), 1324.

DeKeyser, R. (2020). Skill acquisition theory. In *Theories in Second Language Acquisition* (pp. 83–104). Routledge.

Delorme, A., & Makeig, S. (2004). EEGLAB: an open source toolbox for analysis of single-trial EEG dynamics including independent component analysis. *Journal of Neuroscience Methods*, *134*(1), 9–21.

Delplanque, S., Silvert, L., Hot, P., Rigoulot, S., & Sequeira, H. (2006). Arousal and valence effects on event-related P3a and P3b during emotional categorization. *International Journal of Psychophysiology*, *60*(3), 315–322.

De Paola, M., & Gioia, F. (2016). Who performs better under time pressure? results from a field experiment. *Journal of Economic Psychology*, *53*, 37–53.

Dietrich, A., & Kanso, R. (2010). A review of EEG, ERP, and neuroimaging studies of creativity and insight. *Psychological Bulletin*, *136*(5), 822.

Dijkerman, H. C., & De Haan, E. H. (2007). Somatosensory processing subserving perception and action: Dissociations, interactions, and integration. *Behavioral and Brain Sciences*, *30*(2),

224–230.

Dong, A. (2005). The latent semantic approach to studying design team communication. *Design Studies*, *26*(5), 445–461.

Donoso, M., Collins, A. G., & Koechlin, E. (2014). Foundations of human reasoning in the prefrontal cortex. *Science*, *344*(6191), 1481–1486.

Doppelmayr, M., Klimesch, W., Hödlmoser, K., Sauseng, P., & Gruber, W. (2005). Intelligence related upper alpha desynchronization in a semantic memory task. *Brain Research Bulletin*, *66*(2), 171–177.

Dorst, K., & Cross, N. (2001). Creativity in the design process: Co-evolution of problem–solution. *Design Studies*, *22*(5), 425–437.

Dorst, K., & Dijkhuis, J. (1995). Comparing paradigms for describing design activity. *Design Studies*, *16*(2), 261–274.

Duckworth, A. L., Quirk, A., Gallop, R., Hoyle, R. H., Kelly, D. R., & Matthews, M. D. (2019). Cognitive and noncognitive predictors of success. *Proceedings of the National Academy of Sciences*, *116*(47), 23499–23504.

Eekels, J. (2001). On the fundamentals of engineering design science: The geography of engineering design science. part 2. *Journal of Engineering Design*, *12*(3), 255–281.

Eisma, J., Rawls, E., Long, S., Mach, R., & Lamm, C. (2021). Frontal midline theta differentiates separate cognitive control strategies while still generalizing the need for cognitive control. *Scientific Reports*, *11*(1), 1–14.

Engel, A. K., & Fries, P. (2010). Beta-band oscillations—signalling the status quo? *Current Opinion in Neurobiology*, *20*(2), 156–165.

Ericsson, K. A., & Simon, H. A. (1980). Verbal reports as data. *Psychological Review*, *87*(3), 215.

Eriksen, B. A., & Eriksen, C. W. (1974). Effects of noise letters upon the identification of a target letter in a nonsearch task. *Perception & Psychophysics*, *16*(1), 143–149.

Eysenbach, G., & Köhler, C. (2002). How do consumers search for and appraise health information on the world wide web? qualitative study using focus groups, usability tests, and in-depth interviews. *BMJ*, *324*(7337), 573–577.

Fagin, R., Halpern, J. Y., Moses, Y., & Vardi, M. (2004). *Reasoning about knowledge*. MIT press.

Fairclough, S. H., Venables, L., & Tattersall, A. (2005). The influence of task demand and learning on the psychophysiological response. *International Journal of Psychophysiology*, *56*(2), 171–184.

Fernandez Rojas, R., Debie, E., Fidock, J., Barlow, M., Kasmarik, K., Anavatti, S., ... Abbass, H. (2020). Electroencephalographic workload indicators during teleoperation of an unmanned aerial vehicle shepherding a swarm of unmanned ground vehicles in contested environments. *Frontiers in Neuroscience*, *14*, 40.

Fiebelkorn, I. C., & Kastner, S. (2019). A rhythmic theory of attention. *Trends in Cognitive Sciences*, *23*(2), 87–101.

Fink, A., Grabner, R., Neuper, C., & Neubauer, A. (2005). Eeg alpha band dissociation with increasing task demands. *Cognitive Brain Research*, *24*(2), 252–259.

Fodor, Z., Marosi, C., Tombor, L., & Csukly, G. (2020). Salient distractors open the door of perception: alpha desynchronization marks sensory gating in a working memory task. *Scientific Reports*, *10*(1), 1–11.

Freeman, F. G., Mikulka, P. J., Prinzel, L. J., & Scerbo, M. W. (1999). Evaluation of an adaptive automation system using three EEG indices with a visual tracking task. *Biological Psychology*, *50*(1), 61–76.

Freeman, F. G., Mikulka, P. J., Scerbo, M. W., & Scott, L. (2004). An evaluation of an adaptive automation system using a cognitive vigilance task. *Biological Psychology*, *67*(3), 283–297.

Friedman, D., & Johnson Jr, R. (2000). Event-related potential (erp) studies of memory encoding and retrieval: A selective review. *Microscopy research and technique*, *51*(1), 6–28.

Fu, K.-M. G., Foxe, J. J., Murray, M. M., Higgins, B. A., Javitt, D. C., & Schroeder, C. E. (2001). Attention-dependent suppression of distracter visual input can be cross-modally cued as indexed by anticipatory parieto–occipital alpha-band oscillations. *Cognitive Brain Research*, *12*(1), 145–152.

Gabard-Durnam, L. J., Mendez Leal, A. S., Wilkinson, C. L., & Levin, A. R. (2018). The harvard automated processing pipeline for electroencephalography (HAPPE): standardized processing software for developmental and high-artifact data. *Frontiers in Neuroscience*, *12*, 97.

Gabriel, G., Ramallo, M. A., & Cervantes, E. (2016). Workload perception in drone flight training

simulators. *Computers in Human Behavior*, *64*, 449–454.

García-Martínez, B., Martinez-Rodrigo, A., Alcaraz, R., & Fernández-Caballero, A. (2019). A review on nonlinear methods using electroencephalographic recordings for emotion recognition. *IEEE Transactions on Affective Computing*, *12*(3), 801–820.

Gero, J. S. (1990). Design prototypes: A knowledge representation schema for design. *AI Magazine*, *11*(4), 26–26.

Gero, J. S., & Kannengiesser, U. (2004). The situated function–behaviour–structure framework. *Design Studies*, *25*(4), 373–391.

Gero, J. S., & Tang, H.-H. (2001). The differences between retrospective and concurrent protocols in revealing the process-oriented aspects of the design process. *Design Studies*, *22*(3), 283–295.

Gevins, A., & Smith, M. E. (2003). Neurophysiological measures of cognitive workload during human-computer interaction. *Theoretical Issues in Ergonomics Science*, *4*(1-2), 113–131.

Ghani, U., Signal, N., Niazi, I., & Taylor, D. (2020). ERP based measures of cognitive workload: A review. *Neuroscience & Biobehavioral Reviews*.

Gick, M. L., & Holyoak, K. J. (1983). Schema induction and analogical transfer. *Cognitive Psychology*, *15*(1), 1–38.

Gneezy, U., Niederle, M., & Rustichini, A. (2003). Performance in competitive environments: Gender differences. *The Quarterly Journal of Economics*, *118*(3), 1049–1074.

Gobel, E. W., Parrish, T. B., & Reber, P. J. (2011). Neural correlates of skill acquisition: decreased cortical activity during a serial interception sequence learning task. *Neuroimage*, *58*(4), 1150–1157.

Göker, M. H. (1997). The effects of experience during design problem solving. *Design Studies*, *18*(4), 405–426.

Gonzalez-Mulé, E., Carter, K. M., & Mount, M. K. (2017). Are smarter people happier? meta-analyses of the relationships between general mental ability and job and life satisfaction. *Journal of Vocational Behavior*, *99*, 146–164.

Gottfredson, L. S. (1997). *Mainstream science on intelligence: An editorial with 52 signatories, history, and bibliography* (Vol. 24) (No. 1). Citeseer.

Grier, R. A., Warm, J. S., Dember, W. N., Matthews, G., Galinsky, T. L., Szalma, J. L., & Parasuraman, R. (2003). The vigilance decrement reflects limitations in effortful attention, not mindlessness. *Human Factors*, *45*(3), 349–359.

Guderian, S., & Düzel, E. (2005). Induced theta oscillations mediate large-scale synchrony with mediotemporal areas during recollection in humans. *Hippocampus*, *15*(7), 901–912.

Händel, B. F., Haarmeier, T., & Jensen, O. (2011). Alpha oscillations correlate with the successful inhibition of unattended stimuli. *Journal of Cognitive Neuroscience*, *23*(9), 2494–2502.

Hanslmayr, S., Aslan, A., Staudigl, T., Klimesch, W., Herrmann, C. S., & Bäuml, K.-H. (2007). Prestimulus oscillations predict visual perception performance between and within subjects. *Neuroimage*, *37*(4), 1465–1473.

Harmon-Jones, E., & Allen, J. J. (1998). Anger and frontal brain activity: EEG asymmetry consistent with approach motivation despite negative affective valence. *Journal of Personality and Social Psychology*, *74*(5), 1310.

Hart, S. G., & Staveland, L. E. (1988). Development of NASA-TLX (Task Load Index): Results of empirical and theoretical research. In *Advances in Psychology* (Vol. 52, pp. 139–183). Elsevier.

Hasher, L., Zacks, R. T., & May, C. P. (1999). Inhibitory control, circadian arousal, and age.

Hatchuel, A., & Weil, B. (2009). CK design theory: An advanced formulation. *Research in Engineering Design*, *19*(4), 181–192.

Hatfield, B. D., Haufler, A. J., Hung, T.-M., & Spalding, T. W. (2004). Electroencephalographic studies of skilled psychomotor performance. *Journal of Clinical Neurophysiology*, *21*(3), 144–156.

Healey, J. A., & Picard, R. W. (2005). Detecting stress during real-world driving tasks using physiological sensors. *IEEE Transactions on Intelligent Transportation Systems*, *6*(2), 156–166.

Heard, J., Harriott, C. E., & Adams, J. A. (2018). A survey of workload assessment algorithms. *IEEE Transactions on Human-Machine Systems*, *48*(5), 434–451.

Helton, W. S., Hollander, T. D., Warm, J. S., Matthews, G., Dember, W. N., Wallaart, M., … Hancock, P. A. (2005). Signal regularity and the mindlessness model of vigilance. *British*

Journal of Psychology, *96*(2), 249–261.

Herweg, N. A., Solomon, E. A., & Kahana, M. J. (2020). Theta oscillations in human memory. *Trends in Cognitive Sciences*, *24*(3), 208–227.

Hinds, P. J., Roberts, T. L., & Jones, H. (2004). Whose job is it anyway? a study of human-robot interaction in a collaborative task. *Human–Computer Interaction*, *19*(1-2), 151–181.

Hinterberger, T., Zlabinger, M., & Blaser, K. (2014). Neurophysiological correlates of various mental perspectives. *Frontiers in Human Neuroscience*, *8*, 637.

Hjortskov, N., Rissén, D., Blangsted, A. K., Fallentin, N., Lundberg, U., & Søgaard, K. (2004). The effect of mental stress on heart rate variability and blood pressure during computer work. *European Journal of Applied Physiology*, *92*(1), 84–89.

Hohaia, W., Saurels, B. W., Johnston, A., Yarrow, K., & Arnold, D. H. (2022). Occipital alpha-band brain waves when the eyes are closed are shaped by ongoing visual processes. *Scientific Reports*, *12*(1), 1–10.

Holt, D. J., Kunkel, L., Weiss, A. P., Goff, D. C., Wright, C. I., Shin, L. M., ... Heckers, S. (2006). Increased medial temporal lobe activation during the passive viewing of emotional and neutral facial expressions in schizophrenia. *Schizophrenia Research*, *82*(2-3), 153–162.

Horng, W.-B., Chen, C.-Y., Chang, Y., & Fan, C.-H. (2004). Driver fatigue detection based on eye tracking and dynamic template matching. In *IEEE International Conference on Networking, Sensing and Control* (Vol. 1, pp. 7–12).

Hu, J., & Min, J. (2018). Automated detection of driver fatigue based on EEG signals using gradient boosting decision tree model. *Cognitive Neurodynamics*, *12*(4), 431–440.

Hu, W.-L., Booth, J., & Reid, T. (2015). Reducing sketch inhibition during concept generation: Psychophysiological evidence of the effect of interventions. In *International Design Engineering Technical Conferences and Computers and Information in Engineering Conference* (Vol. 57175, p. V007T06A010).

Ismail, L. E., & Karwowski, W. (2020). Applications of EEG indices for the quantification of human cognitive performance: A systematic review and bibliometric analysis. *PLoS One*, *15*(12), e0242857.

Jaimes, A., & Sebe, N. (2007). Multimodal human–computer interaction: A survey. *Computer*

Vision and Image Understanding, *108*(1-2), 116–134.

Jain, A. K. (2010). Data clustering: 50 years beyond k-means. *Pattern Recognition Letters*, *31*(8), 651–666.

Jain, A. K., Murty, M. N., & Flynn, P. J. (1999). Data clustering: A review. *ACM Computing Surveys (CSUR)*, *31*(3), 264–323.

Jansson, D. G., & Smith, S. M. (1991). Design fixation. *Design Studies*, *12*(1), 3–11.

Jaquess, K. J., Lo, L.-C., Oh, H., Lu, C., Ginsberg, A., Tan, Y. Y., ... Gentili, R. J. (2018). Changes in mental workload and motor performance throughout multiple practice sessions under various levels of task difficulty. *Neuroscience*, *393*, 305–318.

Jasper, H. H. (1958). The ten-twenty electrode system of the international federation. *Electroencephalogr. Clin. Neurophysiol.*, *10*, 370–375.

Jaušovec, N., & Jaušovec, K. (2000). EEG activity during the performance of complex mental problems. *International Journal of Psychophysiology*, *36*(1), 73–88.

Jensen, O., & Lisman, J. E. (1998). An oscillatory short-term memory buffer model can account for data on the sternberg task. *Journal of Neuroscience*, *18*(24), 10688–10699.

Jensen, O., & Tesche, C. D. (2002). Frontal theta activity in humans increases with memory load in a working memory task. *European Journal of Neuroscience*, *15*(8), 1395–1399.

Jia, W., von Wegner, F., Zhao, M., & Zeng, Y. (2021). Network oscillations imply the highest cognitive workload and lowest cognitive control during idea generation in open-ended creation tasks. *Scientific Reports*, *11*(1), 1–23.

Jia, W., & Zeng, Y. (2021). EEG signals respond differently to idea generation, idea evolution and evaluation in a loosely controlled creativity experiment. *Scientific Reports*, *11*(1), 1–20.

Johnson, W., Bouchard Jr, T. J., Krueger, R. F., McGue, M., & Gottesman, I. I. (2004). Just one g: Consistent results from three test batteries. *Intelligence*, *32*(1), 95–107.

Johnson, W., te Nijenhuis, J., & Bouchard Jr, T. J. (2008). Still just 1 g: Consistent results from five test batteries. *Intelligence*, *36*(1), 81–95.

Judge, T. A., Colbert, A. E., & Ilies, R. (2004). Intelligence and leadership: A quantitative review and test of theoretical propositions. *Journal of Applied Psychology*, *89*(3), 542.

Kamzanova, A. T., Kustubayeva, A. M., & Matthews, G. (2014). Use of EEG workload indices for

diagnostic monitoring of vigilance decrement. *Human Factors*, *56*(6), 1136–1149.

Kane, M. J., Bleckley, M. K., Conway, A. R., & Engle, R. W. (2001). A controlled-attention view of working-memory capacity. *Journal of Experimental Psychology: General*, *130*(2), 169.

Kane, M. J., & Engle, R. W. (2003). Working-memory capacity and the control of attention: the contributions of goal neglect, response competition, and task set to stroop interference. *Journal of Experimental Psychology: General*, *132*(1), 47.

Kar, S., Bhagat, M., & Routray, A. (2010). EEG signal analysis for the assessment and quantification of driver's fatigue. *Transportation Research Part F: Traffic Psychology and Behaviour*, *13*(5), 297–306.

Karakaş, S. (2020). A review of theta oscillation and its functional correlates. *International Journal of Psychophysiology*, *157*, 82–99.

Karthikeyan, P., Murugappan, M., & Yaacob, S. (2011). ECG signals based mental stress assessment using wavelet transform. In *2011 IEEE International Conference on Control System, Computing and Engineering* (pp. 258–262).

Keil, A., Mussweiler, T., & Epstude, K. (2006). Alpha-band activity reflects reduction of mental effort in a comparison task: a source space analysis. *Brain Research*, *1121*(1), 117–127.

Kerick, S. E., Douglass, L. W., & Hatfield, B. D. (2004). Cerebral cortical adaptations associated with visuomotor practice. *Medicine and Science in Sports and Exercise*, *36*(1), 118–129.

Keye, D., Wilhelm, O., Oberauer, K., & Van Ravenzwaaij, D. (2009). Individual differences in conflict-monitoring: testing means and covariance hypothesis about the simon and the eriksen flanker task. *Psychological Research PRPF*, *73*(6), 762–776.

Khare, S. K., & Bajaj, V. (2020). Entropy-based drowsiness detection using adaptive variational mode decomposition. *IEEE Sensors Journal*, *21*(5), 6421–6428.

Klimesch, W. (1999). EEG alpha and theta oscillations reflect cognitive and memory performance: A review and analysis. *Brain Research Reviews*, *29*(2-3), 169–195.

Klimesch, W. (2012). Alpha-band oscillations, attention, and controlled access to stored information. *Trends in Cognitive Sciences*, *16*(12), 606–617.

Kocher, M. G., & Sutter, M. (2006). Time is money—time pressure, incentives, and the quality of decision-making. *Journal of Economic Behavior & Organization*, *61*(3), 375–392.

Koechlin, E., Ody, C., & Kouneiher, F. (2003). The architecture of cognitive control in the human prefrontal cortex. *Science*, *302*(5648), 1181–1185.

Krall, J., Menzies, T., & Davies, M. (2016). Learning mitigations for pilot issues when landing aircraft (via multiobjective optimization and multiagent simulations). *IEEE Transactions on Human-Machine Systems*, *46*(2), 221–230.

Krathwohl, D. R. (2002). A revision of bloom's taxonomy: An overview. *Theory into Practice*, *41*(4), 212–218.

Kulikowski, K. (2021). Cognitive abilities-a new direction in burnout research. *European Journal of Work and Organizational Psychology*, *30*(5), 705–719.

Kumar, M., Weippert, M., Vilbrandt, R., Kreuzfeld, S., & Stoll, R. (2007). Fuzzy evaluation of heart rate signals for mental stress assessment. *IEEE Transactions on Fuzzy Systems*, *15*(5), 791–808.

Kuncel, N. R., Hezlett, S. A., & Ones, D. S. (2004). Academic performance, career potential, creativity, and job performance: Can one construct predict them all? *Journal of Personality and Social Psychology*, *86*(1), 148.

Kunzelmann, A., & Rigotti, T. (2021). How time pressure is associated with both work engagement and emotional exhaustion: The moderating effects of resilient capabilities at work. *German Journal of Human Resource Management*, *35*(3), 309–336.

Kutas, M., & Federmeier, K. D. (2011). Thirty years and counting: Finding meaning in the n400 component of the event related brain potential (erp). *Annual review of psychology*, *62*, 621.

Law A, K. J. W. B. H. A. S. C. G. T. R., Araujo J, & S., J. (2017).

Leder, J., Häusser, J. A., & Mojzisch, A. (2013). Stress and strategic decision-making in the beauty contest game. *Psychoneuroendocrinology*, *38*(9), 1503–1511.

LePine, J. A., LePine, M. A., & Jackson, C. L. (2004). Challenge and hindrance stress: relationships with exhaustion, motivation to learn, and learning performance. *Journal of Applied Psychology*, *89*(5), 883.

Liang, C., Lin, C.-T., Yao, S.-N., Chang, W.-S., Liu, Y.-C., & Chen, S.-A. (2017). Visual attention and association: An electroencephalography study in expert designers. *Design Studies*, *48*,

76–95.

Liu, S., & Nam, C. S. (2018). Quantitative modeling of user performance in multitasking environments. *Computers in Human Behavior*, *84*, 130–140.

Lopez, N., Previc, F. H., Fischer, J., Heitz, R. P., & Engle, R. W. (2012). Effects of sleep deprivation on cognitive performance by united states air force pilots. *Journal of Applied Research in Memory and Cognition*, *1*(1), 27–33.

Love, P. E., Edwards, D. J., & Irani, Z. (2010). Work stress, support, and mental health in construction. *Journal of Construction Engineering and Management*, *136*(6), 650–658.

Lubinski, D. (2004). Introduction to the special section on cognitive abilities: 100 years after spearman's (1904) "'general intelligence', objectively determined and measured". *Journal of Personality and Social Psychology*, *86*(1), 96.

Maher, M., & Tang, H.-H. (2003). Co-evolution as a computational and cognitive model of design. *Research in Engineering Design*, *14*(1), 47–64.

Maior, H. A., Wilson, M. L., & Sharples, S. (2018). Workload alerts—using physiological measures of mental workload to provide feedback during tasks. *ACM Transactions on Computer-Human Interaction*, *25*(2).

Makeig, S., Debener, S., Onton, J., & Delorme, A. (2004). Mining event-related brain dynamics. *Trends in Cognitive Sciences*, *8*(5), 204–210.

Malach, R., Reppas, J., Benson, R., Kwong, K., Jiang, H., Kennedy, W., ... Tootell, R. (1995). Object-related activity revealed by functional magnetic resonance imaging in human occipital cortex. *Proceedings of the National Academy of Sciences*, *92*(18), 8135–8139.

Malone, T. W. (2018). How human-computer 'superminds' are redefining the future of work. *MIT Sloan Management Review*, *59*(4), 34–41.

Malvankar-Mehta, M. S., & Mehta, S. S. (2015). Optimal task allocation in multi-human multi-robot interaction. *Optimization Letters*, *9*(8), 1787–1803.

Manly, T., Robertson, I. H., Galloway, M., & Hawkins, K. (1999). The absent mind: Further investigations of sustained attention to response. *Neuropsychologia*, *37*(6), 661–670.

Margheim, L., Kelley, T., Pattison, D., et al. (2005). An empirical analysis of the effects of auditor time budget pressure and time deadline pressure. *Journal of Applied Business Research*

(JABR), *21*(1).

McClernon, C. K., McCauley, M. E., O'Connor, P. E., & Warm, J. S. (2011). Stress training improves performance during a stressful flight. *Human Factors*, *53*(3), 207–218.

Meichenbaum, D. (1985). Stress inoculation training. *New York*, *304*.

Michel, C. M., & Koenig, T. (2018). EEG microstates as a tool for studying the temporal dynamics of whole-brain neuronal networks: A review. *Neuroimage*, *180*, 577–593.

Miletić, S., & van Maanen, L. (2019). Caution in decision-making under time pressure is mediated by timing ability. *Cognitive Psychology*, *110*, 16–29.

Mina, T., Kannan, S. S., Jo, W., & Min, B.-C. (2020). Adaptive workload allocation for multi-human multi-robot teams for independent and homogeneous tasks. *IEEE Access*, *8*, 152697–152712.

Miyake, A., Friedman, N. P., Emerson, M. J., Witzki, A. H., Howerter, A., & Wager, T. D. (2000). The unity and diversity of executive functions and their contributions to complex "frontal lobe" tasks: A latent variable analysis. *Cognitive Psychology*, *41*(1), 49–100.

Murray, M. M., Brunet, D., & Michel, C. M. (2008). Topographic ERP analyses: A step-by-step tutorial review. *Brain Topography*, *20*(4), 249–264.

Musslick, S., & Cohen, J. D. (2021). Rationalizing constraints on the capacity for cognitive control. *Trends in Cognitive Sciences*, *25*(9), 757–775.

Nachev, P., Rees, G., Parton, A., Kennard, C., & Husain, M. (2005). Volition and conflict in human medial frontal cortex. *Current Biology*, *15*(2), 122–128.

Nagamachi, M. (1995). Kansei engineering: a new ergonomic consumer-oriented technology for product development. *International Journal of industrial ergonomics*, *15*(1), 3–11.

Neill, T. M., Gero, J. S., & Warren, J. (1998). Understanding conceptual electronic design using protocol analysis. *Research in Engineering Design*, *10*(3), 129–140.

Nguyen, P., Nguyen, T. A., & Zeng, Y. (2018). Empirical approaches to quantifying effort, fatigue and concentration in the conceptual design process. *Research in Engineering Design*, *29*(3), 393–409.

Nguyen, P., Nguyen, T. A., & Zeng, Y. (2019). Segmentation of design protocol using EEG. *AI EDAM*, *33*(1), 11–23.

Nguyen, T. A., Xu, X., Zeng, Y., et al. (2013). Distribution of mental stresses during conceptual

design activities. In *Proceedings of The 19th International Conference on Engineering Design (ICED 13), Design for Harmonies* (Vol. 7, pp. 287–296).

Nguyen, T. A., & Zeng, Y. (2010). Analysis of design activities using EEG signals. In *International Design Engineering Technical Conferences and Computers and Information in Engineering Conference* (Vol. 44137, pp. 277–286).

Nguyen, T. A., & Zeng, Y. (2012). A theoretical model of design creativity: Nonlinear design dynamics and mental stress-creativity relation. *Journal of Integrated Design and Process Science*, *16*(3), 65–88.

Nguyen, T. A., & Zeng, Y. (2014). A physiological study of relationship between designer's mental effort and mental stress during conceptual design. *Computer-Aided Design*, *54*, 3–18.

Nguyen, T. A., & Zeng, Y. (2017). Effects of stress and effort on self-rated reports in experimental study of design activities. *Journal of Intelligent Manufacturing*, *28*(7), 1609–1622.

Nie, D., Wang, X.-W., Shi, L.-C., & Lu, B.-L. (2011). EEG-based emotion recognition during watching movies. In *2011 5th International IEEE/EMBS Conference on Neural Engineering* (pp. 667–670).

Niederée, U., Jipp, M., Teegen, U., & Vollrath, M. (2012). Effects of observability, mood states, and workload on human handling errors when monitoring aircraft automation. In *Proceedings of The Human Factors and Ergonomics Society Annual Meeting* (Vol. 56, pp. 1481–1485).

Niederle, M., & Vesterlund, L. (2007). Do women shy away from competition? do men compete too much? *The Quarterly Journal of Economics*, *122*(3), 1067–1101.

Nolan, H., Whelan, R., & Reilly, R. B. (2010). Faster: Fully automated statistical thresholding for EEG artifact rejection. *Journal of Neuroscience Methods*, *192*(1), 152–162.

Nyhus, E., & Curran, T. (2010). Functional role of gamma and theta oscillations in episodic memory. *Neuroscience & Biobehavioral Reviews*, *34*(7), 1023–1035.

Nystrom, L. E., Braver, T. S., Sabb, F. W., Delgado, M. R., Noll, D. C., & Cohen, J. D. (2000). Working memory for letters, shapes, and locations: fMRI evidence against stimulus-based regional organization in human prefrontal cortex. *Neuroimage*, *11*(5), 424–446.

Oberauer, K., Süß, H.-M., Wilhelm, O., & Sander, N. (2007). Individual differences in working memory capacity and reasoning ability.

Oberauer, K., Süß, H.-M., Wilhelm, O., & Wittman, W. W. (2003). The multiple faces of working memory: Storage, processing, supervision, and coordination. *Intelligence*, *31*(2), 167–193.

Olejniczak, P. (2006). Neurophysiologic basis of EEG. *Journal of Clinical Neurophysiology*, *23*(3), 186–189.

Oostenveld, R., & Praamstra, P. (2001). The five percent electrode system for high-resolution EEG and ERP measurements. *Clinical Neurophysiology*, *112*(4), 713–719.

Palva, S., & Palva, J. M. (2007). New vistas for α-frequency band oscillations. *Trends in Neurosciences*, *30*(4), 150–158.

Parasuraman, R., Barnes, M., Cosenzo, K., & Mulgund, S. (2007). *Adaptive automation for human-robot teaming in future command and control systems* (Tech. Rep.). Army research lab aberdeen proving ground md human research and engineering.

Pascual-Marqui, R. D., Michel, C. M., & Lehmann, D. (1995). Segmentation of brain electrical activity into microstates: Model estimation and validation. *IEEE Transactions on Biomedical Engineering*, *42*(7), 658–665.

Pavlov, Y. G., & Kotchoubey, B. (2017). EEG correlates of working memory performance in females. *BMC Neuroscience*, *18*(1), 1–14.

Payne, L., Guillory, S., & Sekuler, R. (2013). Attention-modulated alpha-band oscillations protect against intrusion of irrelevant information. *Journal of Cognitive Neuroscience*, *25*(9), 1463–1476.

Payne, L., & Sekuler, R. (2014). The importance of ignoring: Alpha oscillations protect selectivity. *Current Directions in Psychological Science*, *23*(3), 171–177.

Peng, C.-K., Havlin, S., Stanley, H. E., & Goldberger, A. L. (1995). Quantification of scaling exponents and crossover phenomena in nonstationary heartbeat time series. *Chaos: An Interdisciplinary Journal of Nonlinear Science*, *5*(1), 82–87.

Petkar, H., Dande, S., Yadav, R., Zeng, Y., & Nguyen, T. A. (2009). A pilot study to assess designer's mental stress using eye gaze system and electroencephalogram. In *International Design Engineering Technical Conferences and Computers and Information in Engineering Conference* (Vol. 48999, pp. 899–909).

Pfeifer, R., Rothenfluh, T., Stolze, M., & Steiner, F. (1992). Mapping expert behavior onto task-level frameworks: The need for "eco-pragmatic" approaches to knowledge engineering. In *Contemporary Knowledge Engineering and Cognition* (pp. 59–77). Springer.

Pfurtscheller, G. (1977). Graphical display and statistical evaluation of event-related desynchronization (ERD). *Electroencephalography and Clinical Neurophysiology*, *43*(5), 757–760.

Pfurtscheller, G. (1992). Event-related synchronization (ERS): An electrophysiological correlate of cortical areas at rest. *Electroencephalography and Clinical Neurophysiology*, *83*(1), 62–69.

Phillips, J. M. (2008). The role of excess cognitive capacity in the relationship between job characteristics and cognitive task engagement. *Journal of Business and Psychology*, *23*(1), 11–24.

Pidgeon, L. M., Grealy, M., Duffy, A. H., Hay, L., McTeague, C., Vuletic, T., … Gilbert, S. J. (2016). Functional neuroimaging of visual creativity: A systematic review and meta-analysis. *Brain and Behavior*, *6*(10), e00540.

Poldrack, R. A. (2006). Can cognitive processes be inferred from neuroimaging data? *Trends in Cognitive Sciences*, *10*(2), 59–63.

Poldrack, R. A. (2011). Inferring mental states from neuroimaging data: From reverse inference to large-scale decoding. *Neuron*, *72*(5), 692–697.

Pope, A. T., Bogart, E. H., & Bartolome, D. S. (1995). Biocybernetic system evaluates indices of operator engagement in automated task. *Biological Psychology*, *40*(1-2), 187–195.

Pourtois, G., Delplanque, S., Michel, C., & Vuilleumier, P. (2008). Beyond conventional event-related brain potential (ERP): Exploring the time-course of visual emotion processing using topographic and principal component analyses. *Brain Topography*, *20*(4), 265–277.

Prewett, M. S., Johnson, R. C., Saboe, K. N., Elliott, L. R., & Coovert, M. D. (2010). Managing workload in human–robot interaction: A review of empirical studies. *Computers in Human Behavior*, *26*(5), 840–856.

Putman, P., Antypa, N., Crysovergi, P., & van der Does, W. A. (2010). Exogenous cortisol acutely influences motivated decision making in healthy young men. *Psychopharmacology*, *208*(2), 257–263.

Radüntz, T. (2020). The effect of planning, strategy learning, and working memory capacity on mental workload. *Scientific Reports*, *10*(1), 1–10.

Raghavachari, S., Kahana, M. J., Rizzuto, D. S., Caplan, J. B., Kirschen, M. P., Bourgeois, B., ... Lisman, J. E. (2001). Gating of human theta oscillations by a working memory task. *Journal of Neuroscience*, *21*(9), 3175–3183.

Ramshur, J. T. (2010). *Design, evaluation, and application of heart rate variability analysis software (HRVAS)* (Unpublished doctoral dissertation). University of Memphis Tennessee.

Rasmussen, J. (1983). Skills, rules, and knowledge; signals, signs, and symbols, and other distinctions in human performance models. *IEEE Transactions on Systems, Man, and Cybernetics*(3), 257–266.

Reddy, U. S., Thota, A. V., & Dharun, A. (2018). Machine learning techniques for stress prediction in working employees. In *2018 IEEE International Cconference on Computational Intelligence and Computing Research (ICCIC)* (pp. 1–4).

Ree, M. J., Earles, J. A., & Teachout, M. S. (1994). Predicting job performance: Not much more than g. *Journal of Applied Psychology*, *79*(4), 518.

Reeves, B., & Nass, C. (1996). *The media equation: How people treat computers, television, and new media like real people*. Cambridge University press.

Reif, J. H. (1985). Depth-first search is inherently sequential. *Information Processing Letters*, *20*(5), 229–234.

Rhodes, G. (1985). Lateralized processes in face recognition. *British Journal of Psychology*, *76*(2), 249–271.

Richardson, P., Sieh, L., & Elkateeb, A. M. (2001). Fault-tolerant adaptive scheduling for embedded real-time systems. *IEEE Micro*, *21*(05), 41–51.

Richman, J. S., & Moorman, J. R. (2000). Physiological time-series analysis using approximate entropy and sample entropy. *American Journal of Physiology-Heart and Circulatory Physiology*, *278*(6), H2039–H2049.

Rieuf, V., Bouchard, C., Meyrueis, V., & Omhover, J.-F. (2017). Emotional activity in early immersive design: Sketches and moodboards in virtual reality. *Design Studies*, *48*, 43–75.

Roberts, R. E., Anderson, E. J., & Husain, M. (2010). Expert cognitive control and individual differences associated with frontal and parietal white matter microstructure. *Journal of Neuroscience*, *30*(50), 17063–17067.

Robertson, I. H., Manly, T., Andrade, J., Baddeley, B. T., & Yiend, J. (1997). Oops!': performance correlates of everyday attentional failures in traumatic brain injured and normal subjects. *Neuropsychologia*, *35*(6), 747–758.

Roozenburg, N. F. (1993). On the pattern of reasoning in innovative design. *Design Studies*, *14*(1), 4–18.

Roux, F., & Uhlhaas, P. J. (2014). Working memory and neural oscillations: Alpha–gamma versus theta–gamma codes for distinct wm information? *Trends in Cognitive Sciences*, *18*(1), 16–25.

Russo, J. E., Johnson, E. J., & Stephens, D. L. (1989). The validity of verbal protocols. *Memory & Cognition*, *17*(6), 759–769.

Ryu, K., & Myung, R. (2005). Evaluation of mental workload with a combined measure based on physiological indices during a dual task of tracking and mental arithmetic. *International Journal of Industrial Ergonomics*, *35*(11), 991–1009.

Salahuddin, L., Cho, J., Jeong, M. G., & Kim, D. (2007). Ultra short term analysis of heart rate variability for monitoring mental stress in mobile settings. In *2007 29th Annual International Conference of The IEEE Engineering in Medicine and Biology Society* (pp. 4656–4659).

Salgado, J. F., Anderson, N., Moscoso, S., Bertua, C., De Fruyt, F., & Rolland, J. P. (2003). A meta-analytic study of general mental ability validity for different occupations in the european community. *Journal of Applied Psychology*, *88*(6), 1068.

Sauerwein, E., Bailom, F., Matzler, K., & Hinterhuber, H. H. (1996). The kano model: How to delight your customers. In *International Working Seminar on Production Economics* (Vol. 1, pp. 313–327).

Sauseng, P., Griesmayr, B., Freunberger, R., & Klimesch, W. (2010). Control mechanisms in working memory: A possible function of EEG theta oscillations. *Neuroscience & Biobehavioral Reviews*, *34*(7), 1015–1022.

Sauseng, P., Klimesch, W., Doppelmayr, M., Pecherstorfer, T., Freunberger, R., & Hanslmayr, S. (2005). EEG alpha synchronization and functional coupling during top-down processing in a working memory task. *Human Brain Mapping*, *26*(2), 148–155.

Sauseng, P., Klimesch, W., Heise, K. F., Gruber, W. R., Holz, E., Karim, A. A., ... Hummel, F. C.

(2009). Brain oscillatory substrates of visual short-term memory capacity. *Current Biology*, *19*(21), 1846–1852.

Schmidt, F. L., & Hunter, J. (2004). General mental ability in the world of work: Occupational attainment and job performance. *Journal of Personality and Social Psychology*, *86*(1), 162.

Schmidt, L. A., & Trainor, L. J. (2001). Frontal brain electrical activity (EEG) distinguishes valence and intensity of musical emotions. *Cognition & Emotion*, *15*(4), 487–500.

Schmitt, A., Ohly, S., & Kleespies, N. (2015). Time pressure promotes work engagement: Test of illegitimate tasks as boundary condition. *Journal of Personnel Psychology*, *14*(1), 28.

Schön, D. A. (2017). *The reflective practitioner: How professionals think in action*. Routledge.

Scott, T. J., & O'Sullivan, M. K. (2005). Analyzing student search strategies: Making a case for integrating information literacy skills into the curriculum. *Teacher Librarian*, *33*(1), 21.

Seitzman, B. A., Abell, M., Bartley, S. C., Erickson, M. A., Bolbecker, A. R., & Hetrick, W. P. (2017). Cognitive manipulation of brain electric microstates. *Neuroimage*, *146*, 533–543.

Sergent, J., & Bindra, D. (1981). Differential hemispheric processing of faces: Methodological considerations and reinterpretation. *Psychological Bulletin*, *89*(3), 541.

Shaw, E. P., Rietschel, J. C., Shuggi, I. M., Xu, Y., Chen, S., Miller, M. W., ... Gentili, R. J. (2019). Cerebral cortical networking for mental workload assessment under various demands during dual-task walking. *Experimental Brain Research*, *237*(9), 2279–2295.

Shurchkov, O. (2012). Under pressure: Gender differences in output quality and quantity under competition and time constraints. *Journal of the European Economic Association*, *10*(5), 1189–1213.

Simon, H. A. (1969). The sciences of the artificial. *Cambridge, MA*.

Slobounov, S., Fukada, K., Simon, R., Rearick, M., & Ray, W. (2000). Neurophysiological and behavioral indices of time pressure effects on visuomotor task performance. *Cognitive Brain Research*, *9*(3), 287–298.

Smagorinsky, P. (1989). The reliability and validity of protocol analysis. *Written Communication*, *6*(4), 463–479.

Snyder, A. C., & Foxe, J. J. (2010). Anticipatory attentional suppression of visual features indexed by oscillatory alpha-band power increases: A high-density electrical mapping study. *Journal*

of Neuroscience, *30*(11), 4024–4032.

Spearman, C. (1961). "general intelligence" objectively determined and measured.

Spezialetti, M., Placidi, G., & Rossi, S. (2020). Emotion recognition for human-robot interaction: recent advances and future perspectives. *Frontiers in Robotics and AI*, *7*.

Starcke, K., Wolf, O. T., Markowitsch, H. J., & Brand, M. (2008). Anticipatory stress influences decision making under explicit risk conditions. *Behavioral Neuroscience*, *122*(6), 1352.

Staudigl, T., & Hanslmayr, S. (2013). Theta oscillations at encoding mediate the context-dependent nature of human episodic memory. *Current Biology*, *23*(12), 1101–1106.

Stavrinides, G. L., & Karatza, H. D. (2018). Scheduling data-intensive workloads in large-scale distributed systems: Trends and challenges. *Modeling and Simulation in HPC and Cloud Systems*, 19–43.

Stipacek, A., Grabner, R., Neuper, C., Fink, A., & Neubauer, A. (2003). Sensitivity of human EEG alpha band desynchronization to different working memory components and increasing levels of memory load. *Neuroscience Letters*, *353*(3), 193–196.

Strenze, T. (2007). Intelligence and socioeconomic success: A meta-analytic review of longitudinal research. *Intelligence*, *35*(5), 401–426.

Sutter, M., Kocher, M., & Strauß, S. (2003). Bargaining under time pressure in an experimental ultimatum game. *Economics Letters*, *81*(3), 341–347.

Suwa, M., Purcell, T., & Gero, J. (1998). Macroscopic analysis of design processes based on a scheme for coding designers' cognitive actions. *Design Studies*, *19*(4), 455–483.

Suwa, M., & Tversky, B. (1997). What do architects and students perceive in their design sketches? A protocol analysis. *Design Studies*, *18*(4), 385–403.

Sweller, J. (2010). Element interactivity and intrinsic, extraneous, and germane cognitive load. *Educational Psychology Review*, *22*(2), 123–138.

Sylcott, B., Cagan, J., & Tabibnia, G. (2011). Understanding of emotions and reasoning during consumer tradeoff between function and aesthetics in product design. In *International Design Engineering Technical Conferences and Computers and Information in Engineering Conference* (Vol. 54860, pp. 165–176).

Tang, Y., Zeng, Y., et al. (2009). Quantifying designer's mental stress in the conceptual design

process using kinesics study. In *Proceedings of The 17th International Conference on Engineering Design (ICED 09)* (Vol. 9, pp. 211–220).

Tesche, C., & Karhu, J. (2000). Theta oscillations index human hippocampal activation during a working memory task. *Proceedings of the National Academy of Sciences*, *97*(2), 919–924.

Thompson-Schill, S. L., Ramscar, M., & Chrysikou, E. G. (2009). Cognition without control: When a little frontal lobe goes a long way. *Current Directions in Psychological Science*, *18*(5), 259–263.

Thorndyke, P. W. (1977). Cognitive structures in comprehension and memory of narrative discourse. *Cognitive Psychology*, *9*(1), 77–110.

Tsarouchi, P., Michalos, G., Makris, S., Athanasatos, T., Dimoulas, K., & Chryssolouris, G. (2017). On a human–robot workplace design and task allocation system. *International Journal of Computer Integrated Manufacturing*, *30*(12), 1272–1279.

Unsworth, N., Brewer, G. A., & Spillers, G. J. (2009). There's more to the working memory capacity—fluid intelligence relationship than just secondary memory. *Psychonomic Bulletin & Review*, *16*(5), 931–937.

Unsworth, N., Fukuda, K., Awh, E., & Vogel, E. K. (2015). Working memory delay activity predicts individual differences in cognitive abilities. *Journal of Cognitive Neuroscience*, *27*(5), 853–865.

Vanheusden, S., Van Gils, T., Caris, A., Ramaekers, K., & Braekers, K. (2020). Operational workload balancing in manual order picking. *Computers & Industrial Engineering*, *141*, 106269.

Veen, V. v., & Carter, C. S. (2006). Conflict and cognitive control in the brain. *Current Directions in Psychological Science*, *15*(5), 237–240.

Verguts, T., & Notebaert, W. (2009). Adaptation by binding: A learning account of cognitive control. *Trends in Cognitive Sciences*, *13*(6), 252–257.

Verma, A., Cherkasova, L., Kumar, V. S., & Campbell, R. H. (2012). Deadline-based workload management for mapreduce environments: Pieces of the performance puzzle. In *2012 IEEE Network Operations and Management Symposium* (pp. 900–905).

Vesin, B., Mangaroska, K., & Giannakos, M. (2018). Learning in smart environments: User-centered design and analytics of an adaptive learning system. *Smart Learning Environments*, *5*(1), 1–21.

Vieira, S., Gero, J., Delmoral, J., Gattol, V., Fernandes, C., Parente, M., & Fernandes, A. (2019). Understanding the design neurocognition of mechanical engineers when designing and problem-solving. In *International Design Engineering Technical Conferences and Computers and Information in Engineering Conference* (Vol. 59278, p. V007T06A037).

Viswanathan, V., Atilola, O., Esposito, N., & Linsey, J. (2014). A study on the role of physical models in the mitigation of design fixation. *Journal of Engineering Design*, *25*(1-3), 25–43.

Von Wegner, F. (2018). Partial autoinformation to characterize symbolic sequences. *Frontiers in Physiology*, 1382.

Wang, X., Nguyen, T. A., Zeng, Y., et al. (2015). Influence of information collection strategy in problem formulation on design creativity through mental stress: A theoretical analysis. In *Proceedings of The 20th International Conference on Engineering Design (ICED 15)* (Vol. 11, pp. 091–100).

Wang, Y., Wu, L., Yuan, X., Liu, X., & Li, X. (2019). An energy-efficient and deadline-aware task offloading strategy based on channel constraint for mobile cloud workflows. *IEEE Access*, *7*, 69858–69872.

Warm, J. S., Parasuraman, R., & Matthews, G. (2008). Vigilance requires hard mental work and is stressful. *Human Factors*, *50*(3), 433–441.

Wästlund, E., Norlander, T., & Archer, T. (2008). The effect of page layout on mental workload: A dual-task experiment. *Computers in Human Behavior*, *24*(3), 1229–1245.

Weiergräber, M., Papazoglou, A., Broich, K., & Müller, R. (2016). Sampling rate, signal bandwidth and related pitfalls in EEG analysis. *Journal of Neuroscience Methods*, *268*, 53–55.

Welford, A. (1978). Mental work-load as a function of demand, capacity, strategy and skill. *Ergonomics*, *21*(3), 151–167.

Whittaker, S. (2005). Supporting collaborative task management in e-mail. *Human–Computer Interaction*, *20*(1-2), 49–88.

Wickens, C. D. (2002). Situation awareness and workload in aviation. *Current Directions in*

Psychological Science, *11*(4), 128–133.

Wickens, C. D. (2008). Multiple resources and mental workload. *Human Factors*, *50*(3), 449–455.

Widiyati, K., & Aoyama, H. (2013). Robust design on emotion for pet bottle shape using taguchi method. In *Emotional Engineering* (Vol. 2, pp. 195–218). Springer.

Wiebe, E. N., Roberts, E., & Behrend, T. S. (2010). An examination of two mental workload measurement approaches to understanding multimedia learning. *Computers in Human Behavior*, *26*(3), 474–481.

Wiegmann, D., & Shappell, S. (1997). Human factors analysis of post-accident data: The taxonomy of unsafe operations. *International Journal of Aviation Psychology*, *9*, 267–291.

Wilczynski, N. L., & Haynes, R. B. (2004). Developing optimal search strategies for detecting clinically sound prognostic studies in MEDLINE: An analytic survey. *BMC Medicine*, *2*(1), 1–5.

Wilhelm, O., Hildebrandt, A., & Oberauer, K. (2013). What is working memory capacity, and how can we measure it? *Frontiers in Psychology*, *4*, 433.

Wong, L., & Abdulla, W. (2006). Time-frequency evaluation of segmentation methods for neonatal EEG signals. In *2006 International Conference of The IEEE Engineering in Medicine and Biology Society* (pp. 1303–1306).

Xu, R., & Wunsch, D. (2005). Survey of clustering algorithms. *IEEE Transactions on neural networks*, *16*(3), 645–678.

Xu, X., Yuan, H., & Lei, X. (2016). Activation and connectivity within the default mode network contribute independently to future-oriented thought. *Scientific Reports*, *6*(1), 1–10.

Yamagishi, N., Callan, D. E., Goda, N., Anderson, S. J., Yoshida, Y., & Kawato, M. (2003). Attentional modulation of oscillatory activity in human visual cortex. *Neuroimage*, *20*(1), 98–113.

Yang, J., Yang, L., Quan, H., & Zeng, Y. (2021). Implementation barriers: A TASKS framework. *Journal of Integrated Design and Process Science*(Preprint), 1–14.

Yerkes, R. M., & Dodson, J. D. (1908). The relation of strength of stimulus to rapidity of habit-formation.

Young, M. S., Brookhuis, K. A., Wickens, C. D., & Hancock, P. A. (2015). State of science: mental

workload in ergonomics. *Ergonomics*, *58*(1), 1–17.

Yuksel, B. F., Oleson, K. B., Harrison, L., Peck, E. M., Afergan, D., Chang, R., & Jacob, R. J. (2016). Learn piano with BACh: An adaptive learning interface that adjusts task difficulty based on brain state. In *Proceedings of The 2016 chi Conference on Human Factors in Computing Systems* (pp. 5372–5384).

Zahabi, M., Nasr, V., Mohammed Abdul Razak, A., Patranella, B., McCanless, L., & Maredia, A. (2021). Effect of secondary tasks on police officer cognitive workload and performance under normal and pursuit driving situations. *Human Factors*, 00187208211010956.

Zeng, Y. (2002). Axiomatic theory of design modeling. *Journal of Integrated Design and Process Science*, *6*(3), 1–28.

Zeng, Y. (2004). Environment-based formulation of design problem. *Journal of Integrated Design and Process Science*, *8*(4), 45–63.

Zeng, Y. (2015). Environment-based design (EBD): A methodology for transdisciplinary design+. *Journal of Integrated Design and Process Science*, *19*(1), 5–24.

Zeng, Y., & Cheng, G. (1991). On the logic of design. *Design Studies*, *12*(3), 137–141.

Zeng, Y., & Gu, P. (1999). A science-based approach to product design theory Part I: Formulation and formalization of design process. *Robotics and Computer-Integrated Manufacturing*, *15*(4), 331–339.

Zhang, Z., & Zhang, J. (2006). Driver fatigue detection based intelligent vehicle control. In *18th International Conference on Pattern Recognition (ICPR'06)* (Vol. 2, pp. 1262–1265).

Zhao, M., Jia, W., Jennings, S., Law, A., Bourgon, A., Grenier, H., … Zeng, Y. (2022). Cognitive control improves and cognitive workload reduces through a skill acquisition process: EEG evidences from a pilot training process. *Nature Human Behaviour (to be submitted)*.

Zhao, M., Jia, W., Yang, D., Nguyen, P., Nguyen, T. A., & Zeng, Y. (2020). A tEEG framework for studying designer's cognitive and affective states. *Design Science*, *6*.

Zhao, M., Qiu, D., & Zeng, Y. (2022). How much workload is a "good" workload for human beings to meet the deadline? *PloS One (to be submitted)*.

Zhao, M., Yang, D., Liu, S., & Zeng, Y. (2018). Mental stress-performance model in emotional engineering. In *Emotional Engineering* (Vol. 6, pp. 119–139). Springer.

Zhao, M., & Zeng, Y. (2019). Influence of information collection strategy on designer's mental stress. In *Proceedings of The Design Society: International Conference on Engineering Design* (Vol. 1, pp. 1783–1792).

Zhu, S., Yao, S., & Zeng, Y. (2007). A novel approach to quantifying designer's mental stress in the conceptual design process. In *International Design Engineering Technical Conferences and Computers and Information in Engineering Conference* (Vol. 48035, pp. 593–600).